An active thumb module for the Symbihand

Assisting Duchenne Muscular Dystrophy patients in ADL

- P. de Groot -

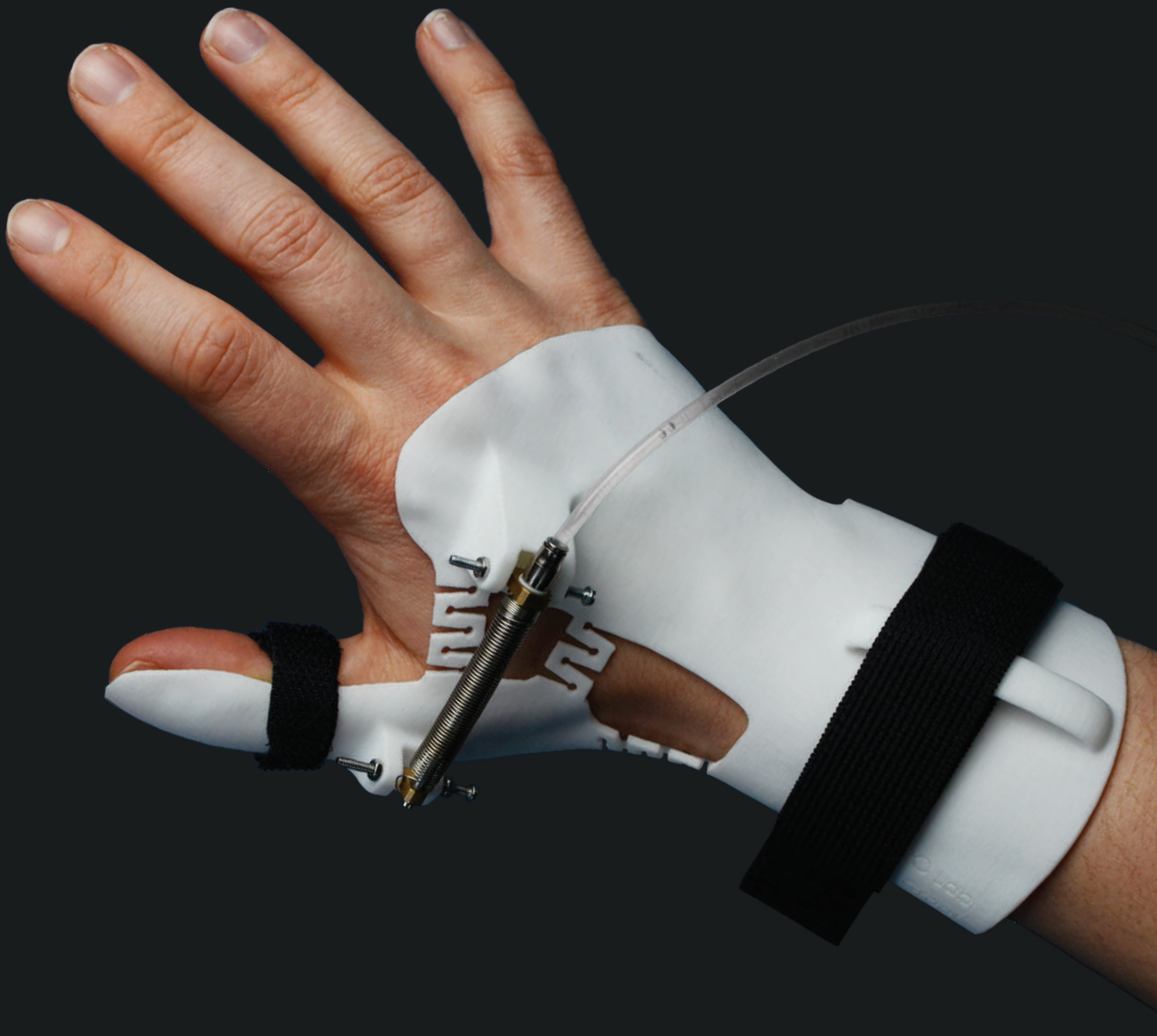

Delft University of Technology, Faculty of Mechanical, Maritime and Materials Engineering
Department of Biomechanical Engineering, Delft Institute of Prosthetics and Orthotics

An active thumb module for the Symbihand

Assisting Duchenne Muscular Dystrophy patients in ADL

by

P. de Groot

to obtain the degree of Master of Science in Biomedical Engineering
at the Delft University of Technology,
Faculty of Mechanical, Maritime and Materials Engineering,
Delft Institute of Prosthetics and Orthotics

to be defended publicly on March 12th 2021

Student number:	4367960		
Project duration:	March 1st, 2020 – March 12th, 2021		
Thesis committee:	Dr. ir.	D.H. Plettenburg,	TU Delft, supervisor
	Prof. Dr.	F.C.T. van der Helm,	TU Delft, chair
	Dr.Ir.	M. Mirakhorlo,	TU Delft, external committee member

TU Delft

Preface

Before you lies the graduation thesis "An active thumb module for the Symbihand: Assisting Duchenne Muscular Dystrophy patients in ADL." Which describes the design process of an hydraulically actuated thumb orthosis. It has been written to fulfill the graduation requirements of the track BioMechatronics of the Master BioMedical Engineering at the TU Delft. I was engaged in researching and writing this thesis for the Dutch Institute of Prosthetics and Orthotics from March 2020 to March 2021.

Ever since I shadowed an orthopedic technician in high school my interest for assistive devices was kindled. I was inspired by the patients and their drive to regain control over their lives. In my opinion technology can be of substantial value in fulfilling this goal and good design can be truly meaningful to this target population. I am content that for my thesis I found a topic by which I could contribute to this cause.

It has been quite the ride, with ups and downs and with uncertainties and changes of perspective along the way. 'Fail often, Fail fast.' Donald A. Norman once said to describe the iterative development process. I have to admit that sometimes I wished I had failed a little faster, a little more often. Corona has been an obstruction of my development process, regarding possibilities such as meeting with Duchenne patients or simply conferring with fellow students.

Luckily, I did not have to do it entirely on my own. I would like to thank my supervisor Dick Plettenburg for our weekly meetings, for encouraging me and for not leaving my side despite your retirement and change of address. Furthermore, I would like to thank Jan van Frankenhuyzen. Thank you for your support in building and developing the prototype, for allowing me to abuse the 3D printers as often as I wished and for the genuine laughs during our meetings.

Moreover, I would like to express my gratitude towards my family, friends and roommates. My parents whom have been incredibly patient and know when to push and when to let me find my own course. My grandparents and little sister for always being proud of me and my little brother for simply taking an interest. I also give thanks to my friends and roommates. You have lifted me up when I was down, listened to my occasional complaining, and kept telling me that I am capable enough.

At last, a special shout-out goes to Simon Stouten and Luuk Lommerse. I had fun being in the same boat as you guys and I am grateful for the feedback you have provided me on several occasions. I hope the same goes for you.

P. DE GROOT
Rotterdam, 21-02-2020

Contents

TABLE OF CONTENTS

TU Delft

LIST OF FIGURES

LIST OF TABLES

Glossary

ABBREVIATIONS AND ACRONYMS

AA	Abduction / Adduction
ABS	Acrylonitrile Butadiene Styrene
ACT Hand	Anatomically Correct Testbed hand
ADL	Activities of Daily Living
aROM	Active Range of Motion
BAR Hand	Bio-mimetic Anthropomorphic Robotic hand
CAD	Computer Aided Design
CE	Cognital Effort
CMC	Carpometacarpal joint
CR	Customer Requirements
DAC	Dual Acting Cylinder
DIP	Distal interphalangeal joint
DMD	Duchenne Muscular Dystrophy
DOF	Degrees of Freedom
DP	Design parameters
DR	Design Requirement
FDM	Fused Deposition Modelling
FE	Flexion / Extension
FEM	Finite Element Modelling
FR	Functional Requirements
fROM	Functional Range of Motion
IP	Interphalangeal joint of the thumb
LE	Lingquistic Effort
MCP	Metacarpophalangeal joint of the fingers
MP	Metacarpophalangeal joint of the thumb
NMD	Neuromuscular disorder
PA	Poly-Amide
PE	Physical Effort
PIP	Proximal interphalangeal joint
PLA	Polylactic Acid
pROM	Passive Range of Motion
PVA	Polyvinyl Alcohol
QOL	Quality of Life
ROM	Range Of Motion
RUD	Radial Ulnar Deviation
SAC	Single Acting Cylinder
SCI	Spinal Cord Injury
sEMG	Surface Electromyography
SLA	Stereolithography
SLM	Selective Laser Melting
SLS	Selective Laser Sintering
SMA	Smart Memory Alloy
SME	Smart Memory Effect
SMP	Smart Memory Polymer
TL	Time Load
UE	Upper Extremity

SYMBOLS

A_{proj}	Projected Area [mm^2]
D	Piston bore diameter [mm]
D_c	Piston bore diameter [mm]
D_g	Piston groove diameter [mm]
d_p	Moment arm of piston cylinder [mm]
d_g	Moment arm of pinch force [mm]
f_c	O-ring compression friction factor [-]
f_h	Fluid pressure friction factor [-]
f_{loss}	Relative actuator losses [-]
F_a	Actuation force [N]
F_p	Piston-cylinder force [N]
F_s	Spring force [N]
F_o	O-ring friction force [N]
F_g	Pinch force [N]
h	End cap overlap height [mm]
H_s	Shore Hardness [°Sh]
k	Spring constant [N/mm]
L	Cylinder length [mm]
L_w	outside circumference of the seal [mm]
m	Mass [gr]
P	Pressure in the system [MPa]
p_g	Pressure gradient [MPa]
t_p	Cylinder wall thickness [mm]
x	Extension [mm]
α	O-ring squeeze [%]
θ	ROM [deg]
ρ	Density [kg/m^2]
σ	Yield strength [MPa]

1.

Introduction

Introduction

The interaction of humans with their environment takes place largely through their hands. Thence during evolution, our hands have developed into intricate machines [1], [2]. How vital dexterous hand function is to us, becomes most evident when impairment occurs. Unfortunately, hand injuries, paralysis or loss of muscle function are widespread consequences from vascular disorders, accidents, degenerative diseases and structural or neuromuscular disorders [3]–[5]. Significant loss of hand function impedes the ability to perform activities of daily living (ADL) and dramatically reduces the quality of life (QOL) [6]. A diminishment in QOL can be bestowed upon psychological distress and obstruction of the person's ability to live safely, independently, and actively participate in social roles [3].

To tackle this problem for Duchenne Muscular Dystrophy (DMD) patients, two PhD students have put their work towards developing the mechanical and control system of the Symbihand [7], [8]. The Symbihand is an orthotic device developed to support DMD patients hand function in ADL. This thesis was executed for the Delft Institute of Prosthetics and Orthotics and continues on the written dissertations. First will be elaborated more on Duchenne Muscular Dystrophy, state of the art in active hand orthoses and the Symbihand.

1. DUCHENNE MUSCULAR DYSTROPHY

Duchenne Muscular Dystrophy is a progressive neuromuscular disease caused by an absence or deficiency of the dystrophin protein [9]. Dystrophin proteins in the body are responsible for the protection of muscle cells from contraction-induced damage. So, absence or abnormalities of the protein result in muscle degeneration [10]. As a consequence of muscle degeneration, patients suffer from muscular weakness. This weakness leads to disuse of the affected muscles, causing muscle stiffness, early fatigue, and deformities of the hand [11], [12]. The condition of DMD is hereditary and X-linked, with an incidence estimated on 1:5000 male newborns and a prevalence of 4.78 [%] worldwide [13]. Most patients are diagnosed around the age of 5, and although there is still no cure to DMD, the life expectancy of these patients has increased significantly over the years [14]. As a result of developments in disease treatment and management, prospects up to 30-40 years of age have become a sound expectation. This increased probability of having a future is accompanied by a desire for independence within the patient population [15]. Hand function plays a vital role in performing ADL, while DMD patients have to live without it for more than 15 years [16]. The disease's progression is reported as highly variable but can be divided into five stages, where hand impairments start to develop from the late ambulatory stage and onwards [9]:

Presymptomatic ⟶ *Early ambulatory* ⟶ <u>*Late ambulatory* ⟶ *Early non-ambulatory*</u> ⟶ *Late non-ambulatory*

Symptoms of DMD occur on both sides of the body and affect both extensor and flexor muscles. As the disease is of muscular origin instead of neurological origin, tactile and proprioceptive functioning remains unblemished [17]. The scope within this project is set to patients in the "Late ambulatory" and "Early non-ambulatory" phase of the disease. These patients are confined to their wheelchairs for most of the day [18]. The average age on which boys with DMD become completely confined to their wheelchair is between 8-14 years old [13], [14], [18]. Patients within these stages of the disease already cope with muscle weakness, emerging muscle stiffness, and mild to moderate deformities of the hand. In addition to muscle degeneration, trophic changes in skin integrity are present [19]. These changes include; coldness, increased skin fragility, tearing, bruising, transparency, and even scleroderma-like changes [20]. The focus is put towards the assistance of the hand in ADL. The hands of the user should at least be able to tolerate a functional passive range of motion for the orthosis to be usable in ADL.

Currently, static splinting of the hand is part of the DMD treatment plan. Static splints are fitted so that the hand stiffens into a functional static position. Splinted positioning is interspersed with passive stretching of the limbs by physical therapists [21]. Passive stretching is performed for contracture prophylaxis and to maintain a passive range of motion (pROM). The passive movements oppose fibrosis and in this way contributes to pain management [22], [23]. These interventions do not affect grip force nor attenuate fatigue. By modifying the hand's structural or functional characteristics with an external device, the ability to perform ADL can be aided [24]. Utilisation of active assistive devices will improve an individual's perceived QOL and enhance their social participation [24]–[26].

The plethora of hand orthoses focuses on stroke and spinal cord injury (SCI) patients. However, DMD patients suffer from different symptoms as their disease is of muscular origin instead of neurological origin. Hand orthoses developed are therefore often not suitable for this patient group, while they have to live with hand impairments for over 15 years. Symptomwise, similarities with stroke and SCI patients can be encountered in the presence of muscle stiffness and consecutive hand deformities. On the other hand, contrasting with stroke and SCI patients; DMD patients maintain proprioception and tactile sensation, have bilateral symptoms in flexion and extension and suffer from loss of skin integrity. These differing symptoms call for different control systems and particular attention to hand-interface design. As high variations are present between patients and within patients over time, it is difficult to establish general requirements to the assistive device relevant during the entire disease course. For this reason, it is decided to narrow it down to a functional assistive device for DMD patients that still have a functional pROM, who suffer from mild to moderate hand deformities and are confined to a wheelchair for a significant part of the day. The design of an assistive hand orthosis for this target group can counteract the effects of disuse and increase their level of independence, plausibly creating a positive effect on their perceived QOL.

2. STATE OF THE ART OF ACTIVE HAND ORTHOSES

Literature on rehabilitation engineering is replete with technical descriptions and analysis of assistive devices intended to enhance the lives of persons with disabilities [27]. The great number of orthotic devices developed in the last decades emphasises the importance of hand function, and many devices have shown promising results [6], [28]. Within the field of assistive devices, powered hand orthoses are a newly emerging technology. Powered hand orthoses consist of systems attached to hand segments, which actively assist digit flexion and extension to aid in the performance of functional grasping by applying forces to appropriate areas of the user's digits [6]. They attempt to restore movements that would typically be challenging or not possible for these individuals to independently achieve and maintain a stable grasp [6]. In practice, a dynamic hand orthosis can make the fingers follow a given trajectory, apply resistant forces to mimic external actions or augment the forces that would be naturally exerted [29]. This way, a distinction can be made between various types of hand orthoses. Most important is the difference between assistive and rehabilitative devices. Rehabilitative devices focus on functional recovery and training of the hand by indirectly enhancing hand function. Assistive devices, contrarily, are meant to restore functional abilities of the hand for the performance of ADL. These assistive orthoses shall be worn throughout the day, and the device takes over hand functioning completely or augments the functionality that has remained [29], [30].

Designs for active orthoses are diverse, and a specific user population is often not clearly described. Ideally, a clinically accessible assistive hand orthosis should be derived from a set of well-defined design specifications based on the input of end-users [6]. Many of the current assistive devices do not suit the needs of the end-users or their environment, which results in device abandonment [31]. Moreover, the majority of the designs have not been validated in patient populations or translated beyond a laboratory environment [6]. Simple assistive tools are easy to control, but not very functional in the performance of ADL. At the same time, more complex tools are often robotic systems that allow more functionality but are very expensive, difficult to control, not portable, and too bulky to use unobtrusively in daily life [31]. Market success would require a device which meets an user's acceptance level of cost, reliability, safety, appearance, and simplicity in ease of use and function [31], [32].

Designing an active hand orthosis for fragile patients is challenging, which explains why such a broad diversity is present between current active hand orthoses. Specific design guidelines regarding a distinct target group must be defined for each intended device [3]. Often, the wish for innovation overshadows the real needs and requirements of the user. Developing a successful product despite these conflicting interests is a real challenge [33]. The design of exoskeleton devices involves a process in which trade-offs must be made constantly through weighting factors upon the specific application and previous experience of the design team [3].

Active hand orthoses for SCI and stroke patients have been researched in abundance. In contrast, the only existing devices to support the hand function of people with DMD are static hand splints [34]. The Symbihand has been developed especially for DMD patients, and opposed to many other studies, this development process has included a DMD patient in a case study for validation of the design [7], [8]. The design of the Symbihand showed promising results and is therefore taken as a starting point for my thesis.

3. THE SYMBIHAND

In 2019 Bos and Nizamis developed a hand orthosis for DMD patients, the Symbihand [7], [8]. Efforts were put towards the physical design as well as towards the control of the Symbihand. Intentions were to carefully design a hand orthosis to accommodate the disabled hand, while addressing the specific needs of the DMD patient [7]. The Symbihand is actuated by an electric motor and uses miniature hydraulics to transfer mechanical work to the four finger digits. As illustrated in Figure 1(a), the orthosis is an under-actuated system where 1 master cylinder controls 8 slave cylinders. The system results in simultaneous bidirectional control of the metacarpophalangeal (MCP) and the proximal interphalangeal (PIP) joints of the fingers. This is facilitated by active protraction with hydraulic cylinders and passive retraction with return springs. Within the custom made piston-cylinders water is used as a medium substance. The orthosis works in close interaction with a human operator, and so the medium should not cause damage to the skin or stain on fabric in case of any leakage, hence no oil can be used. Water has an increased mass compared to gas, but also, has a better energy density and results in a better transparency of the system due to its incompressible nature. Each finger module is connected to an electrically operated valve so that grasp posture can be controlled. The thumb and wrist are splinted in a fixed position so that flexion of the fingers is allowed to result in a 3-jaw chuck grip (thumb between the index and middle finger).

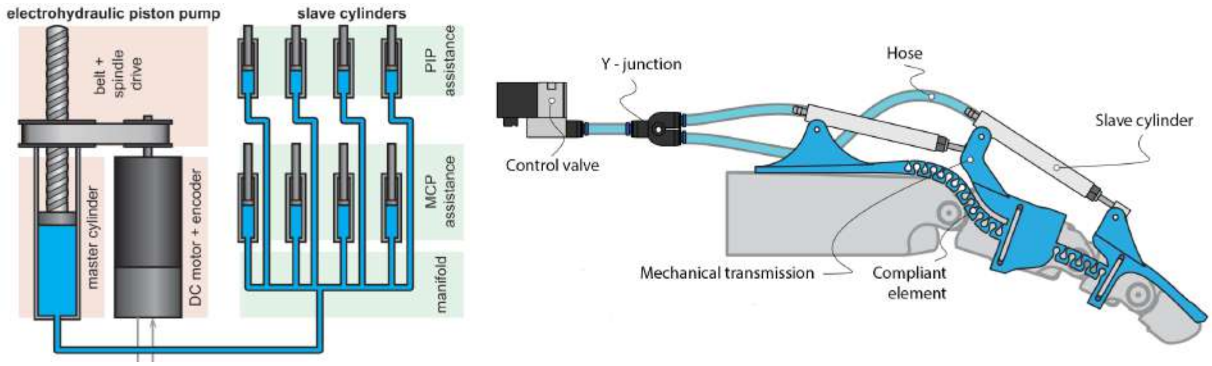

FIGURE 1. Design of the Symbihand. 1(a) Schematic of the hydraulic system, where one master cylinder under-actuates several slave cylinders. Each finger is equipped with two slave cylinders. 1(b) Components of a single finger module. [7].

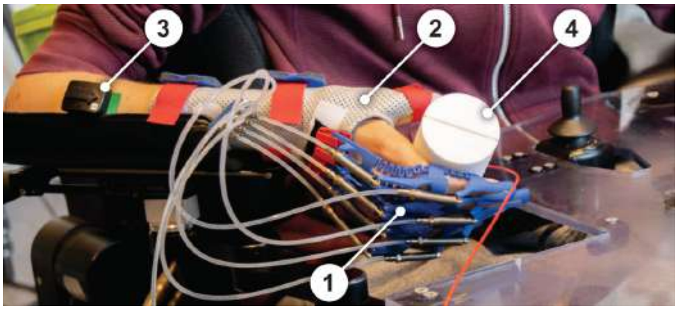

FIGURE 2. Prototype used for case study of the Symbihand with a DMD patient, valves for separate finger control were removed for easier control. Components; [1] Finger modules, [2] Wrist-Thumb splint, [4] Sensorized object for force measurements, [3] sEMG module.

Figure 1(b) and Figure 2 indicate the components of the Symbihand. The finger modules include a compliant mechanism that is meant to absorb shear forces and minimise added stiffness. These compliant structures are manufactured by selective laser sintering (SLS) of Poly-Amide (nylon-PA) flexure elements. Due to the open structures, the modules allow tactile feedback via the users' fingers. By these means, DMD patients are enabled with their natural sensation, which remains intact during disease progression. Operation becomes more straightforward when their own feedback system is employed. The developed control system of the orthosis utilises direct sEMG control based on a 1st order admittance model [8], [35]. This control unit provides verified robust and intuitive control, that the patient adapted to within 10 minutes [7].

A case study of force tracking tasks with one singular DMD patient was performed using the prototype in Figure 2. Electronic control valves were removed from the system for control simplification by allowing direct sEMG control. The fingers were therefore only capable of initiated synergistic flexion motion and passive retraction if no stimulus was applied. Obtained results were promising, increasing hand force from 2.4 to 8 [N]; reduced muscular activation with more than 40 [%]; simple and intuitive control; low pressures in the hydraulic system of <1.5 [MPa]; a fit within a 15 [mm] boundary of the hand and effective self-alignment through the flexure elements.

Experimental results also issued points for improvement. First of all, capabilities of the orthosis were more extensive than the level of assistive forces deemed comfortable by the user. Forces increased from 2.4 to 8 [N], whereas the assistance could possibly be 23 [N] and requiring only 35 [%] of the pump capacity. Although 8 [N] is sufficient for some ADL activities, ideally tolerance should be improved so the range of activities can be expanded. Further optimization of the device by miniaturisation and improvement of comfort is required. An idea to improve comfort is by changing interface materials and by changing the method for donning and doffing of the individual components. During the tests the participant complained of skin irritation due to rough and ragged edges of the 3D printed and polished finger module. Donning and doffing of the orthosis was indicated as uncomfortable as well. Donning discomforts originated from chafing of the modules over the fingers and the cumbersome donning of the wrist-thumb splint due to its tight fit. Lastly, the static position of the wrist-thumb splint to enable a 3-jaw chuck grip was considered an awkward resting position for the thumb. That whilst the thumb is of essential value for the versatility of the hand. Enabling thumb movement would add the key pinch to the executable grasp taxonomy from precision pinch and cylindrical grip. These three grasps are identified as the smallest grasp set with the largest grasp span [36], [37].

It should be noted that the results were obtained through a case study, and so, it is unsure to what extent results can be generalized over the entire DMD patient population. Nevertheless, in Table 1 insights for further experimentation with and development of the Symbihand design are reported. In this thesis, focus will be on the development of a thumb mechanism specifically.

TABLE 1. Possibilities for further experimenting with and development of the Symbihand.

Experimentation	Testing with more participants to evaluate generalization of the results
	Evaluation of the effect of passive wrist support on muscular activation during functional hand use
	Test with other disease pathologies to evaluate extension of the user group
	Evaluate functionality during ADL Activities instead of force tracking tasks
	Analysis on force steadiness and smoothness
	Develop an intervention to address the hand function of DMD patients
	Evaluate the change in force assistance tolerance and acceptation over time
Development & Optimization	Further mass reduction and/or redistribution
	Further miniaturization
	Further improvement of comfort - Contact interface & Donning and doffing mechanism
	Increase portability
	Thumb mechanism for switching between resting and functional position

4. THESIS OUTLINE

Patients who suffer from Duchenne Muscular Dystrophy, have to live with hand impairments for over 15 years. This significantly influences their ability to live independently. Currently, static splinting interspersed with stretching of the hand is the course of treatment for this patient group and developed active hand orthoses focus mainly on stroke and SCI patients.
The Symbihand was developed by R. Bos and K. Nizamis in 2019 [7], [8]. The active hand orthosis is especially designed to assist DMD patients in ADL. Control is intuitive, the self-aligning mechanism prevents inaccurate joint alignment during flexion and the hydraulic finger modules are forceful and can achieve proper ROM. One of the limitations of the device is that the thumb is restricted to an awkward position in order to facilitate grasping abilities. That while, the thumb is of substantial influence on the versatility of the hand and actuation of this digit could be of additional value for functionality by adding the possibility of the key pinch [38]. This thesis describes the design and evaluation of a thumb module for the Symbihand with the aim to release the awkward static position of the splinted thumb. In order to add a thumb module to the system, preservation of the hydraulic actuation and the self-aligning mechanism is imperative.

The design scope of the thumb module becomes as follows: "The design of a hydraulic thumb module for the Symbihand, with the focus on functional assistance of DMD patients who have limited hand function and are wheelchair confined." This can be achieved by assisting the hand in the ROM and force needed for the precision pinch, lateral pinch and cylindrical pinch. It should be taken into account that the addition of a thumb module might complicate control, so added function and diminished ease of control must be in balance [39].

Included in this thesis is a design paper about the thumb module (Section II), a literature study on the fixture design of hand orthoses for DMD patients (Section III) and additional explanations of design choices and requirements in the Appendix.

2.

Scientific Paper

Design of a hydraulic thumb orthosis for Duchenne Muscular Dystrophy patients

P. DE GROOT, Delft Institute of Prosthetics and Orthotics
Delft University of Technology, Faculty of Mechanical, Maritime and Materials Engineering Department of BioMechanical Engineering, The Netherlands

ABSTRACT **INTRO:** Of every 5000 male births, one boy is born with Duchenne Muscular Dystrophy. This disease is marked by progressive muscle deterioration and weakness. Duchenne patients have to live with impaired hand function for more than 15 years, even though the hands are essential tools for autonomy. **GOAL:** To assist the hand in ADL and active hand orthosis was developed in 2019, the Symbihand. In this paper an active thumb module was developed to replace the uncomfortable static splinted thumb of the Symbihand. In ADL the precision pinch, lateral grasp, and cylindrical grip are grasp that can facilitate the broadest grasp span. Hence, the thumb should assist the movement from 0-90 [deg] in the transverse plane and generate a minimum pinch force of 10 [N] to enact these grasps successfully. **RESULTS:** The thumb module prototype is a 3D printed shell structure incorporated with three compliant elements, actuated by one miniature piston-cylinder filled with water. Although the resulting design is lightweight with its 61 [gr], slim with a protrusion of 22 [mm], and allows for cutaneous feedback with its open palmed shell and dorsal actuation, it can not yet meet the force and range of motion requirements for ADL. A pressure of 4 [MPa] was applied to the system, resulting in a pinch force of 2.8 [N] and a ROM of about 75 [%] of the set necessary reach. **CONCLUSION:** The current prototype does not meet the force and range of motion requirements. For improving the system, the compliant elements should be redesigned or replaced, geometric relations should be re-evaluated and the cylinder attachment points should be reshaped.

INDEX TERMS Duchenne Muscular Dystrophy, Active hand orthosis, Thumb module, Miniature hydraulics

1. INTRODUCTION

DUCHENNE Muscular Dystrophy (DMD) is a hereditary X-linked recessive disorder and is, with an incidence of 1:5000 male live births, the most common form of muscular dystrophy in children [13]. Muscle cells of people with Duchenne are highly vulnerable to cell damage, due to an absence or deficiency in the dystrophin protein. As muscle cells are replaced with fat and connective tissue, the disease is characterized by progressive muscle wasting and weakness [10], [21]. Weakness progresses more or less symmetrically from proximal muscle groups to distal muscle groups but affects extensor groups more than flexor muscle groups [40]–[42]. In addition to muscular weakness, joint contractures develop, which can be attributed to limb disuse and the concomitant fibrosis and proliferation of connective tissue [22], [43]. Although Duchenne is present from birth, it is often not diagnosed until the age of 5 [14]. Up to this point, there is no cure for DMD and treatment is mainly aimed at delaying disease progression and preserving functional abilities [44]. As a result of disease retarding treatments, the median survival in DMD boys has risen from 14 in the 1960s to above 30 years since the 2000s [44]. Dysfunction of the lower extremities begets complete wheelchair confinement by the age of 10. Around this age functional limitations of the upper extremities (UE) start to present as well, even though, studies report a decline in UE strength already before this age [42], [45]–[47]. Functional limitations of the lower limbs can be compensated fairly well by wheelchair usage. Oppositely, loss of UE function is much harder to compensate [16]. A decline of hand function initiates around the age of 15 [45], [46], [48]. Considering the current life expectancy, DMD patients are confined to a wheelchair and have to live with impaired hand function for more than 15 years [16].
Humans interact with their environments largely by the use of their hands. So, if left unsupported, the performance of activities of daily living (ADL) and so independence is impeded and social participation is restricted. Hereby quality of life (QOL) is negatively impacted significantly [6]. Following Jones and Lederman (2006), the main categories for hand functioning are tactile sensing, proprioceptive sensing, prehension, and non-prehensile skilled movements. People with DMD experience problems with their prehension and non-prehensile skilled movements but their tactile and proprioceptive senses remain intact [49]–[51]. Current treatment options that have been shown to prolong functionality consist of physical exercises, stretching and the use of splints and arm support [43], [52], [53]. During mild weakness, splints provide enough support. However, as soon as severe weakness is experienced, active support is needed. Such active interventions would be applicable to patients with a Brooke scale grade of 4, 5, or 6, which indicate the stages in the non-ambulatory phase at which the fingers start to dysfunction [16], [54]. Thus, there is a need for interventions that compensate for the loss of hand function. One solution,

can be dynamic hand supports that reduce the effort needed to perform functional activities with the hands and counteract disuse [24]. With the aim to provide Duchenne patients with more autonomy, a portable dynamic hand orthosis has been developed by R. Bos and K. Nizamis (2019). The Symbihand, shown in Figure 15(d), is able to generate movements of the fingers opposed to a static splinted thumb. The design is based on a hydraulic transmission, flexible structures and a self-adaptive grasp, with a high energy density and transparent force transmission. Hydraulic components were customised to fit into a low-profile mechanism while still providing sufficient pressure resilience. Additionally, a custom hydraulic piston pump has been developed to provide the required hydraulic pressure. A case study showed improved grip force from 2.4 to 8 [N], with a pressure limitation set at 1.5 [MPa] of the 5 [MPa] piston pump. One of the drawbacks reported in this case study, is the thumb's uncomfortable static position, needed to enable a 3-jaw chuck grip [7], [8]. Besides the discomfort, also the movable thumb is the main determining factor of the versatility of the hand. Assistance of the thumb will allow for performance of the lateral pinch in addition to the the power grip and precision pinch, hereby expanding the range of tasks that can be performed [36], [37].

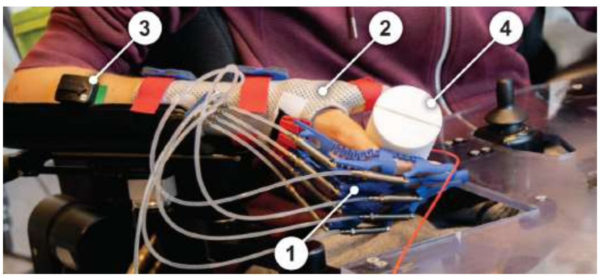

(a) The Symbihand prototype as used in the case study. 1) Custom miniature hydraulic cylinders, 2) Static splinted wrist & thumb, 3) sEMG sensor, 4) Sensorised object to measure grip force.

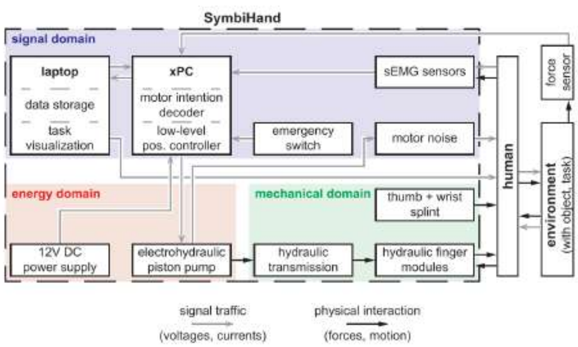

(b) Overview of the Symbihand system and control

FIGURE 3. The Symbihand design: an hydraulically actuated assistive hand orthosis for DMD patients. The prototype consists of 8 miniature piston-cylinders filled with water that move the fingers towards a static splinted thumb when pressure is applied. Pressure is applied by 1 electro-hydraulic piston-pump and controlled by sEMG on the forearm muscles [7], [8].

OUTLINE

The goal of this study is to develop a hydraulic thumb module for the Symbihand that releases the awkward resting position in the current static splint. The design focuses on patients with Brooke scale grades of 4, 5, or 6 and is meant to assist in ADL. Assistance of ADL can be accomplished by facilitating the ROM needed for the precision pinch, lateral pinch, and cylindrical pinch. It is beyond the scope of this study to design the control mechanism of the thumb module. The thumb module was developed by following the design process and tools described in the Delft Design Guide [55]. Based on the user case study performed by Bos et al. [7] and literature searches into current hand orthoses, Duchenne Muscular Dystrophy and grasping, a set of requirements was constructed. These are established in Section 2. Requirements. Utilising the Fish-model, ideas were generated and evaluated for separate elements of the orthoses, after which they were brought together into one concept design, which is presented in Section 3. Thumb module design. This concept has been tested using a custom build test set-up. Of which the results provided new insights into further development of the thumb module. The experimental set-up is outlined in Section 4. Experiment Design, of which the results are described in Section 5. Results and discussed in Section 6. Discussion. Finally, conclusions are drawn in Section 7. Conclusion.

2. REQUIREMENTS

The addition of an active thumb module to the Symbihand is meant to increase the functional autonomy of the DMD patient. It was deducted from literature that when designing for Duchenne patients the following characteristics of DMD should be considered; reduced skin integrity, bilateral symptoms, muscular stiffness and weakness, hand deformities, and high variability between and within patients (Section III). To accomplish acceptance of the device by the patients, the mentioned characteristics should be accounted for.

2.A) GRASPING

The thumb is used in almost 90 [%] of the grasping executions and endures half of the workload of the prehensile hand [1], [56]. To expand functionalities, the thumb module should assist the precision, lateral, and cylindrical grip. This is believed to be a small, versatile grasp set to accommodate the largest grasp span [37], [57]. Precision pinches should be able to achieve values of >10 [N], lateral pinches >10.4 [N], and cylindrical grips >20.6 [N] [58], [59]. With these forces, most of the ADL activities can be performed. Minimal hand opening should be 10 [cm] for the achievement of a successful pre-grasping position [60]. Bidirectional support must be applied, as both flexion and extension are affected in DMD. During assistance of the fingers, only normal forces contribute to grasping forces. Shear forces, on the contrary, can cause skin damage and should be avoided [7]. The joints of the thumb and index finger are indicated in Figure 4, together with their global and local axes. By regard of hand synergies, added function can be achieved by merely assist-

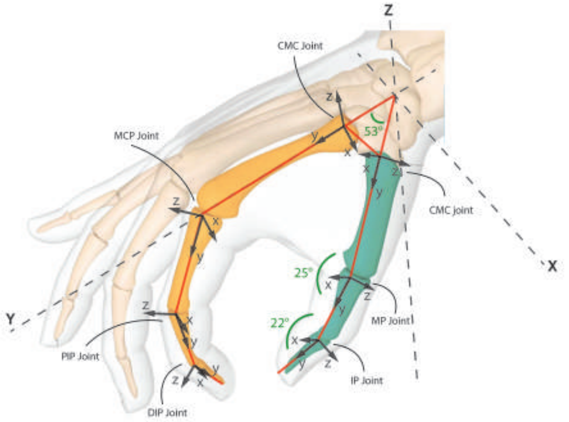

FIGURE 4. Anatomy of the thumb and index finger. Including joint names, their local axes, and the chosen splinting angles of the MP and IP joints of the thumb.

TABLE 2. Design Requirements for dynamic hand orthosis for DMD patients.

Specification		Value	Unit
CMC joint	FE Transverse plane	0 - 90	[deg]
Forces exerted on the hand	Perpendicular	<5	[N]
	Shear	0	[N]
Forces exerted by the hand	Precision pinch	10	[N]
	Lateral pinch	10.4	[N]
	Cylindrical grip	20.6	[N]
Hand opening width		10	[cm]
Mass	Thumb without wrist splint	<50	[gr]
	Total orthosis	<250	[gr]
Cycle time		2	[Hz]
Actuation	Maximal pressure	5	[MPa]
	Hydraulic cylinder with water		
	Bi-directional		
	Placed dorsally		
Portability	Transportable by powered wheelchair		
Control	Allow cutaneous feedback		
Environmental compatibility			
Comfortable and easy donning & doffing			

ing the carpometacarpal (CMC) joint and splinting of the metacarpophalangeal (MP) and interphalangeal (IP) joints [61]. The thumb must be able to move from the resting position to the grasping position, by moving around the CMC joint from 0-90 [deg] in the transverse plane (Figure 4 XZ-plane). Splinting of the MP and IP joints should be in an arched manner at 22 [deg] MP and 25 [deg] IP flexion. Maximal movement of the non-splinted joints can be achieved by splinting the wrist at 35 [deg] dorsal extension and 5 [deg] ulnar deviation [62], [63].

2.B) TRANSPARENT FEEDBACK

Even though control is beyond the design scope, here the topic is raised. This is because some aspects of control, such as allowing tactile feedback, are of great importance and affect the design requirements. As boys with DMD experience bi-lateral symptoms, control of the device must be completely hands-free. The control of the thumb must be separate from the other digits, in order to permit the execution of the identified grasp types. The user should be an integrated part of the control loop. Duchenne patients have intact proprioceptive and tactile capabilities, therefore an open structure must be adopted that allows for tactile feedback. Cutaneous feedback is of significant importance for determining the grip safety margin to apply to the grip force. The safety margin is a function of frictional properties at initial contact and phasic slip-detection [64]. The utilisation of the natural feedback of the DMD patient results in transparent and reliable feedback. It gives the user a feeling of ownership as they can control the applied safety margins themselves. It was indicated by Nizamis et al. (2019), that patients can process signals and respond successfully to signals when the cycle time of the finger movements is no faster than 2 [Hz] [65].

2.C) USAGE IN DAILY LIFE

In case the hand orthosis functions properly, the user shall start to rely on the device's functioning. For this reason, the device should be durable and not break easily. If this unfortunately happens, repair should need low effort. Parts should be replaceable, and maintenance should be easy. As the orthosis is used for assistive purposes, portability is a must. For the disease phase decided on, portability means that a powered wheelchair can transport the complete assistive device. During the day, different environments and tasks shall be encountered. Accordingly, the device must be able to withstand water and dirt and be easily cleanable. The smell must be neutral, noise emission must be kept as low as possible, and the device's exterior must be of low encumbrance. The weight limit for the thumb module without the hydraulic system and the wrist splint is set to 50 [gr], as this is also adopted for the finger modules. The whole orthosis including the hydraulic actuation carried by the hand, all finger modules, the wrist splint and the thumb module should have equivalent weight to the current orthosis of 250 [gr]. Reduced weight and proper mass distribution is beneficial, and the centre of mass should preferably be placed further away from the extremities.

3. THUMB MODULE DESIGN

3.A) ACTUATION

The Symbihand is actuated by 8 custom made hydraulic piston-cylinders. As the thumb module is an addition to the finger modules, actuation shall be facilitated by a hydraulic system as well.

Hydraulic Systems

Hydraulic systems can transport mechanical work through flexible hoses using a working medium. Compared to other actuation systems, hydraulics offer several advantages:

1) As long as miniaturisation is accompanied by an increase in system pressure hydraulic systems have a low effective mass (high stiffness with low mass) and can be more compact and lightweight than an electro-magnetic equivalent [66]–[68].
2) Contrary to pneumatics, where compressible gases are used, hydraulics generally use an incompressible fluid

as medium. Due to the incompressible nature, hydraulic systems are more energy efficient, more accurate, have higher load holding capacities, and allow for a very transparent force transmission [7], [68].
3) The hydraulic system is more flexible to install than Bowden cable systems, as efficiency is independent of hose curvature (low friction), and stiffness is high [68], [69].
4) With hydraulic systems, you can potentially transfer, amplify, and distribute forces and movements inside one system [7].

When implementing a hydraulic system into a design, risk of leakage, strict dimension tolerances, and sealing friction should be taken into account [7], [69]. Various actuators can be used for hydraulic transmission. Elastic hydraulic actuation mechanisms comprise at least one component that deforms elastically under applied pressure. They are uncomplicated to down-scale, yet, they have low force capacity, offer less transparent feedback, have limited stroke length, and are more prone to leakage or failure than inelastic mechanisms [7], [72], [73]. Artificial muscles have a higher force capacity, but, exert pulling instead of pushing forces as they work using contraction. These contraction forces have to be converted to pushing forces on the limb, leading to higher encumbrance and weight due to the added components [72]. Inelastic hydraulic actuators can provide large strokes in small volumes and have high force capacity and stiffness. The miniaturisation of these components is limited by complexity and friction [7]. A new development in piston-cylinder actuation is the application of 3D printing for possible cylinder weight reduction [74]–[76]. However, calculations showed that in this case no weight reduction would be expected at a miniature scale due to limitations of wall thickness in the 3D printing process. In this design, a miniaturised hydraulic cylinder with O-ring sealing developed by Bos (2019) was used [7]. By controlling a master cylinder, fluid is pressed into the hose. Hereby, pressure in the systems increases and the slave cylinder starts to apply a force around the thumb joint.

The piston-cylinder

The piston-cylinder by Bos (2019) has a bore diameter of 4 [mm], a stroke length of 30 [mm] and can withstand pressures up to 5 [MPa]. Figure 5 shows the working principle of the piston-cylinder mechanism for flexion of the four finger digits. The range of motion (ROM) of the finger joints (θ) can be presented in 2D, contrarily, thumb motions are hardly planar [71]. Still, thumb circumduction around the CMC joint with a straight thumb could be described as a conical movement, as illustrated in Figure 6 [70], [71]. By placing proximal connection A on the hand's dorsal side and

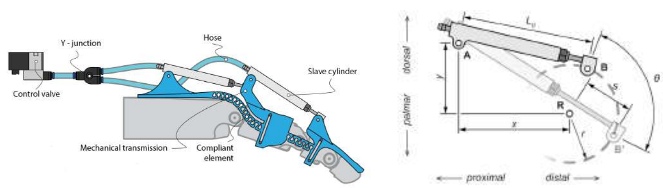

(a) (b)

FIGURE 5. 5(a) Design of the Symihan finger module. 5(b) Illustration showing the relation between the slave actuator's stroke (s), initial length (L0), and placement of the proximal connection (x, y) with the moment arm (r) and resulting joint range of motion (θ) around the finger joint (R). [7]

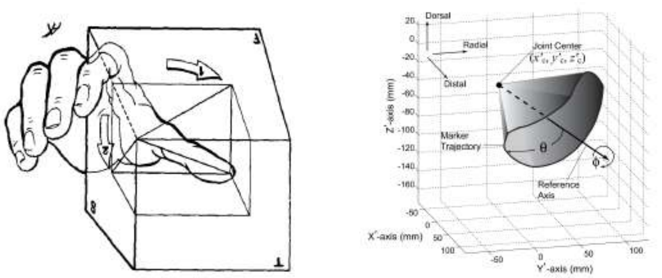

(a) (b)

FIGURE 6. 6(a) thumb motion according to the anatomists' method. Flexion angle 1 and abduction angle 2 are indicated and are in relation to the three classic reference planes: (F) frontal, (S) sagittal and (T) transverse [70]. 6(b) A representative cone circumscribed by the thumb tip marker trajectory in the X-Y-Z local coordinate system, where the joint center indicates the CMC joint of the thumb [71]

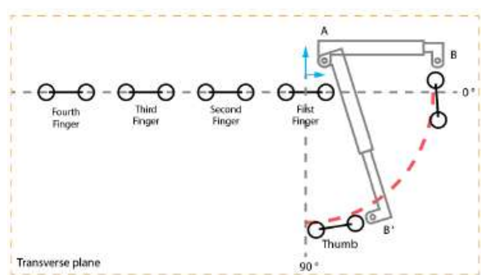

(a) AB represents the unactuated cylinder and AB' the actuated cylinder in the transverse plane.

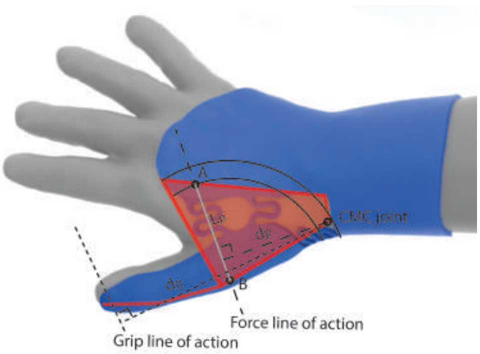

(b) d_p is the moment arm of the piston cylinder, d_g is the moment arm of the grasping force and L_p is the unactuated piston length.

FIGURE 7. Piston cylinder positioning. 7(a) Placement of the cylinder in the transverse plane. Minimal protrusion should lead to maximal ROM. 7(b) Placement of the cylinder in the frontal plane. Find the largest moment arm within the selected area.

distal connection B on the thumb's dorsal side, the orthosis generates a moment around the CMC joint to move the thumb in the transverse plane (FE 0-90 [deg]). Positioning of the piston-cylinder in the transverse plane is shown in Figure 7(a). When determining the placement of the cylinder, the cylinder should be aligned with the circumduction plane to minimise shear forces. When looking at Figure 7(b), connection B must be as distal as possible without crossing the imaginary line between the index's MCP and the thumbs MP joint. B can also not be placed further than the thumbs MP joint, to avoid MP flexion. Furthermore, the moment arm must be as large as possible within these region limits, and connection A must be placed medially to create the largest ROM without protruding.

O-ring friction

In miniature hydraulics, surface effects such as friction drag of seals and viscous drag of gaps become significant at small bores and impact overall efficiency [67]. Stronger seals introduce more friction, whilst weaker seals introduce more leakage. O-ring contact seals are implemented in the custom cylinder for their high attainable fluid pressures, low leakage rates, and ease of miniaturisation [7]. Following the method of Martini (1984) and Plettenburg (2002) the O-ring friction for the custom made cylinder was calculated. The total friction loss ratio should be <0.33, so that the differential pressure is able to overcome the maximum break-out force of 3x the running friction [7], [77], [78]. At application of 4 [MPa] pressure with an O-ring of Shore hardness 70A, the O-ring frictional force is estimated on 3.63 [N], which corresponds to a frictional loss of 7 [%].

Retraction Mechanism

To return the piston-cylinder to its initial position after actuation, a stainless steel tension spring with a spring rate of 0.01 [N/mm] (T40740E, Tevema Technical Supply BV, Almere, Netherlands) is used.

Medium

The inserted hydraulic fluid is water. Water has a lower viscosity than most hydraulic fluids and so is more prone to leakage. Though, in case of leakage it does not stain and is not harmful to the skin. Water has already been used in other miniature hydraulic systems [7], [79]. Therefore, water is a suitable medium for this application.

Tubing

The master cylinder is connected to the pressure transducer and the pressure transducer to the slave cylinder by the use of a hose. In general more flexible hoses have lower radial stiffness, but they also have more radial expansion compared to more rigid hoses. Expansion adds hysteresis to the system. At higher applied pressures more expansion shall occur and radial stiffness becomes more important. The hose is a <Ø3 [mm] semi-rigid PA tubing material (Legris 1025P03 00 18, Parker Hannifin Corporation, Cleveland, OH, USA), so the tubing is somewhat flexible with a bending radius of 6 [mm], whilst still being energy efficient. Losses in efficiency due to tubing are related to wall friction and small friction coefficients due to smooth bends [7], [80]. These were assumed negligible compared to O-ring friction in the actuators.

3.B) ORTHOTIC DESIGN

In pursuance of an anthropometrically fitting design, a 3D scan of the hand was made. Onto this scan, a shell structure was created by CAD modelling in SolidWorks. This shell consists of a part for wrist fixation, a part for fixation of the MP and IP joints and compliant elements connecting the thumb to the wrist. This shell was 3D printed by the process of SLS printing with Oceanz Nylon PA12 material [81]. Figure 10 shows a picture of one of the prototypes.

Fixture

The 3D printed shell structure is connected to the hand by the use of two velcro straps. One enwinds the proximal phalanx of the thumb fastening the thumb splint. The other enwinds the wrist, thereby fixating the wrist in position.

Compliant Elements

For prototyping, three structures have been realized in the CAD model for 3D printing. Structure 1 is the flexure element, as implemented in the Symbihand [7]. Performance of this structure is good in terms of bending; however, does not allow stretch. This structure was reverse engineered and used as a reference structure. Structure 2 has a similar shape to structure 1, but with an increased height from 6 to 10 [mm]. This structure should allow for some more displacement, with similarly experienced stresses according to FEM simulations. Structure type 3 consists of a more rounded shape with a height of 15 [mm]. Here, more displacement should be allowed, whilst maintaining the stresses and strains within acceptable limits. However, whether or not the structure is too flexible for opposing the shear forces remains the question. The three structure types are indicated in Figure 8.

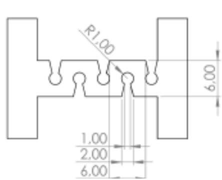

(a) Structure 1

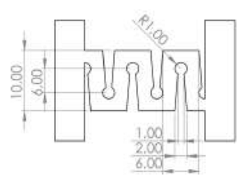

(b) Structure 2

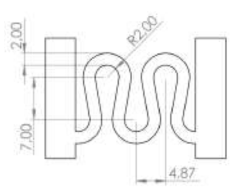

(c) Structure 3

FIGURE 8. Structure types implemented in the orthosis prototypes. 8(a) Structure 1, is the compliant element as implemented by Bos (2019). 8(b) Structure 2, is structure 2 with increased height from 6 to 10 [mm]. 8(c) Structure 3, is a rounded structure with a total height of 15 [mm].

Piston Force

The force exerted by the piston cylinder (F_p) can be calculated by multiplying the actuation pressure with the piston surface area, where the bore diameter (D) is 4 [mm]. Forces exerted by the return spring (F_s) can be calculated by Hooke's Law, where the spring constant (k) is 0.01 [N/mm] and x, the extension (slave cylinder stroke), is 30 [mm]. Pinch forces (F_g) needed for ADL are 10 [N] as established in Section 2. O-ring friction (Fo) is assumed to be 3.63 [N], which is the calculated O-ring friction at 4 [MPa].

$$F_p = P \cdot \frac{\pi \cdot D^2}{4} \tag{1a}$$

$$F_s = k \cdot x \tag{1b}$$

$$F_g = 10 \tag{1c}$$

$$F_o = 3.63 \tag{1d}$$

The pressure (P) that should be applied to the system to generate enough grip force, can then be calculated by the application of the moment equilibrium:

$$\begin{aligned} F_g \cdot d_g &= (F_p - F_s - F_o) \cdot d_p \\ F_g \cdot d_g &= \left(P \cdot \frac{\pi \cdot D^2}{4} - k \cdot x - 3,63 \right) \cdot d_p \\ P &= \frac{\frac{d_g}{d_p} \cdot F_g + k \cdot x + 3,63}{\frac{1}{4} \cdot \pi \cdot D^2} \end{aligned} \tag{2}$$

The moment arm of the piston cylinder (d_p) and so also the return spring is $\sim$ 31 [mm]. This is 2.7 times smaller than the moment arm of the grip force (d_g), which is $\sim$ 84 [mm]. Pressure that should be applied to the system then results in 2.46 [MPa]. It should be noted that in these calculations, resistance of the flexure elements and joint stiffness are not included. The real applied pressures for achieving the desired 10 [N], shall therefore be higher.

4. EXPERIMENT DESIGN

Two experiments have been executed with the three developed prototypes. First, a close test was carried out to verify the the thumb module's ability to achieve a precision pinch grasp taxonomy. Secondly, a pinch test has been performed to evaluate the thumb module's grasping force.

4.A) VARIABLES

Variables that have been tested are:

Dependent variables

- Pressure [MPa]: Pressure in the hydraulic system as a result of master cylinder stroke.
- Stroke of the slave cylinder [mm]: Displacement of the slave cylinder piston, due to pressure in the hydraulic system.
- Pinch force [N]: Force exerted by the thumb after applying a pressure of 4 [MPa] with an object angle of 33 [deg] relative to the plane of motion of the index finger.

Independent variables

- Stroke of the master cylinder [mm]: Input is the displacement of the master cylinder piston. Stroke is increased until the desired pressures of 1.5, 3, or 4 [MPa] are achieved.

4.B) TESTBED

In order to evaluate the grasping function of the thumb module, a mock-up hand was developed. This mock-up hand consists of a hand base obtained from the 3D scanned hand used to create the orthosis, the index finger inserts for the two test set-ups and the movable thumb. The movable thumb is based on 3D scanned bone models [82, Pinshape.com] and connected by pin joints, as indicated in the design of the ACT Hand [83]–[86]. This hand was then attached to the test bench developed by Smit and Plettenburg (2010), which is equipped with a linear displacement sensor (LVDT: Schaevitz: LCIT 2000) and a custom pinch force sensor (Double leave spring with strain gauges) [87]. A pressure transducer with a range of 0-4 [MPa] (Gems 3500 series pressure transducer) was added to the test bench to measure the system's pressure. A master cylinder with a bore diameter of 9 [mm] was used, which increases pressure in the system by pulling the piston. An image of the test set-up is shown in Figure 9. By rotating the test bench's spindle a pulling force is put on the master cylinder, and so, the stroke of the master cylinder can be controlled. For measuring the stroke of the slave cylinder as a result of increased pressures, a digital calliper was used.

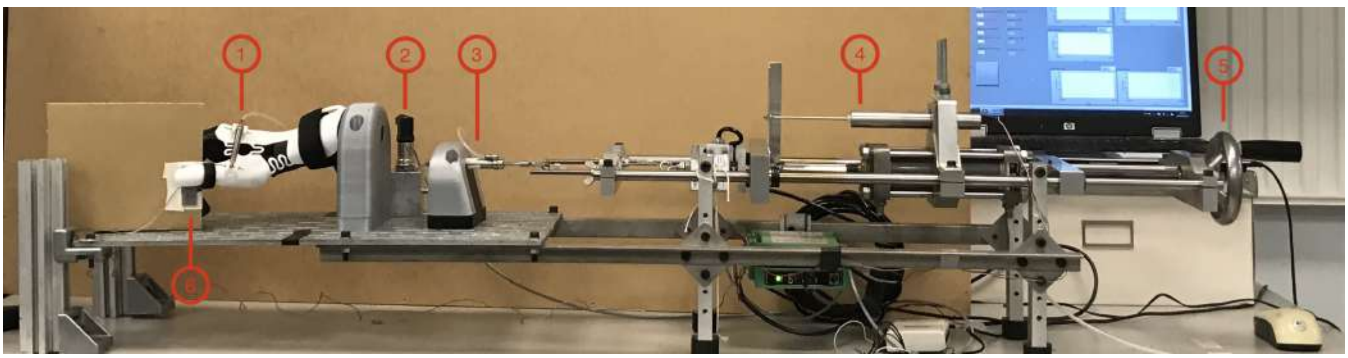

FIGURE 9. Test set up. 1) Slave cylinder, 2) Pressure transducer, 3) Master cylinder, 4) Linear displacement sensor, 5) Spindle, and 6) Pinch force cylinder.

4.C) PROTOCOL

Each test was executed for subsequent three flexure element designs resulting in 3 test repetitions.

Close test

The close test was executed to review the thumb motion as a result of the applied pressures. During each trial, pressure was applied, held for 10 [sec], and then released. Displacement of the master cylinder, pressure in the system, and stroke of the slave cylinder were measured for three different pressure values of 1.5, 3, and 4 [MPa]. Each condition was tested 3 times, resulting in a total of 9 measurements. Strokes of the slave cylinder were measured before, at the maximum, and after applying pressure. Each trial was filmed, and the thumb's position at the maximum pressure could be identified as either a successful or unsuccessful precision pinch.

Pinch test

The pinch test was performed for identifying the grasping forces that can be applied by the thumb. The pinch sensor was placed at the end-point of thumb movement after applying 4 [MPa]. Forces were then measured for the application of the maximum pressure of 4 [MPa]. Pressure was applied, held for 10 [sec], and then released. This test was repeated three times, resulting in 9 measurements.

4.D) DATA ANALYSIS

Photos taken of the thumb position at 4 [MPa], were used to identify whether or not the pinch grip was successful. In a successful precision pinch the thumb tip, meets the tip of the index finger. The grip was either indicated as successful or unsuccessful. Measured data was acquired using LabView and then imported into Matlab for analysis. Data arrays were trimmed, so that the data was analysed from the moment the displacement exceeded 0 [mm] in the close test and from the moment the force exceeded 0 [N] in the pinch test. Data was plotted for master cylinder stroke vs actuation pressure and for actuation pressure vs pinch force. Furthermore, hysteresis was calculated for the full closing-reopening cycle. Hereby, the three different flexure designs could be compared. The developed Matlab script can be found in Appendix I.

Hysteresis

Hysteresis, or energy expenditure of the system, is a measure of the efficiency of the actuation mechanism. It is defined as the difference between the amount of work required to close the device and the amount of work returned by the mechanism during reopening [87]. Hysteresis can be estimated by integrating the measured pressure over the stroke length [7], [88]. Low hysteresis indicates an energy efficient mechanism. Energy expenditure (work) can be estimated by integrating the measured pressure over the master cylinder displacement. The loading curve determines the input energy and the unloading curves the output energy [Nmm]. By substracting one from the other, the hysteresis can be calculated.

5. RESULTS

5.A) PROTOTYPE

The resulting three prototypes are 2 [mm] thick 3D printed structures. The orthosis is fixed to the hand by two velcro straps, and the hydraulic actuator is attached with two M2 nuts and bolts. The shell structures all weigh approximately 50 [gr], and the miniature actuator including 21 [cm] of hose filled with water 11 [gr]. With the assembled actuator, the system protrudes from the hand's dorsal side with 22 [mm].

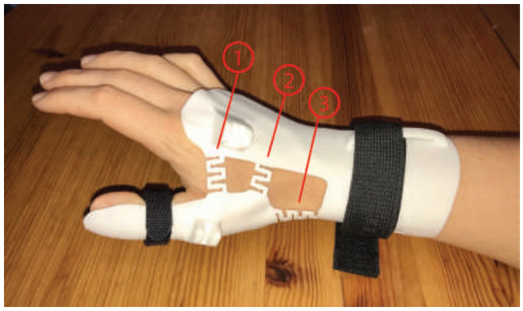

FIGURE 10. One of the three 3D printed Nylon PA12 shell structures of the orthoses, without the hydraulic cylinder and fixated to the hand by one wrist and one thumb strap. Compliant elements are numbered in red. The two protruding parts are for assembling the piston-cylinder.

(a) Structure 1: sagittal view.

(b) Structure 2: sagittal view.

(c) Structure 2: frontal view

(d) Structure 3: sagittal view.

(e) Structure 3: frontal view.

(f) Structure 3, 1 element: sagittal view.

(g) Structure 3, 1 element: frontal view.

FIGURE 11. Close test results. Thumb position at 4 [MPa] with structure 1, 2, and 3, and at 2.2 [MPa] with only 1 compliant element.

5.B) CLOSE TEST

Slave cylinder stroke

Table 3 presents the mean stroke lengths of the three trials before, during, and after applying 1.5, 3, and 4 [MPa] of pressure. As can be seen from this table, structure 3 has larger slave cylinder stroke lengths at similar pressures than structure 1 and 2. As can be seen in the same table, none of the structures returns to its initial stroke length after the pressure is removed.

TABLE 3. Slave cylinder stroke lengths, before after and during applied pressures. Maximum stroke of the cylinder is 30 [mm]

	Before	Pressure	After	Difference
	1.5 [MPa]			
Structure 1	6.60 ± 0.26	11.73 ± 0.06	8.28 ± 0.26	1.67 ± 0.02
Structure 2	7.74 ± 0.12	11.93 ± 0.07	8.22 ± 0.18	2.37 ± 0.58
Structure 3	6.71 ± 0.16	15.96 ± 0.17	8.15 ± 0.08	2.88 ± 0.16
	3 [MPa]			
Structure 1	6.33 ± 0.33	14.31 ± 0.21	8.70 ± 0.25	0.56 ± 0.24
Structure 2	7.51 ± 0.11	14.67 ± 0.09	8.55 ± 0.04	1.04 ± 0.15
Structure 3	6.53 +- 0.12	21.93 ± 0.62	9.03 ± 0.17	1.35 ± 0.18
	4 [MPa]			
Structure 1	6.05 ± 0.17	15.81 ± 0.10	6.65 ± 0.11	1.43 ± 0.24
Structure 2	7.66 ± 0.16	16.88 ± 0.34	8.93 ± 0.05	2.50 ± 0.06
Structure 3	6.97 ± 0.25	26.70 ± 2.22	12.13 ± 1.16	5.31 ± 0.94

Thumb position at 40 [MPa]

Figure 11 shows the end-point positions of the thumb at an actuation pressure of 4 [MPa]. Figures 11(c) and 11(e) show that none of the prototypes reach the plane of motion of the index finger. Figure 11(a), 11(b) and 11(d) show that structure 1 and 2 reach to about 50 [%] of the distance needed to reach the thumb tip. Structure 3 can reach further to about 75 [%] of the needed distance. After the assessment of the prototypes, 2/3 of the flexure elements of structure 1 and 2/3 of the flexure elements of structure 3 were broken. Structure 2 showed no signs of failure.

5.C) PINCH TEST

Forces exerted by the thumb on a gripping plane were measured with the pinch test. Figure 13 shows the exerted forces against the actuation pressure. Maximum measured forces are 2.8 ± 0.17 [N] for structure 1, 2.69 ± 0.21 [N] for structure 2, 1.32 ± 0 [N] for structure 3 at 3 [MPa], and 0.58 ± 0.58 [N] for structure 3 at 4 [MPa]. It should be noted that during the force measurement of structure 3 at 4 [MPa], the flexure elements had already failed.

5.D) HYSTERESIS

Hysteresis was calculated by subtracting the amount of work returned when the pressure is removed from the amount of work needed for the thumb movement. Energy loss in the system for structure 1 is 144.32 ± 11.25 [Nmm], for structure 2 is 90.55 ± 15.80 [Nmm], and for structure 3 is 207.84 ± 13.47 [Nmm]. Relative to the input energy, these are percentual energy losses of respectively 52.40, 65.46, and 51.73 [%].

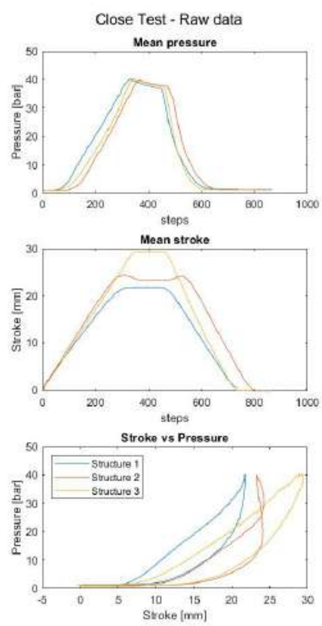

FIGURE 12. Measurements from the Close test for structure 1 (blue), structure 2 (red), and structure 3 (yellow) for an applied pressure of 4 [MPa]. Upper: pressure measurements, middle: master cylinder stroke measurements, lower: pressure as a result of master cylinder stroke.

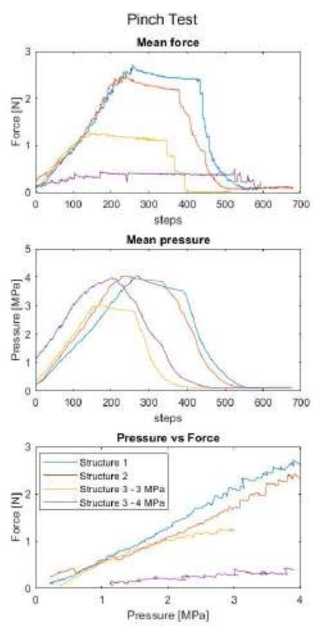

FIGURE 13. Measurements from the Pinch test for structure 1 (blue), structure 2 (red), and structure 3 at 3 [MPa] (yellow) and 4 [MPa] (purple). Upper: force measurements, middle: pressure measurements, lower: force as a result of actuation pressure.

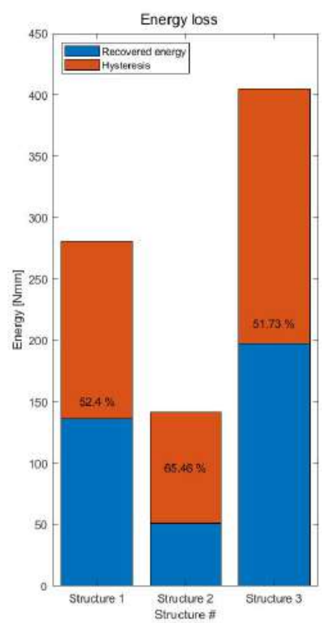

FIGURE 14. Calculated energy values for each tested structure. The total height of the bar indicates the energy put into the system when applying 4 [MPa] of pressure. The red part of the bar indicates the amount of energy not returned to the system after the pressure is back to 0.1 [MPa]. The percentages indicate how much energy is lost relative to the input energy.

5.E) TRIAL ON A HEALTHY HAND

Trials with structure 2 did not result in a different ROM than with the testbed hand. The applied forces were not experienced as uncomfortable to the healthy hand and no pinch points were appointed. Despite the two fixating straps, the orthosis showed a tendency to rotate around the wrist during pressure application.

5.F) TRIAL WITHOUT FLEXURE ELEMENT 1 & 2

A trial without flexure element 1 and 2 of structure 1, resulted in solely an abduction-adduction (AA) motion of the thumb. No rotation towards the index finger was present. The stroke limit was reached at an applied pressure around 2.2 [MPa]. The position of the thumb at maximal stroke length is shown in Figure 11(f) & 11(g).

6. DISCUSSION AND FURTHER RECOMMENDATIONS

6.A) DESIGN IN GENERAL

Weight

The prototype weighs 61 [gr] including the wrist splint and the filled hydraulic actuator. The requirement of 50 [gr] for the thumb module, excluding the wrist splint, is hereby met. After adding the weight of the 4 finger modules of the Symbihand, the total orthosis shall weigh 204 [gr] [7]. This weight is about 45 [%] of the adult male hand weight and is lighter than the Symbihand prototype with a splinted thumb of 250 [gr] [92], [93]. This is also lighter than the thumb modules found in literature which are indicated in Figure 15. Aubin (2013) [89] developed an orthosis of 230 [gr] to assist the thumb of paraplegic children, Cempini (2015) [90] an orthosis of 438 [gr] to assist the thumb and index finger, and Lambercy (2013) [91] adds 126 [gr] to the hand to assist merely thumb motion. Although the thumb module is well in weight compared to the other designs, it is still an extra half hand of weight the user has to carry around. Adding weight to the body is tiresome, and so, lighter systems are advantageous.

Encumbrance

Regarding the system's encumbrance, the design can be seen as a relatively 'flat' design. The module protrudes from the hand with 22 [mm], which is smaller than the 30 [mm] protrusion of the HX developed by Cempini (2015), and the 33 [mm] protrusion of the Symbihand finger modules. A comparison with Aubin (2013) and Lambercy (2013) can only be made from Figure 15. Nevertheless, it can be observed that the thumb module design is less cumbersome.

3D printed orthosis shell

The shell structure was modelled on a 3D scan of a hand. This modelling technique resulted in a proper fit to the scanned hand that is fastened to the user's hand with only one thumb and one wrist strap. Donning and doffing of the device is of low effort and the thumb tip and the hand palm are open for tactile feedback. Still, the current shell design must be reformed:

- The orthosis can only fit one user and is not a parametric design that can quickly be adjusted.
- The orthosis tends to rotate around the wrist when pressure is applied and does not keep its position.
- The shell is not stiff enough and endures deformation, hereby not maintaining attachment A in position.
- Despite the open palm structure, the shell is completely closed and could cause sweat problems. This problem is well known for the designs of prosthetic sockets [94].

The rotation around the wrist could resolve itself when the finger modules are combined with the thumb module. If not, the rotation around the wrist needs to be counteracted, conjointly with the deformation of the shell structure. This can be realised in two manners; first, by optimising the orthosis shell and piston attachments, regarding shape, thickness, and material, so that forces are exerted in a more oblique direction; secondly, an additional strap across the upper palm can be a solution. The palmar strap would take away some sensory information from the hand. Nevertheless, this should not induce any problems, as the hand palm is less innervated than the digits and contact forces are spread over the entire hand. During optimisation of the shell structure, it should also be attempted to create a more open structure on the hand's dorsal side. Sweat is a known factor of irritation in prosthetic sockets. It could cause severe problems to the sensitive and fragile skin of the DMD patients, especially during long term use. When the final shape of the orthosis is determined, the model must be described either parametrically, so it can simply be adjusted to the individual, or the design should be made to fit different hand sizes and deformations.

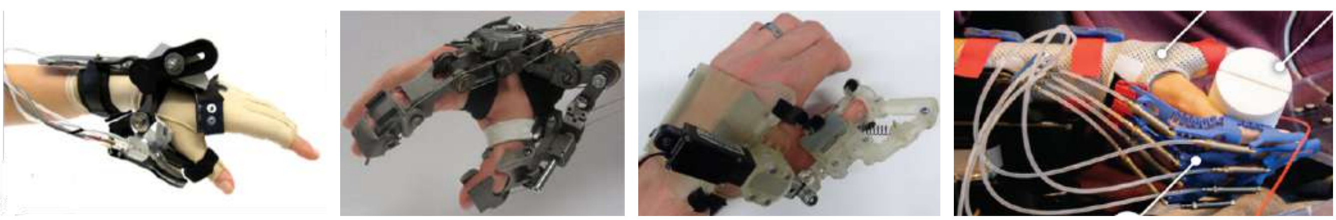

(a) Aubin (2013) [89]. (b) Cempini (2015) [90]. (c) Lambercy (2013) [91]. (d) Bos (2019) [7].

FIGURE 15. Designs of active thumb modules found in literature

6.B) PERFORMANCE

To achieve a successful precision or lateral pinch, the tip of the thumb must reach the plane of motion of the index finger, at a place the index fingertip can reach as well. The performance requirements that were set are the ROM and force to execute a pinch grip. For the ROM this meant a conical movement from 0 to 90 [deg] in the transverse plane. This workspace was implemented in the testbed, as can be seen in Figure 11. None of the prototypes was able to complete a precision pinch. The maximal ROM obtained with structure 3, reached to about 75 [%] of the required motion. Also the measured forces with a maximum of 2.8 [N] are lower than the requirement of 10 [N]. It is to be expected that the increased joint stiffness of Duchenne patients causes additional resistance to movement and shall further limit the pinch force.

Measured hysteresis in the system is 51-65 [%] which are not insurmountable losses, as the user is not responsible for providing the actuation force. An estimated 7 [%] can be ascribed to O-ring friction. Besides O-ring friction, other components that contribute to energy loss are; friction in the hose, the test-bed thumb, and the bearings, in addition to the deformation of the flexure elements. As the medium is of low viscosity and the hose has a good radial stiffness, friction in the hose was assumed negligible. The medium was also assumed truly incompressible, however it should be reviewed if the system can be enhanced by degassing the water and by removing the pressure transducer. The pressure transducer is connected to the system with an adapter block where some air could have accumulated that is compressible.

The thumb module should be improved, therefore the components of the system and their effect on the results are discussed separately. They are presented with further recommendations for improvement.

Compliant elements

The more the compliant element can stretch, the closer to the final position the thumb is able to get. Structure 3 comes closest to about 75 [%] of the necessary reach. Still, structure 1, 2, and 3 all thwart the thumb from reaching the index finger's plane of motion. Simultaneously, the flexure elements are essential for guiding the thumb motion. After testing without compliant elements 1 and 2, the thumb's motion remained planar, restricted to AA.

In Section 3., it was calculated that, without the flexure elements, a force of 10 [N] should be achieved at a pressure of 2.46 [MPa]. Instead, the maximum pinch force measured was 2.8 [N] measured at a pressure of 4 [MPa]. The theoretical value deviates substantially from the measured forces, which implies that much of the exerted force is needed to deform the compliant elements. Between structure 1 and structure 2, no large force difference exists. Contrarily, structure 3 can exert lower forces, as can be interpreted from the pressure-force relationship's steepness in Figure 13. The lower forces can be attributed to the increased amount of thumb movement with this compliant element, or to the guiding direction of the thumb, changing the force direction onto the pinch sensor. This difference in direction would explain why the pinch force after failure of the flex elements of structure 3 is much lower, as can be seen from the purple line in Figure 13.

The compliant elements also contribute to the hysteresis within the system. Energy is required for their deformation, which is not returned after the pressure drops. The retraction spring puts in effort to get them back to their original shape. However, as can be seen from the discrepancies between the stroke length before and after pressure application, the original shape is not immediately achieved. The presence of strain in the material eventually leads to the failure of the flexure elements, a great point of energy loss. Structure 1 and 3 have failed during the trials of testing, and even though structure 2 remained whole, this structure is too stiff and experiences some twist during movement.

Either, the flexure elements should be optimised, regarding material, shape, and placement. By for example, applying a more elastic material, increasing the structure width, and placement of the elements where stresses are minimal and loading in bending without twist. Alternatively, the flexure elements can be replaced with a rigid mechanism that steers the thumb movement. Replacement would require more knowledge about the origin of the thumbs' conical movement for proper alignment of this structure, or a remote joint to maintain anatomical compliance.

Piston-cylinder

A limiting factor in achieving the required ROM, is the stroke length of the piston-cylinder. As can be seen from Table 3 structure 3 is at the stroke limit when 4 [MPa] is applied, but has not reached the desired ROM. This indicates that the stroke length of the piston cylinder is too small to reach the desired end point.

This problem can be addressed by implementing a cylinder with an increased stroke length. However, increasing the stroke length would affect the resting position of the thumb. Moreover, it would increase the protrusion from the hand. The resting position is determined by the cylinder length without stroke. To compensate for this additional length, attachment A would have to be placed more lateral on the hand. Consequently, the attachment height should be increased as was shown in Figure 7(a).

Another possibility to improve the ROM is to re-evaluate the positioning of the piston cylinder. The current design aims for a conical thumb motion. By repositioning the cylinder, perhaps the grasp taxonomy can be accomplished. The thumb orthosis of Lambercy (2013), applies a similar actuation principle to the thumb module. It operates by using a linear actuator to assist the thumb motion. Lambercy's orthosis has a ROM of FE angles of 0-40 [deg] and AA angles of 0-12 [deg] measured from the resting position. In combination with unassisted FE of the MP and IP joints, this was deemed enough for carrying out a precision pinch. It should be considered that by repositioning the cylinder in this manner, the moment arm becomes less, and forces shall be lower.

TABLE 4. Overview of the requirements and the measured results

Specification		Value	Measured	Unit	Sufficient
Pinch Force	Precision pinch	10	2.8	[N]	×
ROM	Transverse plane	0-90 [deg]	$\pm 75[\%]$	[-]	×
Hand opening width		10	not measured	[cm]	-
Mass	Total orthosis	<250	204	[gr]	✓
	Maximal pressure	5	4	[MPa]	-
Actuation	Bi-directional	return spring			✓
	Placed dorsally	protrusion 2.2		[cm]	✓
Control	Allow cutaneous feedback	open tip & palm			✓
Comfortable and easy donning & doffing		2 straps			✓

The geometric relations in the actuation mechanism are not ideal for optimal force transmission. The piston force's direction with respect to the thumb joint is rather inefficient, due to its small moment arm compared to the moment arm of force at the thumb tip. It is questionable whether redesigning the flexure elements and repositioning the piston-cylinder is enough for achieving high enough pinch forces. Most likely, a cylinder with a larger bore diameter shall be needed to meet the pinch force requirement. Increasing the bore diameter is paired with more protrusion and more weight, so shall have a negative effect on the overall design.
Instead of increasing the bore diameter, a second cylinder could be added. As can be deduced from Lambercy's design, the inclusion of MP assistance or adjustment of the splinting angles could advance the ROM. Adding a second cylinder to the MP joint, would allow for an additional force that shall increase the pinch force. Adding an additional cylinder will increase the weight and encumbrance of the system. It should be evaluated which option, increasing the bore diameter or adding another cylinder is beneficial regarding weight and encumbrance.

Cylinder Attachment

The attachments of the cylinders should be reshaped to improve the design. Reshaping attachment A can influence how forces are directed onto the orthosis shell. Hereby, it can be made sure that the shell of the orthosis does not deform during pressure application.
Reshaping attachment B can be an alternative to increasing the stroke length of the piston cylinder. By lengthening the attachment towards attachment A the lack of stroke can be compensated for. Adjusting the attachment in this manner shall result in more rotation around the thumb joint and so increase the ROM.

Locking Mechanism

During optimisation one could find that, to meet the force requirement, the system would become too bulky. A decision could be to refrain from the set force requirement of 10 [N] pinch. Instead this requirement can be changed into resisting a 10 [N] force. A locking mechanism must then be designed that locks the thumb at the pinch position, after which the fingers can exert the grasping force on the object. This would still release the awkward position of the splinted thumb, but the execution of the lateral pinch will then be inoperable, as no force can be exerted by the thumb. An example of a locking mechanism is closing the control valve.

7. CONCLUSION

A preliminary design of a hydraulic thumb actuating orthosis for DMD patients with incipient hand dysfunction has been discussed. The thumb module was designed to release the awkward resting position due the currently used thumb-wrist splint of the Symbihand developed by Bos (2019). The prototype uses a miniature hydraulic cylinder to facilitate conical thumb movement towards the index finger. Experimentation with a custom built testbed hand showed that the required forces and ROM for ADL can not be achieved. Limitations are caused by the designed complaint elements which connect the thumb to the wrist brace. These elements are needed to guide the thumb along the conical path, instead of heading into pure AA of the thumb in the frontal plane. Still the the design has potential as it is lightweight, slim, and allows for cutaneous feedback. For further development compliant elements should be redesigned or replaced by another guiding mechanism, geometrical relations should be reassessed, cylinder attachment points should be reshaped, and stiffness of the wrist brace should be increased.

ACKNOWLEDGEMENTS

Supervisor

Dr.ir. D.H. Plettenburg

Delft University of Technology, Faculty of Mechanical, Maritime and Materials Engineering, Department of BioMechanical Engineering, Delft Institute of Prosthetics and Orthotics, The Netherlands.

Chair

Prof.dr. F.C.T. van der Helm

Delft University of Technology, Faculty of Mechanical, Maritime and Materials Engineering, Department of BioMechanical Engineering, The Netherlands.

Prototyping

Ir. J. van Frankenhuyzen

Delft University of Technology, Faculty of Mechanical, Maritime and Materials Engineering, Department of BioMechanical Engineering, Delft Institute of Prosthetics and Orthotics, The Netherlands.

3D scanning

B.J. Naagen

Delft University of Technology, Faculty of Industrial Design and Engineering, Department of Human Centered Design, The Netherlands.

3D modelling approach

Ir. R. Schönfeld

Delft University of Technology, Faculty of Industrial Design and Engineering, Department of Integrated Product Design, The Netherlands.

3.

Literature Study

Literature Review: Dynamic Hand Orthoses for Duchenne Muscular Dystrophy

P. DE GROOT, Delft Institute of Prosthetics and Orthotics

Delft University of Technology, Faculty of Mechanical, Maritime and Materials Engineering Department of BioMechanical Engineering, The Netherlands

ABSTRACT For Duchenne Muscular Dystrophy (DMD) patients currently no assistive hand orthoses are available on the market. Precise design requirements for achieving a successful design are hard to find within design articles. Quantification of parameters is difficult as data of DMD patients obtained is most often on functional scales. Besides that, the fixture between hand and orthosis is often not designed for. Fixture design is however of large value to the wearability of the device, as it concerns the connection between the human and the machine. The aim of this research is to create an overview of reported design requirements, the special needs of DMD patients and current fixture designs and relate them to one-another. In total 50 articles were evaluated for retrieving design requirements, 47 for identifying patient characteristics and 91 articles for the evaluation of fixture designs. All articles were retrieved from either PubMed, Scopus or WebOfScience or from the reference lists of the articles found here. The main identified customer requirements resulting were "Adaptability" due to high variability within and between patients, "Tolerability" due to reduced muscle and skin integrity, and lastly, "Ownership" as it is an assistive device that should increase the feeling of independence.

INDEX TERMS Duchenne Muscular Dystrophy, Dynamic Hand Orthosis, Design Requirements, Fixture

1. INTRODUCTION

This literature research has been conducted within the Delft Institute of Prosthetics and Orthotics which is currently developing an assistive hand orthosis for patients with Duchenne Muscular Dystrophy. The review continues on previous studies by Bos et al. [28] and Baan [73] on the designs of dynamic hand orthoses. Together they have made a structured overview of over 200 dynamic hand orthoses, based on categorization in a signal, energy and mechanical domain. Optimization of these three domains are however not the only critical values for a successful dynamic hand orthosis. Therefore a new literature survey is conducted directed to the design requirements of dynamic hand orthoses. As within their research Bos et al. and Baan only focussed on actuation mechanisms, the design of the interface between user and mechanism, is a prior focus within this review.

DUCHENNE Muscular Dystrophy (DMD) is a hereditary disease with an incidence estimated on 1:5000 male newborns and a prevalence of 4.78 [%] world wide [13]. It is a rapidly progressive neuromuscular disorder where an absence or deficiency in the protein dystrophin leads to continuous muscle degeneration [9]. First symptoms are noticeable between the age of 1 and 3 years old, ambulation is lost by the age of 8 to 14, respiratory failure starts around the age of 20 and eventually an early death is expected between 30 to 40 years of age [9], [13], [14]. As there is no cure for DMD current treatment options focus on alleviation of symptoms and management of complications [14]. Developments in treatment and management have increased life expectancy significantly, as it was expected at 20 years of age at the beginning of the 1990s [44] [95]. Accordingly, young people with DMD should be looking forward to living independently, as adults, with appropriate support, [96]. As it is now, boys with DMD will live with impaired upper extremity (UE) function for more than 15 years. Loss of hand function has a great impact on the performance of Activities of Daily Living (ADL) and restricts social participation [16], [24], [30], [97], [98]. Assistive devices have the potential to help perform ADL and so improve the Quality of Life (QOL). Still, use of these devices by DMD patients is scarce. Of the 213 respondents reported by Janssen et al. in 2014 merely 9 [%] used an assistive device [16]. Increased chances of acceptation of assistive technologies and a reduction of device abandonment can be addressed by user-based input [99]. "Comfort" and "Wearability" are important aspects of user input and can be translated to the design of the hand-orthosis interface. Aims of this review are to create an overview of reported design requirements in the development of dynamic hand orthoses. It then tries to draw a line between these criteria, the special needs of Duchenne patients and current hand-mechanism interfaces. The report was split into three sections. The first section reports design requirements extracted from literature and the reasoning behind them. The second section of this report looks into the physical status of Duchenne Muscular Dystrophy patients in order to identify specific needs for the patient group as well as variations within the patient group. The third section evaluates existing devices to identify good potential design solutions for improving the interface between the users' hand and the orthosis.

Types of Hand Orthoses;

There are many different kinds of hand orthoses used for rehabilitation purposes. Before looking into literature, one must be aware of the distinctions between them.

Dynamic vs Static Orthoses; The overall function of an orthosis is to support, immobilize, or treat muscles, joints or skeletal parts which are weak, ineffective, deformed or injured [100], [101]. This can either be done by limiting the range of motion (ROM) in order to give a body part time to heal by non-use, a static orthosis. Otherwise, this can be done by an orthosis that supports movements a user can not perform without help in order to train or maintain muscle integrity and function. This is called a dynamic orthosis [102].

Active vs Passive Orthoses [28] [30]; Dynamic orthoses can assist motions in two ways. First energy can be added to the system passively, e.g. by the use of springs. These passive orthoses can only be used in patients who have enough muscle power to initiate movement themselves with a certain amount of force. If this is not the case, active orthoses can be a solution. Here energy is added to the system by use of external power, e.g. a battery. This can help move limbs of patients that have very limited muscle function and activation. Actuation can be achieved by many different systems.

Rehabilitation vs Assistive Orthoses [30] [103] [104]; Lastly a distinction can be made between the purposes of the orthoses. Some orthoses are developed for rehabilitation. They facilitate functional recovery and train the musculo-skeletal system by indirectly enhancing hand function. The main aim is that over time the orthosis will be superfluous. These therapeutic orthoses are only worn during the duration of a training session. Regaining muscle function is not a prospect for all patients. Muscle function loss might be permanent or even progressive. Assistive devices enhance hand function directly so that patients with very limited muscle function can still perform activities of daily living. Therefore they are worn throughout the day and can take over the complete functioning of the hand.

2. DESIGN REQUIREMENTS IN CURRENT ORTHOSIS DESIGNS

This subsection creates an overview of the design requirements that are currently used when designing hand orthoses and evaluates their quality.

2.A) METHOD

A literature search was performed in September 2019 in three different databases: PubMed, Scopus and WebOfScience. Search indications used the words: "Hand Orthosis OR Hand Exoskeleton" AND "Criteria OR Requirements", exact insertions can be seen in Figure 16. Results were then selected based on the following criteria: The article was written in English; The orthosis was designed specifically for the hand; The article contained a physical orthosis design; The orthosis was dynamic, not a splint; The article mentioned design criteria either explicitly or implicitly; The article described a complete orthosis design not just one component; Orthosis was usable for ADL; Finally results were also included specifically about design requirements in exoskeleton design or user perspectives on the matter. For further completion of the literature listing, reference lists of selected articles were reviewed for more detailed information.

2.B) RESULTS

From the data search the number of suggested articles were; 640 by PubMed, 64 by Scopus and 120 by WebOfScience. After reviewing the articles by use of the selection criteria 31 articles were selected from PubMed, an additional 8 from Scopus and another 18 from WebOfScience. Reviewing their references added another 3 articles to the analysis, resulting in the final 50 articles.

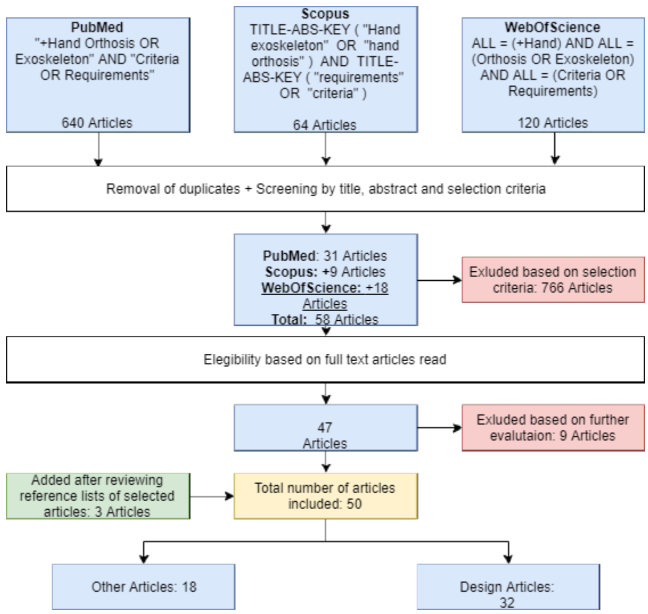

FIGURE 16. Literature Search Query for design requirements in dynamic hand orthoses.

Taxonomy

The obtained article selection consisted of 32 design articles and 18 other articles that were either reviews, standards or user perspectives.

The design articles mainly focus on design for stroke patients and some others on more generic orthosis design, only 1 by Bos et al. [34] looked into the design for Duchenne Muscular Dystrophy. All design articles described prototypes, instead of commercially available assistive devices. Furthermore only 15 out of the 32 design articles contained a section dedicated to criteria. Others put their focus elsewhere and mentioned them throughout the whole article.

Content of the non-design articles varied as well. Different aspects of current hand orthosis technologies were compared in 6 articles. Defining design requirements was specific focus in 7 articles, the aspect of touch in assistive robotics was

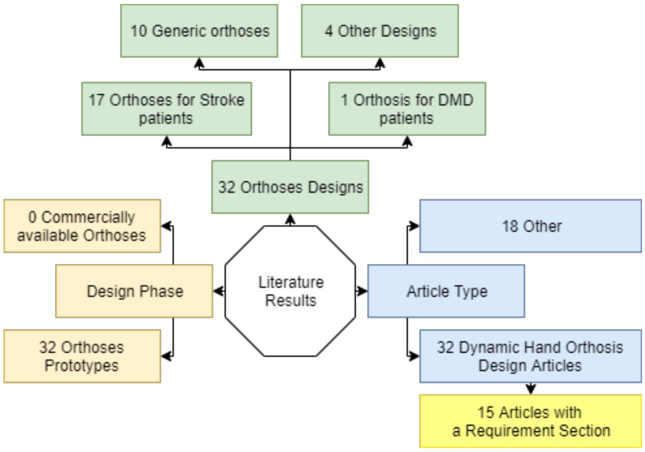

FIGURE 17. Literature Taxonomy for design requirements in dynamic hand orthoses.

discussed in 1 article, a quick overview of standards within exoskeleton design was given in 1 article and user perspectives were described in 4 articles.

Requirements

Selected articles were read and design requirements were extracted. Of all design articles, few design objectives were supported with scientific research. Most often requirements were briefly mentioned without clear definition or quantification. The concept selection process then relied on the personal experience (intuition), creativity and subjective judgment of the developers(s) [3].

Retrieved requirements were structured into Customer Requirements (CRs), Functional Requirements (FRs) and Design Parameters (DPs) as is done in the design method described by Yang et al. (2018) [105]. The obtained overview can be found in Appendix C, were the number of times a certain requirement was mentioned is indicated between the brackets.

The overview shows that very few quantified design requirements have been used in the development of dynamic hand orthoses over the years. At the same time different design parameters and functional requirements are used to describe the same user requirement. Criteria, including synonyms, with the highest level of recognition were:

1) Wearability: 23 times
2) Encumbrance: 21 times
3) Weight: 19 times
4) Safety: 17 times
5) Portability: 16 times
6) Variability in hand dimensions: 15 times

In addition to above criteria, requirements with respect to grasping are greatly present in literature as well. They have the highest variation in functional requirements and design parameters but also contain the highest number of quantified design parameters.

From the literature reviews more additional information on the design requirements could be retrieved. Definitions of design requirements as stakeholder needs were drafted by Veale et al. in 2016 [106]. Sarac er al. in 2019 evaluated design requirements in general, but also for different purposes: rehabilitation, assistance and haptics [104]. Prange et al. described design requirements for assistance and devided them into 3 categories: 'Functionality', 'Safety' and 'Usability'.

In all literature reviews the need for user input has been indicated, as otherwise design requirements cannot be adequately defined [32]. Stanger et al. even claimed that market success is determined by the user's acceptance regarding level of cost, reliability, appearance, ease of use and function [32]. An equation has been given by Heller et al. in 2008, called Bakers' ergonomic equation [107]. Baker's ergonomic equation 3, defines the success of assistive technologies (AT) purely based on user costs vs. user desire. The higher the outcome of the equation, the higher the chance of success of the assistive device. Best results would be obtained if there is much user motivation, opposite to low effort for using the device.

$$\text{Success or Failure of AT use} = \frac{\text{M}}{\text{PE} + \text{CE} + \text{LE} + \text{TL}} \quad (3)$$

1) M = Motivation of the user to perform a task
2) PE= Physical effort which includes movement exertion, motor strength, endurance, fatigue, and limitations in ROM.
3) CE = Cognitive load is the amount of thinking involved in the use of the device in the performance of the task
4) LE = Linguistic effort refers to the amount of symbolic interpretation and processing needed to operate a device.
5) TL = Time load is the amount of time needed to perform a task using assistive technology.

2.C) DISCUSSION

CRs represent the needs of the users terms like 'wearable', or 'portable' which can be interpreted in different ways. FRs are customer demand information translated into product technical goals to ensure products meet the needs of customers. Lastly DPs are parameters by which can be tested that the FRs have been met. They are specific parameters that preferably can be quantified

As products are chosen by users based on their functions, functions are commonly used as performance measures. Performance is therefore often validated in an laboratory environment instead of translated to a patient population [30] [105] [6]. As a consequence designs are based on designer experiences without truly looking at the details of user requirements. This is supported by results found in the selected literature as only 16 of the 31 articles found were supported design requirements with scientific research.

Additionally it is not clearly described which user group the assistive devices are designed for and what the specifications of these users are. This results in designs that are not optimized for the intended user population [6]. No single optimal design solution exist as there has to be dealt with high inter-

and intra-subject variability. Differences can be identified from diagnosis, disease stages, but also expression levels of the disease. These variations make it it even more important to create well-defined design specifications based on user's and professionals opinions [3] [6]. Following a user centered design process devices will improve likeliness of retention and thus will reduce the reported numbers of non-use [108]. A suggested process, is the one described by Yang et al. [105], which is also used to structure the collected design requirements. Here CRs represent the needs of the users in terms like 'wearable', or 'portable' which can be interpreted in different ways. FRs are customer demands translated into product technical goals. These ensure that products meet the needs of customers. Lastly DPs are parameters by which can be tested that the FRs have been met. They are specific parameters that preferably can be quantified.
Because researchers do not perform detailed analyses of user requirements for a specific patient population, design articles written contain vague descriptions of criteria and lack quantification of the design parameters. When a value is assigned to one of these parameters there are large differences between reports. These assigned values are also based on healthy subjects most of the time and so are not necessarily applicable to a diseased hand which can have completely different properties. The knowledge gap that can be identified within this area of design is hereby underlined.
Another point of interest emerging from the overview of design requirements concerns the absence of attention to developing the interface between the hand and the orthosis. As the most reported criterion is 'Wearability', this is unlogical. A lot of effort is put into the actuator configuration, but what is overseen is that if the device can not be worn due tot the fixture, the device will not succeed.

2.D) CONCLUSION

The design process of dynamic hand orthoses requires improvements. All starts at proper definitions of design requirements that target a specific user group. These requirements should be obtained by user input and knowledge of disease stages, specifications and needs. All ends with validation of the design by translation to the target population instead of solely by laboratory research or healthy subjects. This also includes detailed reporting of the steps taken and the decisions made within the design process, so that others can learn and improve.

3. SPECIFICATIONS AND SYMPTOMS OF DUCHENNE MUSCULAR DYSTROPHY PATIENTS

The previous subsection identified controversies between design requirements stated in literature and the method by which the criteria were obtained. In order to specify good requirements, one must truly know whom to design for. The target group for this literature survey are patients with DMD, a patient group not frequently designed for in articles about dynamic hand orthoses. This subsection will explore specifications of these patients, so that crucial design factors can be determined. DMD functioning is described in relation to healthy hand performance, which has been described in many articles and books, i.a. the book written by Controzzi et al. in 2014 [109] .

3.A) METHODS

The search for DMD patient characteristics was performed in three databases; PubMed, Scopus and WebOfScience. As the aim of this literature survey is to look for design requirements for a dynamic hand orthosis search terms used included: "DMD OR Duchenne Muscular Dystrophy" and "Hand" " Impairment OR Function OR Dexterity". The search results were then selected by the following criteria; 1. Article was written in English; 2. About hand function, not about lower limb function or arm function; 3. Indications of functioning over time.
As assistive devices not only have an purpose of fulfilling ADL, but should also limit disease progression, another literature search was performed. Keywords used were; "DMD OR Duchenne Muscular Dystrophy" AND "Rehabilitation OR Therapy OR Exercise" in order to identify the influence of training on the disease progression and the guidelines used for prescribing optimal therapy. Here articles were selected based on: 1. Article is written in English; 2. Relevance to distal UE rehabilitation or physical therapy; 3. About the effect of exercise based on disease pathology;
Within the articles some secondary symptoms were mentioned. Based on these symptoms, a small scale literature search has been done in Google Scholar in order to complete the patient characteristics. These articles have also been added to the literature list.

3.B) RESULTS

Within Figure 18 the results from the search queries used are visualized. First terms about hand performance resulted in 165 articles in PubMed, 132 in Scopus and 107 in WebOfScience. Second terms about exercise and physical treatment resulted in 404 results in PubMed. After screening based on the selection criteria 55 articles were left. Thorough reading eliminated another 14 articles, but also added 16 articles from the small scale Google Scholar searches and reference lists. The eventual number of articles reviewed is 47.

Taxonomy

As can be seen in Figure 17, from the selected articles 4 contained information about the aetiology of DMD, within these articles pathophysiology was described. 11 Articles described the progression of the disease for DMD patients, 16 reported specific hand function of DMD patients. From the 10 articles selected in the literature search about physical treatment and exercise, 7 were eventually used. Lastly 16 articles reported about symptoms of DMD that were not specifically about hand functioning but were still relevant for dynamic orthosis design.

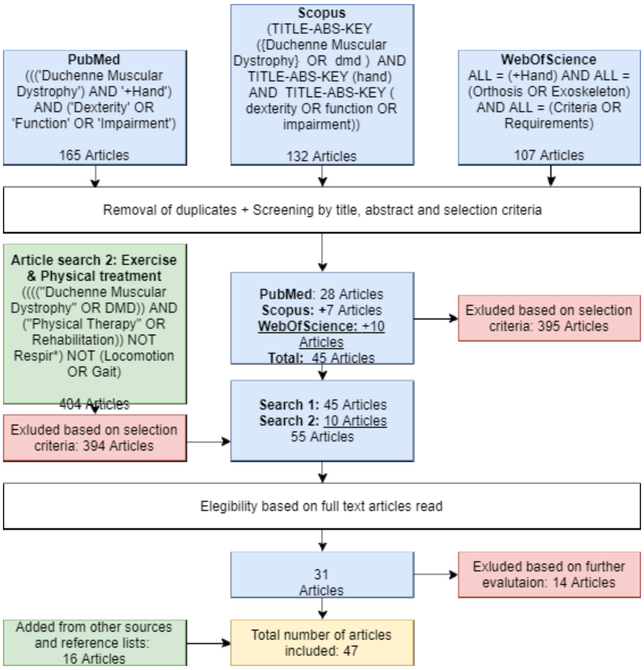

FIGURE 18. Literature Search Query DMD patient characteristics.

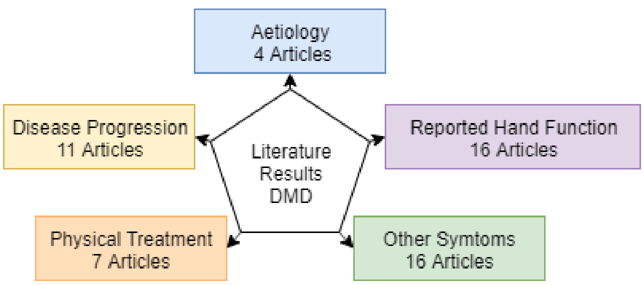

FIGURE 19. Literature taxonomy for patient characteristics.

Patient Characteristics

Aetiology; In the introduction some basic knowledge about DMD was already described. The disease is genetic X-chromosome linked and affects the synthesis of the dystrophin protein due to a mutation in the dystrophin gene. As a consequence, boys with this disease are incapable of producing the dystrophin protein or produce defected proteins. The dystrophin protein is a part of a complex that connects the extracellular matrix through the sarcolemma to the intracellular cytoskeleton and so provides stability to the muscle membrane [110]. It is essential for the transmission of force generated by contractile proteins [111]. Therefore it is responsible for protecting muscle cells from contraction-induced damage [10]. Absence or abnormalities of dystrophin proteins lead to muscle degeneration caused by sarcolemmal instability, membrane tears and muscle cell necrosis. By cause of lost regenerative capacity muscle fibers are gradually replaced by fibrous or adipose tissue [21]. This process induced by the dystrophin mutation over time results in weak and stiff muscles that first cause impairments and eventually early death.

Disease progression; Described by Bushby et al. in 2010, where the course of DMD is divided into five stages; Stage 1. Presymptomatic stage; Stage 2. Early ambulatory stage; Stage 3. Late ambulatory stage; Stage 4. Early non-ambulatory stage and Stage 5. Late non-ambulatory stage [9]. On average first symptoms are expressed between 1-3 years of age, however diagnosis of the disease is often not made until the age of 5. The non-ambulatory stage (4) is entered around the age of 8-14 and instead patients use wheelchairs for ambulation [13] [14]. Upper extremity weakness initiates in the early ambulatory stage (2) and progresses from proximal to distal and first affects extensor groups before flexor groups [112] [41] [42]. Progression of the disease has been monitored by use of many different scales on muscular and functional levels [113]–[115]. Nunes et al. reported in 2016 that muscle strength and motor function were not correlated to age [116]. Similar findings were proclaimed in 2018 by Pane et al. who stated that progression is non-linear and therefore a wide variability can be observed between patients [117]. These progressive decreases in muscle strength and function are the primary cause of the loss of functional abilities [43].

Reported Hand Function; As the disease becomes more severe muscle weakness and stiffness present themselves in the hands and cause impairment. Simultaneously increase of the DMD life expectancy makes distal UE function important as it plays a key factor in maintaining functional independence and in the interaction between a person and it's environment [118] [48] [52]. Accordingly loss of hand function results in a great loss of independence, this whilst it presents itself at an age where adolescents and young adults develop a greater desire for independence [96] [15]. Also due to their confinement to a wheelchair dependency on their arm and hand function is even higher [21] [41] [11]. UE function has been confirmed to be of highest priority to the patient group in a research in 2007 by the Dutch Duchenne Parent Project. Reasoning behind this prioritization was that wheelchairs can take over ambulation but compensation for the loss of arm function is less evident [24]. Research into treatment of the disease has not been able to preserve muscle function. The lack of dystrophin leads to muscle weakness, leading to reported grip and pinch strengths far below normal [11]. Before the first decade strength has still shown an increase as development in relation to age and growth is larger than degeneration in relation to the disease [42]. Still after the age of 10 muscle weakening occurs and has reported correlation to the loss of functional ability [41] [119]. Grip and pinch strength have been measured by Seferian et al. in 2015 and showed large variation between strength loss and time after loss of ambulation, as can be seen in Figure 20 [41]. VanderVelde et al. found that 73 [%] of the research group consisting of DMD, Becker Muscular Dystrophy and Limb Girlde Muscular Distrophy patients, had quantifiable Grip Strength impairments in their dominant limb and 78

[%] in their non-dominant limb [120]. As muscle weakness propagates it becomes a prior cause to limb disuse due to limitation of the active range of motion (ROM) [21]. Wagner et al. studied the occurrence of pain within 18 participants. Pain during passive finger flexion occured in 15 [%] of the fingers of 8-14 year olds and in 25 [%] of the 18.7-24 year olds [11].

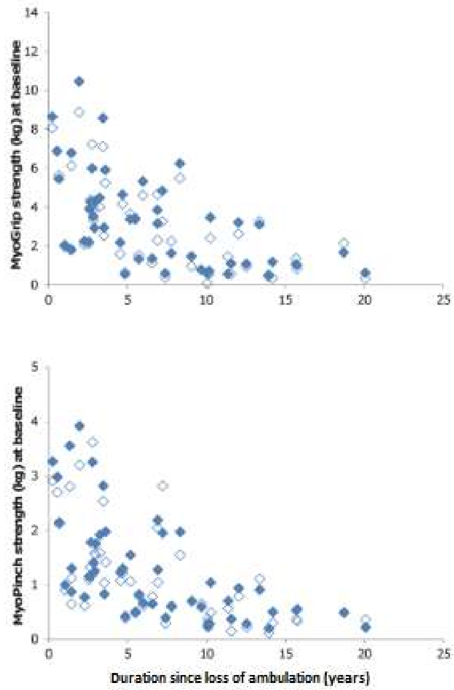

FIGURE 20. Grip and Pinch strength over time after loss of ambulation, reported by Seferian et al. in 2015 [41]

.

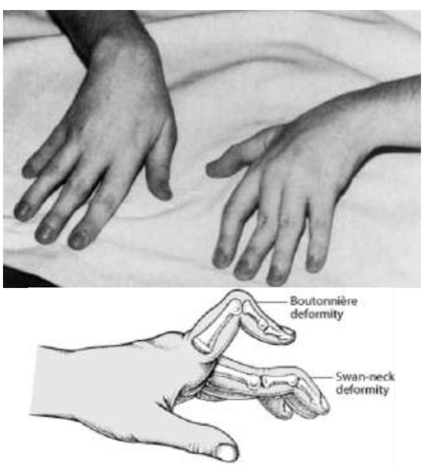

FIGURE 21. Hand deformity configurations. A) Muscle imbalance and joint contractures of a DMD patient of 14-18-year-old. shortness of the long finger flexors and ulnar deviators; swan neck and boutonniere posturing of the digits [11]. B) Schematic representation of Swan Neck and Boutonniere deformities [12]

When limbs are in static positioning for longer periods fibrosis and proliferation of connective tissue precipitate and muscle stiffening emerges [22], [43]. These contractures confine the passive ROM due to the occurrence of pain and further allow for infiltration and stiffening [11] [16] [8]. Muscle contractures are rare before the age of 9, but by the age of 13 most of the DMD patients suffer from them [121]. According to Wagner et al. finger deformities that mostly occur are Swan Neck and Boutonniere deformities as represented in Figure 21. Swan Neck deformities have a pattern of metacarpal phalangeal (MCP) flexion, proximal interphalangeal (PIP) hyper-extension and distal interphalangeal (DIP) flexion, whereas Boutonniere deformities are inverse showing MCP hyper-extension, PIP flexion and DIP hyper-extension [11].

Physical Treatment; Besides medicinal treatment of DMD the prescription of physical and exercise treatment has been up for discussion [8], [26], [43], [52], [53], [122], [123]. Physical treatment mostly refers to passive stretching of the stiff limbs by therapists and the use of night braces in order to remain passive ROM for as long as possible. Exercise means active participation to some extend and is used for preserving muscle strength for as long as possible [8]. Discussion within these treatment options are about the possible adverse effects of overexercise, as the regenerative capabilities of DMD patients are flawed. So exercise might not always be as beneficial as it is for healthy subjects. Abresch et al. concluded in 2009 that there is a contraindication for dystrophinopathy patients with large muscle weakness, due to their increased susceptibility to exercise-induced damage adverse to little gain [124]. In contradiction, exercise can be beneficial to individuals who are still mildly affected and whose muscles are less sensitive to overexertion and overwork weakness [26]. Muscle pain, a sorely uncomfortable feeling or extreme fatigue during or prolonged post-exercise have been indicated as signs for overstrain [43].

Other reported symptoms/characteristics; Apart from the manifestation of hand impairments there are several additional user group characteristics that are relevant. Senses of DMD patients are still completely intact. This includes tactile as well as proprioceptive functioning as the disease is of muscular and no neurological origin [17]. Additionally it has been noted in literature that fibrosis or extensive corticosteroid use also affect skin integrity [9], [125]–[128]. Trophic changes become more common in the later stages of the disease and occur in the skin of extremities [20]. Symptoms assigned to this skin atrophy include coldness, increased skin fragility, tearing, bruising, transparency and even scleroderma like changes [20]. Skin condition influences DMD patients moving and handling methods, as it is more sensitive to soreness, rubbing and shear forces [19]. Furthermore it is mentioned that DMD children are on average 4.3 [cm] shorter than their peers and by the age of 18 they fall below the fifth percentile on growth curves [129]. However it has also been stated that this lag in growth does not regard hand sizes, which are claimed to be similar to healthy individuals [130]. Lastly Lacourpaille in 2014 found a longer delay between the onset of fascicle motion and the onset of force production

in DMD patients compaired to healthy subjects [111]. This is due to the extensive loss of contractile elements in the muscles causing significant impairment of the excitation-contraction coupling. Duchenne patients are compelled to increase their overall activation effort to perform the same movements as healthy controls [24] [111] [8]. This might result in increased fatigability according to Jansen et al. in 2017 who encountered increased sEMG levels that demonstrated more use of muscle capacity by DMD patients than healthy subjects to perform daily activities [123]. In order to reduce this fatigue and to still be able to complete daily activities despite muscle weakness, DMD patients develop compensatory strategies or adopt awkward postures. Movements hereby become less efficient, which also explains their higher activity measures [21] [120] [39].
Lastly the perception of DMD patients towards assistive technology as reported by Andrews et al in 2018. Within this report it is stated that typically these technologies are seen as a positive improvement when described due to functional deterioration, as it elevates quality of life through impediment reduction [129]. Same results were found in a report written by Cassel et al in 2011. where attitude towards the transition into a wheelchair was described [131].

3.C) DISCUSSION

The results described previously can be used in order to create CRs as described by Yang et al. [105] and will then be related to design requirements mentioned in Chapter 2.. An overview of the DMD characteristics discussed in the results can be found in Table 5 and the design requirements of Chapter 2. can be found in Appendix C.
First of all many researches stress the high patient variability between DMD patients. Variations can be found within the disease course on many levels and milestones occur at a wide range of ages. Although the rate of disease progression is highly variable, a pattern in the disease course has been described [9]. DMD patients experience muscle loss from a young age and on. At this time they are in a period marked by growth and development indicating the need for a hand orthosis that can facilitate changes in limb size and proportions. Their hand dimensions however do not differ from those of healthy boys, therefore anthropometric measures of healthy individuals can be used for creating an ergonomic orthosis. The importance of hand dimensions has been described within the literature of design requirements, however are of particular importance in a population that is still within phase of high growth.
High variability can also be found in the amount of muscle weakness and thus also the amount of assistance needed will differ. This will also change during the course of the disease. When muscle strength is only beginning to decline the purpose of the orthosis worn will be to maintain muscle strength and counteract disease progression. The assistive device will then be more like a rehabilitation device and should then encourage active user participation and assist as little as possible. Overwork should be avoided at all costs and is indicated by muscle pain or soreness. As the disease progresses, active ROM will decrease and more assistance will be needed to keep hand function for ADL. This calls for adjustable assistive forces, highly related to user input. Also as extensor muscles are influenced before flexor muscles, assistance of extension will be needed first, however assistance of flexion might not be necessary yet. Lastly as DMD patients are more easily fatigued, the need of limb assistance might even change during the day. The desired activities to perform are personal as well. In the end the aim is to preserve function and user forces + assistive forces should be enough for ADL at all time. Adaptability to the change in user needs will enhance the feeling of ownership by the user as stated in Appendix C "Ownership". An important note to make is that once muscle stiffness and hand deformities are extremely severe a hand orthosis might not be able to be of any functional benefit at all [8] and priorities should be changed.
Assistive devices can supply forces to help movement of the hands, but still at some point muscle stiffening will occur, limiting passive ROM and increasing resistance towards assistive movements. Here pain becomes a significant limiting factor of movement, and should kept as a leading factor to ensure safety. At this moment muscle stiffness will limit actuation speed and through muscle pain will limit passive ROM. Avoiding static positioning becomes critical for preventing unwanted contractures and severe hand deformities for as long as possible. Accommodating change in passive ROM should be taken into account with regard to safety considerations as represented in Appendix C "unwanted/unnatural movements". Might hand deformities still occur, a closer look should be taken at bio-mechanical compatibility. This is due to the changing positioning of the DIP, PIP and MCP joints that will demand different alignments and force transmissions of the orthosis. Deformities also have influence on the donning and doffing of the orthosis as sliding anything rigid over the fingers would be difficult due to irregular shapes. Modular designs are thus needed as also has been noted by Nizamis et al. in 2019 who have tested their hand orthosis with the user group [8]. Easy donning and doffing can therefore be highlighted in Appendix C.
Independent donning and doffing by the user as indicated in the same schedule might be of lesser value. DMD patients need care every morning to even get out of bed and so already have access to the help getting them into their assistive device. The device will then be worn throughout the day, emphasizing the need for comfortable wearing for longer periods of time. As the skin of DMD patients is fragile and sensitive to tearing or bruising special attention must be paid towards comfort and tolerance. Even small pressure points, irregularities, chafing or slightly rough surfaces can be experienced as highly uncomfortable according to Nizamis et al. [8].
Senses, tactile as well as proprioceptive, are not affected in DMD patients. An assistive device should therefore allow the use of these senses, as it would increase their sense

TABLE 5. DMD characteristics related Design Requirements.

DMD Patient Characteristics	Related Design Requirements
Extensor weakness before flexor weakness	Assistive device must support opening and closing
High patient variability	Adjustable to user size, performance and needs
Muscle Weakness –> loss of strength + loss of active ROM	Starts off wit focus on preserving muscle strength = assist as needed
UE weakness initiates from the early ambulatory stage	
Loss of ambulation (age 8 - 14)	Confinement to wheelchair so portability has extended options
Muscle Stiffness –> loss of passive ROM	At some point need for passive stretching as well as assistance When passive ROM too severely reduced, ADL function by assistance might not be possible anymore
Hand deformities due to static positioning	Compliance for joint alignment & pressure distribution Challenge for Donning and Doffing
Fatigue due to disturbed excitation-contraction coupling	Need for assistance can change during the day –> Adjustability
Muscle pain due to overwork	
Tactile and proprioceptive senses remain intact	Accommodate for natural sensation of finger and hand palms
Reduced skin integrity	Soft interface, no chafing, no tightness, pinching, good pressure distribution
"Normal" hand size but during period of growth	Should fit different hand dimensions and adjustable over time
Compensatory Movements	
Symptoms in both left and right extremities	Control can not be done by unaffected hand as, so different method

of ownership and independence. Tomlinson et al. in 2007 indicated that "friction is an essential part of the feedback and feedforward control system of grip" [17]. The user should exert as much force as he can, which they need feedback for to know when sufficient force is applied [132]. This has also been stated in the DR section 2., where the importance of palmar sensation and an open finger tip structure are indicated in the DR scheme of Appendix C.
Besides issues discussed above, a different definition of "Portability" can be defined for DMD patients. Where it is described as small lightweight systems for stroke patients in Section 2., for DMD patients this only accounts for the orthosis itself. As the user is already wheelchair bound, more options for power supply and forms of actuation are possible. The user does not have to carry the load of the entire system themselves, but weight can be positioned on the wheelchair. At more severe cases patients use a powered wheelchair, making added weight to the wheelchair of even less concern. The ability to move freely without encumbrance are still to be taken into account with regard to movement of the UE limbs.
Some final commentary notes are, that although the disease course of DMD is clear, quantification of the design requirements is still difficult. The use of many different measurements and metrics impede the comparison of different studies to one another. Also scales that are used, are most often based on functions instead of measurements disallowing usable quantification of performance. In addition research groups often consist of not only DMD but also Becker Muscular Distrophy or Limb Girdle Dystrophy patients. This influences the data obtained as there are large discrepancies in disease progression between these types of NMDs. As a result there is a lot of absent knowledge about the effects of physical treatment and exercise on the DMD patient group as well. Stating guidelines of requirements to aim for and to prevent is thereby obstructed.

3.D) CONCLUSION

This section has attempted to identify specific design requirements for the design of an assistive hand orthosis for a DMD patient group. Quantification was deemed important, but found impossible due to absence of measurements of DMD hand capabilities. The optimal assistive orthosis is highly adjustable to user size, performance and needs throughout the disease course. Within the DMD user group must be dealt with high muscle stiffness, muscle pain, severe hand deformities and skin fragility. Higher attention thus must be paid towards comfort, tolerability and donning/doffing especially as the orthosis is assistive and shall be worn for longer periods of time. This also means higher focus on fixture design is needed. Furthermore portability has a different meaning for this patient group as they are wheelchair bound. This increases possibilities for actuation with regard to power supply and load carrying.

4. CURRENT FIXTURES BETWEEN THE ORTHOSIS AND THE USERS HAND

The fixture design for the interface between the hand and the actuator is scarcely reported within literature. Nevertheless this part is of high significance as DMD patients have to deal with hand deformities and decreased skin integrity, whilst wearing the assistive device for full days. This subsection will review fixture methods currently used in prototypes and work towards the description of a 'good' fixture.

4.A) METHODS

Literature found in Section 2. was sufficient for evaluation of fixture designs. Additionally more fixture designs were gathered from the literature reviews selected in Section 2.. Articles have been dismissed when no description nor an image of the fixture design was included.

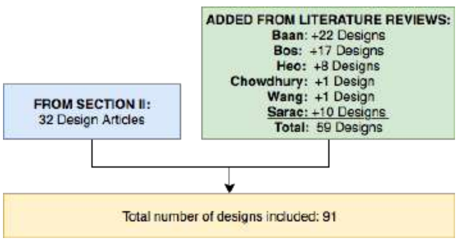

FIGURE 22. Literature Search Query for fixture designs.

4.B) RESULTS

In Section 2. 32 orthosis designs were included. To this number Heo et al. added 8 designs, Bos et al. another 17, Sarac et al. 10, Chowdhury 1, Baan 22 and lastly from Wang et al. 1 [28], [30], [104], [133], [134]. In total 91 dynamic hand orthosis designs were evaluated and grouped according to their fixture design.

Taxonomy

The fixtures of the designs included were reviewed based on images and descriptions. The three articles of Suarez-Escobar [3], Liang [98] and Pu [135] did not contain an description nor an image and were left out. As can be seen in Figure 23, fixtures were grouped according to their fixture method: "Glove" (23), "Straps" (25), "Endpoint inserts" (3), "Finger inserts" (5), "Hybrid" (29) or "Miscellaneous"(6). Within the literature 1 of the designs by Bos et al. [34] was tested with a DMD patient and so provided feedback on the designed hand-orthosis interface.

Fixture Designs

Xiloyannis et al. described the function of the fastening system in two components: 1. The fastening must adhere to the body of the user and 2. The fastening must keep everything in place [136]. These functions must be executed without constraining muscle expansion during motion, slipping during operation and peak pressure appearances. Also it should accomodate larger range of hand sizes and contain a soft interface between the hand-anchorpoints and the fixture [136]. For these reasons glove and strap type of fixtures are mostly used for wearable hand systems [137].

Glove Type: The use of glove type connections as in Figure 24(g) are considered beneficial for several reasons. Gloves are simple to use and already come in different sizes, where finger length is the only constraint when deciding on a size [97] [137]. Besides that a snug connection is created between the hand and the actuators, whilst still in compliance with change of rotation points is integrated within the design [97]. Moreover components can simply be added to the glove by sewing or adhesives [138]. A drawback to this has been difficulties to create a proper adherence between the glove and the actuator, one that does not allow for slip or looseness of the actuator [97]. Besides that In et al. reported that loosening of the glove occurred during testing their orthosis design. This loosening was considered unfavourable as it would change the relationship between actuator and fingertip force [103]. Also fabrics of gloves absorb sweat, but cleaning them including all assistive components is difficult [138]. Gloves are often used for cable actuated systems, as they provide a separating surface between hand and cables everywhere. Palmar and dorsal structures are added for guidance and application of cables for flexion and extension. Also many prototypes consist of gloves as it is readily available allowing for quick testing of the prototypes [137].

Strap Type: Straps as used in Figure 24(a) are created by different mechanisms such as velcro, elastic bands, buckles or even BOA fasteners [139]. They accommodate better for differences in hand sizes, creating a one size fits all fastening method [140]. However more time is needed to donn the orthosis [137], when too tight pressure points can appear [97] and when too loose slipping can occur and allow for misalignment [97].

Others used *endpoint fixation* only by using fingertip inserts as can be seen in Figure 24(b). The use of this type of fastening allows for some variation in finger tip lengths, easy donning and natural finger motion. On the contrary, fingertips can slip out of the finger inserts when not properly pushed inside or when forces are not properly exerted [133].

Several designs also employed *finger inserts* as fastening method. Of these 5 designs 4 were made of rigid materials [148]–[151] and 1, shown in Figure 24(i) was made of a more flexible material [138]. These inserts have reported advantages over the use of gloves. They are easily cleanable

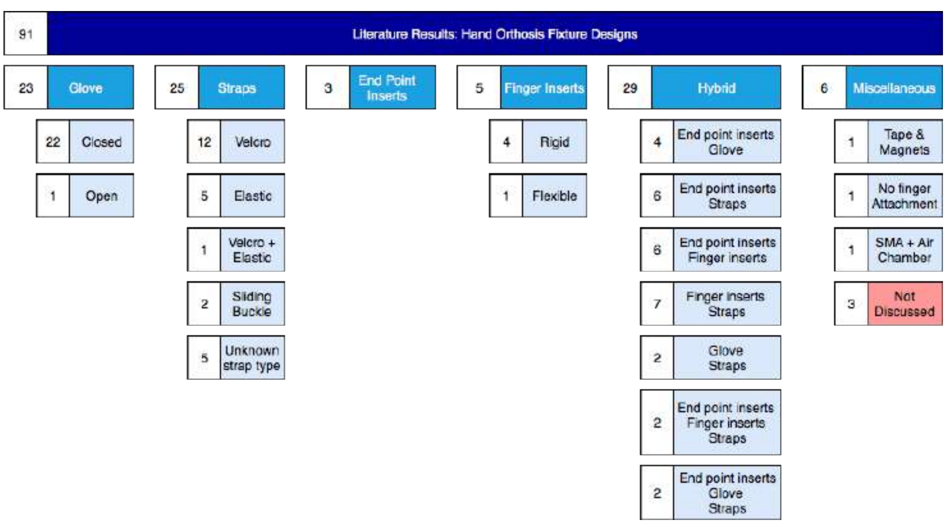

FIGURE 23. Overview of hand orthosis designs sorted by fastening method.

as simply wipes can be used to remove dirt and sweat, they maintain structural shape by itself and they have a stronger force transmission [138]. However adjusting the finger inserts to different hand sizes is more difficult invoking the need for modular designs [8]. The flexible material configuration used by Kang et al. is one proposed solution to this problem [138]. Limitations of this fastening method have also been described. One is that these rigid materials do not absorb sweat nor allow ventilation so an open structure must be used [138]. Another is that donning and doffing are experienced as uncomfortable by DMD patients, due to the tight sliding motion over their sensitive skin [8]. The design by Weiss et al. in 2013 used 3D printing to create the rigid hand orthosis structure, by 3D printing the orthosis could be fully adjusted to the user [149]. Structures that are 3D printed even when polished however are not smooth enough for comfortable wear [8]. The structures of the finger inserts all contain separate fixture elements for each finger segment, so that movements can be supported per segment allowing for independent assistance [150].

Hybrids: All separate fastening types have their upsides and downsides. Therefore, hybrid interface solutions have been reported as well. Different configurations shown in literature can be seen in Figure 23. Endpoint inserts allow for easy donning, Straps for more adjustability, rigid structures for good force transmission and gloves for good alignment and soft interfaces. Gloves are mostly combined with other attachment types as liners [89], [152] or finger tips are removed and they function as a connection to the wrist [153]–[156]. Finger inserts and endpoint inserts are often combined so that the most distal part of the finger insert is not an open but a closed structure. This has consequences though for the force transmission, as en endpoint inserts forces are only applied to the distal segment, whereas in finger inserts force transmission is applied to all finger segments. Also the open structure of finger inserts allow for tactile feedback, whereas the endpoint inserts create a barrier [157]. One of the finger inserts with endpoint insert has also been made in a flexible material to enable for extra comfort and compliance [158]. Straps are added to improve the fit of finger inserts, as too loose or too tight fits of these inserts are to be avoided. The design of Xiloyannis in Figure 24(d) combined straps for easy donning, with gloves for a snug fit and added rigid anchoring in order to allow for efficient force transmission [136].

The last category of fixture designs is *Miscellaneaous*, here fastenings methods were included that were one of a kind or not described/shown. The AMADEO design of Tyromotion in Figure 24(h) used tape to secure magnets to the fingers, these magnets then facilitated linkage of the fingers to the exoskeleton [159]. Another orthosis design that was sorted into this category is by Cui et al. in 2015. Their design was not attached to the fingers, but assisted in finger flexion and resisted in extension therefore not needing direct finger connection [157].

Added to fixture designs described above are firstly that the designs of Brokaw et al. [160] and Gasser et al. [143] linked all four fingers together so that no independent movement was possible. The design of Gasser et al. is shown in Figure 24(c), both created a rigid dorsal plate and binded this to the back of the fingers. Brokaw et al. used straps for attachment, whilst Gasser still used separate endpoint inserts for each finger [143], [160]. A second note is that Nizamis et al. found that the extensive contractures and deformities present in DMD patients call for modular hand orthoses to enable comfortable donning and doffing [8]. Patino et al. also developed a modular hand orthosis with exchangeable finger parts as in Figure 24(e). Finally the actuator decided on

(a) Maeder-York et al. [141] (b) HEXOTRAC by Sarakoglou et al. [142] (c) Vanderbilt by Gasser et al. [143] (d) Synergy glove by Xiloyannis et al. [136] (e) Patino et al. [144]

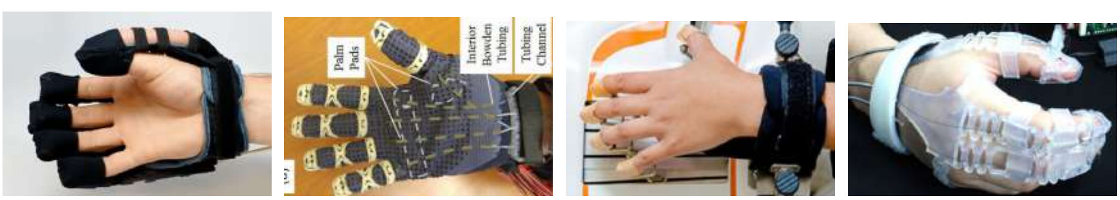

(f) Polygerinos et al. [145] (g) HEXOES by Burns et al. [146] (h) AMADEO by Tyromotion [147] (i) Exoglove Poly by Kang et al. [138]

FIGURE 24. Examples of fixture designs of orthoses retrieved from literature.

also plays a key factor in the decision on fastening method. Cable actuated systems mostly use gloves, as rigid structures here result in more encumbrance and they provide a snug fit between the actuator and the hand [136]. Finger inserts, rigid endpoint inserts and straps are used in linkage or pneumatic systems. Soft actuators use soft endpoint inserts as done in the design of Polygerinos et al. in Figure 24(f).

4.C) DISCUSSION

There are four main categories for attaching the orthosis to the hand. Although some design articles describe their fastening method shortly most often little attention is paid towards this crucial aspect of the design. As assistive devices will be worn throughout the day a comfortable and wearable design is of great importance for the success of the assistive device. As the skin integrity of DMD patients is affected obtaining a comfortable fixture design is a greater challenge. Tolerances are lower for shearing, chafing, chipping, pinching, etc.. Surfaces should therefore be smooth and soft and forces should be distributed uniformly [8]. This would indicate that glove-like structures would be a preferable option compared to rigid finger insets or straps. However as was indicated by Kang et al. glove type hand orthoses are far more difficult to clean. Difficulties in cleanability create problems in assistive devices. Assistance in ADL requires the device to be used in all sorts of environments and whilst performing all sorts of tasks, increasing the risk of the device becoming fouled. At the same time, gloves do absorb sweat and thus should be cleaned on a regular basis to avoid skin irritation [138]. Gloves also create an entirely closed environment for the hand limiting the tactile senses of the wearer, which has been identified as an important design requirement for orthosis design (Section 2.). For DMD patients these senses remain intact and as motor performance is limited these senses are meaningful to them. They are needed to find optimal muscle use, minimization of effort to perform a certain task in order to prolong the time before fatigue occurs as described in Section 3.. From this point of view end point inserts are disadvantageous and instead open structures such as finger inserts and the use of straps are more beneficial. These inserts and straps also allow for more easy donning and doffing of the device. This requirement is often stressed within literature, which is striking as still many designers decide on the use of gloves. Gloves are very inadequate for easy donning as they have a snug fit to the fingers. The hands of DMD patients also suffer from hand deformities making them unable to get the hand into the stretched and spread finger position needed for easily putting on a glove. Besides these hand deformities which vary per individual, this variability also accounts for finger dimensions between individuals, finger dimensions within the individual due to growth, disease progression and changes in dimensions during the day. Demand for adjustable or modular designs is thus amplified for the DMD focus group. This is more easily facilitated by designs that contain straps or finger inserts. The urge for flexible designs vs. rigid designs also increases as flexible designs have more intrinsic ability to adjust to small changes due to their compliance. Intrinsic compliance is also favourable for biomechanical compatibility, having more potential for quick and proper joint alignment.
In the end no perfect fastening method exists. Needs, wishes and tolerances of the user change over time highlighting different requirements from the list in Appendix C. Many designers have attempted to combine the different fastening methods. Some of these hybrid fastenings make sense. Such as the combination of finger inserts with straps, where one provides rigidity for force transmission and the other enables bigger adjustability. Others are less clear such as the use of gloves as liner for their strap fasteners as done by Aubin (2013) and Li (2011) [89], [152]. The benefit of the open strap structure is being opposed by glove that is used to provide a soft structure. Gloves that are combined with end point inserts are more sensible, as actually just an more open structure to the glove is created whilst still preserving the compliance and soft interface benefits of a glove fastening. A final remark about fastening methods is that appearance does matter. Patients have to wear their orthosis every day during a lifetime and the goal is for the orthosis to be fully accepted. Fastening should therefore be personal and aim to facilitate as slim and low encumbrance actuator mechanisms as possible. This will reduce not only practical things like hindrance but also increase the feeling of ownership by expressing personality and freedom.

4.D) CONCLUSION

All orthosis designs need an interface between the human and the device, however not always attention is paid to this connection. Especially for the DMD user group higher standards are required as the device is daily worn over the course of years, by people with deformities and reduced skin and muscle integrity. Gloves are compliant soft interfaces but at the cost of tactile, cleaning and force transmission properties. Finger inserts in contrary have more efficient force transmission, can be made modular, have better cleaning properties and have a more open structure. However, they have worse intrinsic compliance and the rigid configurations cause discomfort due to shear whilst putting them over the fingers. Strap types are suitable regarding adjustability to different hand sizes and differences during the day. They do however require more donning time and they can become tighter or more loose during the day. Combining several methods is a possibility however should only be done when both methods strengthen each others advantages.

5. DISCUSSION

Within Section 2. Baker's ergonomic equation (3) was given. This equation describes the chances for success or failure of assistive technology use. The elements it contains should be kept in mind when designing a dynamic hand orthosis. The numerator consists of "Motivation" only, for DMD patients this element can be expected to be high. An assistive device can help them perform ADL activities and so become more independent but also increase options for social participation. To that end success or failure of the device can be accounted purely to the quality of the design on the four elements in the denominator; "Physical Effort (PE)", "Cognitive Effort (CE)", "Linguistic Effort (LE)" and "Time Load (TL)". These elements can be used to define design requirements by the method of Yang et al. [105]. Linguistic Effort is negligible as it is only related to the control interface, which is disregarded within this review. This leaves PE, CE and TL as key factors for the success of dynamic hand orthosis for DMD patients. From these three aspects, combined with the patient characteristics described in Section 3., customer requirements can be identified from Appendix C. These then can be transferred into functional requirements by the same means, including the existing fixture designs from Section 4..

PE relates to movement exertion, motor strength, endurance, fatigue and ROM limitations [107]. Due to the symptoms of their disease for DMD patients this effort shall be relatively high. Physical effort should be reduced to the minimum, and thus some design aspects should be kept in mind:

Adaptability of the device is of great importance and can be interpreted in several ways. First, DMD patients have different needs throughout disease progression. In the beginning, it is mainly for rehabilitation purposes to maintain as much muscle function as possible. Then it will pass into assistance instead to keep independent functioning. Finally the device will only be for therapeutic aims trying to prevent hand deformations and pain due to muscle stiffness in the form of passive stretching. Preferred assistance also changes during the day as DMD patients are easily fatigued. The device should thus be adaptable to Assist As Needed at all times. A second way in which adaptability is essential in the physical domain is that the device needs to have biomechanical compatibility with different hand sizes. Not only because hand sizes differ between different users, but also as fingers of DMD patients still grow, might swell or slink during the day and deform over the long haul. The properties should, therefore, be either adjustable or modular. A last definition for adaptability is that the device is worn all day, thus should be usable in different environments. It helps perform all sorts of functions so should be able to adapt to the needs of the environment quickly.

Tolerability refers to how a user is affected by wearing the device. Tolerance is an issue when designing for DMD patients. It is hampered by different aspects of the disease. Soft snug interfaces are needed to prevent skin damage of the fragile and sensitive DMD skin. This also means the device should contain some intrinsic compliance to avoid chafing. This compliance is also needed for the second interpretation of tolerability. Joint alignment is needed for biomechanical compatibility but is difficult when dealing with upcoming hand deformities. Compliant properties of the fixture and actuator are then needed for properly aligned force transmission. A last objective for compliance is that it avoids blood vessel obstruction allowing blood flow into the fingers. A third call for tolerance can be assigned to changes in muscle integrity. As muscles become stiffer their tolerance towards applied forces will decrease. At some point, limiting motion of the dynamic hand orthosis to natural hand movement is not enough for the diseased hand muscles. Good sense of applied and required forces should be present and adjusted to the different disease stages. This also counts for the speeds at which the motion is powered, as stiff muscles can not endure too fast motions. Lastly, tolerance is of importance for the donning and doffing of the device. Sliding movements over the fingers, like used in finger inserts, are easily experienced as painful or uncomfortable. When too uncomfortable to put on the device will not be worn at all.

When looking at the CE domain it is about the amount of thinking involved in the use of the device. Although this is mostly related to the actuation and control of the system, it can also be related to pain levels. Tolerance, in this way, would also influence the cognitive effort of the user. Pain thresholds are highly personal, but overall are lowered within DMD patients. Experienced control by the user, as defined as *"Ownership"* within the design requirement overview of Appendix C, can be established by some embodiment aspects. A feeling of ownership is important as the assistive device is used to improve independence of the user instead of translating it from family or caretaker to a device. The orthosis should, therefore, incorporate open fingertip and palm structures for natural sensation and sense user intention. The hand orthosis this way will become an extension of oneself.

Lastly, TL is a determinant for success. Within dynamic hand orthoses, this refers to two aspects. First, it depends on the actuation speed of the orthosis. An endeavour is that the assisted hand moves as quickly as a healthy hand when performing the same task. However, as muscle tolerances to assisted grasp speeds lower due to stiffness, this is not a consistently realistic aim. As the device transfers from assistive to therapeutic, this aspect will become eventually redundant. The second aspect inverses this importance. Donning and doffing of the device can take a little longer when a long wearing time is opposite to it. This is in rehabilitative and assistive devices that are worn for the full day after donning. However when the purpose becomes therapeutic donning and doffing should be done quicker as the duration of wearing is only for an hour or so and occurs several times a day.

Functional and customer requirements that are deemed important are described above and shown in Table 6. Some of them have also been described by the literature in Section 2.. Such as "Wearability" and "Safety" which combined in meaning are similar to "Tolerability". Another one is "Variability in hand dimensions", which in Section 2. strictly referred to between patient variability, but here was broadened into "Adaptability". Other requirements that were identified as important based on the number of times it was mentioned within the literature are of less meaning for DMD patients due to their characteristics. For example "Portability", which in this case is different as DMD patients are wheelchair-bounded. Same accounts for "Weight" as heavy power supplies can be carried by the wheelchair and do not need to be carried around by the user himself.

Now there are many dynamic hand orthosis designs, however none of them have made it to market yet. The hand is a complex body part to assist, as it is fragile, used for many varying tasks and has a difficult anatomy. Nevertheless what was found within Section 2. and 4., is that the fundamentals of design processes are missing. Design requirements are either not clearly defined or lack of scientific backup. Same accounts for closing the design process. Validation of concepts outside of the lab is missing, and user feedback is kept out of the loop or is limited to a small group of healthy subjects. This stagnates the development of dynamic hand orthoses as it is all within the chaos. This can be seen within the designs of fastening systems where many different mechanisms have been attempted. It is still unclear which type of fixtures have highest potential as very little attention is paid to it. For further improvement of the hand-orthosis interface design requirements established in Table 6 need to be taken into account. These adjustments to embodiment design of the orthoses will through the CE, PE and TL elements of Bakers ergonomic equations increase the acceptance and use of assistive devices for DMD patients.

TABLE 6. Design Requirements for dynamic hand orthosis for DMD patients.

CRs	FRs
Adaptability	
Assist As Needed	From high user participation to complete assistance to passive stretching
	Assistance of extension before flexion as extensors are affected first
	Different assistance levels during the day due to fatigue.
Hand sizes	Modularity for between patient differences
	Adjustability for within patient differences
	Compatibility to hand deformities
Environmental Compatibility	Usable in different environments performing varying task
	Material choice and modularity for easy cleaning
Tolerability	
Skin Integrity	Soft snug interface to prevent skin damage/discomfort
Muscle Integrity and Overwork	Natural movement until limbs are not capable of these anymore
	Fitting grasp speed
Compliance	Prevent blood vessel obstruction
	Joint and force alignment to deformities
	No chafing between orthosis and the skin
Comfortable Donning/Doffing	Avoid sliding motions during donning/doffing
Ownership	
Natural Sensation	Open finger tip and palm structure
User in Control	Sense user intention
Time Load	
Grasp Speed	Rehabilitation and Assistance need fast actuation speeds that are comparable to normal hand functioning
	Therapeutic needs slow activaton as the stiff muscles can not withstand fast speeds
Donning/Doffing	Rehabilitation and Assistance are fine with longer donning and doffing times
	Therapeutics need quick donning and doffing

Before the functional requirements become useful, they should be translated into design parameters. Hence the requirements should be either further specified, quantified or both. Achieving design parameters for dynamic hand orthoses for DMD patients is challenging. Limitations and needs are time variable, highly personal or not measured before. This urges for setting outer boundaries, allowing different settings within this range, and for more research and measurements of certain parameters. Some parameters can be based on measurements of healthy subjects. For example, when the device is in the assistive phase, minimal requirements could be functional ROM and functional force exertion for task completion of which values indicated can be seen in C. Maximal requirements can be set to those of healthy hands, so avoiding hyperextension or too high compressing forces. Normal ROM of the hands compared to functional ROM of the hands were described by Hume et al. in 1990 [161]. Speed of actuation must be fast, because when task performance is faster without the orthosis, the orthosis shall likely not be worn. Duration of closing movement was indicated as ~ 1 [s] by Bützer (2019) [162], actuation speed has been mentioned twice. Once as 0.2 [Hz] by Wang et al. (2018) [134] and once as 1.5 [Hz] by Gasser et al. (2015) [163]. Both values are claimed to be sufficient for ADL use. Data here is thus controversial and should be investigated further.

When in the rehabilitative phase, limitations can be based on muscle contraction values, as overuse should be avoided. Fatigue free muscle contraction has been identified as 20 [%] of maximal voluntary muscle contraction [164]. And so could be used as an outer boundary for allowable muscle contraction for DMD patients in early disease phases, before assistance should occur. Actuation speeds should be adjusted to what is allowed by the muscular changes. No information about this has been found, and lower boundaries should also be identified as when the device is too slow to be functional. However, as the hand can not function without the orthosis, the user shall be less bothered by slower movements. As the device is used for passive stretching, boundaries of applied forces and ROM should be related to pain thresholds of the patients and the amount of muscular resistance. Within the literature found in the different sections above, none described or researched these thresholds and therefore limits are unknown. Maximal ROM of the device should for now be set to those of the normal ROM of healthy hands and further research into pain thresholds should be conducted. Actuation speed during passive stretching is not essential and is strictly limited to pain thresholds of the user. No information was found on these thresholds, and more research in this field should be conducted.

Hand sizes could also be based on those of healthy subjects. No literature search on statistical hand dimensions has been performed. Neither has research been performed of fluctuations of finger diameters during the days or seasons. However, perhaps some information on this can be found within the jewellery industry or anthropometric databases. These 'normal' dimensions should then be altered according to the severity and type of hand deformities that start to occur over time. Occurrence of deformities have been described by Wagner et al. in 1989 and 1993 [11], [48]. Here is stated

that deformities and functioning are age related. Severity is indicated by function loss instead of joint measurements and data indicated here are thus not useful for creating design requirements.
More research should also be conducted into pain thresholds of DMD patients towards several interactions. Firstly actuation speeds, as already described above, secondly passive ROM and lastly tolerances towards clamping forces. The fit between fingers and fastening should be snug enough to avoid chafing, and loose enough to avoid blood vessel obstruction and skin damage. Values here are unknown and should be measured and tested with the real user group. No indication of values can now be given.
Lastly, the time needed for donning and doffing should be surveyed. How quickly should this be done when the device is taken off and put on several times a day, and how do these limits change when this action has to be performed once a day. Donning and doffing time limitations have been reported within the found literature once. Kuswanto et al. (2018) found values of less than 1 minute for quick donning and doffing [165]. This requirement was obtained by testing their hand exoskeleton design with three different users. No other researches have been found for comparison.
So to some extent, boundaries of requirements can be defined. However, values are still controversial, lack solid argumentation or are taken as outer boundaries based on healthy subjects. These values can be used now, until further research is conducted with DMD patients.

6. CONCLUSION

This literature survey was conducted within the Delft Institute of Prosthetics and Orthotics as an addition to the development of dynamic hand orthosis for DMD patients. It continues on previous reviews done by Bos et al. [28] and Baan [73], who created an overview of over 200 dynamic hand orthoses based on their actuation systems. Within their reports it was not addressed how these mechanism have been connected to the user, making them wearable. The aim of this research was to look into the design requirements used in dynamic hand orthoses, relate them to the user group of DMD patients and further look into the embodiment design of the hand-orthosis interface.
From current design articles it was established that many iterations are still lying within the future. However in order to obtain an efficient design process it is important that documentation of design choices and their testing results are reported with care. This starts by clear definition of design requirements for a specific user group, and ends with validation of the concept by including the end user. To obtain fitting design requirements a look was taken at the characteristics of DMD patients. From literature found here a few conclusions could be established, beginning with the fact that quantification and measurement of the disease progress as done now is not usable for creating accurate design parameters. This is due to the fact that scales currently used rely on subjective functional scales instead of parameter values that are measurable. Still some patient characteristics could be used to draft some customer requirements. High variability between and within patient dimensions and disease progression call for adjustable and modular properties, reduced skin and muscle integrity demand higher attention to tolerability and donning/doffing methods. Furthermore as the device is assistive, shall be worn all day and is meant to conserve some independence, the feeling of ownership of the user over the device must be established. This should not only be done by creating a good controller, but also by preservation of natural sensation. Some other customer requirements that were deemed important in Section 2. can be differently interpret for DMD patients. So the definition of portability can be broadened as the confinement to a wheelchair creates possibilities for other actuation systems and power supplies. When evaluating current embodiment designs of hand orthoses, many different fastening mechanism could be identified as shown in Figure 23. All have their benefits and drawbacks and no ideal fixture can be identified yet. Important properties are soft and snug interfaces, some intrinsic compliance, adjustability and/or modularity, easy cleaning and comfortable donning and doffing. Combining different fastening mechanisms has potential, but should only be done when they reinforce each others benefits.

ACKNOWLEDGEMENTS

Chair

Prof.dr. F.C.T. van der Helm
Delft University of Technology, Faculty of Mechanical, Maritime and Materials Engineering, Department of BioMechanical Engineering, The Netherlands.

Supervisor

Dr.ir. D.H. Plettenburg
Delft University of Technology, Faculty of Mechanical, Maritime and Materials Engineering, Department of BioMechanical Engineering, Delft Institute of Prosthetics and Orthotics, The Netherlands.

4.

Final Remarks

Final Remarks

During my graduation year I did an internship, performed a literature study and designed a hydraulic thumb module for the Symbihand. Here I will try to bring these experiences together and translate them into some take home messages.

ASSISTIVE DEVICES AND REHABILITATION TECHNOLOGY ARE EMERGING.

Literature was replete with all sorts of assistive and rehabilitative devices focused on hand function. However it is striking that few of the designs are commercially available or implemented in the medical field. Apparently, despite the scientific attention technology is either not there yet, or it has not yet seeped into the protocols of the care givers. As was recently stressed in a seminar of the Technologie en Zorgacademie (TZA), it is often unclear to the caregivers for whom and for what reason to implement healthcare technology. Design projects should therefor have a defined target group and design requirements that implicate for what situation the product is developed. This thesis focused on assisting Duchenne Muscular Dystrophy patients with a Brooke scale of 4,5 or 6 in activities of daily living.

THE USER SHOULD BE INCLUDED IN THE DESIGN PROCESS MORE PROMINENTLY.

In the field of orthotics, technology and the user could not work closer together. During my internship I met some SCI patients at de Hoogstraat revalidatie and experienced how valuable it is to meet your target group. Literature makes more sense and the effect of the disease becomes much more clear. Due to the corona virus, to my regret I did not attempt to meet Duchenne patients, however I am sure it would have shifted my perspective somehow. It is in contradiction that as emerged from my literature review inclusion of the user in the design process is a scarce phenomenon. This is reflected in current design results. Devices are bulky, heavy, noisy, cover the entire hand with straps or a glove and little attention is paid towards comfort and usability. In the Symbihand and the thumb module these elements were taken into account, however should be implemented further. Main points of improvement are the hand-shell interface which should be padded, adjustability to various hand sizes and the comfort of donning and doffing.

THE NEED FOR CLEAR DESIGN REQUIREMENTS.

Due to high variability between and within patients regarding the disease course and expression, it is often difficult to state clear requirements for the design of active orthoses. In Duchenne Muscular Dystrophy there is also the case that quantification and measurement of the disease progress is not usable for creating accurate design parameters, since they are based on functional scales. As I stated in my literature review a method that can be used to determine requirements is by translating customer requirements (CRs) into functional requirements (FRs) and then quantify them with design parameters (DPs). In this thesis I endeavored to apply this method for grasping properties and by stressing the need for ownership and the concomitant need for tactile feedback. It is not only important to have clear requirements for a specified target group during your design process, it is also important to document them in literature appropriately. By evaluating the design as well as your requirements, others can continue on your findings, resulting in more efficient design processes and acceleration of innovation.

THE COMPLEXITY OF THE HAND.

The hand is an essential, but complex part of the human body. As has been stressed more often throughout this thesis, the hand is our main way of humans interacting with their environment. Grasping is achieved based on visual, proprioceptive and tactile feedback, and every person executes this in their own manner. To account for the most functional grasps of the hand according to literature, grasping taxonomies can be reduced to three grasp types: the lateral pinch, precision pinch and cylindrical grasp should be implemented. These grasps can be executed by controlling the thumb separately, from the simultaneous control of the four finger digits. It is difficult to precisely predict the trajectory of the assisted thumb, as the movements are highly related to the anatomic structures and limitations. An incredibly simplified mock-up thumb has been implemented to represent merely the restrictions of the bone shapes, however it could be more accurate by implementing artificial tendons and ligaments.

THE POTENTIAL OF HYDRAULICS IN ACTIVE HAND ORTHOSES.

Even though, hydraulic actuation of the hand is not the most efficient way of assisting the hand, hydraulics are a valid option for the design of active orthoses. The prototype uses a miniature hydraulic cylinder to facilitate conical thumb movement towards the index finger. Hereby, it is meant to facilitate the lateral and precision pinch as well as the cylindrical grip. The device is advantageous due to the light weight, relative slimness and the allowance of tactile feedback. Lamentably, the design is not able to achieve the necessary range of motion and force levels. To reach better levels of its potential, the device should be improved by it compliant elements, geometric relations and the custom piston-cylinder attachment or dimensions. Then before presenting it to a panel of potential users, improvements must be made regarding comfort.

References

REFERENCES

[1] A. E. Flatt, "Our Thumbs," Baylor University Medical Center Proceedings, vol. 15, no. 4, pp. 380–387, 2002.

[2] B. Hirt, H. Seyhan, M. Wagner, and R. Zumhasch, Hand and Wrist Anatomy and Biomechanics; A Comprehensive Guide. Thieme, 2017.

[3] M. Suarez-Escobar, J. A. Gallego-Sanchez, and E. Rendon-Velez, "Mechanisms for linkage-driven underactuated hand exoskeletons: conceptual design including anatomical and mechanical specifications," International Journal on Interactive Design and Manufacturing, vol. 11, no. 1, pp. 55–75, 2017.

[4] P. Aqueveque, P. Ortega, E. Pino, F. Saavedra, E. Germany, and B. Gómez, "After Stroke Movement Impairments - A review of current technologies for rehabilitation," in Physical Disabilities - Therapeutic Implications, ch. 7, p. 13, Intech, 2016.

[5] A. Pedrocchi, S. Ferrante, E. Ambrosini, M. Gandolla, C. Casellato, T. Schauer, C. Klauer, J. Pascual, C. Vidaurre, M. Gföhler, W. Reichenfelser, J. Karner, S. Micera, A. Crema, F. Molteni, M. Rossini, G. Palumbo, E. Guanziroli, A. Jedlitschka, M. Hack, M. Bulgheroni, E. D 'amico, P. Schenk, S. Zwicker, A. Duschau-Wicke, J. Miseikis, L. Graber, and G. Ferrigno, "MUNDUS project: MUltimodal Neuroprosthesis for daily Upper limb Support," Journal of NeuroEngineering and Rehabilitation, vol. 10, p. 1, 2013.

[6] Q. Boser, M. Dawson, D. G. Schofield, J.S, and J. Hebert, "Defining the design requirements for an assistive powered hand exoskeleton: A pilot explorative interview study and case series," Prosthetics and Orthotics International, 2020.

[7] R. Bos, Mechanical design of dynamic hand orthoses; Expanding technology with comprehensive overviews and alternative pathways. PhD thesis, Delft University of Technology, 2019.

[8] K. Nizamis, Hand Neuro-Motor Characterization and Motor Intention Decoding in Duchenne Muscular Dystrophy . PhD thesis, University of Twente, 2019.

[9] K. Bushby, R. Finkel, D. J. Birnkrant, L. E. Case, P. R. Clemens, L. Cripe, A. Kaul, K. Kinnett, C. McDonald, S. Pandya, J. Poysky, F. Shapiro, J. Tomezsko, and C. Constantin, "Diagnosis and management of Duchenne muscular dystrophy, part 1: diagnosis, and pharmacological and psychosocial management," The Lancet Neurology, vol. 9, pp. 77–93, 1 2010.

[10] D. J. Blake, A. Weir, S. E. Newey, and K. E. Davies, "Function and genetics of dystrophin and dystrophin-related proteins in muscle," Physiological Reviews, vol. 82, no. 2, pp. 291–329, 2002.

[11] M. B. Wagner, P. J. Vignos, and C. Carlozzi, "Duchenne muscular dystrophy: A study of wrist and hand function," Muscle & Nerve, vol. 12, pp. 236–244, 3 1989.

[12] D. R. Steinberg, "Bone, Joint, and Muscle Disorders - Swan Neck Deformity," MD manual Consumer version, 2020, May. Retrieved from https://www.msdmanuals.com/home/bone,-joint,-and-muscle-disorders/hand-disorders/swan-neck-deformity.

[13] M. C. Walter and P. Reilich, "Recent developments in Duchenne muscular dystrophy: facts and numbers," Journal of Cachexia, Sarcopenia and Muscle, vol. 8, no. 5, pp. 681–685, 2017.

[14] S. Ryder, R. M. Leadley, N. Armstrong, M. Westwood, S. De Kock, T. Butt, M. Jain, and J. Kleijnen, "The burden, epidemiology, costs and treatment for Duchenne muscular dystrophy: An evidence review," Orphanet Journal of Rare Diseases, vol. 12, no. 1, pp. 1–21, 2017.

[15] D. J. Birnkrant, K. Bushby, C. M. Bann, S. D. Apkon, A. Blackwell, M. K. Colvin, L. Cripe, A. R. Herron, A. Kennedy, K. Kinnett, J. Naprawa, G. Noritz, J. Poysky, N. Street, C. J. Trout, D. R. Weber, and L. M. Ward, "Diagnosis and management of Duchenne muscular dystrophy, part 3: primary care, emergency management, psychosocial care, and transitions of care across the lifespan," The Lancet Neurology, vol. 17, pp. 445–455, 5 2018.

[16] M. M. H. P. Janssen, A. Bergsma, A. C. H. Geurts, and I. J. M. de Groot, "Patterns of decline in upper limb function of boys and men with DMD: an international survey," Journal of Neurology, vol. 261, pp. 1289–1290, 7 2014.

[17] S. E. Tomlinson, R. Lewis, and M. J. Carré, "Review of the frictional properties of finger-object contact when gripping," Proceedings of the Institution of Mechanical Engineers, Part J: Journal of Engineering Tribology, vol. 221, no. 8, pp. 841–850, 2007.

[18] Parent Project Muscular Dystrophy, "Ten Year Registry Report," tech. rep., 2017.

[19] K. Stone, T. C., J. Blakeney, A. Howarth, H. McAndrew, N. Traynor, M. McCutcheon, and R. Johnston, Occupational Therapy and Duchenne Muscular Dystrophy. John Wiley & Sons, 2007.

[20] A. E. Emery, F. Muntoni, and R. C. M. Quinlivan, Duchenne Muscular Dystrophy. Oxfort University Press, 4th editio ed., 2015.

[21] J. Weichbrodt, B. M. Eriksson, and A. K. Kroksmark, "Evaluation of hand orthoses in Duchenne muscular dystrophy," Disability and Rehabilitation, vol. 40, no. 23, pp. 2824–2832, 2018.

[22] J. P. J. Bakker, I. J. M. de Groot, A. Beelen, G. J. Lankhorst, D. Behm, A. Blazevich, A. Kay, M. McHugh, L. Doglio, E. Pavan, I. Pernigotti, P. Petralia, C. Frigo, C. Minetti, A. M. Glanzman, J. M. Flickinger, K. H. Dholakia, C. G. Bönnemann, R. S. Finkel, I.-Y. Jung, J. H. Chae, S. K. Park, J. H. J. Y. Kim, J. H. J. Y. Kim, S. J. Kim, M. S. Bang, R. K.J., B. J., N. K.N., H. N. Lee, H. Sawnani, P. Horn, I. Rybalsky, L. Relucio, B. L. Wong, C. M. McDonald, R. T. Abresch, G. T. Carter, W. M. Fowler Jr., E. R. Johnson, D. D. Kilmer, B. J. Sigford, M. Of, L. Contractures, N. Diseases, S. Pandya, J. M. Florence, W. M. King, J. D. Robison, M. Oxman, M. A. Province, C. R. Senesac, D. J. Lott, S. C. Forbes, S. Mathur, I. Arpan, E. S. Senesac, G. A. Walter, K. Vandenborne, A. J. Skalsky, C. M. McDonald, and M. Sussman, "Prevention and Management of Limb Contractures in," Phys Ther, vol. 23, no. 3, pp. 675–687, 2012.

[23] K. Bushby, R. Finkel, D. J. Birnkrant, L. E. Case, P. R. Clemens, L. Cripe, A. Kaul, K. Kinnett, C. McDonald, S. Pandya, J. Poysky, F. Shapiro, J. Tomezsko, and C. Constantin, "Diagnosis and management of Duchenne muscular dystrophy, part 2: implementation of multidisciplinary care," The Lancet Neurology, vol. 9, pp. 177–189, 2 2010.

[24] A. Bergsma, J. Lobo-Prat, E. Vroom, P. Furlong, J. L. Herder, M. Corrigan, I. de Groot, A. Faisal, N. Goemans, J. Han, M. Iodice, A. Kennedy, B. Koopman, J. L. Prat, M. Main, B. Mathie, F. Muntoni, M. N. Castro, M. Paalman, J. Porter, T. Rahman, J. Schneider, A. Stienen, P. Verstegen, and C. Walsh, "1st Workshop on Upper-Extremity Assistive Technology for People with Duchenne: State of the art, emerging avenues, and challenges. April 27th 2015, London, United Kingdom.," Neuromuscular Disorders, vol. 26, no. 6, pp. 386–393, 2016.

[25] R. F. Pangalila, G. A. Van Den Bos, B. Bartels, M. P. Bergen, M. J. Kampelmacher, H. J. Stam, and M. E. Roebroeck, "Quality of life of adult men with Duchenne muscular dystrophy in the Netherlands: Implications for care," Journal of Rehabilitation Medicine, vol. 47, no. 2, pp. 161–166, 2015.

[26] M. K. Colvin, J. Poysky, K. Kinnett, M. Damiani, M. Gibbons, J. Hoskin, S. Moreland, C. J. Trout, and N. Weidner, "Psychosocial management of the patient with Duchenne muscular dystrophy," Pediatrics, vol. 142, no. October, pp. S99–S106, 2018.

[27] A. I. Batavia and G. S. Hammer, "Toward the development of consumer-based criteria for the evaluation of assistive devices," Journal of Rehabilitation Research and Development, vol. 27, no. 4, pp. 425–436, 1990.

[28] R. A. Bos, C. J. Haarman, T. Stortelder, K. Nizamis, J. L. Herder, A. H. Stienen, and D. H. Plettenburg, "A structured overview of trends and technologies used in dynamic hand orthoses," Journal of NeuroEngineering and Rehabilitation, vol. 13, p. 62, 12 2016.

[29] M. Troncossi, "An Original Classification of Rehabilitation Hand Exoskeletons," Journal of Robotics and Mechanical Engineering Research, vol. 1, no. 4, pp. 17–29, 2016.

[30] P. Heo, G. Gu, S. Lee, K. Rhee, and J. Kim, "Current Hand Exoskeleton Technologies for Rehabilitation and Assistive Engineering," International Journal of Precision Engineering and Manufacturing, vol. 13, no. 5, pp. 807–824, 2012.

[31] B. Radder, A. I. R. Kottink, N. Van Der Vaart, D. Oosting, J. H. Buurke, S. M. Nijenhuis, G. B. Prange, and J. S. Rietman, "User-centred input for a wearable soft-robotic glove supporting hand function in daily life," IEEE International Conference on Rehabilitation Robotics, vol. 2015-Septe, pp. 502–507, 2015.

[32] C. A. Stanger, C. Anglin, W. S. Harwin, and D. P. Romilly, "Devices for Assisting Manipulation: A Summary of User Task Priorities," IEEE Transactions on Rehabilitation Engineering, vol. 2, no. 4, pp. 256–265, 1994.

[33] G. Aumayr, D. Bleier, G. Chroust, and N. Sturm, "Understanding needs and requirements of the target group: Systematic perspective on interaction between system and environment," 25th International Conference on Software, Telecommunications and Computer Networks, SoftCOM 2017, 2017.

[34] R. A. Bos, K. Nizamis, D. H. Plettenburg, and J. L. Herder, "Design of an Electrohydraulic Hand Orthosis for People with Duchenne Muscular

Dystrophy Using Commercially Available Components," Proceedings of the IEEE RAS and EMBS International Conference on Biomedical Robotics and Biomechatronics, vol. 2018-Augus, pp. 305–311, 2018.
[35] J. Lobo-Prat, K. Nizamis, M. M. Janssen, A. Q. Keemink, P. H. Veltink, B. F. Koopman, and A. H. Stienen, "Comparison between sEMG and force as control interfaces to support planar arm movements in adults with Duchenne: A feasibility study," Journal of NeuroEngineering and Rehabilitation, vol. 14, no. 1, pp. 1–17, 2017.
[36] S. F. Duncan, C. E. Saracevic, and R. Kakinoki, "Biomechanics of the hand," Hand Clinics, vol. 29, no. 4, pp. 483–492, 2013.
[37] I. M. Bullock, T. Feix, and A. M. Dollar, "Finding small, versatile sets of human grasps to span common objects," Proceedings - IEEE International Conference on Robotics and Automation, pp. 1068–1075, 2013.
[38] J. J. Crisco, T. Patel, E. Halilaj, and D. C. Moore, "The envelope of physiological motion of the first carpometacarpal joint," Journal of Biomechanical Engineering, vol. 137, no. 10, pp. 1–8, 2015.
[39] K. Nizamis, A. H. A. Stienen, D. G. Kamper, T. Keller, D. H. Plettenburg, E. J. Rouse, D. Farina, B. F. J. M. Koopman, and M. Sartori, "Transferrable Expertise From Bionic Arms to Robotic Exoskeletons: Perspectives for Stroke and Duchenne Muscular Dystrophy," IEEE Transactions on Medical Robotics and Bionics, vol. 1, no. 2, pp. 88–96, 2019.
[40] M. M. Janssen, J. Harlaar, B. Koopman, and I. J. de Groot, "Unraveling upper extremity performance in Duchenne muscular dystrophy: A biophysical model," Neuromuscular Disorders, vol. 29, no. 5, pp. 368–375, 2019.
[41] A. M. Seferian, A. Moraux, M. Annoussamy, A. Canal, V. Decostre, O. Diebate, A. G. Le Moing, T. Gidaro, N. Deconinck, F. Van Parys, W. Vereecke, S. Wittevrongel, M. Mayer, K. Maincent, I. Desguerre, C. Thémar-Noël, J. M. Cuisset, V. Tiffreau, S. Denis, V. Jousten, S. Quijano-Roy, T. Voit, J. Y. Hogrel, and L. Servais, "Upper limb strength and function changes during a one-year follow-up in non-ambulant patients with duchenne muscular dystrophy: An observational multicenter trial," PLoS ONE, vol. 10, no. 2, 2015.
[42] F. L. Mattar and C. Sobreira, "Hand weakness in Duchenne muscular dystrophy and its relation to physical disability," Neuromuscular Disorders, vol. 18, no. 3, pp. 193–198, 2008.
[43] M. Jansen, I. Jm De Groot, N. Van Alfen, and A. C. Geurts, "Physical training in boys with Duchenne Muscular Dystrophy: the protocol of the No Use is Disuse study," BMC Pediatrics, vol. 10, no. 55, 2010.
[44] M. Eagle, S. V. Baudouin, C. Chandler, D. R. Giddings, R. Bullock, and K. Bushby, "Survival in Duchenne muscular dystrophy: improvements in life expectancy since 1967 and the impact of home nocturnal ventilation," Neuromuscular Disorders, vol. 12, pp. 926–929, 12 2002.
[45] J. P. Lord, M. M. Portwood, J. S. Lieberman, W. M. Fowler Jr, and P. Berck, "Upper extremity functional rating for patients with Duchenne muscular dystrophy.," Archives of physical medicine and rehabilitation, vol. 68, no. 3, pp. 151–154, 1987.
[46] M. Kohler, C. Clarenbach, C. Bahler, T. Brack, E. Russi, and K. Bloch, "Disability and Survival in Duchenne Muscular Dystrophy," Journal of Neurology, Neurosurgery & Psychiatry, vol. 80, no. 3, pp. 320–325, 2009.
[47] B. Bartels, R. F. Pangalila, M. P. Bergen, N. A. Cobben, H. J. Stam, and M. E. Roebroeck, "Upper limb function in adults with Duchenne muscular dystrophy," Journal of Rehabilitation Medicine, vol. 43, no. 9, pp. 770–775, 2011.
[48] M. Wagner, P. Vignos, C. Carlozzi, and A. Hull, "Assessment of Hand Function in Duchenne Muscular Dystrophy," Archives of Phyisical Medicine and Rehabilitation, vol. 74, no. 8, pp. 801–804, 1993.
[49] L. A. Jones and S. J. Lederman, Human Hand Function. Oxford University Press, 2006.
[50] M. Backhouse, L. Harding, S. Rodger, and N. Hindman, "Investigating sensory processing patterns in boys with Duchenne muscular dystrophy using the sensory Profile," British Journal of Occupational Therapy, vol. 75, no. 6, pp. 271–280, 2012.
[51] D. Green, "Are proprioceptive functions affected in Duchenne muscular dystrophy?," Developmental Medicine and Child Neurology, vol. 56, no. 9, pp. 805–806, 2014.
[52] M. M. Janssen, J. C. Hendriks, A. C. Geurts, and I. J. de Groot, "Variables associated with upper extremity function in patients with Duchenne muscular dystrophy," Journal of Neurology, vol. 263, no. 9, pp. 1810–1818, 2016.
[53] I. Alemdaroglu, A. Karaduman, O. T. Yilmaz, and H. Topaloglu, "Different types of upper extremity exercise training in Duchenne muscular dystrophy: Effects on functional performance, strength, endurance, and ambulation," Muscle and Nerve, vol. 51, no. 5, pp. 697–705, 2015.
[54] Y. Lu and Y. Lue, "Strength and Functional Measurement for Patients with Muscular Dystrophy," in Muscular dystrophy, vol. 32, ch. 7, pp. 671–688, Intech, 2012.
[55] A. Van Boeijen, J. Daalhuizen, R. van der Schoor, and J. Zijlstra, Delft Design Guide: Design strategies and methods. Bis B.V., Uitgeverij (BIS Publishers), 1st ed., 2014.
[56] G. Cotugno, K. Althoefer, and T. Nanayakkara, "The Role of the Thumb: Study of Finger Motion in Grasping and Reachability Space in Human and Robotic Hands," IEEE Transactions on Systems, Man, and Cybernetics: Systems, vol. 47, no. 7, pp. 1061–1070, 2017.
[57] V. Gracia-Ibáñez, J. L. Sancho-Bru, and M. Vergara, "Relevance of grasp types to assess functionality for personal autonomy," Journal of Hand Therapy, vol. 31, no. 1, pp. 102–110, 2018.
[58] A. Kargov, C. Pylatiuk, J. Martin, S. Schulz, and L. Döderlein, "A comparison of the grip force distribution in natural hands and in prosthetic hands," Disability and Rehabilitation, vol. 26, no. 12, pp. 705–711, 2004.
[59] N. Smaby, M. E. Johanson, B. Baker, D. E. Kenney, W. M. Murray, and V. R. Hentz, "Identification of key pinch forces required to complete functional tasks," Journal of Rehabilitation Research and Development, vol. 41, no. 2, pp. 215–223, 2004.
[60] M. Kutz, Biomedical Engineering and Handbook; Volume 1: Fundamentals, vol. 1. McGraww-Hill, 2nd ed., 2009.
[61] H. T. Lin, L. C. Kuo, H. Y. Liu, W. L. Wu, and F. C. Su, "The three-dimensional analysis of three thumb joints coordination in activities of daily living," Clinical Biomechanics, vol. 26, no. 4, pp. 371–376, 2011.
[62] L. Smulders, G. Prange, A. Stienen, and J. V. Wijngaarden, "Requirements for an assistive device for the hemiparetic patient : an orthosis for the supporting hand in bimanual activities," pp. 1–8.
[63] W. J. Mallon, H. R. Brown, and J. A. Nunley, "Digital ranges of motion: Normal values in young adults," Journal of Hand Surgery, vol. 16, no. 5, pp. 882–887, 1991.
[64] A. S. Augurelle, A. M. Smith, T. Lejeune, and J. L. Thonnard, "Importance of cutaneous feedback in maintaining a secure grip during manipulation of hand-held objects," Journal of Neurophysiology, vol. 89, no. 2, pp. 665–671, 2003.
[65] K. Nizamis, W. Schutte, J. J. Grutters, J. Goseling, N. H. Rijken, and B. F. Koopman, "Evaluation of the cognitive-motor performance of adults with Duchenne Muscular Dystrophy in a hand-related task," PLoS ONE, vol. 15, no. 1, pp. 1–17, 2020.
[66] W. Durfee, J. Xia, and E. Hsiao-wecksler, "Tiny Hydraulics for Powered Orthotics," 2011.
[67] J. Xia and W. K. Durfee, "Analysis of small-scale hydraulic actuation systems," Journal of Mechanical Design, Transactions of the ASME, vol. 135, no. 9, pp. 1–11, 2013.
[68] L. J. Love, R. F. Lind, and J. F. Jansen, "Mesofluidic actuation for articulated finger and hand prosthetics," 2009 IEEE/RSJ International Conference on Intelligent Robots and Systems, IROS 2009, pp. 2586–2591, 2009.
[69] G. Smit, D. H. Plettenburg, and F. C. van der Helm, "Design and evaluation of two different finger concepts for body-powered prosthetic hand," Journal of Rehabilitation Research and Development, vol. 50, no. 9, pp. 1253–1266, 2013.
[70] A. I. Kapandji, "Clinical evaluation of the thumb's opposition," Journal of Hand Therapy, vol. 5, no. 2, pp. 102–106, 1992.
[71] X. Zhang, P. Braido, S. W. Lee, R. Hefner, and M. Redden, "A normative database of thumb circumduction in vivo: Center of rotation and range of motion," Human Factors, vol. 47, no. 3, pp. 550–561, 2005.
[72] M. De Volder and D. Reynaerts, "Pneumatic and hydraulic microactuators: A review," Journal of Micromechanics and Microengineering, vol. 20, no. 4, 2010.
[73] M. Baan, "Designs of Dynamic Flat Hand Orthoses," Master Thesis TU Delft, 2019.
[74] I. M. de Apellaniz Goenaga, "Development of a 3D printed hydraulic piston-cylinder system," Master Thesis TU Delft, 2019.
[75] C. L. Nall and P. A. Bhounsule, "A miniature 3D printed on-off linear pneumatic actuator and its demonstration into a cartoon character of a hopping lamp," Actuators, vol. 8, no. 4, 2019.
[76] J. Krause and P. Bhounsule, "A 3D printed linear pneumatic actuator for position, force and impedance control," Actuators, vol. 7, no. 2, 2018.
[77] L. Martini, Practical Seal Design. New York: Taylor & Francis, 1984.
[78] D. H. Plettenburg, "A Sizzling Hand Prosthesis; On the design and development of a pneumatically powered hand prosthesis for children," Doctoral Dissertation, TU Delft, 2002.

[79] G. Smit, D. H. Plettenburg, and F. C. Van Der Helm, “The lightweight Delft Cylinder hand: First multi-articulating hand that meets the basic user requirements,” IEEE Transactions on Neural Systems and Rehabilitation Engineering, vol. 23, no. 3, pp. 431–440, 2015.

[80] L. Janssen and M. Warmoeskerken, Transport Phenomena Data Companion. VSSD, 3rd ed., 2006.

[81] Oceanz, “OCEANZ PA12 Datasheet for flexible polyamide parts produced by Selective Laser Sintering,” tech. rep., 2020. Retrieved from https://www.oceanz.eu/producten-en-service/materialen/Oceanz-PA12/.

[82] G. Grayson, “Biomimetic Robotic Prosthetic Hand,” Pinshape.com. Retrieved from https://pinshape.com/items/36355-3d-printed-biomimetic-robotic-prosthetic-hand.

[83] L. Y. Chang and Y. Matsuoka, “A kinematic thumb model for the ACT hand,” Proceedings - IEEE International Conference on Robotics and Automation, vol. 2006, no. May, pp. 1000–1005, 2006.

[84] A. Hollister, W. Buford, L. Myers, D. Giurintano, and A. Novick, “The axes of rotation of the thumb carpometacarpal joint,” Journal of Orthopedic Research, vol. 10, pp. 454–460, 1993.

[85] A. Hollister, D. J. Giurintano, W. L. Buford, L. M. Myers, and A. Novick, “The axes of rotation of the thumb interphalangeal and metacarpophalangeal joints,” Clinical Orthopaedics and Related Research, no. 320, pp. 188–193, 1995.

[86] A. Hollister and D. J. Giurintano, “Thumb Movements, Motions, and Moments,” Journal of Hand Therapy, vol. 8, no. 2, pp. 106–114, 1995.

[87] G. Smit and D. H. Plettenburg, “Efficiency of voluntary closing hand and hook prostheses,” Prosthetics and Orthotics International, vol. 34, no. 4, pp. 411–427, 2010.

[88] J. Cool, Werktuigkundige systemen. Delft Academic Press, 3e ed., 2013.

[89] P. Aubin, H. Sallum, C. Walsh, L. Stirling, and A. Correia, “A Pediatric Robotic Thumb Exoskeleton for at-home rehabilitation,” in IEEE 13th International Conference on Rehabilitation Robotics (ICORR), IEEE, 2013.

[90] M. Cempini, M. Cortese, and N. Vitiello, “A powered finger-thumb wearable hand exoskeleton with self-aligning joint axes,” IEEE/ASME Transactions on Mechatronics, vol. 20, no. 2, pp. 705–716, 2015.

[91] O. Lambercy, D. Schröder, S. Zwicker, and R. Gassert, “Design of a thumb exoskeleton for hand rehabilitation,” i-CREATe 2013 - International Convention on Rehabilitation Engineering and Assistive Technology, in Conjunction with SENDEX 2013, pp. 8–11, 2013.

[92] W. de Jong, T. Lotgering, M. van Leeuwen, K. Berghman, L. van den Elshout, and J. Molenbroek, “DINED - Antropometric database: Dutch students 2016,” 2018. TU Delft - 4TU.Centre for Research Data, Retrieved from https://dined.io.tudelft.nl/en.

[93] W. Dempster and G. Gaughran, “Properties of Body segments based on size and weight,” American Journal of Anatomy, vol. 120, pp. 33–54, 1967.

[94] K. Ghoseiri and M. R. Safari, “Prevalence of heat and perspiration discomfort inside prostheses: Literature review,” Journal of Rehabilitation Research and Development, vol. 51, no. 6, pp. 855–867, 2014.

[95] J. Rahbek, B. Werge, A. Madsen, J. Marquardt, B. F. Steffensen, and J. Jeppesen, “Adult life with Duchenne muscular dystrophy: Observations among an emerging and unforeseen patient population,” Pediatric Rehabilitation, vol. 8, no. 1, pp. 17–28, 2005.

[96] D. Abbott, J. Carpenter, and K. Bushby, “Transition to adulthood for young men with Duchenne muscular dystrophy: Research from the UK,” Neuromuscular Disorders, vol. 22, no. 5, pp. 445–446, 2012.

[97] B. Kim, H. In, D. Y. Lee, and K. J. Cho, “Development and assessment of a hand assist device: GRIPIT,” Journal of NeuroEngineering and Rehabilitation, vol. 14, no. 1, pp. 1–14, 2017.

[98] R. Liang, G. Xu, M. Li, S. Zhang, A. Luo, and T. Tao, “A Novel Variable Stiffness Compliant Finger Exoskeleton for Rehabilitation Based on Electromagnet Control,” Proceedings of the Annual International Conference of the IEEE Engineering in Medicine and Biology Society, EMBS, vol. 2018-July, pp. 3926–3929, 2018.

[99] G. Prange, L. Smulders, J. van Wijngaarden, G. Lijbers, S. Nijenhuis, P. Veltink, J. Buurke, and A. Stienen, “User requirements for assistance of the supporting hand in bimanual daily activities via a robotic glove for severely affected stroke patients,” in 2015 IEEE International Conference on Rehabilitation Robotics (ICORR), pp. 357–361, IEEE, 8 2015.

[100] P. Eunson, “Spasticity in children and young people with non-progressive brain disorders : management of spasticity and co-existing motor disorders and their early musculoskeletal complications,” National Institute for Health and Clinical Excellence Guideline, pp. 1–302, 2012.

[101] T. Rahman, W. Sample, R. Seliktar, M. Alexander, and M. Scavina, “A body-powered functional upper limb orthosis,” Journal of Rehabilitation Research and Development, vol. 37, no. 6, pp. 675–680, 2000.

[102] C. Glasgow, L. Tooth, and J. Fleming, “Which Splint? Dynamic versus Static Progressive Splinting to Mobilise Stiff Joints in the Hand,” The British Journal of Hand Therapy, vol. 13, no. 4, pp. 104–110, 2008.

[103] H. K. In, K. J. Cho, K. R. Kim, and B. S. Lee, “Jointless structure and under-actuation mechanism for compact hand exoskeleton,” IEEE International Conference on Rehabilitation Robotics, no. 2010, pp. 1–6, 2011.

[104] M. Sarac, M. Solazzi, and A. Frisoli, “Design Requirements of Generic Hand Exoskeletons and Survey of Hand Exoskeletons for Rehabilitation, Assistive or Haptic Use,” IEEE Transactions on Haptics, vol. PP, no. 601165, p. 1, 2019.

[105] J. Yang, Q. Peng, J. Zhang, and P. Gu, “Design of a Hand Rehabilitation Device Using integrated Axiomatic and Benchmarking Methods,” Procedia CIRP, vol. 78, pp. 295–300, 2018.

[106] A. J. Veale and S. Q. Xie, “Towards compliant and wearable robotic orthoses: A review of current and emerging actuator technologies,” Medical Engineering and Physics, vol. 38, no. 4, pp. 317–325, 2016.

[107] K. W. Heller, P. J. Mezei, and M. J. T. Avant, “Meeting the Assistive Technology Needs of Students with Duchenne Muscular Dystrophy,” Journal of Special Education Technology, vol. 23, no. 4, pp. 15–30, 2008.

[108] R. Wessels, B. Dijcks, M. Soede, G. J. Gelderblom, and L. De Witte, “Non-use of provided assistive technology devices, a literature overview,” Technology and Disability, vol. 15, no. 4, pp. 231–238, 2003.

[109] M. Controzzi, C. Cipriani, and M. C. Carrozza, Design of artificial hands: A review, vol. 95. Springer Tracts in Advanced Robotics, 2014.

[110] C. Y. Tsao and J. R. Mendell, “The childhood muscular dystrophies: Making order out of chaos,” Seminars in Neurology, vol. 19, no. 1, pp. 9–23, 1999.

[111] L. Lacourpaille, F. Hug, A. Guével, Y. Péréon, A. Magot, J. Y. Hogrel, and A. Nordez, “New insights on contraction efficiency in patients with Duchenne muscular dystrophy,” Journal of Applied Physiology, vol. 117, no. 6, pp. 658–662, 2014.

[112] M. M. Janssen, A. C. Geurts, and I. J. de Groot, “Towards a short questionnaire for stepwise assessment of upper limb function, pain and stiffness in Duchenne muscular dystrophy,” Disability and Rehabilitation, vol. 40, no. 7, pp. 842–847, 2018.

[113] H. Arora, “Commonly available outcome measures for use in Indian boys with Duchenne muscular dystrophy,” Neurology India, vol. 66, no. 5, pp. 1279–1285, 2018.

[114] L. B. Hiller and C. K. Wade, “Upper extremity functional assessment scales in children with duchenne muscular dystrophy: A comparison,” Archives of Physical Medicine and Rehabilitation, vol. 73, no. 6, pp. 527–534, 1992.

[115] E. S. Mazzone, G. Vasco, C. Palermo, F. Bianco, C. Galluccio, V. Ricotti, A. D. Castronovo, M. S. D. Mauro, M. Pane, A. Mayhew, and E. Mercuri, “A critical review of functional assessment tools for upper limbs in Duchenne muscular dystrophy,” Developmental Medicine & Child Neurology, vol. 54, pp. 879–885, 10 2012.

[116] M. F. Nunes, M. E. Hukuda, F. M. Favero, A. B. Oliveira, M. C. Voos, and F. A. Caromano, “Relationship between muscle strength and motor function in Duchenne muscular dystrophy,” Arquivos de Neuro-Psiquiatria, vol. 74, no. 7, pp. 530–535, 2016.

[117] M. Pane, G. Coratti, C. Brogna, E. S. Mazzone, A. Mayhew, L. Fanelli, S. Messina, A. D. Amico, M. Catteruccia, M. Scutifero, S. Frosini, V. Lanzillotta, G. Colia, F. Cavallaro, E. Rolle, R. De Sanctis, N. Forcina, R. Petillo, A. Barp, A. Gardani, A. Pini, G. Monaco, M. G. D. Angelo, R. Zanin, G. L. Vita, C. Bruno, T. Mongini, F. Ricci, E. Pegoraro, L. Bello, A. Berardinelli, R. Battini, V. Sansone, E. Albamonte, G. Baranello, E. Bertini, L. Politano, M. P. Sormani, and E. Mercuri, “Upper limb function in Duchenne muscular dystrophy: 24 month longitudinal data,” PLoS ONE, vol. 13, no. 6, pp. 4–11, 2018.

[118] K. Nizamis, N. H. Rijken, A. Mendes, M. M. Janssen, A. Bergsma, and B. F. Koopman, “A novel setup and protocol to measure the range of motion of the wrist and the hand,” Sensors (Switzerland), vol. 18, no. 10, pp. 1–14, 2018.

[119] J. Y. Hogrel, C. Wary, A. Moraux, N. Azzabou, V. Decostre, G. Ollivier, A. Canal, C. Lilien, I. Ledoux, M. Annoussamy, N. Reguiba, T. Gidaro, A. G. Le Moing, R. Cardas, T. Voit, P. G. Carlier, and L. Servais, “Longitudinal functional and NMR assessment of upper limbs in Duchenne muscular dystrophy,” Neurology, vol. 86, no. 11, pp. 1022–1030, 2016.

[120] L. Vandervelde, P. Y. Van Den Bergh, A. Renders, N. Goemans, and J. L. Thonnard, “Relationships between motor impairments and activity limitations in patients with neuromuscular disorders,” Journal of Neurology, Neurosurgery and Psychiatry, vol. 80, no. 3, pp. 326–332, 2009.
[121] C. M. Mcdonald, “Profiles of Neuromuscular Diseases; Duchenne Muscular Dystrophy,” American journal of physical medicine & rehabilitation, vol. 74, no. 5, pp. 70–92, 1995.
[122] R. W. Grange and J. A. Call, “Recommendations to define exercise prescription for duchenne muscular dystrophy,” Exercise and Sport Sciences Reviews, vol. 35, no. 1, pp. 12–17, 2007.
[123] M. M. Janssen, J. Harlaar, B. Koopman, and I. J. De Groot, “Dynamic arm study: Quantitative description of upper extremity function and activity of boys and men with duchenne muscular dystrophy,” Journal of NeuroEngineering and Rehabilitation, vol. 14, no. 1, 2017.
[124] R. T. Abresch, J. J. Han, and G. T. Carter, “Rehabilitation management of neuromuscular disease: The role of exercise training,” Journal of Clinical Neuromuscular Disease, vol. 11, no. 1, pp. 7–21, 2009.
[125] S. Black and R. I. Cook, Duchenne Muscular Dystrophy; Methods and Protocols. Springer Nature, 2018.
[126] S. Schoepe, H. Schäcke, E. May, and K. Asadullah, “Glucocorticoid therapy-induced skin atrophy,” Experimental Dermatology, vol. 15, no. 6, pp. 406–420, 2006.
[127] T. P. Zanto, K. Hennigan, M. Östberg, W. C. Clapp, and A. Gazzaley, “NIH Public Access,” vol. 46, no. 4, pp. 564–574, 2011.
[128] C. Angelini and E. Peterle, “Old and new therapeutic developments in steroid treatment in Duchenne muscular dystrophy,” Acta Myologica, vol. 31, no. May, pp. 9–15, 2012.
[129] J. Andrews and R. Wahl, “Duchenne and Becker muscular dystrophy in adolescents: current perspectives,” Adolescent Health, Medicine and Therapeutics, no. 9, pp. 53–63, 2018.
[130] A. G. Le Moing, A. M. Seferian, A. Moraux, M. Annoussamy, E. Dorveaux, E. Gasnier, J. Y. Hogrel, T. Voit, D. Vissière, and L. Servais, “A movement monitor based on magneto-inertial sensors for non-ambulant patients with Duchenne muscular dystrophy: A pilot study in controlled environment,” PLoS ONE, vol. 11, no. 6, pp. 1–17, 2016.
[131] J. Cassel, R. Cassel, F. Down, S. Fowler, P. Gage, R. Geall, L. Inman, S. Manning, P. Martin, J. McConnell, and M. Morrow, “Wheelchair Provision for Children and Adults with Muscular Dystrophy and other Neuromuscular Conditions, Best Practice Guidelines,” Muscular Dystrophy Campaign, 2011.
[132] P. Beckerle, R. Kõiva, E. A. Kirchner, R. Bekrater-Bodmann, S. Dosen, O. Christ, D. A. Abbink, C. Castellini, and B. Lenggenhager, “Feel-good robotics: Requirements on touch for embodiment in assistive robotics,” Frontiers in Neurorobotics, vol. 12, no. December, pp. 1–7, 2018.
[133] A. Chowdhury, S. S. Nishad, Y. K. Meena, A. Dutta, and G. Prasad, “Hand-Exoskeleton Assisted Progressive Neurorehabilitation Using Impedance Adaptation Based Challenge Level Adjustment Method,” IEEE Transactions on Haptics, vol. 12, no. 2, pp. 128–140, 2019.
[134] D. Wang, Q. Meng, Q. Meng, X. Li, and H. Yu, “Design and Development of a Portable Exoskeleton for Hand Rehabilitation,” IEEE Transactions on Neural Systems and Rehabilitation Engineering, vol. 26, no. 12, pp. 2376–2386, 2018.
[135] S. W. Pu, S. Y. Tsai, and J. Y. Chang, “Design and development of the wearable hand exoskeleton system for rehabilitation of hand impaired patients,” IEEE International Conference on Automation Science and Engineering, vol. 2014-Janua, pp. 996–1001, 2014.
[136] M. Xiloyannis, L. Cappello, K. D. Binh, C. W. Antuvan, and L. Masia, “Preliminary design and control of a soft exosuit for assisting elbow movements and hand grasping in activities of daily living,” Journal of Rehabilitation and Assistive Technologies Engineering, vol. 4, p. 205566831668031, 2017.
[137] Y. Park, I. Jo, J. Lee, and J. Bae, “A Dual-cable Hand Exoskeleton System for Virtual Reality,” Mechatronics, vol. 49, no. December 2017, pp. 177–186, 2018.
[138] B. B. Kang, H. Lee, H. In, U. Jeong, J. Chung, and K. J. Cho, “Development of a polymer-based tendon-driven wearable robotic hand,” Proceedings - IEEE International Conference on Robotics and Automation, vol. 2016-June, pp. 3750–3755, 2016.
[139] C. G. Rose and M. K. O'Malley, “Hybrid Rigid-Soft Hand Exoskeleton to Assist Functional Dexterity,” IEEE Robotics and Automation Letters, vol. 4, no. 1, pp. 73–80, 2019.
[140] J. Parker and P. Paker, Duchenne Muscular Dystrophy; medical dictionary, bibliography, and Annotated Research Guide to Internet References. ICON Group International, Inc., 2004.
[141] P. Maeder-York, T. Clites, E. Boggs, R. Neff, P. Polygerinos, D. Holland, L. Stirling, K. Galloway, C. Wee, and C. Walsh, “Biologically inspired soft robot for thumb rehabilitation,” Journal of Medical Devices, Transactions of the ASME, vol. 8, no. 2, pp. 29–31, 2014.
[142] I. Sarakoglou, A. Brygo, D. Mazzanti, N. G. Hernandez, D. G. Caldwell, and N. G. Tsagarakis, “Hexotrac: A highly under-actuated hand Exoskeleton for finger tracking and force feedback.,” IEEE International Conference on Intelligent Robots and Systems, vol. 2016-Novem, pp. 1033–1040, 2016.
[143] B. W. Gasser, D. A. Bennett, C. M. Durrough, and M. Goldfarb, “Design and preliminary assessment of Vanderbilt hand exoskeleton,” IEEE International Conference on Rehabilitation Robotics, pp. 1537–1542, 2017.
[144] A. G. Patiño, A. Ferrone, C. G. D. Gastélum, and C. Menon, “A Novel Biomedical Technology Based on the Use of Artificial Muscles to Assist with Hand Functions,” 2018 IEEE 9th Annual Information Technology, Electronics and Mobile Communication Conference, IEMCON 2018, pp. 620–625, 2018.
[145] P. Polygerinos, Z. Wang, K. C. Galloway, R. J. Wood, and C. J. Walsh, “Soft robotic glove for combined assistance and at-home rehabilitation,” Robotics and Autonomous Systems, vol. 73, pp. 135–143, 11 2015.
[146] M. K. Burns, K. Van Orden, V. Patel, and R. Vinjamuri, “Towards a wearable hand exoskeleton with embedded synergies,” Proceedings of the Annual International Conference of the IEEE Engineering in Medicine and Biology Society, EMBS, pp. 213–216, 2017.
[147] S. W. Lee, K. A. Landers, and H. S. Park, “Development of a biomimetic hand exotendon device (BiomHED) for restoration of functional hand movement post-stroke,” IEEE Transactions on Neural Systems and Rehabilitation Engineering, vol. 22, no. 4, pp. 886–898, 2014.
[148] H. Yamaura, K. Matsushita, R. Kato, and H. Yokoi, “Development of hand rehabilitation system for paralysis patient - Universal design using wire-driven mechanism,” Proceedings of the 31st Annual International Conference of the IEEE Engineering in Medicine and Biology Society: Engineering the Future of Biomedicine, EMBC 2009, pp. 7122–7125, 2009.
[149] P. Weiss, L. Heyer, T. F. Munte, M. Heldmann, A. Schweikard, and E. Maehle, “Towards a parameterizable exoskeleton for training of hand function after stroke,” IEEE International Conference on Rehabilitation Robotics, 2013.
[150] A. Rahman and A. Al-Jumaily, “Design and development of a bilateral therapeutic hand device for stroke rehabilitation,” International Journal of Advanced Robotic Systems, vol. 10, pp. 1–12, 2013.
[151] W. Sarwar, W. Harwin, B. Janko, and G. Bell, “Multi-Compliance Printing Techniques for the Fabrication of Customisable Hand Exoskeletons,” 2019 IEEE 16th International Conference on Rehabilitation Robotics (ICORR), pp. 488–493, 2019.
[152] J. Li, R. Zheng, Y. Zhang, and J. Yao, “iHandRehab: An interactive hand exoskeleton for active and passive rehabilitation,” IEEE International Conference on Rehabilitation Robotics, no. 50975009, pp. 1–6, 2011.
[153] L. Cappello, J. T. Meyer, K. C. Galloway, J. D. Peisner, R. Granberry, D. A. Wagner, S. Engelhardt, S. Paganoni, and C. J. Walsh, “Assisting hand function after spinal cord injury with a fabric-based soft robotic glove,” Journal of NeuroEngineering and Rehabilitation, vol. 15, no. 1, pp. 1–10, 2018.
[154] P. W. Ferguson, B. Dimapasoc, Y. Shen, and J. Rosen, “Design of a hand exoskeleton for use with upper limb exoskeletons,” Biosystems and Biorobotics, vol. 22, pp. 276–280, 2019.
[155] Z. Ma, P. Ben-Tzvi, and J. Danoff, “Hand Rehabilitation Learning System with an Exoskeleton Robotic Glove,” IEEE Transactions on Neural Systems and Rehabilitation Engineering, vol. 24, no. 12, pp. 1323–1332, 2016.
[156] R. Conti, B. Allotta, E. Meli, and A. Ridolfi, “Development, design and validation of an assistive device for hand disabilities based on an innovative mechanism,” Robotica, vol. 35, no. 4, pp. 892–906, 2017.
[157] L. Cui, A. Phan, and G. Allison, “Design and fabrication of a three dimensional printable non-assembly articulated hand exoskeleton for rehabilitation,” Proceedings of the Annual International Conference of the IEEE Engineering in Medicine and Biology Society, EMBS, vol. 2015-Novem, pp. 4627–4630, 2015.
[158] A. Mohammadi, J. Lavranos, P. Choong, and D. Oetomo, “Flexo-glove: A 3D Printed Soft Exoskeleton Robotic Glove for Impaired Hand Rehabilitation and Assistance,” Proceedings of the Annual International Conference of the IEEE Engineering in Medicine and Biology Society, EMBS, vol. 2018-July, pp. 2120–2123, 2018.

[159] J. Lee, W. Park, S. Kim, and J. Bae, "Design of a wearable hand rehabilitation system for quantitative evaluation of the stroke hand," International Conference on Control, Automation and Systems, vol. 0, no. Iccas, pp. 419–422, 2016.
[160] E. B. Brokaw, I. Black, R. J. Holley, and P. S. Lum, "Hand Spring Operated Movement Enhancer (HandSOME): A portable, passive hand Exoskeleton for stroke rehabilitation," IEEE Transactions on Neural Systems and Rehabilitation Engineering, vol. 19, no. 4, pp. 391–399, 2011.
[161] M. C. Hume, H. Gellman, H. McKellop, and R. H. Brumfield, "Functional range of motion of the joints of the hand," Journal of Hand Surgery, vol. 15, no. 2, pp. 240–243, 1990.
[162] T. Butzer, J. Dittli, J. Lieber, H. J. van Hedel, A. Meyer-Heim, O. Lambercy, and R. Gassert, "PEXO - A Pediatric Whole Hand Exoskeleton for Grasping Assistance in Task-Oriented Training," IEEE 16th Interntional Conference on Rehabilitation Robotics (ICORR), pp. 108–114, June 24-28, 2019.
[163] B. W. Gasser and M. Goldfarb, "Design and performance characterization of a hand orthosis prototype to aid activities of daily living in a post-stroke population," Proceedings of the Annual International Conference of the IEEE Engineering in Medicine and Biology Society, EMBS, vol. 2015-Novem, pp. 3877–3880, 2015.
[164] H. Monod, "Contractility of muscle during prolonged static and repetitive dynamic activity," Ergonomics, vol. 28, no. 1, pp. 81–89, 1985.
[165] D. Kuswanto, B. Iskandriawan, and P. S. Mahardhika, "Power Grip Exoskeleton Design as Rehabilitation Devices for Post-Stroke Survivors," Proceedings - 2018 1st International Conference on Bioinformatics, Biotechnology, and Biomedical Engineering, BioMIC 2018, vol. 1, pp. 1–6, 2018.
[166] D. D. Neumann, Kinesiology of the musculoskeletal system; Foundations for Rehabilitation. Elsevier Inc., 2nd ed., 2010.
[167] A. Roda-Sales, M. Vergara, J. L. Sancho-Bru, V. Gracia-Ibáñez, and N. J. Jarque-Bou, "Human hand kinematic data during feeding and cooking tasks," Scientific data, vol. 6, no. 1, p. 167, 2019.
[168] M. R. Cutkosky, "On Grasp Choice, Grasp Models, and the Design of Hands for Manufacturing Tasks," IEEE Transactions on Robotics and Automation, vol. 5, no. 3, pp. 269–279, 1989.
[169] T. Iberall, "Human prehension and dexterous robot hands," International Journal of Robotics Research, vol. 16, no. 3, pp. 285–299, 1997.
[170] I. M. Bullock, S. Member, J. Z. Zheng, S. D. L. Rosa, C. Guertler, and A. M. Dollar, "Grasp Frequency and Usage in Daily Household and Machine Shop Tasks," IEEE Transactions on Haptics, vol. 6, no. 3, 2015.
[171] G. I. Bain, N. Polites, B. G. Higgs, R. J. Heptinstall, and A. M. McGrath, "The functional range of motion of the finger joints," Journal of Hand Surgery: European Volume, vol. 40, no. 4, pp. 406–411, 2015.
[172] T. Feix, J. Romero, H. B. Schmiedmayer, A. M. Dollar, and D. Kragic, "The GRASP Taxonomy of Human Grasp Types," IEEE Transactions on Human-Machine Systems, vol. 46, no. 1, pp. 66–77, 2016.
[173] A. Saudabayev, Z. Rysbek, R. Khassenova, and H. A. Varol, "Data Descriptor : Human grasping database for activities of daily living with depth , color and kinematic data streams," Scientific Data 5, 180101, pp. 1–13, 2018.
[174] B. Gasser, Design of an upper-limb exoskeleton for functional assitance of bimanual activities of daily living. PhD thesis, Vanderbilt University, 2019.
[175] M. Kutz, Biomedical Engineering and Design Handbook, vol. 2. McGraww-Hill, 2nd ed., 2009.
[176] V. Gracia-Ibáñez, M. Vergara, J. L. Sancho-Bru, M. C. Mora, and C. Piqueras, "Functional range of motion of the hand joints in activities of the International Classification of Functioning, Disability and Health," Journal of Hand Therapy, vol. 30, no. 3, pp. 337–347, 2017.
[177] J. Lin, Y. Wu, and T. S. Huang, "Modeling the constraints of human hand motion," Proceedings - Workshop on Human Motion, HUMO 2000, no. May 2014, pp. 121–126, 2000.
[178] A. L. Hutchison and R. L. Hutchison, "Fibonacci, Littler, and the Hand: A Brief Review," Hand, vol. 5, no. 4, pp. 364–368, 2010.
[179] S. Biggar and W. Yao, "Design and Evaluation of a Soft and Wearable Robotic Glove for Hand Rehabilitation," IEEE Transactions on Neural Systems and Rehabilitation Engineering, vol. 24, no. 10, pp. 1071–1080, 2016.
[180] M. Mirakhorlo, N. Van Beek, M. Wesseling, H. Maas, H. E. Veeger, and I. Jonkers, "A musculoskeletal model of the hand and wrist: model definition and evaluation," Computer Methods in Biomechanics and Biomedical Engineering, vol. 21, no. 9, pp. 548–557, 2018.
[181] P. Jenmalm and R. S. Johansson, "Visual and somatosensory information about object shape control manipulative fingertip forces," Journal of Neuroscience, vol. 17, no. 11, pp. 4486–4499, 1997.
[182] K. Nizamis, W. Schutte, J. Goseling, and B. F. Koopman, "Quantification of information transfer rate of the human hand during a mouse clicking task with healthy adults and one adult with Duchenne muscular Dystrophy," IEEE International Conference on Rehabilitation Robotics, pp. 1227–1232, 2017.
[183] E. Versluis, "Bio Mechanical Engineering Design of a Hydraulic Prosthetic Hand Adding an active thumb to the Delft Cylinder Hand," Master Thesis TU Delft, 2015.
[184] V. Punsola-Izard, D. Salas-Gómez, E. Sirvent-Rivalda, and J. Esquirol-Caussà, "Functional patterns of thumb key pinch and their influence on thumb strength and stability," Hand Therapy, vol. 17, no. 4, pp. 78–86, 2012.
[185] C. Pylatiuk, A. Kargov, S. Schulz, and L. Döderlein, "Distribution of grip force in three different functional prehension patterns," Journal of Medical Engineering and Technology, vol. 30, no. 3, pp. 176–182, 2006.
[186] S. Ueki, H. Kawasaki, S. Ito, Y. Nishimoto, M. Abe, T. Aoki, Y. Ishigure, T. Ojika, and T. Mouri, "Development of a hand-assist robot with multi-degrees-of-freedom for rehabilitation therapy," IEEE/ASME Transactions on Mechatronics, vol. 17, no. 1, pp. 136–146, 2012.
[187] C. J. Nycz, T. B. Meier, P. Carvalho, G. Meier, and G. S. Fischer, "Design criteria for hand exoskeletons: Measurement of forces needed to assist finger extension in traumatic brain injury patients," IEEE Robotics and Automation Letters, vol. 3, no. 4, pp. 3285–3292, 2018.
[188] V. K. Nanayakkara, G. Cotugno, N. Vitzilaios, D. Venetsanos, T. Nanayakkara, and M. N. Sahinkaya, "The Role of Morphology of the Thumb in Anthropomorphic Grasping: A Review," Frontiers in Mechanical Engineering, vol. 3, no. June, 2017.
[189] G. Cotugno, V. Mohan, K. Althoefer, and T. Nanayakkara, "Simplifying grasping complexity through generalization of kinaesthetically learned synergies," Proceedings - IEEE International Conference on Robotics and Automation, no. May, pp. 5345–5351, 2014.
[190] R. Vinet, Y. Lozac'h, N. Beaudry, and G. Drouin, "Design methodology for a multifunctional hand prosthesis," Journal of Rehabilitation Research and Development, vol. 32, no. 4, pp. 316–324, 1995.
[191] W. Cooney, M. Lucca, E. Chao, and R. Linscheid, "The kinesiology of the thumb trapesiometacarpal joint.PDF," The journal of bone and joint surgery, vol. 63-A, no. 9, 1981.
[192] G. Stillfried and P. van der Smagt, "Movement model of a human hand based on magnetic resonance imaging (MRI)," International Conference on Applied Bionics and Biomechanics (ICABB), 2010.
[193] P. Heo and J. Kim, "Power-assistive finger exoskeleton with a palmar opening at the fingerpad," IEEE Transactions on Biomedical Engineering, vol. 61, no. 11, pp. 2688–2697, 2014.
[194] A. Alutei, A. Vaida, D. Mandru, and M. O. Tatar, "Development of an active upper-limb orthosis," IFMBE Proceedings, vol. 26, pp. 405–408, 2009.
[195] H. Al-Fahaam, S. Davis, and S. Nefti-Meziani, "The design and mathematical modelling of novel extensor bending pneumatic artificial muscles (EBPAMs) for soft exoskeletons," Robotics and Autonomous Systems, vol. 99, pp. 63–74, 2018.
[196] D. Leonardis, M. Barsotti, C. Loconsole, M. Solazzi, M. Troncossi, C. Mazzotti, V. P. Castelli, C. Procopio, G. Lamola, C. Chisari, M. Bergamasco, and A. Frisoli, "An EMG-controlled robotic hand exoskeleton for bilateral rehabilitation," IEEE Transactions on Haptics, vol. 8, no. 2, pp. 140–151, 2015.
[197] J. Arata, K. Ohmoto, R. Gassert, O. Lambercy, H. Fujimoto, and I. Wada, "A new hand exoskeleton device for rehabilitation using a three-layered sliding spring mechanism," Proceedings - IEEE International Conference on Robotics and Automation, pp. 3902–3907, 2013.
[198] A. Chiri, F. Giovacchini, N. Vitiello, E. Cattin, S. Roccella, F. Vecchi, and M. C. Carrozza, "HANDEXOS: Towards an exoskeleton device for the rehabilitation of the hand," 2009 IEEE/RSJ International Conference on Intelligent Robots and Systems, IROS 2009, pp. 1106–1111, 2009.
[199] C. J. Nycz, T. Butzer, O. Lambercy, J. Arata, G. S. Fischer, and R. Gassert, "Design and Characterization of a Lightweight and Fully Portable Remote Actuation System for Use with a Hand Exoskeleton," IEEE Robotics and Automation Letters, vol. 1, no. 2, pp. 976–983, 2016.
[200] H. I. Baqapuri, H. A. Nizami, S. Siddiqui, J. Iqbal, and U. Shahbaz, "Prefabrication design of an actuated exoskeleton for traumatized and paralytic hands," 2012 International Conference on Robotics and Artificial Intelligence, ICRAI 2012, pp. 108–111, 2012.

[201] A. Borboni, M. Mor, and R. Faglia, “Gloreha-Hand Robotic Rehabilitation: Design, Mechanical Model, and Experiments,” Journal of Dynamic Systems, Measurement and Control, Transactions of the ASME, vol. 138, no. 11, 2016.

[202] A. Chiri, M. Cempini, S. M. M. De Rossi, T. Lenzi, F. Giovacchini, N. Vitiello, and M. C. Carrozza, “On the design of ergonomic wearable robotic devices for motion assistance and rehabilitation,” Proceedings of the Annual International Conference of the IEEE Engineering in Medicine and Biology Society, EMBS, pp. 6124–6127, 2012.

[203] J. Chen, D. Nichols, E. B. Brokaw, and P. S. Lum, “Home-based therapy after stroke using the hand spring operated movement enhancer (HandSOME),” IEEE Transactions on Neural Systems and Rehabilitation Engineering, vol. 25, no. 12, pp. 2305–2312, 2017.

[204] Z. C. Puzo, T. A. Clark, and B. L. Ulrey, “Development of an assistive device controlled by surface electromyogram signals,” Proceedings of the IEEE Annual Northeast Bioengineering Conference, NEBEC, vol. 2014-Decem, pp. 1–2, 2014.

[205] N. Benjuya and S. Kenney, “Myoelectric Hand Orthosis,” Journal of Prosthetics and Orthotics, vol. 2, no. 2, pp. 149–154, 1990.

[206] E. M. Refour, B. Sebastian, R. J. Chauhan, and P. Ben-Tzvi, “A General Purpose Robotic Hand Exoskeleton With Series Elastic Actuation,” Journal of Mechanisms and Robotics, vol. 11, no. 6, pp. 1–9, 2019.

[207] P. Dollfus and M. Oberlé, “Technical note: Preliminary communication a tridigital dynamic orthosis for tetraplegic patients,” Paraplegia, vol. 22, no. 2, pp. 115–118, 1984.

[208] Y. Chen, S. Le, Q. C. Tan, O. Lau, F. Wan, and C. Song, “A lobster-inspired robotic glove for hand rehabilitation,” Proceedings - IEEE International Conference on Robotics and Automation, pp. 4782–4787, 2017.

[209] I. H. Ertas, E. Hocaoglu, and V. Patoglu, “AssistOn-Finger: An under-actuated finger exoskeleton for robot-assisted tendon therapy,” Robotica, vol. 32, no. 8, pp. 1363–1382, 2014.

[210] S. S. Nishad, A. Dutta, and A. Saxena, “Design and control of a three finger hand exoskeleton for translation of a slender object,” 2014 11th International Conference on Ubiquitous Robots and Ambient Intelligence, URAI 2014, no. Urai, pp. 179–184, 1997.

[211] E. Refour, B. Sebastian, and P. Ben-Tzvi, “Two-digit robotic exoskeleton glove mechanism: Design and integration,” Journal of Mechanisms and Robotics, vol. 10, no. 2, pp. 1–9, 2018.

[212] C. Ferraresi, Mechanisms and Machine Science 49 Advances in Service and Industrial Robotics. Springer, Proceedings of the 26th International conference on Robotics in Alpe-Adria-Danube Region, 2017.

[213] L. Connelly, M. E. Stoykov, Y. Jia, M. L. Toro, R. V. Kenyon, and D. G. Kamper, “Use of a pneumatic glove for hand rehabilitation following stroke,” Proceedings of the 31st Annual International Conference of the IEEE Engineering in Medicine and Biology Society: Engineering the Future of Biomedicine, EMBC 2009, pp. 2434–2437, 2009.

[214] Y. Fu, Q. Zhang, F. Zhang, and Z. Gan, “Design and development of a hand rehabilitation robot for patient-cooperative therapy following stroke,” 2011 IEEE International Conference on Mechatronics and Automation, ICMA 2011, pp. 112–117, 2011.

[215] D. S. Richards, I. Georgilas, G. Dagnino, and S. Dogramadzi, “Powered exoskeleton with palm degrees of freedom for hand rehabilitation,” Proceedings of the Annual International Conference of the IEEE Engineering in Medicine and Biology Society, EMBS, vol. 2015-Novem, pp. 4635–4638, 2015.

[216] M. Takagi, K. Iwata, Y. Takahashi, S. I. Yamamoto, H. Koyama, and T. Komeda, “Development of a grip aid system using air cylinders,” Proceedings - IEEE International Conference on Robotics and Automation, pp. 2312–2317, 2009.

[217] S. Gobee, V. Durairajah, and N. Mohammadullah, “Portable soft-exoskeleton for finger rehabilitation,” ACM International Conference Proceeding Series, vol. Part F1319, pp. 65–70, 2017.

[218] J. Guo, S. Yu, Y. Li, T. H. Huang, J. Wang, B. Lynn, J. Fidock, C. L. Shen, D. Edwards, and H. Su, “A soft robotic exo-sheath using fabric EMG sensing for hand rehabilitation and assistance,” 2018 IEEE International Conference on Soft Robotics, RoboSoft 2018, pp. 497–503, 2018.

[219] K. Tadano, M. Akai, K. Kadota, and K. Kawashima, “Development of grip amplified glove using bi-articular mechanism with pneumatic artificial rubber muscle,” Proceedings - IEEE International Conference on Robotics and Automation, pp. 2363–2368, 2010.

[220] A. P. Tjahyono, K. C. Aw, H. Devaraj, W. Surendra, E. Haemmerle, and J. Travas-Sejdic, “A five-fingered hand exoskeleton driven by pneumatic artificial muscles with novel polypyrrole sensors,” Industrial Robot, vol. 40, no. 3, pp. 251–260, 2013.

[221] C. J. Gearhart, B. Varone, M. H. Stella, and B. F. Busha, “An effective 3-fingered augmenting exoskeleton for the human hand,” Proceedings of the Annual International Conference of the IEEE Engineering in Medicine and Biology Society, EMBS, vol. 2016-Octob, pp. 590–593, 2016.

[222] Y. Jiang, D. Chen, P. Liu, X. Jiao, Z. Ping, Z. Xu, J. Li, and Y. Xu, “Fishbone-inspired soft robotic glove for hand rehabilitation with multi-degrees-of-freedom,” 2018 IEEE International Conference on Soft Robotics, RoboSoft 2018, pp. 394–399, 2018.

[223] C. J. Haarman, E. E. Hekman, H. S. Rietman, and H. van der Kooij, “Pushing the limits: A novel tape spring pushing mechanism to be used in a hand orthosis,” Biosystems and Biorobotics, vol. 22, no. 13525, pp. 475–479, 2019.

[224] W. A. Surendra, A. P. Tjahyono, and K. C. Aw, “Portable and wearable five-fingered hand assistive device,” 2012 19th International Conference on Mechatronics and Machine Vision in Practice, M2VIP 2012, pp. 431–435, 2012.

[225] M. B. Hong, S. J. Kim, T. Um, and K. Kim, “KULEX: An ADL power-assistance demonstration,” 2013 10th International Conference on Ubiquitous Robots and Ambient Intelligence, URAI 2013, pp. 542–544, 2013.

[226] P. Heo, S. J. Kim, and J. Kim, “Powered finger exoskeleton having partially open fingerpad for flexion force assistance,” 2013 IEEE/ASME International Conference on Advanced Intelligent Mechatronics: Mechatronics for Human Wellbeing, AIM 2013, vol. 2, pp. 182–187, 2013.

[227] K. Y. Tong, S. K. Ho, P. M. Pang, X. L. Hu, W. K. Tam, K. L. Fung, X. J. Wei, P. N. Chen, and M. Chen, “An intention driven hand functions task training robotic system,” 2010 Annual International Conference of the IEEE Engineering in Medicine and Biology Society, EMBC’10, pp. 3406–3409, 2010.

[228] S. Kudo, K. Oshima, M. Arizono, Y. Hayashi, and S. Moromugi, “Electric-powered glove for CCI patients to extend their upper-extremity function,” 2014 IEEE/SICE International Symposium on System Integration, SII 2014, pp. 638–643, 2014.

[229] T. Jiralerspong, K. H. Heung, R. K. Tong, and Z. Li, “A Novel Soft Robotic Glove for Daily Life Assistance,” Proceedings of the IEEE RAS and EMBS International Conference on Biomedical Robotics and Biomechatronics, vol. 2018-Augus, pp. 671–676, 2018.

[230] G. Herrmann, M. Studley, M. Pearson, A. Conn, C. Melhuish, M. Witkowski, J.-H. Kim, and P. Vadakkepat, Advances in Autonomous Robotics. Springer, Joint proceedings of the 13th Annual TAROS Conference and the 15th Annual FIRA RoboWorld Congress, 2012.

[231] E. R. Triolo, M. H. Stella, and B. F. Busha, “A force augmenting exoskeleton for the human hand designed for pinching and grasping,” Proceedings of the Annual International Conference of the IEEE Engineering in Medicine and Biology Society, EMBS, vol. 2018-July, pp. 1875–1878, 2018.

[232] Y. Kadowaki, T. Noritsugu, M. Takaiwa, D. Sasaki, and M. Kato, “Development of soft power-assist glove and control based on human intent,” Journal of Robotics and Mechatronics, vol. 23, no. 2, pp. 281–291, 2011.

[233] C. L. Jones, F. Wang, R. Morrison, N. Sarkar, and D. G. Kamper, “Design and development of the cable actuated finger exoskeleton for hand rehabilitation following stroke,” IEEE/ASME Transactions on Mechatronics, vol. 19, no. 1, pp. 131–140, 2014.

[234] J. Iqbal, N. G. Tsagarakis, and D. G. Caldwell, “Four-fingered lightweight exoskeleton robotic device accommodating different hand sizes,” Electronics Letters, vol. 51, no. 12, pp. 888–890, 2015.

[235] J. Makaran, D. Dittmer, R. Buchal, and D. MacArthur, “The SMART wrist-hand orthosis (WHO) for quadriplegic patients,” Journal of Prosthetics and Orthotics, vol. 5, no. 3, 1993.

[236] M. X. Lin, G. Y. Ma, F. Q. Liu, Q. S. Sun, and A. Q. Song, “Design and Dynamic Modeling of Flexible Rehabilitation Mechanical Glove,” IOP Conference Series: Materials Science and Engineering, vol. 320, no. 1, 2018.

[237] A. Lince, N. Celadon, A. Battezzato, A. Favetto, S. Appendino, P. Ariano, and M. Paleari, “Design and testing of an under-actuated surface EMG-driven hand exoskeleton,” IEEE International Conference on Rehabilitation Robotics, pp. 670–675, 2017.

[238] J. Iqbal, N. G. Tsagarakis, A. E. Fiorilla, and D. G. Caldwell, “A portable rehabilitation device for the hand,” 2010 Annual International Conference of the IEEE Engineering in Medicine and Biology Society, EMBC’10, pp. 3694–3697, 2010.

[239] J. H. Low, M. H. Ang, and C. H. Yeow, “Customizable soft pneumatic finger actuators for hand orthotic and prosthetic applications,” IEEE

International Conference on Rehabilitation Robotics, vol. 2015-Septe, pp. 380–385, 2015.
[240] A. McConnell, X. Kong, and P. A. Vargas, “A novel robotic assistive device for stroke-rehabilitation,” IEEE RO-MAN 2014 - 23rd IEEE International Symposium on Robot and Human Interactive Communication: Human-Robot Co-Existence: Adaptive Interfaces and Systems for Daily Life, Therapy, Assistance and Socially Engaging Interactions, pp. 917–923, 2014.
[241] S. Moromugi, T. Ishimatsu, H. Matsui, T. Ikeda, M. Mizuta, T. Koga, T. Tateishi, T. Saoyama, and M. Takashima, “An electrical prehension orthosis operated through activity of mastication muscle,” Proceedings of the SICE Annual Conference, pp. 2030–2033, 2010.
[242] V. D. Niestanak, A. A. Moshaii, and M. M. Moghaddam, “A New Underactuated Mechanism of Hand Tendon Injury Rehabilitation,” 5th RSI International Conference on Robotics and Mechatronics, IcRoM 2017, no. IcRoM, pp. 400–405, 2018.
[243] P. Brown, D. Jones, and S. K. Singh, “Exoskeleton glove for control of paralyzed hands,” Proceedings - IEEE International Conference on Robotics and Automation, vol. 1, pp. 642–647, 1993.
[244] L. Cheng, M. Chen, and Z. Li, “Design and Control of a Wearable Hand Rehabilitation Robot,” IEEE Access, vol. 6, pp. 74039–74050, 2018.
[245] T. Otsuka and Y. Sankai, “Development of exo-finger for grasp-assistance,” SCIS and ISIS 2010 - Joint 5th International Conference on Soft Computing and Intelligent Systems and 11th International Symposium on Advanced Intelligent Systems, pp. 410–415, 2010.
[246] Y. Hasegawa, Y. Mikami, K. Watanabe, and Y. Sankai, “Five-fingered assistive hand with mechanical compliance of human finger,” Proceedings - IEEE International Conference on Robotics and Automation, pp. 718–724, 2008.
[247] M. A. Delph, S. A. Fischer, P. W. Gauthier, C. H. Luna, E. A. Clancy, and G. S. Fischer, “A soft robotic exomusculature glove with integrated sEMG sensing for hand rehabilitation,” IEEE International Conference on Rehabilitation Robotics, pp. 1–7, 2013.
[248] D. Sasaki, T. Noritsugu, M. Takaiwa, and H. Yamamoto, “Wearable power assist device for hand grasping using pneumatic artificial rubber muscle,” Proceedings - IEEE International Workshop on Robot and Human Interactive Communication, pp. 655–660, 2004.
[249] G. R. Tan, N. P. Robson, and G. S. Soh, “Motion generation of passive slider multiloop wearable hand devices,” Journal of Mechanisms and Robotics, vol. 9, no. 4, pp. 1–9, 2017.
[250] H. In, B. B. Kang, M. K. Sin, and K. J. Cho, “Exo-Glove: A wearable robot for the hand with a soft tendon routing system,” IEEE Robotics and Automation Magazine, vol. 22, no. 1, pp. 97–105, 2015.
[251] M. Ghassemi, J. M. Ochoa, N. Yuan, D. Tsoupikova, and D. Kamper, “Development of an Integrated Actuated Hand Orthosis and Virtual Reality System for Home-Based Rehabilitation,” Proceedings of the Annual International Conference of the IEEE Engineering in Medicine and Biology Society, EMBS, vol. 2018-July, pp. 1689–1692, 2018.
[252] M. Slack and D. Berbrayer, “A myoelectricallly controlled wrist-hand orthosis for brachial plexus injury: A case study,” Journal of Prosthetics and Orthotics, vol. 4, no. 3, 1992.
[253] K. Shiota, S. Kokubu, T. V. Tarvainen, M. Sekine, K. Kita, S. Y. Huang, and W. Yu, “Enhanced Kapandji test evaluation of a soft robotic thumb rehabilitation device by developing a fiber-reinforced elastomer-actuator based 5-digit assist system,” Robotics and Autonomous Systems, vol. 111, pp. 20–30, 2019.
[254] Z. J. Tang, S. Sugano, and H. Iwata, “A novel, MRI compatible hand exoskeleton for finger rehabilitation,” 2011 IEEE/SICE International Symposium on System Integration, SII 2011, pp. 118–123, 2011.
[255] A. Hadi, K. Alipour, S. Kazeminasab, and M. Elahinia, “ASR glove: A wearable glove for hand assistance and rehabilitation using shape memory alloys,” Journal of Intelligent Material Systems and Structures, vol. 29, no. 8, pp. 1575–1585, 2018.
[256] Z. Sun, Z. Guo, and W. Tang, “Design of wearable hand rehabilitation glove with soft hoop-reinforced pneumatic actuator,” Journal of Central South University, vol. 26, no. 1, pp. 106–119, 2019.
[257] S. Toochinda and W. Wannasuphoprasit, “Design and Development of an Assistive Hand Device for Enhancing Compatibility and Comfortability,” 2018 2nd International Conference on Engineering Innovation, ICEI 2018, pp. 1–6, 2018.
[258] K. Toya, T. Miyagawa, and Y. Kubota, “Power-Assist Glove operated by predicting the grasping mode,” Nihon Kikai Gakkai Ronbunshu, C Hen/Transactions of the Japan Society of Mechanical Engineers, Part C, vol. 75, no. 756 PART C, pp. 2267–2273, 2009.
[259] K. Watanabe, H. Morishtea, T. Mori, and T. Sato, “Grasping objects with the prototype of index-finger PIP joint motion amplifier for assisting rheumatoid arthritis patients,” IEEE/ASME International Conference on Advanced Intelligent Mechatronics, AIM, vol. 2, pp. 875–880, 2005.
[260] H. K. Yap, P. M. Khin, T. H. Koh, Y. Sun, X. Liang, J. H. Lim, and C. H. Yeow, “A Fully Fabric-Based Bidirectional Soft Robotic Glove for Assistance and Rehabilitation of Hand Impaired Patients,” IEEE Robotics and Automation Letters, vol. 2, no. 3, pp. 1383–1390, 2017.
[261] A. Wege, K. Kondak, and G. Hommel, “Development and control of a hand exoskeleton for rehabilitation,” Human Interaction with Machines Proceedings of the 6th International Workshop held at the Shanghai JiaoTong University, 2005, no. 1, pp. 149–157, 2006.
[262] S. Moromugi, K. Kawakami, K. Nakamura, T. Sakamoto, and T. Ishimatsu, “A tendon-driven glove to restore finger function for disabled,” ICCAS-SICE 2009 - ICROS-SICE International Joint Conference 2009, Proceedings, pp. 794–797, 2009.
[263] X. Lu, Z. Yang, Y. Chen, and J. Wang, “Structure Design of a Wearable Device for Hand Rehabilitation,” Proceedings - 2016 9th International Symposium on Computational Intelligence and Design, ISCID 2016, vol. 1, pp. 93–96, 2016.
[264] H. K. Yap, N. Kamaldin, J. H. Lim, F. A. Nasrallah, J. C. H. Goh, and C. H. Yeow, “A Magnetic Resonance Compatible Soft Wearable Robotic Glove for Hand Rehabilitation and Brain Imaging,” IEEE Transactions on Neural Systems and Rehabilitation Engineering, vol. 25, no. 6, pp. 782–793, 2017.
[265] C. J. Nycz, M. A. Delph, and G. S. Fischer, “Modeling and design of a tendon actuated soft robotic exoskeleton for hemiparetic upper limb rehabilitation,” Proceedings of the Annual International Conference of the IEEE Engineering in Medicine and Biology Society, EMBS, vol. 2015-Novem, pp. 3889–3892, 2015.
[266] L. A. Martinez, O. O. Olaloye, M. V. Talarico, S. M. Shah, R. J. Arends, and B. F. BuSha, “A power-assisted exoskeleton optimized for pinching and grasping motions,” Proceedings of the 2010 IEEE 36th Annual Northeast Bioengineering Conference, NEBEC 2010, pp. 1–2, 2010.
[267] H. K. Yap, J. H. Lim, J. C. H. Goh, and C. H. Yeow, “Design of a soft robotic glove for hand rehabilitation of stroke patients with clenched fist deformity using inflatable plastic actuators,” Journal of Medical Devices, Transactions of the ASME, vol. 10, no. 4, pp. 5–10, 2016.
[268] M. Nilsson, J. Ingvast, J. Wikander, and H. Von Holst, “The Soft Extra Muscle system for improving the grasping capability in neurological rehabilitation,” 2012 IEEE-EMBS Conference on Biomedical Engineering and Sciences, IECBES 2012, no. December, pp. 412–417, 2012.
[269] H. K. Yap, J. H. Lim, F. Nasrallah, J. C. Goh, and R. C. Yeow, “A soft exoskeleton for hand assistive and rehabilitation application using pneumatic actuators with variable stiffness,” Proceedings - IEEE International Conference on Robotics and Automation, vol. 2015-June, no. June, pp. 4967–4972, 2015.
[270] F. Zhang, L. Hua, Y. Fu, H. Chen, and S. Wang, “Design and development of a hand exoskeleton for rehabilitation of hand injuries,” Mechanism and Machine Theory, vol. 73, pp. 103–116, 2014.
[271] J. M. Ochoa, Y. Jia, N. Dev, and D. G. Kamper, “Development of a portable actuated orthotic glove to facilitate gross extension of the digits for therapeutic training after stroke,” Proceedings of the 31st Annual International Conference of the IEEE Engineering in Medicine and Biology Society: Engineering the Future of Biomedicine, EMBC 2009, pp. 6918–6921, 2009.
[272] M. B. Hong, S. J. Kim, Y. S. Ihn, G. C. Jeong, and K. Kim, “KULEX-Hand: An Underactuated Wearable Hand for Grasping Power Assistance,” IEEE Transactions on Robotics, vol. 35, no. 2, pp. 420–432, 2019.
[273] L. Saharan, M. J. De Andrade, W. Saleem, R. H. Baughman, and Y. Tadesse, “IGrab: Hand orthosis powered by twisted and coiled polymer muscles,” Smart Materials and Structures, vol. 26, no. 10, 2017.
[274] A. P. R. Ong and N. T. Bugtai, “A bio-inspired design of a hand robotic exoskeleton for rehabilitation,” AIP Conference Proceedings, vol. 1933, no. February, 2018.
[275] S. W. Pu, J. Y. Chang, Y. C. Pei, C. C. Kuo, and M. J. Wang, “Anthropometry-based structural design of a hand exoskeleton for rehabilitation,” M2VIP 2016 - Proceedings of 23rd International Conference on Mechatronics and Machine Vision in Practice, pp. 1–6, 2017.
[276] T. B. W. William, M. Weilin, and S. Y. L. Cynthia, “Development of a puppetry robotic glove system for the rehabilitation of upper limb functions,” i-CREATe 2011 - International Convention on Rehabilitation Engineering and Assistive Technology, pp. 125–128, 2011.

[277] J. Yang, H. Xie, and J. Shi, "A novel motion-coupling design for a jointless tendon-driven finger exoskeleton for rehabilitation," Mechanism and Machine Theory, vol. 99, pp. 83–102, 2016.

[278] M. Almenara, M. Cempini, C. Gómez, M. Cortese, C. Martín, J. Medina, N. Vitiello, and E. Opisso, "Usability test of a hand exoskeleton for activities of daily living: an example of user-centered design," Disability and Rehabilitation: Assistive Technology, vol. 12, no. 1, pp. 84–96, 2017.

[279] S. Grosu, L. De Rijcke, V. Grosu, J. Geeroms, B. Vanderboght, D. Lefeber, and C. Rodriguez-Guerrero, "Driving Robotic Exoskeletons Using Cable-Based Transmissions: A Qualitative Analysis and Overview," Applied Mechanics Reviews, vol. 70, no. 6, 2018.

[280] B. J. Lee, A. Williams, and P. Ben-Tzvi, "Intelligent Object Grasping with Sensor Fusion for Rehabilitation and Assistive Applications," IEEE Transactions on Neural Systems and Rehabilitation Engineering, vol. 26, no. 8, pp. 1556–1565, 2018.

[281] G. Onose, N. Popescu, C. Munteanu, V. Ciobanu, C. Sporea, M. D. Mirea, C. Daia, I. Andone, A. Spînu, and A. Mirea, "Mobile mechatronic/robotic orthotic devices to assist-rehabilitate neuromotor impairments in the upper limb: A systematic and synthetic review," Frontiers in Neuroscience, vol. 12, no. SEP, 2018.

[282] M. Palanivendhan, M. Wadhawan, and R. Selvagandhi, "Upper-limb shape memory alloy orthosis for restoration or improvement of basic hand functions," Indian Journal of Science and Technology, vol. 8, no. 27, 2015.

[283] C. Hansen, F. Gosselin, K. Ben Mansour, P. Devos, and F. Marin, "Design-validation of a hand exoskeleton using musculoskeletal modeling," Applied Ergonomics, vol. 68, no. February 2017, pp. 283–288, 2018.

[284] S. Bahrami and P. Dumond, "Testing of Coiled Nylon Actuators for Use in Spastic Hand Exoskeletons," Proceedings of the Annual International Conference of the IEEE Engineering in Medicine and Biology Society, EMBS, vol. 2018-July, pp. 1853–1856, 2018.

[285] B. D. Lowe, W. G. Billotte, and D. R. Peterson, "ASTM F48 Formation and Standards for Industrial Exoskeletons and Exosuits," IISE Transactions on Occupational Ergonomics and Human Factors, pp. 1–7, 2019.

[286] M. Bianchi, M. Cempini, R. Conti, E. Meli, A. Ridolfi, N. Vitiello, and B. Allotta, "Design of a Series Elastic Transmission for hand exoskeletons," Mechatronics, vol. 51, no. October 2017, pp. 8–18, 2018.

[287] R. B. Walters, Hydraulic and Electric-Hydraulic Control Systems. Springer, 2nd ed., 2000.

[288] M. Rabie, Fluid Power Engineering. McGraw-Hill, 2009.

[289] R. Inamuddin and M. Abdullah, Actuators; Fundamentals, Principles, Materials and Applications. John Wiley & Sons, Inc., 1st ed., 2020.

[290] R. Sindrey and G. M. Bone, "Position tracking control of a miniature water hydraulic rotary actuator," Journal of Dynamic Systems, Measurement and Control, Transactions of the ASME, vol. 131, no. 6, pp. 1–8, 2009.

[291] J. P. Whitney, M. F. Glisson, E. L. Brockmeyer, and J. K. Hodgins, "A low-friction passive fluid transmission and fluid-tendon soft actuator," IEEE International Conference on Intelligent Robots and Systems, no. Iros, pp. 2801–2808, 2014.

[292] Granta Design Limited, "CES Edupack Software - Material Level 3," 2020.

[293] Ultimaker, "Technical data sheet ABS," tech. rep., Ultimaker, 2018. Retrieved from https://support.ultimaker.com/hc/en-us/articles/360012759139-Ultimaker-ABS-TDS.

[294] FormLabs, "Materials Data Sheet; Photopolymer resin for Form1+ and Form 2," tech. rep., Formlabs, Inc., 2019. Retrieved from https://archive-media.formlabs.com/upload/XL-DataSheet.pdf.

[295] Parker Hannifin Corporation O-ring Division, "Parker O-Ring Handbook - ORD 5700," tech. rep., Clevelang, OH, 2018.

[296] Oceanz, "OCEANZ FLEXIBLE: Datasheet for flexible TPE parts produced by Selective Laser Sintering," tech. rep., 2020. Retrieved from https://www.oceanz.eu/materialen/oceanz-flexible/.

[297] CES Edupack, "Material Universe Level 3: Polymers - All: Thermoplastics: PA(Polyamide/Nylon): PA12 : Unfilled: Semi - Flexible," 2019.

[298] CES Edupack, "Material Universe Level 3: Polymers - All: Thermoplastics: PA(Polyamide/Nylon): PA12 : Unfilled: Rigid," 2019.

[299] M. V. Weghe, M. Rogers, M. Weissert, and Y. Matsuoka, "The ACT hand: Design of the skeletal structure," Proceedings - IEEE International Conference on Robotics and Automation, vol. 2004, no. 4, pp. 3375–3379, 2004.

[300] A. D. Deshpande, Z. Xu, M. J. V. Weghe, B. H. Brown, J. Ko, L. Y. Chang, D. D. Wilkinson, S. M. Bidic, and Y. Matsuoka, "Mechanisms of the Anatomically Correct Testbed Hand," ASME Transactions on Mechatronics, vol. 18, no. 1, pp. 238–250, 2013.

[301] M. B. Bhadugale, "Anthropomorphically Inspired Design of a Tendon-Driven Robotic Prosthesis for Hand Impairments," 2018.

[302] J. A. Hughes, P. Maiolino, and F. Iida, "An anthropomorphic soft skeleton hand exploiting conditional models for piano playing," Science Robotics, vol. 3, no. 25, pp. 1–13, 2018.

[303] J. A. Hughes, P. Maiolino, and F. Iida, "Supplementary Materials for; An anthropomorphic soft skeleton hand exploiting conditional models for piano playing," Science Robotics, vol. 3, no. 25, 2018.

[304] B. Miloradović, B. Çürüklü, M. Vujović, S. Popić, and A. Rodić, "Low – cost anthropomorphic robot hand with elastic joints – early results," Conference Proceedings IcETRAN, vol. 2, no. June, 2015.

[305] Z. Xu and E. Todorov, "Design of a highly biomimetic anthropomorphic robotic hand towards artificial limb regeneration," Proceedings - IEEE International Conference on Robotics and Automation, vol. 2016-June, pp. 3485–3492, 2016.

[306] A. Mohammadi, J. Lavranos, H. Zhou, R. Mutlu, G. Alici, Y. Tan, P. Choong, and D. Oetomo, "A practical 3D-printed soft robotic prosthetic hand with multi-articulating capabilities," PLoS ONE, vol. 15, no. 5, pp. 1–23, 2020.

[307] H. A. Varol, M. Goldfarb, S. Dalley, and T. Wiste, "The Human Hand as an Inspiration for Robot Hand Development," ch. 20, pp. 431 – 452, Springer, 2014.

[308] H. Zhou, A. Mohammadi, D. Oetomo, and G. Alici, "A Novel Monolithic Soft Robotic Thumb for an Anthropomorphic Prosthetic Hand," IEEE Robotics and Automation Letters, vol. 4, no. 2, pp. 602–609, 2019.

[309] S. Yousaf, V. Joshi, J. Britt, C. Rose, and M. O'Malley, "Design and characterization of a passive instrumented hand," in Proceedings of the ASME 2019, dynamic systems and controls conference, 2019.

[310] N. Sarkany, G. Cserey, and P. Szolgay, "An introduction of the biomimetic hand testbed: Skeletal structure and actuation," ROSE 2013 - 2013 IEEE International Symposium on Robotic and Sensors Environments, Proceedings, pp. 43–48, 2013.

[311] L. K. Saharan, "iGRAB hand orthosis: design and development using twisted anc coiled polymer muscles," Doctoral Dissertation, The University of Texas, 2017.

[312] S. Shimawaki, T. Murai, M. Nakabayashi, and H. Sugimoto, "Measurement of flexion angle of the finger joint during cylinder gripping using a three-dimensional bone model built by X-ray computed tomography," Applied Bionics and Biomechanics, vol. 2019, 2019.

[313] A. Buryanov and V. Kotiuk, "Proportions of Hand Segments," International Journal of Morphology, vol. 28, no. 3, pp. 755–758, 2010.

[314] J. Herder, In de greep van de handschoen. PhD thesis, TU Delft, 1992.

[315] J. H. Coert, G. A. van Dijke, S. E. Hovius, C. J. Snijders, and M. F. Meek, "Quantifying thumb rotation during circumduction utilizing a video technique," Journal of Orthopaedic Research, vol. 21, no. 6, pp. 1151–1155, 2003.

[316] Y. Hasegawa and T. Suzuki, "Thin and active fixture to hold finger for easy attachment and comfort of grasping support exoskeleton," Proceedings - IEEE International Conference on Robotics and Automation, vol. 2015-June, no. June, pp. 4973–4978, 2015.

[317] WMF Group, "For me, for you. With KAISER.." Retrieved from https://www.wmf.com/en/company/global-consumer-goods/brands/kaiser.html.

[318] Slap Wraps, "SlapWraps; The instant eaqual Grip." Retrieved from www.slapwrap.net.

[319] P. Webb, A. Golan, V. Sumini, and H. Ishii, "Auto-inflatables: Chemical inflation for pop-up fabrication," Conference on Human Factors in Computing Systems - Proceedings, pp. 1–6, 2019.

[320] T. Hiramitsu, K. Suzumori, H. Nabae, and G. Endo, "Experimental evaluation of textile mechanisms made of artificial muscles," in 2nd IEEE International Conference on Soft Robotics (RoboSoft), (Seoul, Korea (South)), IEEE, 2019.

[321] T. Ranzani, S. Russo, N. W. Bartlett, M. Wehner, and R. J. Wood, "Increasing the Dimensionality of Soft Microstructures through Injection-Induced Self-Folding," Advanced Materials, vol. 30, no. 38, pp. 1–6, 2018.

[322] M. Wehner, R. L. Truby, D. J. Fitzgerald, B. Mosadegh, G. M. Whitesides, J. A. Lewis, and R. J. Wood, "An integrated design and fabrication strategy for entirely soft, autonomous robots," Nature, vol. 536, no. 7617, pp. 451–455, 2016.

[323] A. Lendlein, H. Jiang, O. Jünger, and R. Langer, "Light-induced shape-memory polymers," Nature, vol. 434, no. April, pp. 695–697, 2005.

[324] J. Leng, X. Lan, Y. Liu, and S. Du, "Shape-memory polymers and their composites: Stimulus methods and applications," Progress in Materials Science, vol. 56, no. 7, pp. 1077–1135, 2011.
[325] A. Papadopoulou, J. Laucks, and S. Tibbits, "Auxetic materials in design and architecture," Nature Reviews Materials, vol. 2, pp. 1–3, 2017.
[326] A. Papadopoulou, H. Lienhard, S. . Kernizan, J. Laucks, and S. Tibbits, "Self-assembly lab: Active Auxetics," MIT. Retrieved from https://selfassemblylab.mit.edu/active-auxetics.
[327] R. Granberry, K. Eschen, B. Holschuh, and J. Abel, "Functionally Graded Knitted Actuators with NiTi-Based Shape Memory Alloys for Topographically Self-Fitting Wearables," Advanced Materials Technologies, vol. 4, no. 11, pp. 1–11, 2019.
[328] Y. Mao, Z. Ding, C. Yuan, S. Ai, M. Isakov, J. Wu, T. Wang, M. L. Dunn, and H. J. Qi, "3D Printed Reversible Shape Changing Components with Stimuli Responsive Materials," Scientific Reports, vol. 6, no. January, pp. 1–13, 2016.
[329] T. Franssen, "Shape-Memory Alloy in 3D Printing," Master Thesis TU Delft, pp. 4–5, 2017.
[330] K. . Sibbel, P. Azalbert, and B. Ching, "Re:Flex," Retrieved from https://www.materialreflex.com.
[331] J. Ou, Z. Ma, J. Peters, S. Dai, N. Vlavianos, and H. Ishii, "KinetiX - designing auxetic-inspired deformable material structures," Computers and Graphics (Pergamon), vol. 75, pp. 72–81, 2018.
[332] M. A. Skylar-Scott, J. Mueller, C. W. Visser, and J. A. Lewis, "Voxelated soft matter via multimaterial multinozzle 3D printing," Nature, vol. 575, no. 7782, pp. 330–335, 2019.
[333] Y. Kim, H. Yuk, R. Zhao, S. A. Chester, and X. Zhao, "Printing ferromagnetic domains for untethered fast-transforming soft materials," Nature, vol. 558, no. 7709, pp. 274–279, 2018.
[334] Y. Kim, "Printing ferromagnetic domains in soft materials : mechanism, modeling, and applications," S.M. Massachusetts Institute of Technology, 2018. Retrieved from https://dspace.mit.edu/handle/1721.1/118709.
[335] Suzumori Endo Robotics Laboratory, "Active Textile made of Thin McKibben Muscles," 2019. retrieved from https://www.youtube.com/watch?v=PYSqkEhVe6k.
[336] S. Kernizan, A. Moorman, M. Fu, B. Sparrman, J. Laucks, and S. Tibbits, "Self Assembly Lab; Active Textiles," MIT, 2018. Retrieved from https://selfassemblylab.mit.edu/active-textile.
[337] J. M. Ochoa, D. G. Kamper, M. Listenberger, and S. W. Lee, "Use of an electromyographically driven hand orthosis for training after stroke," IEEE International Conference on Rehabilitation Robotics, pp. 1–5, 2011.
[338] A. Stilli, A. Cremoni, M. Bianchi, A. Ridolfi, F. Gerii, F. Vannetti, H. A. Wurdemann, B. Allotta, and K. Althoefer, "AirExGlove-A novel pneumatic exoskeleton glove for adaptive hand rehabilitation in post-stroke patients," 2018 IEEE International Conference on Soft Robotics, RoboSoft 2018, pp. 579–584, 2018.
[339] A. Polotto, F. Modulo, F. Flumian, Z. G. Xiao, P. Boscariol, and C. Menon, "Index finger rehabilitation/assistive device," Proceedings of the IEEE RAS and EMBS International Conference on Biomedical Robotics and Biomechatronics, pp. 1518–1523, 2012.
[340] D. Popov, I. Gaponov, and J. H. Ryu, "Portable exoskeleton glove with soft structure for hand assistance in activities of daily living," IEEE/ASME Transactions on Mechatronics, vol. 22, no. 2, pp. 865–875, 2017.
[341] O. Sandoval-Gonzalez, J. Jacinto-Villegas, I. Herrera-Aguilar, O. Portillo-Rodiguez, P. Tripicchio, M. Hernandez-Ramos, A. Flores-Cuautle, and C. Avizzano, "Design and development of a hand exoskeleton robot for active and passive rehabilitation," International Journal of Advanced Robotic Systems, vol. 13, no. 2, 2016.
[342] I. Jo, J. Lee, Y. Park, and J. Bae, "Design of a wearable hand exoskeleton for exercising flexion/extension of the fingers," IEEE International Conference on Rehabilitation Robotics, pp. 1615–1620, 2017.
[343] H. B. Hoffman and G. L. Blakey, "New design of dynamic orthoses for neurological conditions," NeuroRehabilitation, vol. 28, no. 1, pp. 55–61, 2011.

Appendices

APPENDIX A THE HUMAN HAND

1. THE HAND AND IT'S GRASPING ABILITIES

The hand is an incredibly versatile instrument. So, in furtherance of an usable hand orthosis, knowledge must be gathered about its structure and functionalities. When simplifying the hand to its most minimal form, the limb can be perceived as a stable wrist with two digits, that are able to oppose each other with some power. In this minimal form, one digit can be stable, so the other has motion to move against a stable post [36]. Be that as it may, the hand, in reality, is composed of twenty-nine muscles that drive 19 bones that construct the 5 fingers of the hand [166]. Anatomically the hand has five fingers consisting of 3 phalanges in the fingers and 2 phalanges in the thumb. These phalanges are connected at joints, and the fingers are merged into the hand through the carpals. Tendon structures guided from muscles in the forearm generate motions around the finger joints. Twenty-three degrees of freedom (DOF) are taken into consideration. Movements between the metacarpal joints have been taken out of account for the purpose of simplicity. These 23 DOF include flexion/extension (FE), abduction/adduction (AA) and radial/ulnar deviation (RUD) in the fingers and wrist [7]. Anatomy and motions of the fingers are indicated in Figure 25. Distal interphalangeal (DIP) and proximal interphalangeal (PIP) joints can move only in a FE manner, resulting in 1 DOF. The metacarpal phalangeal (MCP) joints and the carpometacarpal phalangeal (CMC) joint of the thumb are also capable of AA, thus have 2 DOF [2], [3], [167]. For clarity, the MCP and DIP joint of the thumb will be referred to as MP and IP, respectively.

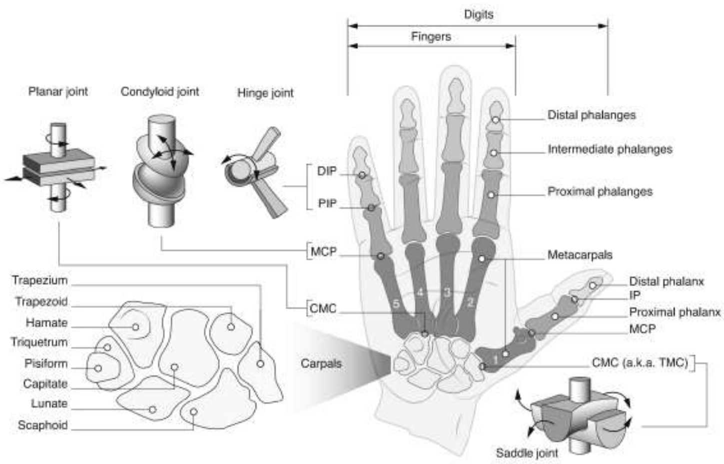

(a) Bones and joints of the hand [3]

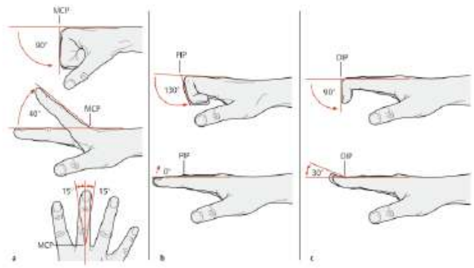

(b) Passive range of motion of the finger joints [2]

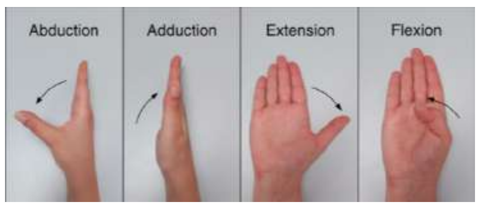

(c) Movements of the thumb CMC joint [167]

FIGURE 25. Hand anatomy of the 19 finger bones and the 21 finger DOF; DIP (1DOF), PIP (1DOF), MCP (2DOF) and the CMC(2DOF).

Humans interact with their environment mainly through grasping. Accordingly, many studies have been performed on the topic of hand function. Grasping attributes related to successful prehension have been defined by Cutkosky et al.(1989) as [168]:

1) *Sensitivity*; how accurately the fingertips can pick up small vibrations and small changes in force and position.
2) *Precision*; how accurately the fingers can impart small motions or forces to the object.
3) *Dexterity*; similar to precision but implies that larger motions can be imparted to the object.
4) *Stability*; how well a grasp will return to its nominal position after being disturbed, and the ability of the grasp to resist external forces without slipping.
5) *Security*; related to stability, but is most closely associated with resistance to slipping.

The prominence of the attributes vary between grasp types. For grasping small, irregular, lightweight objects, more emphasis is on dexterity and precision. These grasps are indicated as precision grips. Contrarily, if the focus is more on stability and security, it is spoken of power grasps [168]. Over the years, many other grasping taxonomies have been developed and were used to evaluate grasp frequencies and usage [62], [168]–[173]. Three popular grasp taxonomies are shown in Figure 26. Classification is based on force production and thumb position. Although grasp taxonomies are quite extensive, it is unnecessary to achieve all of the different grasps. Many tasks can be completed by several grasping approaches [168]. Gracia-Ibanez et al. conducted a study in 2018 to identify the most critical grasps for achieving personal autonomy. Within this study, pad-to-pad pinch, lumbrical, cylindrical and special pinch, together with non-prehensile grasps were identified as most relevant. Relative importance was determined based on dependency versus disability scales and bimanual versus unimanual actions [57]. Another study conducted by Bullock et al. (2013), attempted to identify small, versatile grasp sets to accommodate the largest grasp span. Results suggest that a general-purpose power grasp (e.g. medium wrap), a lateral pinch, and a precision fingertip grasp are all important for versatile object handling with the human hand. The medium wrap and lateral pinch grasp have been identified to handle the broadest range of objects [37]. Bimanual ADL are characterized by asymmetric hand function. One will require power and dexterity, while the other will fulfil a supportive function [62], [174]. Grasp types of the supporting hand that are of use in the majority of bimanual ADL tasks are the cylindrical, spherical and platform power grasp.

Grasping can be divided into two phases. The pre-grasping posture is the position the hand adopts in preparation for grasping an object. Most crucial in the approaching position is a large enough hand opening to envelop the approached object [171]. Kutz et al. (2009) defined a functional opening width of 10 [cm] for power grasps and 5 [cm] for precision pinches [175]. Pre-grasping is followed by the grasping posture itself, by which the configuration the hand uses while holding the object is meant [171]. Hand postures needed for succeeding ADL activities comfortably and effectively, determine the functional range of motion (fROM) [161], [171], [176]. The set of use-full grasps decided on here are the cylindrical grasp, lateral pinch and precision pinch.

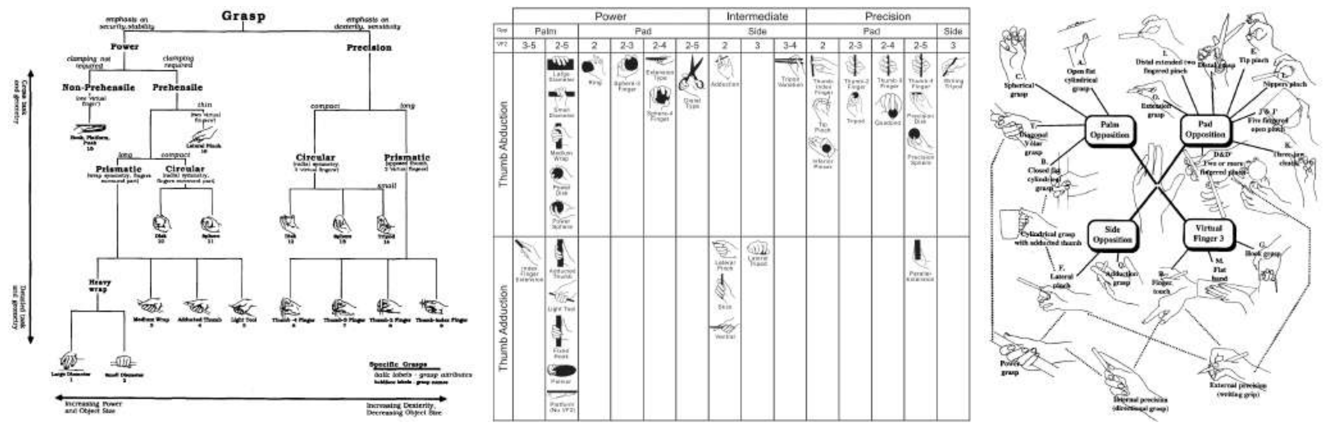

(a) Cutkosky et al. (1989) [168]

(b) Modified taxonomy of Feix et al. (2009) by Bullock et al (2015) [170]

(c) Iberall et al. (1997) [169]

FIGURE 26. Different grasp taxonomies based on force exertion and thumb position.

Motions of the hand are constraint by three elements. Constraint I: *anatomic limitations of the hand*; determine the passive range of motion (pROM) of the hand in Figure 25(c). Constraint II: *joint synergies*; finger joints are underactuated by the same tendons, resulting in simultaneous FE with a ratio between angles of $DIP : PIP = 2 : 3$. Constraint III: *simultaneous motions of individual fingers*; due to neural and muscular synergies originating from motor units that perform specific movements. As a result of these synergies, the 4 fingers are planar manipulators [177]. The functional length of the finger phalanges closely fit the Fibonacci ratio, so the fingers follow an equiangular spiral of joint motion arcs [36], [178]. In flexion, the digits of the hand form longitudinal arches, which are known to resist greater forces than other structures [36]. A straight line of force between the tips of the index and the middle finger and the thumb results from hand the synergies, providing a good strength and consistency in pinch grip [179]. The three constraints brought together, dictate the active ranges of motion of the hand (aROM). It has been reported that individual joint contributions to the total flexion arc of the finger are, 3 [%] DIP, 20 [%] PIP and 77 [%] MCP [36]. All finger tendons cross the wrist, causing mechanical consequences of the relative position of the wrist on hand function [180]. Mallon et al. (1991) found that active and passive flexion abilities of the fingers increased with dorsal extension of the wrist [63]. For optimal finger freedom, the wrist should be positioned in 35 [deg] dorsal extension and 5 [deg] of ulnar deviation [62].

TABLE 7. aROM, pROM and fROM of the finger joints reported in literature. Negative signs (-) signify extension, signless values indicate flexion.

All units are in [deg]		Rest (index)	aROM		pROM	fROM		
		Kamper 2003 hand on thigh	Hume 1990 from straight	Bain 2015 from straight	Hirt 2017 from straight	Bain 2015 from straight	Hume 1990 from straight	Gracia-Ibanez 2017 from straight
Fingers (FE)	DIP	1.1	0/85	-6/84	-30/90	10/64	20/61	-1.8/51.5
	PIP	10.5	0/105	-7/101	0/130	23/87	36/86	4.6/88.9
	MCP	5	0/100	-19/90	-40/90	19/71	33/73	not measured

The anatomical hand can operate at speeds in excess of 40 [rad/s] (2290 [deg/s]) and grasps involving all fingers can exert up to 400 [N] of force. Even though these are achievable values, average physiological speeds for everyday pick-and-place tasks are specified in the range of 3-4 [rad/s] (172-200 [deg/s]) [175]. This corresponds to cycle frequencies between 0.5-1.6 [Hz] in ADL for healthy people [7]. Generation of proper speeds and forces for grasping within the hand is entirely force controlled. For this reason, using the hands does not necessarily require visual feedback. Conversely, cutaneous feedback is of significant importance for determination of the grip safety margin. The safety margin is a function of frictional properties at initial contact and phasic slip-detection [64]. If tactile sensation is diminished, visual feedback is combined with sensorimotor memories that have been obtained by proprioception in previous tasks, and automatic grasp stability can still be achieved [181]. Importance of tactile sensation and proprioception is reflected in the grasp attribute of sensitivity by Cutkosky et al. (1989) [168]. DMD patients have intact proprioceptive and tactile capabilities. Patients can process signals and respond successfully with finger movements no faster than 2 [Hz], was implied in a case study performed by Nizamis et al. (2017) [182].

Regarding forces, most ADL require prehensile forces of 0-67 [N], depending on the coefficient of friction between the grasping surface and the object [175]. Smaby et al. (2004) found values ranging from 1.4 - 31.4 [N] needed for ADL tasks performed with lateral pinches. Nine out of the twelve tasks could be performed with forces below 10.4 [N]. These force levels are far below the average male and female maximum lateral pinch strength of 55-115 [N] determined by Versluis in 2015 [183]. They are also lower than and those reported by Punsola-Izard et al. of 65.4 [N] in 2012 [184]. Precision pinches for opening and closing a zipper on a horizontal surface are within the same force range reported for lateral pinches. Absolute maximum values needed for the thumb are below 6.7 [N] and for the index finger lower than 9.9 [N], as indicated by Pylatiuk et al. (2006) [185]. The task selected requires low forces. Still values are substantially below the maximal exertable lateral pinch strength. Pylatiuk et al. additionally looked into grip distributions in cylindrical grasps. Results showed that the sum of all contact forces exerted by the fingers is 14.1 [N] for holding and pouring out of a 522 [gr] bottle (S), and 20.6 [N] for a bottle of 1620 [gr] (L). Of these forces, 2.6 [N] (S) and 6.0 [N] (L) is exerted by the thumb and 2.4 [N] (S) and 2.6 [N] (L) by the index finger [185]. These forces can be related to forces acquired by Kargov et al. (2004) of 16.7 [N] summed over all 20 sensors, with the highest sensor value of 6.3 [N] for a 522 [gr] bottle. Maximal values at the tip of the thumb were reported as 1.3 [N] and 2.8-4.5 [N] [58]. Forces reported by Kargov et al. have been calculated into torque values of the separate joints. Thumb joint torques; 0.08 [Nm] at the MP joint and 0.02 [Nm] at the IP joint. Index joint torques; 0.09 [Nm] at the MCP, 0.05 [Nm] at the PIP and 0.01 [Nm] at the DIP [58]. Other joint torque measurements for the thumb reported in the literature are; 0.3 [Nm] by Kawasaki et al. (2007) and 0.06-1.4 [Nm] by Cooney et al. (1977) for FE and AA in the CMC joint [91]. Lastly, Ueki et al. (2012) reported maximal values for torques on the thumb joints with values of 0.3 [Nm] at the CMC joint (FE & AA) and 0.26 [Nm] at the MP and IP joints (FE) [186]. Torques mentioned before have been used for the assistance of finger flexion. Torques needed for passive thumb abduction with a fROM of 60 [deg] around the CMC joint in children with hemiplegia or stroke were indicated as maximal 0.285 [Nm], with a mean of 0.168 ±0.076 [Nm]. [89]. For adults, these extension torques needed are larger with values of 0.45 ±0.31 [Nm] reported by Smulders et al. (n.d) [62] and 0.17-1.06 [Nm] by Nycz et al. (2018) [187].

When assisting in thumb function, torques applied should be large enough to facilitate grasping, without exceeding thumb limitations. Torque requirements are set at 0.2 [Nm] to allow of grasping various items with a margin of 0.1 [Nm] from maximal values. By these torques, the exerted forces should be at least 10.4 [N] for lateral pinch, 20.6 [N] for cylindrical grip strength and 10 [N] for precision pinch. During assistance of the fingers, only normal forces contribute to grasping forces. Shear forces in the contrary can cause skin damage and should be avoided [7].

2. THE THUMB

The most important evolutionary advancement of the humans and primates is the possibility to oppose the thumb towards the other fingers. The thumb is used in almost 90 [%] of the grasping executions and endures half of the workload of the prehensile hand [1], [56]. The control of the thumb during grasping is synergistic with the rest of the other fingers of the hand, but can also be independently controlled. This makes the thumb the most independent digit and exceptional in terms of anatomy, kinematics, size and strength of its muscles [188]. Thumb motion can determine which posture is used, while the index and middle finger provide information about object geometry. For this reason, many grasping taxonomies are based largely on thumb position [56], [169], [172]. Analysis shows that although the movement of the thumb during grasping is less compared to the other fingers, adequate placement of the thumb at the right moment determines whether the grasp is successful or not. Therefore, similar thumb motions can be used to grasp different shapes [56], [189]. For example, lateral pinch, tridigital and power grip motions share the same characteristics of thumb joint motion, with only slight variation in the CMC joint angles [61], [190].

The thumb's metacarpal orientation in the anatomic rest position corresponds to a pre-grasp position, e.g. an open hand [190]. The metacarpal orientation is also rotated 80-90 [deg] medially (pronated & flexed) relative to the other digits with their palmar surfaces facing anteriorly [36], [166]. When looked at from a medial perspective, the thumb lies anterior to the finger metacarpals and just out at an angle of 45 [deg] [1]. It can be assumed that thumb opposition is a circular cone motion in which the tip of the cone is located in the wrist, and the orientation of the thumb is almost constant with respect to the cone center axis. Hence, the AA and FE motions of the CMC joint are homologous, respectively, to the circular cone motion and a vertex angle motion, which adjusts the vertex angle of the cone. [186]. The natural thumb uses a preferred plane of motion, which intersects the plane of flexion of the middle finger in the plane of the palm, with an angle ranging from 45 to 55 [deg] [190]. Vinet et al. (1995) state that the only difference between lateral and tridigital modes is the angle of inclination of the thumb (25 or 59 [deg]). The angle of inclination was measured between the plane of the thumb and a plane perpendicular to the plane of the palm, having a 45 [deg] line of the thumb as axis [190]. The oblique arches formed by the thumb help to stabilize orientations and positions of the fingers for in-hand manipulation [188]. Considering almost equal characteristics of IP and MP position in a lateral pinch, precision/tridigital pinch and cylindrical power grasp, in addition to the relevance of these postures in grasp versatility, autonomy and unimanual as well as bimanual tasks, these postures are selected for assistance.

Theoretically, the most advantageous position for performing pinch from a biomechanical perspective is in an arched position, such that there is flexion in the sagittal plane in the IP and MP joint and extension of the CMC joint. During this 'neutral position' of the CMC joint, there is maximal articular contact, ligaments are relaxed, and muscles have a central position which makes them more efficient [184]. For each kilogram of force exerted by the thumb against the fingertip, 12 [kg] of compressive force is applied to the CMC joint. However, in spite of the theoretically ideal arched pattern, this position is not most commonly used [184]. ROMs of the thumb joints in various ADL tasks have been reported by various researchers; Lin et al. (2011) determined the three thumb joint angles and their normalized values in six ADLs; tip pinch, palm pinch, lateral pinch, cylinder grip, spherical grip and power grip [61]. Cooney et al. (1981) measured the fROM of the CMC joint in resting, flexion, extension, abduction, tip pinch and grasp [191]. Vinet et al. (1995) calculated the flexion joint angles of his prosthetic design with a fixed MP joint of 10 [deg] with respect to its reference position in five situations; hand open (resting), tridigital approaching, lateral approaching, tridigital closed, and lateral closed [190]. Hume et al. (1990) reported task-specific positions of the CMC joint [161]. Lastly, it was pointed out in Nanayakkara et al. (2017), that up to 76 [%] of the thumb's workspace related to the maximal ROM is not used to fulfil simple activities [188]. Within this same article, thumb joint ROM is reported as 69 [deg] FE, 48 [deg] AA at the CMC and 93 [deg] FE at the MCP joint [192], which is consistent with values reported by Cooney et al. (1981) [191]. It is challenging to compare identified fROMs, as often different measurement techniques and tasks are used, while the ROM and grasping approaches of participants are already highly variable.

TABLE 8. aROM and pROM of the thumb joints reported in literature. Negative signs (-) signify extension or adduction, signless values indicate flexion or abduction.

Units are in [deg]		aROM				pROM	
		Barakat 2013 line CMC-1st MC	Cooney 1981 from neutral position	Hume 1990 from straight	Stillfried 2010 Sum angular displacement	White 2018 line CMC-1st MC	AAOS line CMC-1st MC
Thumb	IP	-12/88	not measured	5-73	103	not measured	
	MCP	-8/60		0/56	92		
	CMC (FE)	-31/61	-32/15	not measured	48	-20/22	-20/15
	CMC (AA)	10/63	-3/39		69	51	70

TABLE 9. Joint angles reported for ADL grasps. negative signs (-) signify extension, adduction or external rotation, signless values indicate flexion, abduction or internal rotation.

All units are in [deg]		Cooney 1981 [191] Positions with respect to Rest			Lin 201 [61] Mean of Max joint angles with respect to neutral position			Hume 1990 [161] Task specific positions				Gracia-Ibanez 2017 [176] fROM in 24 ICF ADL activities with respect to hand flat on table
		Rest	Tip	Grasp	Tip	Lateral	Cylindrical	Tip	Lateral	Grasp	Grip	Global fROM
CMC	FE	20.5	7.5	4.1	-9/14	-9/4	-16/15	Not measured				-11.2/33.9
	AA	-23.2	5	33	-4/9	-7/6	-1/16					5.4/21.2
	IE	13.6	5.1	6.2	-9/10	-16/6	-15/11					Not measured
MCP	FE	Not measured			-11/9	8/24	-23/1	22	20	10	23	-17.1/14.3
IP	FE				0/36	0/22	37	25	16	28	36	-7.2/80.6

3. IN CONCLUSION

The hand is an essential instrument for ADL and autonomy, where the thumb is the main determining factor of versatility [36]. As the Symbihand only consist of finger modules, a thumb module should be developed [7]. This thumb module should assist lateral, precision and cylindrical grasp in order to increase functional autonomy of the DMD patient [57]. Due to hand synergies, added function can be achieved by merely assisting the CMC joint, while splinting the MP and IP joints [61]. Splinting of the

MP and IP joints should be in an arched manner at 22 [deg] MP and 25 [deg] IP flexion. Maximal movement of the non-splinted joints can be achieved by splinting the wrist at 35 [deg] dorsal extension and 5 [deg] ulnar deviation [62], [63]. Opposition can be seen as a combination of CMC flexion/extension (FE) and abduction/adduction (AA), with intersecting and orthogonal axes of rotation. For ADL CMC FE angles of 13-22 [deg] are sufficient combined with 13-20 [deg] of AA. Overextension should be avoided with the range of safe assistance set to maximal 53 [deg] FE and 42 [deg] AA [186]. However, for control simplicity, only FE will be assisted. The CMC joint will be splinted in the AA plane at an angle of 53 [deg]. In combination with the the finger motions of the Symbihand a hand opening of 10 [cm] should be achieved for proper pre-grasping. During the grasping itself the fingertips of the index and middle finger should meet the tip of the thumb for adequate precision pinch and lateral pinch. Torques for taking this position may not exceed 0.3 [Nm], but should be around 0.2 [Nm]. As a result precision pinch forces should be able to achieve values of >10 [N], lateral pinch forces >10.4 [N], and cylindrical grip forces >20.6 [N]. The torques should be by virtue of normal forces from the orthosis on the thumb, and no shear forces should be present [7]. Lastly, tactile and proprioceptive feedback are a large part of successful grasping and studies imply that DMD patients can process signals themselves. The hand orthosis should not obstruct this feedback loop. DMD patients cannot respond successfully to actuation speeds faster than 2 [Hz] [182]. By these elements hopefully an orthotic thumb can be added to the Symbihand, whilst satisfying the grasping attributes described by Cutkosky et al. (1989) [168].

APPENDIX B STATE OF THE ART IN THUMB ASSISTANCE

1. THUMB ASSISTANCE STATED IN LITERATURE

To capture an idea of the state of the art for thumb modules, designs were gathered from several reviews; Bos et al. (2016) [28], Baan (2019) [73], Heo et al. (2012) [30] and Sarac et al. (2019) [104]. These reviews were obtained from the literature search in Section III on the fixture designs of hand orthoses for DMD patients, of which the acquired designs from this review were added to the depository as well. A first screening was performed, which included designs for functional assistance of the hand. The screening resulted in a depository of 131 designs. Soft robotics were eliminated as their operation method differs too much from the Symbihand. Out of the 108 selected designs, 79 included the thumb; 19 by splinting, 5 by manual/passive adjustment and 55 by active actuation of thumb in some manner. An overview of the evaluated designs can be seen in Appendix K. Precision pinches and cylindrical grips can be achieved by splinting the thumb in opposition and limiting actuation to the index and middle finger [7]. In some cases, thumb positions can be adjusted manually. These mechanisms are implemented for two main reasons: to obtain the desired alignment of thumb and index finger regardless variability in hand dimensions [143], or to allow for movement of the thumb at times when no gripping is occurring [193]. Manual repositioning of the thumb might be a good option for users who suffer from unilateral symptoms, but, DMD patients are affected bilaterally and are not capable of manual repositioning. In cases where thumb assistance was included, often it was decided to assist precision pinches and cylindrical grasps. The thumb for these cases is assisted in the MP and IP joint by FE. Though, despite a more bio-mimetic hand motion, no additional function is obtained by these movements. In general, the thumb needs to have more than one DOF to improve hand functionality as a whole [188].

TABLE 10. Overview of selected hand orthoses.

Active thumb module				Splinted thumb module		Pneumatic soft robotics	Excluding thumb
CMC joint		MP & IP joint					
	Aubin 2013 [89]		Cui 2015 [157]	Splinted Thumb	Alutei 2009 [194]	Al-Fahaam 2018 [195]	Cempini 2013 [90]
	Brokaw 2011 [160]		Leonardis 2015 [196]		Arata 2013 [197]	Baan 2019 [73]	Chiri 2009 [198]
	Cempini 2015 [90]		Nycz 2016 [199]		Baqapuri 2012 [200]	Borboni 2016 [201]	Chiri 2012 [202]
	Chen 2017 [203]		Puzo 2014 [204]		Benjuya 1990 [205]	Cappello 2018 [153]	Conti 2017 [156]
	Lambercy 2013 [91]		Refour 2019 [206]		Dollfus 1984 [207]	Chen 2017 [208]	Ertas 2014 [209]
	Nishad 1997 [210]		Refour 2018 [211]		Ferraresi 2017 [212]	Connelly 2009 [213]	Fu 2011 [214]
	Richards 2015 [215]		Takagi 2009 [216]		Gasser 2015 [163]	Gobee 2017 [217]	Guo 2018 [218]
	Tadano 2010 [219]		Tjahyono 2013 [220]		Gearhart 2016 [221]	Jiang 2018 [222]	Haarman 2019 [223]
	Ueki 2012 [186]		Surendra 2012 [224]		Hong 2013 [225]	Jiang 2017 [?]	Heo 2013 [226]
Endpoint effectors	Chowdhury 2019 [133]		Tong 2010 [227]		Kudo 2014 [228]	Jiralerspong 2018 [229]	Herrmann 2012 [230]
	Ferguson 2019 [154]		Triolo 2018 [231]		Kuswanto 2018 [165]	Kadowaki 2011 [232]	Jones 2014 [233]
	Iqbal 2015 [234]		Wang [134]		Makaran 1993 [235]	Lin 2018 [236]	Lince 2017 [237]
	Iqbal 2010 [238]	Tendon	Biggar 2016 [179]		Mohammadi 2018 [158]	Low 2015 [239]	McConnell 2014 [240]
	Sarakoglou 2016 [142]		Burns 2017 [146]		Moromugi 2010 [241]	Patino 2018 [144]	Niestanak 2018 [242]
Tendon	Brown 1993 [243]		Cheng 2018 [244]		Otsuka 2010 [245]	Polygerinos 2015 [145]	Pu 2014 [135]
	Hasegawa 2008 [246]		Delph 2013 [247]		Pedrocchi 2013 [5]	Sasaki 2014 [248]	Tan 2017 [249]
	In 2015 [250]		Ghassemi 2018 [251]		Slack 1992 [252]	Shiota 2019 [253]	Tang 2011 [254]
	Kim 2017 [97]		Hadi 2018 [255]		Bos 2019 [34]	Sun 2019 [256]	Toochinda 2018 [257]
	Lee 2014 [147]		In 2011 [103]		Bos 2018 [34]	Toya 2009 [258]	Watanabe 2005 [259]
	Li 2011 [152]		Kang 2016 [138]	Adjustable	Butzer 2019 [162]	Yap 2017 [260]	Wege 2006 [261]
	Moromugi 2009 [262]		Lu 2016 [263]		Gasser 2017 [143]	Yap 2017 [264]	Weiss 2013 [149]
	Nycz 2015 [265]		Martinez 2010 [266]		Gasser 2019 [174]	Yap 2016 [267]	Yamaura 2009 [148]
	Rahman 2013 [150]		Nilsson 2012 [268]		Heo 2014 [193]	Yap 2015 [269]	Zhang 2014 [270]
	Rose 2019 [139]		Ochoa 2009 [271]		Hong 2019 [272]		
	Saharan 2017 [273]		Ong 2018 [274]				
	Xiloyannis 2017 [136]		Park 2018 [140]				
			Pu 2017 [275]				
			William 2011 [276]				
			Yang 2016 [277]				

More than half of the 55 active thumb mechanisms are based on tendon actuation systems. This system is highly common probably because the design for the fingers is easily transferable onto the thumb [138], [247]. Within these actuation systems, no specific evaluation of thumb movements is present. Also, support is limited to the FE movements of the MP and IP thumb joints and AA of the CMC joint. Individual MCP and IP joint motions may not be effective because the CMC joint mechanism predominantly controls the thumb linkage [188]. Assistance of the CMC joint, without the use of tendon mechanisms, was found in 14 designs. Howbeit, that 5 of these designs were endpoint effectors controlled in a planar manner, thus only controlling the tip of the thumb, hereby, merely inheriting CMC motion [133], [142], [154], [234].

In the end, only 5 designs appeared relevant within the design scope, where the CMC joint is assisted, and the MP and IP joints are splinted. Thumb designs including assistance of the CMC joint are developed by Ueki et al. (2012) [186], Aubin et al. (2013) [89], Lambercy et al. [91], Richards et al. (2015) [215] and Cempini et al. (2015) [90]. The designs are represented in Figure 27. These designs may support the CMC joint, but they do not suffice all requirements for assisting hand function. For starters, most of the designs are quite cumbersome and would be of hindrance in ADL. Secondly, the designs are connected to the hand in manners that do not allow for tactile sensation or easy donning and doffing with hand deformities. The orthoses designed by Heo et al. (2014) [193], Refour et al. (2018) [211] and Takagi et al. (2009) [216], use hydraulic or pneumatic air cylinders for actuation, as was done by Bos et al. (2019) in the Symbihand. These designs were limited to FE motions of the thumb joint for precision and cylindrical grasps.

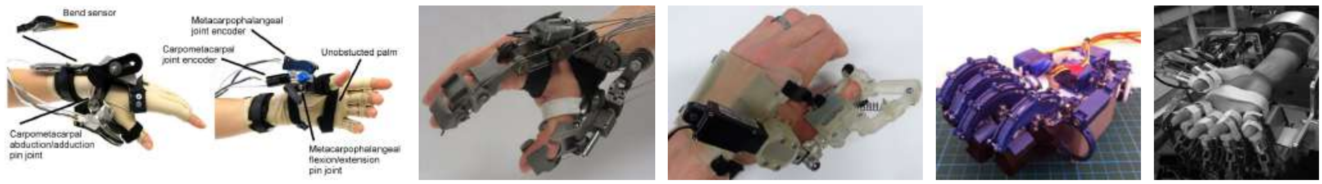

(a) (b) (c) (d) (e)

FIGURE 27. Current thumb designs that assist the thumb's CMC joint. 27(a) Aubin et al. (2013) [89]; 27(b) Cempini et al. (2015) [90]; 27(c) Lambercy et al. (2013) [91]; 27(d) Richards et al. (2015) [215]; 27(e) Ueki et al. (2012) [186].

2. IN CONCLUSION

Over the years hand orthoses have been developed in abundance. Despite the vast amount of attention towards the subject, few orthoses have made it to market. The scope of this design project is to add a thumb module to the Symbihand hand orthosis for DMD patients to assist the CMC joint. From the evaluation of current designs of hand orthoses, it can be concluded that a minority includes a functional thumb design. Often the MP and IP joints of the thumb are supported, even though, support of these joints does not broaden the functional abilities of the hand orthosis. Simply splinting the thumb in opposition would result in equal capabilities, while being less cumbersome. The few orthoses that support the CMC joint are often incredibly ponderous as the MP and IP joint are integrated as well. The design of a slim CMC joint mechanism would therefore be a relevant design scope.

APPENDIX C DESIGN REQUIREMENTS STATED IN LITERATURE

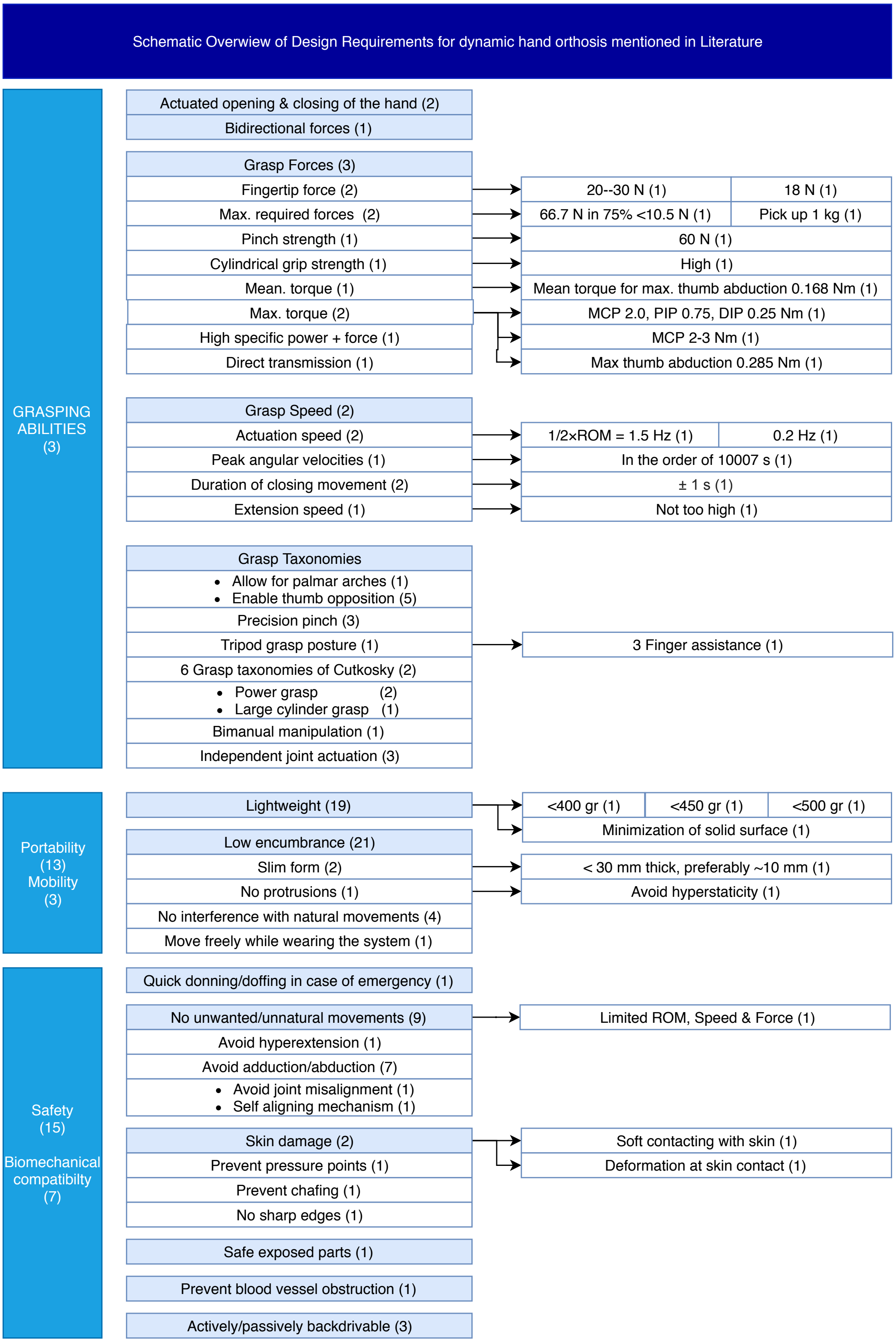

[3], [7], [30], [89], [90], [97], [99], [103]–[106], [132], [133], [137], [139], [144], [146], [151], [155], [156], [159], [162], [163], [165], [215], [233], [234], [238], [249], [256], [268], [278]–[286]

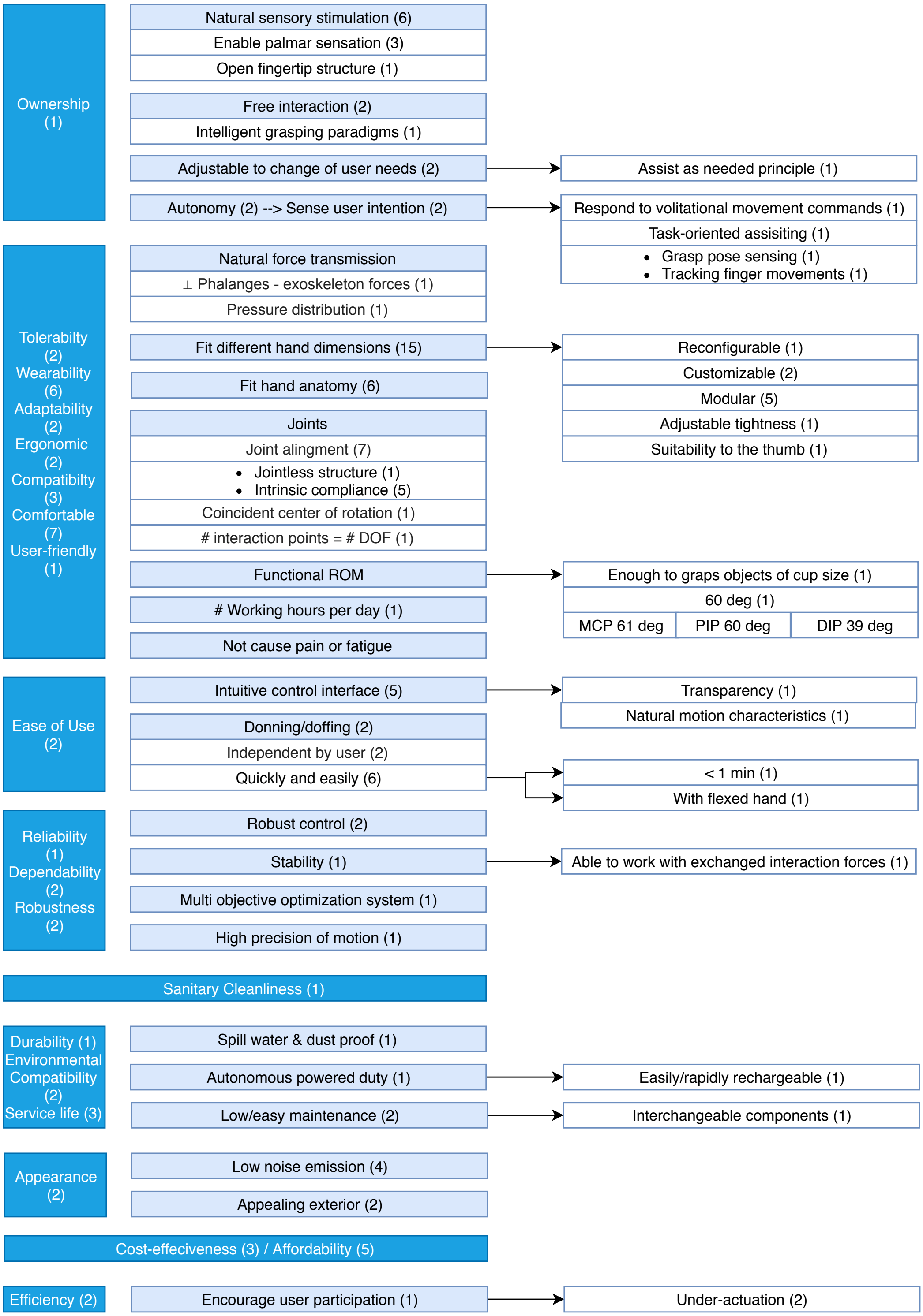

[3], [7], [30], [89], [90], [97], [99], [103]–[106], [132], [133], [137], [139], [144], [146], [151], [155], [156], [159], [162], [163], [165], [215], [233], [234], [238], [249], [256], [268], [278]–[286]

APPENDIX D REQUIREMENTS FOR THE THUMB MODULE

Within Appendix A and B, several capabilities and limitations of the hand and hand orthoses have been discussed. Hereby, design requirements for a Symbihand thumb module can be deducted. Assistance of flexion and extension of the CMC joint will be combined with arched splinting of the MP and IP joints at flexion angles of 25 [deg] and a CMC abduction angle of 53 [deg]. The thumbs most significant added value is its opposition property, flexion and extension of the CMC joint should facilitate an angle 0-90 [deg] flexion between the thumb and index finger within the transverse plane. Fingers can be flexed furthest with the wrist in 5 [deg] ulnar deviation and 35 [deg] dorsal extension, and therefore these are chosen as splinting positions of the wrist.

Flexion and extension movements of the thumb are prioritised, as they can facilitate change from precision to lateral grasp. However, in order to make these grasps functional, the thumb must be controlled independently. Finger joints can withstand torques up to 0.3 [Nm], which is identified as the maximum of applicable torques. Minimum torque levels are set to 0.2 [Nm] to facilitate grasping of objects of >1 [kg] and to factor in some muscle stiffness. Forces exerted on the fingers should be purely perpendicular and the shear component should be 0 [N]. Only perpendicular forces are of assistance in grip and shear forces can lead to skin damage. Contact pressure should be below 4300 [Pa] in order to prevent blood flow obstruction. This is applicable to clamping forces, as well as resultant forces.

With the 0.2 [Nm] applied to the thumb and to the finger modules of the Symbihand, Precision pinches should be able to achieve values of >10 [N], lateral pinches >10.4 [N] and cylindrical grips >20.6 [N]. With these forces, many ADL activities can be performed. Minimal hand opening should be 10 [cm] for the achievement of a successful pre-grasping position. Bidirectional support must be applied, as both flexion and extension is affected in DMD.

The assistive device is meant to be worn throughout the day, imposing high requirements regarding comfort. This attribute starts by donning of the device. Within the Symbihand evaluation, this was experienced as highly uncomfortable. Fixture of the thumb module should be modular, cause no chafing over the fingers and hand deformities should be no problem. Clamping pressure of the fixture should be below 32 [mmHg] (4300 [Pa]), to prevent blood vessel obstruction. After appropriate donning of the device, several aspects of fixture design are of importance. Surfaces should be smooth, soft and without protrusions, so no harm is done to the incredibly sensitive skin of the DMD patient. Furthermore, Tightness should be adjustable, so it can cope with fluctuations that result from environmental and daily changes. Appropriate alignment with the finger joints can be accomplished by implementing the self-aligning mechanism designed for the Symbihand.

The probability of success of the orthosis, for a large part relies on control as well. Due to the bilateral symptoms of DMD patients, control must be completely hands-free. The control method must be simple and intuitive, make use of the users capabilities and not cause any additional fatigue. The user should be an integrated part of the control loop. An open structure that allows for tactile feedback must be adopted, and fixture displacement that causes skin stretch must be prevented. The utilisation of the natural feedback of the DMD patient results in transparent and reliable feedback and gives the user a feeling of ownership as they can control the applied safety margins themselves. It was indicated by Nizamis et al. (2019) that a cycle time of 2 [Hz] is sufficient for DMD patients [8].

If the hand orthosis functions properly, the user shall start to rely on the functioning of the device. For this reason, the device should not break easily. If this unfortunately happens, repair should need low effort. Parts should be replaceable, and also maintenance should be easy. Lastly, some additional requirements must be added which are less specific. As the orthosis is for assistive purposes, portability is a must. For the disease phase decided on, portability means that the complete assistive device can be transported by powered wheelchair. During the day, different environments and tasks shall be encountered. Accordingly, the device must be able to withstand water and dirt and be easily cleanable. The smell must be neutral, noise emission must be as low as possible, and the exterior of the device must be of low encumbrance. Weight limit for the thumb module itself is set to 50 [gr], as this is also adopted for the finger modules. Reduced weight and proper mass distribution is always better and the centre of mass should preferably be placed further away from the extremities. Table 11 shows an overview of the selected design criteria.

TABLE 11. Design requirements for the thumb module for the Symbihand.

Specification			Value	Unit
Fixation angles	IP (Flexion)		25	[deg]
	MP (Flexion)		22	
	CMC (Abduction)		53	
	Wrist	Ulnar Deviation	5	
		Dorsal Extension	35	
CMC	FE transverse plane	Min	0	[deg]
		Max	90	
Joint Torques	Min		0.2	[Nm]
	Max		0.3	
Forces exerted on the hand	Perpendicular		<5	[N]
	Shear		0	
	Contact pressure		<4000	[Pa]
Forces exerted by the hand	Precision pinch		>10	[N]
	Lateral pinch		>10.4	[N]
	Cylindrical grip		>20.6	[N]
Hand Opening			10	[cm]
Cycle Time			2	[Hz]
Mass			<50	[gr]
Actuation			Hydraulic cylinder with water	
			Planar movements	
			Bidirectional	
			Independent thumb	
			Placed dorsally	
Interface & Fixture			Allow cutaneous feedback	
			Smooth surface	
			Soft interface	
			No protrusions	
			Adjustable tightness	
			No blood vessel obstruction (<32 mmHg)	
			Joint self-alignment	
Donning & Doffing			No chafing	
			With hand deformities	
			Modularity	
Control & Grasp attributes			Hands free/ intention decoding	
			Intuitive control/Simplicity	
			Human-in -the-loop	
			Human safety margins	
			Transparency & Reliability	
Portability			Can be transported by powered wheelchair	
Environmental compatibility			Cleanable	
			Can withstand water	
			Can withstand dirt	
			Can fall without breaking	
Appearance			Neutral smell	
			Low noise emission	
			Slim exterior	

APPENDIX E HYDRAULIC ACTUATION

Fluidic systems: a working fluid with a certain momentum, which can be inflicted by pressure forces, gravity forces or viscous forces [34]. Hydraulics work according to the Pascal's Principle, which states that pressure is uniform and acts in all directions in a fluid at rest. Hence, by coupling the chambers of two fluidic cylinders, force can be transmitted in the form of fluid pressure [7]. The source of pressurized fluid can thus be housed in a base station and flexible hoses can be used to transport the fluid to the actuators located at the periphery of the machine [67]. Compared to Bowden systems, hydraulic systems have several advantages: efficiency is independent of hose curvature; installation flexibility and high system stiffness. They are however bulkier, have strict dimension tolerances, are dependent on sealing properties and are subjected to stiffening of the hoses as pressure is increased [69]. Hydraulic actuation can be either provided by elastic or inelastic actuators, both of which will be discussed in this section [72].

Love et al. (2009) states that: "Metrics clearly indicate that fluidic systems have the near term potential to achieve the required stress, strain stiffness and bandwidth, while also providing low friction, low effective mass and compact packaging for future prosthetic devices" [68]. Also, "as long as miniaturisation is coupled with an increase in system pressure, hydraulic systems can be more compact and light weight than an electromagnetic equivalent" [34], [66], [67].

A hydraulic system consists of several components: a power source in the form of a compressor, which creates fluid flow; hoses, that guide the fluid to the actuator; an accumulator for leakage and temperature compensation, as well as emergency back-up and faster response; valves, which control the fluid flow to separate actuators and the hydraulic actuators themselves. In the Symbihand system the used medium is water, as it is incompressible, harmless to the user and does not create any filthiness in case of leakage. Pressure in the actuators control the force production, and the flow rate controls the speed of the actuation [68]. Fluid pressure in the master and slaves are equal to each other at every moment [79].

As described in Appendix D points of attention for the actuation system are: *force production and transmission, weight, space, joint alignment, durability, environmental compatibility, and safety*.

1. ELASTIC HYDRAULIC ACTUATORS

Elastic fluidic actuators: comprise at least one component that deforms elastically under the applied pressure [72]. These actuators have no sliding parts and so have nearly no friction, wear, sealing and leakage issues [34], [72]. Elastic actuators are relatively easy to fabricate and are classified in membrane, balloon, bellows and artificial muscle actuators as illustrated in Figure 28(b) [72].

1) *Membranes:* consist of a flat or corrugated membrane that is deflected by the driving pressure.
2) *Balloon:* rely on a 3D balloon to generate a bending motion.
3) *Bellow:* comprise a folded geometry that focuses the expansion in one direction rather than the nearly isotropic expansion of the balloons. By making non-symmetric bellows structures, it is also possible to fabricate bending actuators.
4) *Artificial muscles:* generate a contraction upon pressurization. They typically consist of an elastic balloon with embedded fibres or other structures that transform the expansion of the balloon in a contraction force. In these devices the stroke of artificial muscles has an upper limit which is never exceeded independent of the driving pressure.

All elastic actuators depend on the expansion of a material to provide enough stroke, whereas the material should be strong enough to withstand high enough pressures for output force. Most elastic actuators operate in a radial direction. Increased actuator forces are accompanied by a decrease in stroke and vice versa. At maximum actuation all the potential energy is stored in the elastic material in the form of elastic energy and nothing is left to be converted into mechanical work [7]. The force-pressure relationship is stroke dependent as it is related to the material deformation. Maximum forces are confined by the material properties and so the burst pressure of the actuator.

Hand orthoses that use elastic actuators are emerging [28], [73], however the main problem of these actuators is low force production. In order to achieve high strokes, thin compliant membranes are needed, which yield low burst pressures and therefore low actuation forces. On the other hand, high output forces require high pressures and therefore more robust membranes [72].

2. INELASTIC HYDRAULIC ACTUATORS

Inelastic hydraulic actuators work with inelastic materials and so do not depend on material deformation for actuation. Instead, they have sliding parts that can generate rotating or linear motions as a result of pressure generation [7], [72], [287]–[289]. Inelastic hydraulic actuators can provide the maximum rated force over the full range of stroke and do not have the disadvantage of limited pressures due to bursting of elastic material or decreasing output force with increasing stroke. They are, however, as strong as their sealing element. Stronger seals introduce more friction, and weaker seals introduce more leakage [34].

Leakage: undesired mass transport of the working fluid outside of the fluidic circuit [34].

HYDRAULIC LINEAR ACTUATORS OR CYLINDERS

These actuators consist of a piston that can slide freely in a cylinder and can be pushed in two directions depending on which side of the piston is pressurized. Piston–cylinder actuators can combine large strokes with high actuation forces and velocities [72], [289]. They can be classified into the following categories and some are indicated in Figure 28(a) [287]–[289].

1) *Single-Acting Cylinders (SACs):* The piston, or plunger, is driven hydraulically in one direction. In the other direction, the piston moves under the action of an external force or a built-in spring.
2) *Double-Acting Cylinders (DACs):* The piston of a double-acting hydraulic cylinder is driven hydraulically in both directions of motion. DACs can be either single-rod, twin-rod symmetrical or twin-rod non-symmetrical. By hydraulic extension and retraction control over the system is increased.
3) *Tandem Cylinders:* two pistons interlinked in a serial formation. Pressurized air is enforced to both ends of pistons, resulting in augmented force for the same barrel diameter.
4) *Three Position Cylinders:* one cylinder has two separate pistons and piston rods and three ports for fluid supply. The result is a piston cylinder with three operational positions.
5) *Telescopic Cylinders:* provide long cylinder strokes with relatively small installation space. The extension of the telescopic cylinder has different phase, each phase has a sleeve which fits within the previous phase. Telescopic cylinders can be DACs as well as SACs.

Mechanical Locking elements: The position locking of hydraulic cylinders can be realized hydraulically or mechanically. For hydraulic position locking, single- or twin-pilot operated check valves are used. Mechanical locking elements keep the cylinder piston in the required position regardless of the variation of the loading force [288].

HYDRAULIC ROTARY ACTUATORS

Convert fluid energy into mechanical energy by providing rotary motion like clockwise or counterclockwise by the application of pressure similar to electrical drives. This type of actuators is competent in restricted angular movements which can be partial rotations or less than 360 [deg] is more normal [287]–[289].

1) *Rack & Pinion drives:* Figure 28(b). The central part of the piston is formed into a rack. The rectilinear motion of the piston is converted into the rotary motion of a pinion. Swivel angles up to 360 deg and more are possible, depending on the piston stroke and gear ratio [288], [290], [291].
2) *Timing Belts:* A timing belt connects two parallel pistons to one another. By alternatively pressurizing the pistons the belt moves and the motion is converted to rotation of a pinion [291].
3) *Parallel Piston Rotary Actuators:* Figure 28(b), two pistons move parallel to each other. They are alternatively pressurized hydraulically. The pressure force is transmitted through the piston rods, and then transformed into the output torque. This class of rotary actuators rotates within 100 [deg] [288].
4) *Vane Rotary Actuators:* Figure 28(a). Essentially non-continuous motors, consist of a cylindrical body to which one or two vanes are rigidly attached. The rotation angle of a single-vane unit is limited to about 320 [deg], while that of a double vane is limited to 150 [deg] [287], [288].

HYDRAULIC MOTORS

Hydraulic motors are displacement machines converting the supplied hydraulic power into mechanical power. They perform continuous rotary motion, where the motor speed depends on the flow rate, while the supply pressure depends mainly on the motor loading torque [288]. Hydraulic motors come with high-torque:low-speed or high-speed:low-torque, of which latter can be divided into gear motors, vane motors and axial piston motors [287]–[289]. For the actuation of a hand orthosis, continuous actuation is however not necessary, and rotary or linear actuators are more suitable.

3. RETURN MECHANISMS

Returning the mechanism back to initial position can be achieved by various mechanisms. Mostly applied are return springs or the use of double hydraulic actuation, springs can be either integrated in the hydraulic actuator or externally applied as in the Delft Cylinder Hand [69]. For vertically applied cylinders, gravity return is also a possibility, however in hand orthoses this is not applicable [287]–[289].

4. MINIATURISATION AND 3D PRINTING OF HYDRAULIC ACTUATORS

In the development of hand orthoses encumbrance and weight are of great importance. Optimization of the actuation system should therefor take into consideration possibilities for miniaturisation and weight reduction. Bos (2019) indicates that miniaturisation potential is related to complexity and friction. At larger inelastic actuators frictional forces are low compared

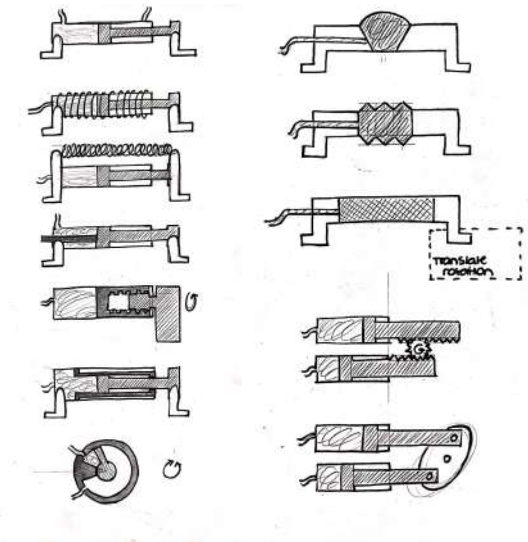

(a) (b)

FIGURE 28. Overview of hydraulic actuators based on Bos (2019), Rabie (2009) and de Volder (2010). 28(a) (Upper to lower) Double acting, single acting with integrated retraction spring, single acting with external retraction spring, single acting with return cable, rotary piston cylinder, telescopic cylinder and a rotary vane actuator. 28(b) (Upper to lower) Balloon elastic actuator, Bellow elastic actuator, Artificial muscle, Pinion & drive rotary actuator, Parallel piston rotary actuator. [7], [72], [288].

to forces due to pressure, however at smaller scales frictional forces become significant for functional instead of optimization purposes [7]. A barrier for increased hydraulic power density at reasonable efficiency is the seals. Too tight and friction dominates. Too loose and the pressurized fluid will leak past the seal. in a cylinder, force is proportional to area while weight is proportional to volume. Surface effects such as friction drag of seals and viscous drag of gaps become significant at small bores and impact overall efficiency. On the other hand, the thickness, and thus the weight, of a cylinder wall required to contain a fixed pressure goes down with bore [67].

Balloon-, bellow-, artificial muscle- and piston-type actuators are considered to be the most feasible for miniaturisation by Bos (2019) . The very small strokes of membrane actuators make them however more suited for micro-scale instead of meso-scale (<20 [mm]) applications, and the other inelastic actuators are generally more complex and require more (moving) parts. Within his dissertation, Bos also compares several readily-available miniature elastic an inelastic actuators. Especially with the application of an orthosis, large strokes are required in very small volumes. Therefore, inelastic piston-type actuators are considered to be most feasible [7]. Besides miniaturisation recently the application of 3D printing for fluidic systems is brought up for consideration. Only three sources of literature could be obtained on this subject: Krause (2018) [76], Nall (2019) [75] and de Apellaniz Goenaga (2019) [74].

Krause et al. (2018), developed an Polylactic Acid (PLA) piston cylinder with a steel piston rod and a 3D printed piston head. The actuator was obtained by Fused Deposition Modelling with an Ultimaker 3 Extended. The piston cylinder was post-processed by sanding the inner surface for friction reduction and closing of the pores. To take into consideration is the heat production in the cylinder, as the plastic could melt when the temperature exceeds the plastic deformation temperature. An O-ring was used for sealing the piston, however a rolling diaphragm was mentioned for possible friction reduction [291]. The actuator created by Krause et al. had a weight of 340 [gr], with a bore diameter o 27 [mm] and a stroke length of 140 [mm]. The seal decided upon was effective up to 1.03 [MPa] [76]. Force-to-weight ratio reported by de Apellaniz Goenaga (2019) of this piston cylinder system is 13.9.

Nall and Bhounsule (2019), developed an Acrylonitrile butadiene styrene (ABS) 3D printed pneumatic actuator with a weight of 12 [gr] and a peak force of 3 [N] at a pressure of 275.8 [kPa]. The actuator consisted of an ABS cylinder post-processed with Acetone for: sealing of pores; reduction of the surface friction and strengthening of the cylinder surface. The cylinder piston is made of galvanised steel, assembled with Loctite to a 3D printed piston head. The sealing used was an O-ring and water proof grease was used to reduce friction even further. The 3D printed actuator by Nall et al. has been compared to a similar injection molded pneumatic actuator by Lego Technic, and the 3D printed version was able to generate more force, speed and power whilst being of similar weight and size [75].

de Apellaniz Goenaga (2019), also focused on developing a 3D printed hydraulic actuator. Here it was looked at different printing processes: FDM, Stereolithography (SLA) and Selective Laser Melting (SLM), with different materials: PLA, resin and Titanium. These processes were compared to conventional hydraulic piston cylinders of Aluminium. Best results were obtained by the SLA printed piston-cylinder with a weight of 28 [gr], pressures of 4 [MPa], dynamic friction force of 6.6 [N] and a stick-slip friction force of 9.9 [N]. During the dynamic tests the cylinders were able to lift 22.25 [kg] with pressures lower than 1.11 [MPa]. The force to weight ratio of the SLA system is 3565. The system consisted of only 3D printed components and an O-ring seal. For post processing parts were threaded, reamed and adhered. With SLA printing UV curing is needed then adhesion was created with Loctite, same as used for the FDM printed parts. Titanium is too strong for post processing and an aluminium end cap was threaded and used, adhered with Araldite AV 138 glue. The SLM printed piston-cylinder was not tested as the prototype was too porous [74]. Compared to the results of the miniaturised machined piston-cylinders of the Symbihand, which could increase hand force from 2.4 to 8 [N] (possibly up to 23 [N]) with pressures < 1.5 [MPa], 3D printed piston-cylinder actuators might be a possibility for further optimization of the actuator system [7].

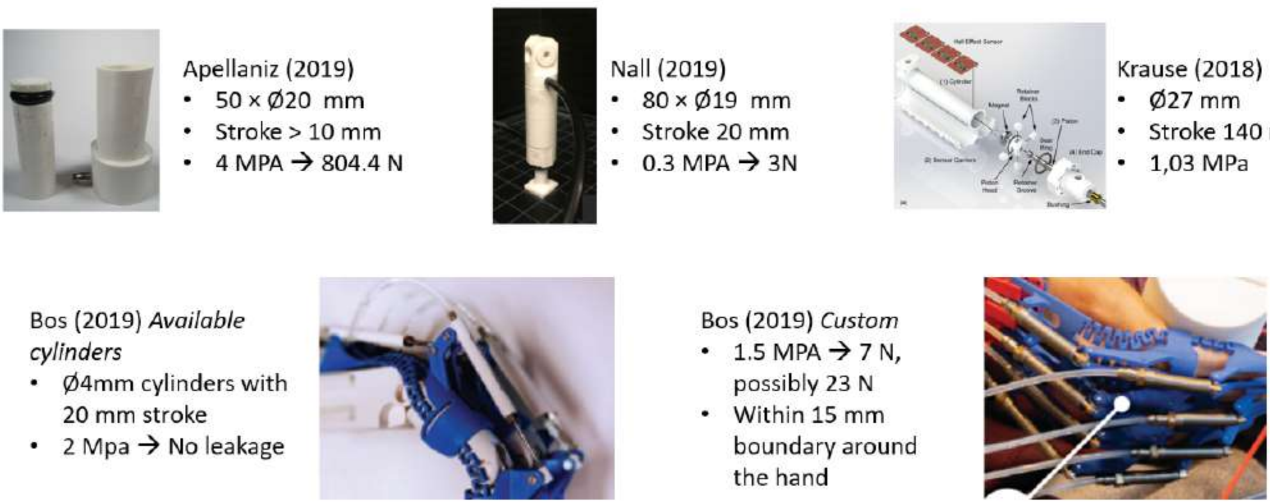

FIGURE 29. Overview of 3D printed piston-cylinder systems and the two Symbihand designs.

FEASIBILITY OF WEIGHT REDUCTION BY 3D PRINTING PISTON-CYLINDERS

As discussed above, the 3D printing of piston cylinder hydraulic actuators might be an option for weight reduction of the hand orthosis. In order to assess the potential for weight reduction in miniaturised actuators, mass of a stainless steel (AISI 304), an ABS FDM printed and an SLA printed actuator are calculated. Parameters which are equal for all three actuators are:

1) L = length of the cylinder = 63 [mm]
2) D = inner diameter of the cylinder = 4 [mm]
3) P = internal pressure = 3 [MPa]
4) h = end cap overlap heigth = 10 [mm]
5) t = piston thickness, depending on O-ring thickness = 2 [mm]

One hydraulic actuator consists of: a hollow cylinder, two end caps, a piston and a piston rod. The piston rod, however can not be printed as it would not be strong enough [74]–[76]. Therefor, the weight is excluded from the mass calculation.

$$\begin{aligned} m_{cylinder} &= \rho \cdot \pi \cdot D \cdot t \cdot L \\ m_{piston} &= \rho \cdot \pi \cdot r^2 \cdot t \\ m_{endcaps} &= \rho \cdot t \cdot \pi \cdot (\frac{D}{2} + 2 \cdot t)^2 + 2 \cdot h \cdot \rho \cdot t \cdot \pi \cdot (D + 2 \cdot t) \qquad + \\ \hline m_{total} &= m_{cylinder} + m_{piston} + m_{endcaps} \\ m_{total} &= \frac{\pi \cdot D^2 \cdot \rho \cdot t_p}{4} + \rho \cdot t \cdot \pi \cdot (\frac{D}{2} + 2 \cdot t)^2 + \pi \cdot D \cdot L \rho \cdot t + 2 \cdot h \cdot \rho \cdot t \cdot \pi \cdot (D + 2 \cdot t) \end{aligned} \tag{4}$$

TABLE 12. Mass and material properties of stainless steel (AISI 304), ABS and cured SLA resin and the resulting mass of similar piston cylinder actuators without the piston rod.

	density (ρ) $[kg/m^3]$	yield strength (σ) [MPa]	required wall thickness (t) [mm]	lowest wall thickness (t) [mm]	calculated mass (m) [gr]
SS AISI 304 [88], [292]	7800	240	0.025	0.15	0.7327
ABS [292], [293]	1030	30	0.2	1	0.6355
SLA [294]	1160	30	0.2	0.6	0.4796

After inserting the values of L, D, P, t_p the equation becomes:

$$m_{total} = 2.51e^{-8} \cdot \rho + 7.92e^{-4} \cdot \rho \cdot t + 3.14 \cdot \rho \cdot t \cdot (2.0 \cdot t + 0.002)^2 + 0.0628 \cdot \rho \cdot t \cdot (2.0 \cdot t + 0.004) \tag{5}$$

Within the equations above, ρ is the material density $[kg/m^3]$, which is 7800 for stainless steel [88], [292], 1030 for ABS [292], [293] and 1160 for cured SLA resin [294]. The material thickness needed is referred to by t in [m], which depends on the pressure the cylinder must be able to endure, the strength of the material and the diameter of the cylinder, as in the following equation:

$$t = \frac{D \cdot P}{2 \cdot \sigma} \tag{6}$$

Where the strength of the material is the yield strength σ in [MPa], 240 for stainless steel [88], [292] and 30 for ABS and cured SLA resin [292]–[294]. If the required wall thickness is lower than can be produced, the lowest wall thickness possible should be used. Wall thicknesses should be t >0.15 [mm] for stainless steel, t >1 [mm] for ABS and t >0.6 [mm] for SLA. According to equation 6, required wall thicknesses are t = 0.025 [mm] for stainless steel and t = 0.2 [mm] for ABS and SLA. These wall thicknesses are all lower than possible in production, therefor the lowest possible wall thicknesses are used for the mass calculations. Results can be found in Table 12.

As can be seen from the calculated masses, due to the higher wall thicknesses needed with 3D printed pistons not much weight reduction can be achieved. Additionally, stainless steel actuators are much easier to manufacture, have better surface properties and have higher durability compared to 3D printing as well.

5. IN CONCLUSION

In hindsight, hydraulic actuation has great potential for developing light weight and forceful actuation mechanisms. The main drawback is the force transmission that should convert linear actuation forces to rotation of the joints in an efficient manner. The current Symbihand prototype has a greater force capacity than the comfort force level of the user in a case study. It is unknown whether discomfort must be assigned to shear forces, or merely to the skin sensitivity and the rough surface finish of the current production method.

Within this thesis I have decided to put my focus towards further optimization of the current actuation mechanism that uses miniaturised hydraulic piston-cylinders. By 3D printing the piston-cylinders weight can be further reduced and modularity/customization can be further increased, however from calculations it was found that in miniaturised piston-cylinder systems weight is not reduced by 3D printing, due to the manufacturing limitations for the wall thickness.

Regarding the hydraulic system, the simpler, the easier the actuator can be miniaturised. Elastic hydraulic actuation mechanisms are uncomplicated to down-scale, yet, they have low force capacity, are less transparent, and are more prone to leakage or failure. Artificial muscles are of higher force capacity, but, exert pulling instead of pushing forces as they work by contraction. These contraction forces have to be converted to pushing forces on the limb which would lead to higher encumbrance and weight due to the added components. Inelastic rotary vane actuators consist of various components, and because, are less suitable for miniaturisation as with each moving component friction is added. Besides frictional problems, dual-piston mechanisms would demand too much space for comfortable application of the rotary actuation mechanism. A simple single-acting cylinder (SAC) is decided upon. Dual-acting cylinders (DAC) would increase controllability, but would also need additional control components and signals. Control would thus be further complicated, which is less favorable for the user.

So, a stainless steel single acting piston-cylinder actuator will remain to be used in the thumb module. Then, by taking a proper look at the embodiment design of the Symbihand, hopefully the human-hand interface can become more user friendly and the discomfort can be assigned to either the force transmission or the problem can be solved.

APPENDIX F O-RING FRICTION

According to Plettenburg (2002), O-ring friction can be broken down into two components; Friction caused by the applied pressure and Friction due to initial compression of the O-ring [78]. Which can be calculated by:

$$F_O = f_c(\alpha, H_s) \cdot L_w + f_h(p_g) \cdot A_{proj} \tag{7}$$

Where f_c indicates the friction factor due to O-ring compression, depending on the squeeze (α [%]) and the O-ring hardness (H_s [° Sh]). This squeeze factor is multiplied by the length of the seals rubbing surface, which is equal to the outside circumference of the seal ($L_w = \pi D_c$ [mm]). f_h indicates the friction factor caused by the fluid pressure and so depends on the pressure difference over the O-ring seal (p_g) [MPa]). This is multiplied by the seal's projected area on which the pressure is applied ($A_{proj} = \frac{\pi}{4}(D_c{}^2 - D_g{}^2)$ [mm^2]).D$_c$ indicates the piston bore diameter [mm] and D_g the piston groove diameter [mm]. Parker Seal Company supplies two graphs based on empirical data to determine the coefficients f_c and f_h. Data was obtained from tests using standard O-rings reciprocating against R = 0.4 [μm] finished chrome-plated surfaces at speeds greater than 0.005 m/s and lubricated with hydraulic oil [MIL-H-56061] at environmental room temperature [295]. On the same set of empirical data Martini (1984) fitted an equation to calculate the dynamic O-ring friction. Coefficients can be calculated by:

$$f_c = 1.75 \cdot 10^4(-0.884 + 0.0206 \cdot H_s - 0.0001 \cdot H_s{}^2) \cdot \alpha \tag{8a}$$

$$f_h = 0.78 \cdot p_g^{0.61} \tag{8b}$$

At the initiation of movement a much higher friction must be overcome, which is called the break-out friction. The break out friction can be maximal 3x the running friction (F_O). The actuator output force (F_A [N]) can be calculated by subtracting the O-ring friction from the actuator force by the pressure ($= p \cdot (\frac{1}{2} \cdot D_c)^2$).:

$$\begin{aligned} F_A =& \frac{\pi}{4} \cdot D_c{}^2 \cdot p_g - \frac{17.1 \cdot \pi}{4}(D_c{}^2 - D_g{}^2) \cdot p_g{}^{0.61} \\ & - 17.5 \cdot 10^4 \cdot \pi \cdot (-0.0884 + 0.206 \cdot H_s \\ & - 0.0001 \cdot H_s{}^2) \cdot \alpha \cdot D_c \end{aligned} \tag{9}$$

Hysteresis of an elastomeric O-ring system is the ratio of the O-ring friction to the motivating force. The relative losses of the actuator due to O-ring running friction can then be estimated according to [7]:

$$f_{loss} = \frac{F_O}{\frac{\pi}{4} \cdot D_c{}^2} \tag{10}$$

The total friction loss should be <0.33. In case this value is exceeded, the differential pressure is no longer able to overcome the maximum break-out force of 3x the running friction [7], [77], [78]. In our design case, an O-ring is used with a shore hardness of 70A, a bore diameter of 4 [mm], a piston groove diameter of 1 [mm] and a relative squeeze of 10 [%]. At application of a 4 [MPa] pressure, the O-ring friction force is 3.63 [N], which corresponds to a frictional loss of 0.07 or 7 [%].

APPENDIX G COMPLIANT ELEMENTS

Within his dissertation, R. Bos has developed a complaint element to oppose the shear forces generated by the piston-cylinders. Although, the shape of these elements can be obtained from images it is not clear whether or not this shape is optimal for connecting the thumb module to the orthosis base.

The shape used for the Symbihand finger modules is deducted from a notched flexure hinge. This shape is known to reduce bending stresses, due to the removal of material in the corners (the notch). Whilst, by maintaining material on the outer sides, the structure is not able to bend as well in the x-y plane and is more resistant to stretch. As the second to fifth digit move in an in-planar manner, it is okay for the structure to allow for very little stretch. However, as the thumb makes a more complex movement which is somewhat unpredictable, some more stretch in the elements must be allowed. For contemplation of the adjustments that can be made to the structure, several SolidWorks Simulations have been performed. These simulations are only rough estimations, made for comparisons of the structures, as many of the variables are uncertain or unknown. Material properties used are gained from the Oceanz PA12 data sheet and supplemented by use of the CES Edupack Database with the values indicated in Table 13 [296]–[298]. However, as the structure is 3D printed the data obtained from CES Edupack likely to be incorrect. The 3D printing process affects material properties as these are dependent on dependent on printing temperature, density and direction, whilst the properties indicated in CES Edupack are based on homogenous materials. Nevertheless, a custom material was created with a density of 0.93 [g/cm^3], a yield strength of 35 [MPa], a tensile modulus of 1650 [MPa], a tensile strength of 42 [MPa].

TABLE 13. Material properties of Nylon PA 12, according to the Oceanz Data sheet [296] and the CES Edupack Database [?], [297]

Material Properties		Oceanz Data Sheet	CES Edupack	
		PA 12	PA 12 Rigid	PA 12 Semi-flexible
Density	[g/cm^3]	0.93	1-1.02	1.02-1.03
Yield Strength	[MPa]	-	34.8-43.4	28-30
Tensile Modulus	[MPa]	1650	1080-1350	440-550
Tensile strength	[MPa]	xy: 48 z: 42	45-55	35-40
Strain @ break	[%]	xy: 18 z: 4	41-59	340-350
Strain @ yield	[%]	-	7.03-13.3	20-25
Shore Hardness	-	75D	69-71D	64-65D

Another uncertainty, is the load case scenario of the structure. The exact amount of pulling force, and displacement that must be counteracted or facilitated is obscure. At the same time, it is ensured that the structure developed by Bos, is great with regards to bending. Therefor, this structure will be recreated and adjusted in different manners. These have then been compared with regard to their stretching abilities in two load case scenarios. First, by applying a pulling force of 5 [N], and second, by applying a displacement of 15 [mm]. In what manner the loads and displacements have been applied, can be seen in Figure 30. The geometry of the evaluated structures are represented in Figure 31 and results of the various structures are presented in Tables 14,15 and 16. A safety factor should be taken into account, which is set to 0.8x the yield strength. Values exceeding the yield strength are indicated in red, values exceeding the safety limit of 28 [MPa] are indicated in orange and values below the safety margin are indicated in green. Same accounts for the strain at break which is 18 [%] and the safety limit which then is 14.4 [%].

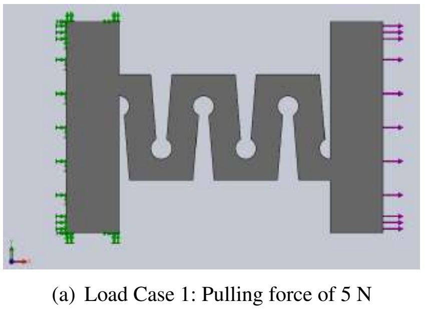

(a) Load Case 1: Pulling force of 5 N

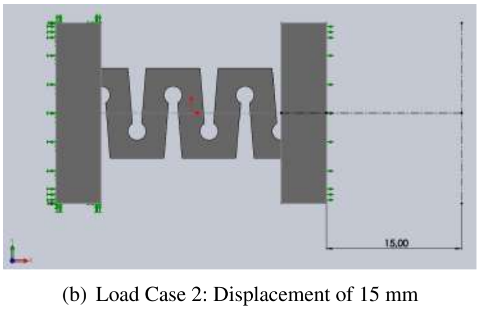

(b) Load Case 2: Displacement of 15 mm

FIGURE 30. Fixtures and Forces applied to the 3D structure in the SolidWorks Simulations.

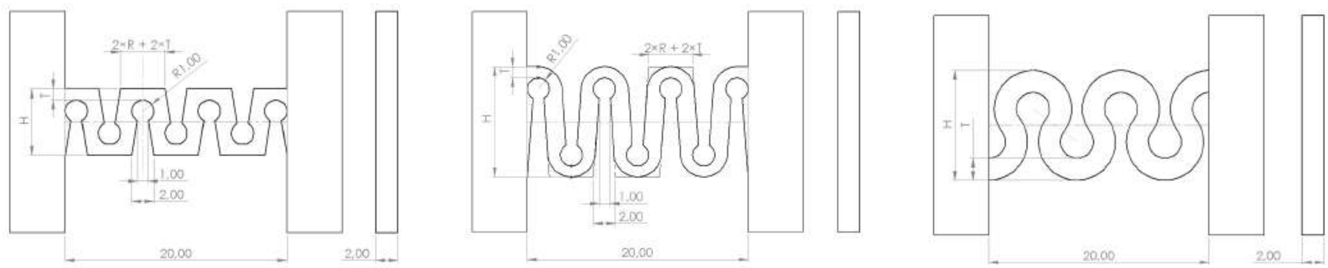

(a) Structure Type 1: Geometry by R. Bos. In the Symbihand H = 6 and T = 1 mm. H has been evaluated with values 6, 10 and 15 mm. T has been evaluated with values of 1 and 2 mm.

(b) Structure Type 2: Geometry of R. Bos, with rounded corners. H as been evaluated for the values of 6, 10 and 15 mm. T has been evaluated with values of 1 and 2 mm and R with 1 and 2 mm.

(c) Structure Type 3: Geometry a more curly structure without Notches, but with a constant thickness. Circles are either defined as tangent to one another, or connected by a tangent line. The structure has been evaluated with H of 10 and 15 mm and T of 1, 2 and 3 mm.

FIGURE 31. Evaluated structure geometries.

TABLE 14. Results of the SolidWorks simulation performed with Structure type 1, as shown in Figure 31(a). All values are Maximum values, as these indicate the likeliness of failure.

		Load Case 1: Pulling force [5N]				Load Case 2: Displacement [15mm]		
Thickness [mm]	Height [mm]	Von Mises Stress [%]	Displacement [mm]	Equivalent Strain [%]	1st principal Strain [%]	Von Mises Stress [MPa]	Equivalent Strain [%]	1st Principal Strain [%]
T = 1	6	37.7	13.8	14.2	23.8	47.5	18.1	29.3
	10	26	16.4	10.5	16.3	26	10.4	16.1
	15	54.8	77.8	20.8	33.4	8.9	3.2	5.5
T = 1.5	6	20.8	4.5	8.4	12.8	91.6	38.3	56.3
T = 2	6	11.9	1.8	4.5	7.4	135	58.1	82.4
	10	21.0	7.6	7.0	12.7	46.8	16.1	28.6
	15	30.4	22.9	12.5	18.9	21.5	8.7	13.2

TABLE 15. Results of the SolidWorks simulation performed with Structure type 2, as shown in Figure 31(b). All values are Maximum values, as these indicate the likeliness of failure.

			Load Case 1: Pulling force [5N]				Load Case 2: Displacement [15mm]		
Thickness [mm]	Notch [mm]	Height [mm]	Von Mises Stress [%]	Displacement [mm]	Equivalent Strain [%]	1st principal Strain [%]	Von Mises Stress [MPa]	Equivalent Strain [%]	1st Principal Strain [%]
T = 1	2	10	48.2	43	18.8	29.8	15.2	6.0	9.6
T = 2			22.2	8.7	9.2	13.9	43.5	18.4	26.9
T = 1	4		42.4	40	15.8	26.4	13.9	5.3	8.4
T = 2			19.5	8.6	7.9	12.2	44.5	16.7	23.5

TABLE 16. Results of the SolidWorks simulation performed with Structure type 3, as shown in Figure 31(c). All values are Maximum values, as these indicate the likeliness of failure.

		Load Case 1: Pulling force [5N]				Load Case 2: Displacement [15mm]		
Thickness [mm]	Height [mm]	Von Mises Stress [%]	Displacement [mm]	Equivalent Strain [%]	1st principal Strain [%]	Von Mises Stress [MPa]	Equivalent Strain [%]	1st Principal Strain [%]
T = 1	10	40.2	44	15.7	25	11	4.1	6.8
T = 2		20.7	10.3	8.4	12.8	33	13.9	20.4
T = 2	15	27.2	27.1	11.9	16.9	16.4	7.1	10.1
T = 3		15.2	6.0	6.6	9.2	59.7	26.8	36.4

Figure 32(a) shows visualisations of the structure type 1 as designed by Bos with H = 6, R = 2 and T = 1.5 [mm]. Table 14 shows that, stress and strain as a result of Load Case 1 (LC1) are all lower than the safety limit, but as expected, the displacement is rather small and the structure is not performing great in Load Case 2 (LC2). Thinning the structure, would reduce the stresses in LC2, but would also lead to failure in LC1. Thickening the structure, would further reduce the stresses experienced during LC1, however would also further increase the stresses and strains experienced during LC2. Lengthening the height of the structure initially allows for larger displacements and strains of the structure in LC1 and for smaller stresses and strains in LC2. Although, it should be noticed that increasing the height, also affects the stresses in LC1. Simulation visuals of structure type 1 with H = 6, T = 1.5 (Bos original); H = 6, T = 1; and H = 10, T = 2 are illustrated in Figure 32(a), 34 and 32(b).

From Table 15 it can be seen that removing the angular corners of the original Bos to obtain structure type 2, only has small effects on the structures performance. Slight increases in stresses and strain in LC1 and also small differentiation in LC2. From the same Table, it can also be stated that increasing the notch diameter from 2 to 4 [mm], has no significant effect on the structures performance in both scenarios. As an example, the simulation results of structure type 2 with H = 10 and T = 2 is shown in Figure 36.

Table 16 presents the results of structure type 3, which is more different from the original structure than structure type 2. The structure allows for a little more displacement in LC1, combined with lower experienced stresses. Meanwhile, stresses and strains in LC2 are significantly decreased. The simulation result of structure type 3 with H = 15 and T = 2 can be found in Figure 37.

For manufacturing, three structures have been realized in the CAD model for 3D printing. First of all the original structure will be fabricated, as this is our reference point. Secondly, structure type 1 is selected with an increased height of 10 [mm]. This structure allows for some more displacement, with similar experienced stresses in LC1 and performs better in LC2, though according to the simulation stresses and strains would still be too large. Therefore, structure type 3 with a height of 15 [mm] and a thickness of 2 [mm] is selected third. Here, even more displacement is allowed in LC1, whilst maintaining the stresses and strains in LC2 within acceptable limits. Here however it is the question whether or not the structure is not too flexible for opposing the shear forces.

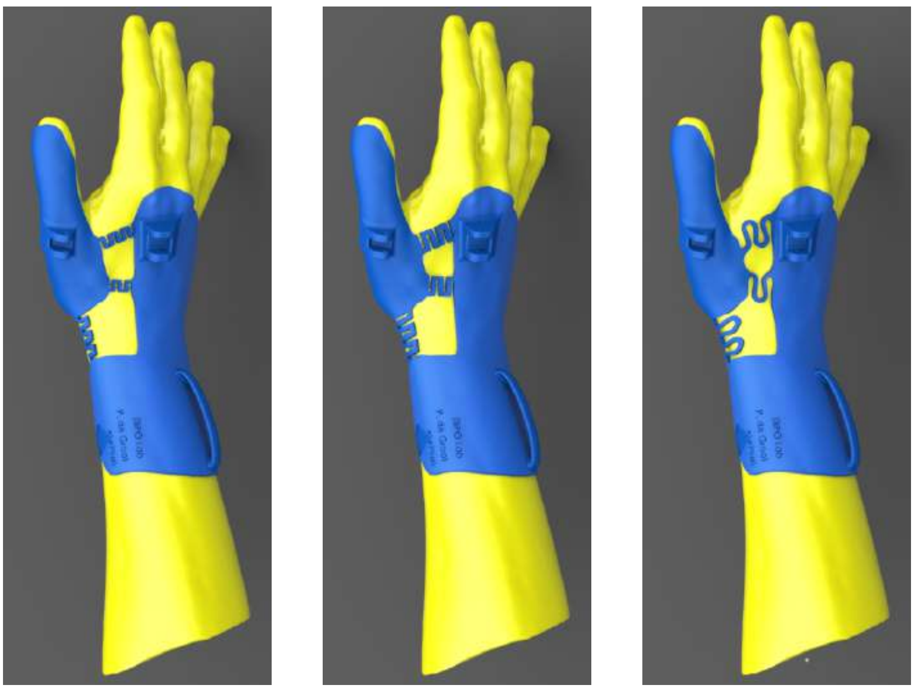

(a) Structure 1: H = 6, R = 1, T = 1.5, as was applied in the Symbihand.

(b) Structure 1: H = 10, R = 1, T = 2, should allow some more displacement.

(c) Structure 3: H = 15, T = 2, should allow even more displacement.

FIGURE 32. SolidWorks models of the structures implemented in the thumb module.

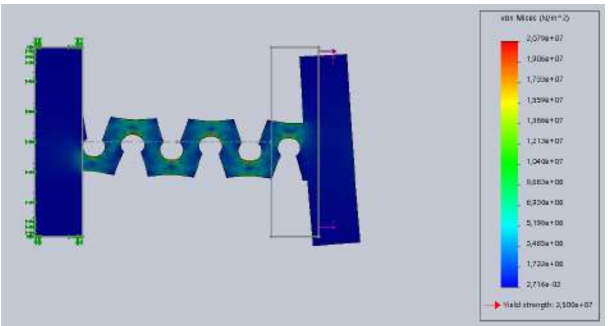

(a) The Von Mises Stress in the structure as a result of Load Case 1: 5N of pulling force in the X-direction.

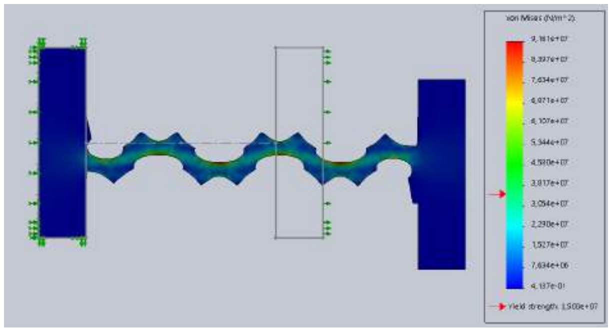

(b) The Von Mises Stress in the structure as a result of Load Case 2: 15 mm displacement in the X-direction.

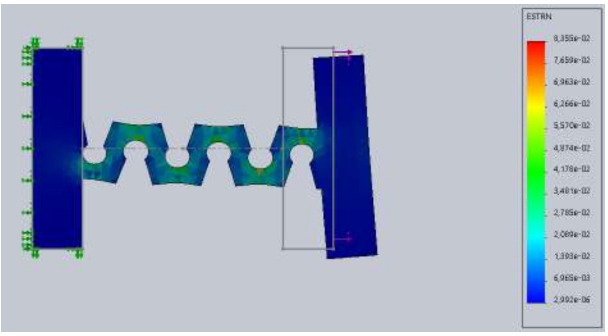

(c) The equivalent strain in the structure as a result of Load Case 1: 5N of pulling force in the X-direction.

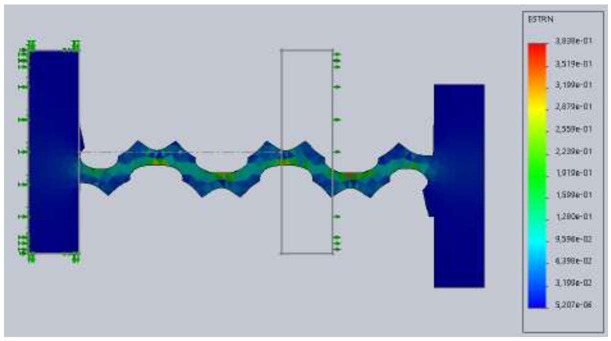

(d) The equivalent strain in the structure as a result of Load Case 2: 15 mm displacement in the X-direction

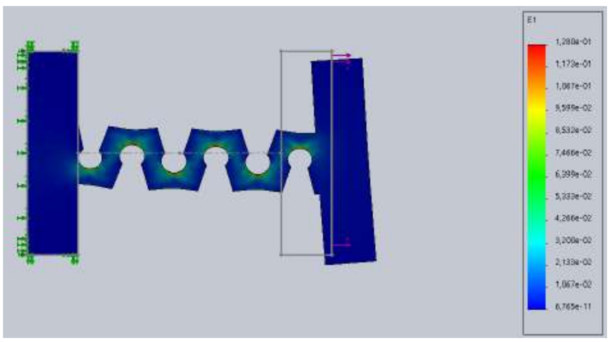

(e) The First principal strain in the structure as a result of Load Case 1: 5N of pulling force in the X-direction.

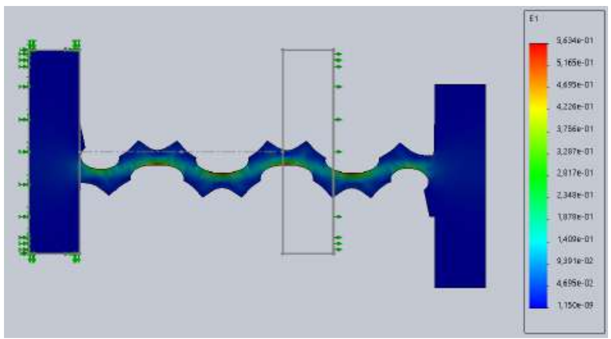

(f) The First principal strain in the structure as a result of Load Case 2: 15 mm displacement in the X-direction

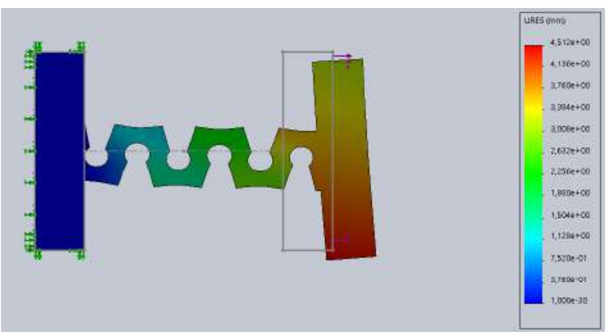

(g) The displacement in the structure as a result of Load Case 1: 5N of pulling force in the X-direction.

FIGURE 33. Visualisation of the simulation results of Load Case 1 and 2, performed with Structure Type 1, H = 6, R = 2, T = 1.5.

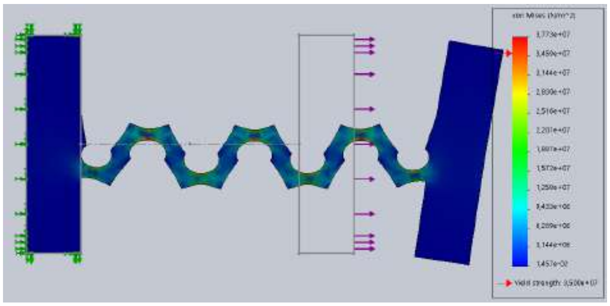

(a) The Von Mises Stress in the structure as a result of Load Case 1: 5N of pulling force in the X-direction.

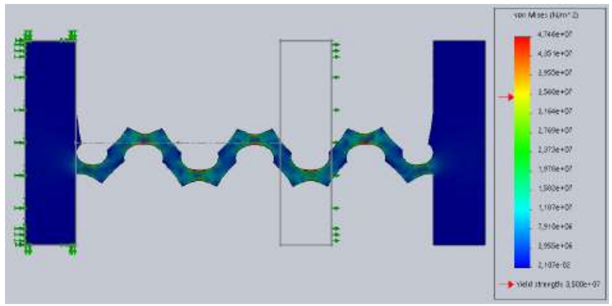

(b) The Von Mises Stress in the structure as a result of Load Case 2: 15 mm displacement in the X-direction.

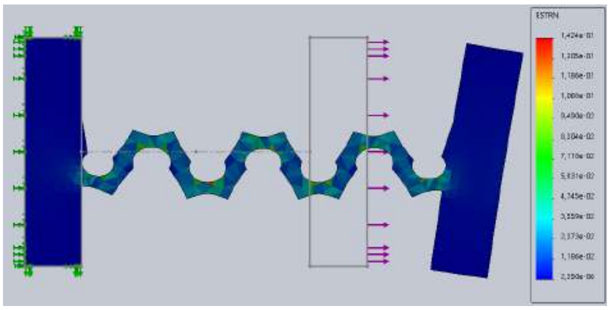

(c) The equivalent strain in the structure as a result of Load Case 1: 5N of pulling force in the X-direction.

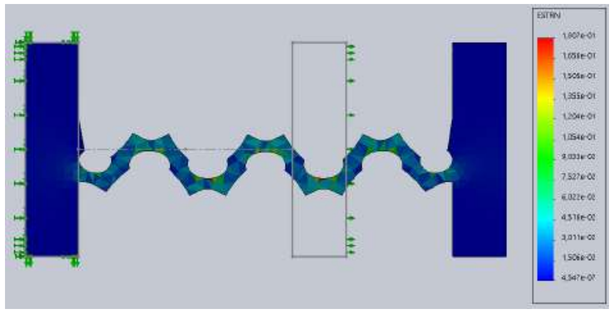

(d) The equivalent strain in the structure as a result of Load Case 2: 15 mm displacement in the X-direction

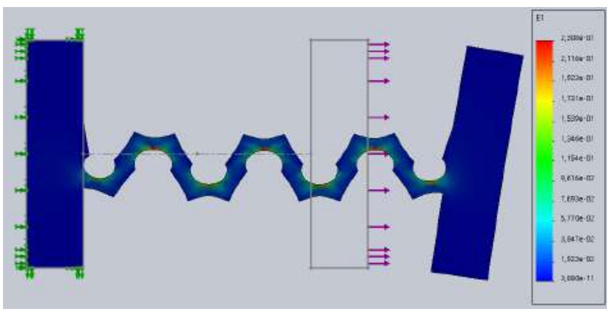

(e) The First principal strain in the structure as a result of Load Case 1: 5N of pulling force in the X-direction.

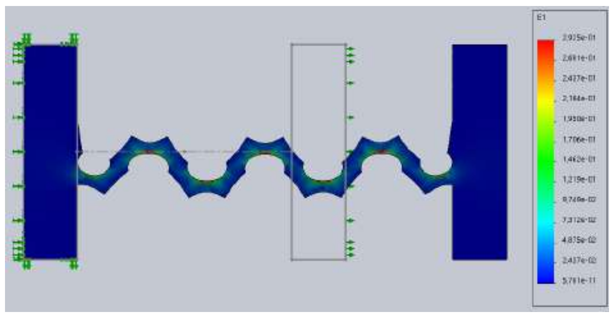

(f) The First principal strain in the structure as a result of Load Case 2: 15 mm displacement in the X-direction

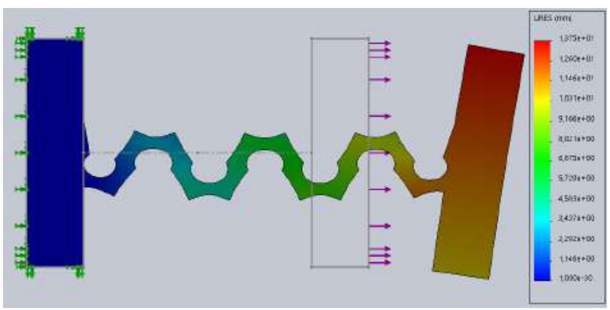

(g) The displacement in the structure as a result of Load Case 1: 5N of pulling force in the X-direction.

FIGURE 34. Visualisation of the simulation results of Load Case 1 and 2, performed with Structure Type 1, H = 6, R = 2, T = 1.

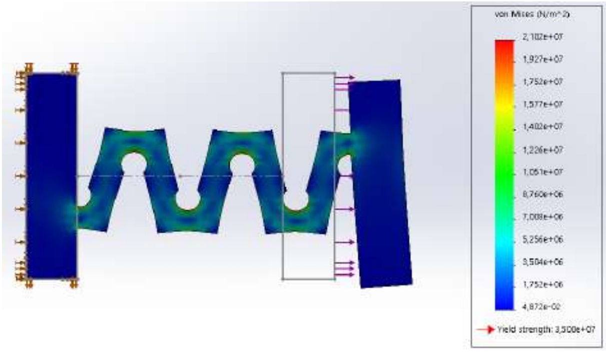

(a) The Von Mises Stress in the structure as a result of Load Case 1: 5N of pulling force in the X-direction.

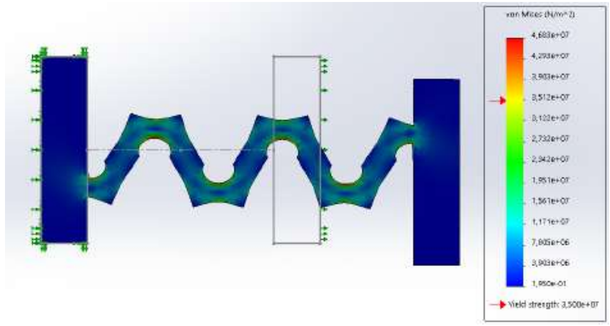

(b) The Von Mises Stress in the structure as a result of Load Case 2: 15 mm displacement in the X-direction.

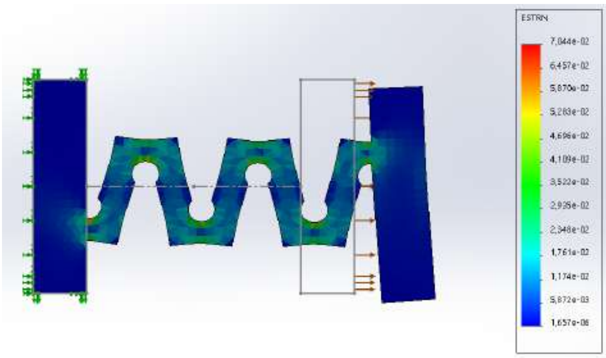

(c) The equivalent strain in the structure as a result of Load Case 1: 5N of pulling force in the X-direction.

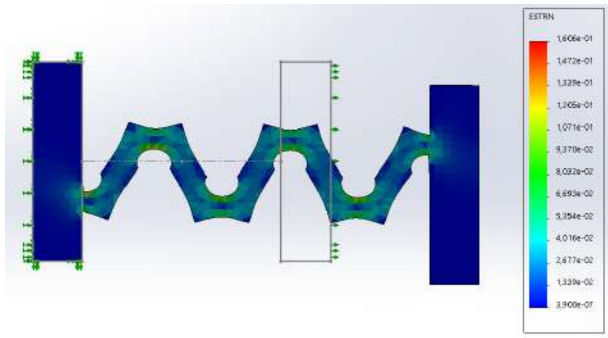

(d) The equivalent strain in the structure as a result of Load Case 2: 15 mm displacement in the X-direction

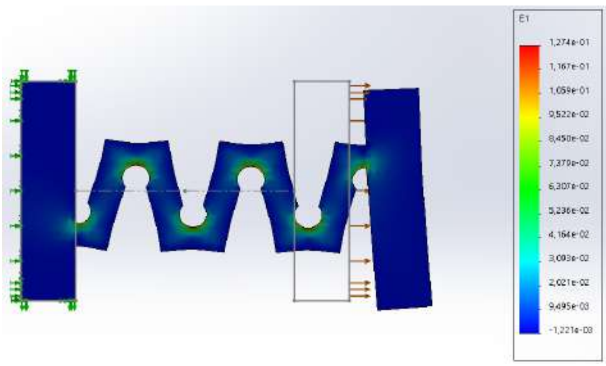

(e) The First principal strain in the structure as a result of Load Case 1: 5N of pulling force in the X-direction.

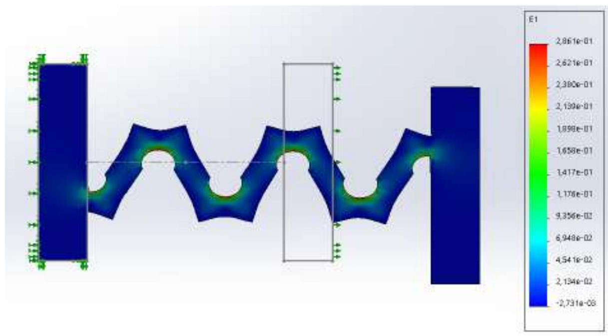

(f) The First principal strain in the structure as a result of Load Case 2: 15 mm displacement in the X-direction

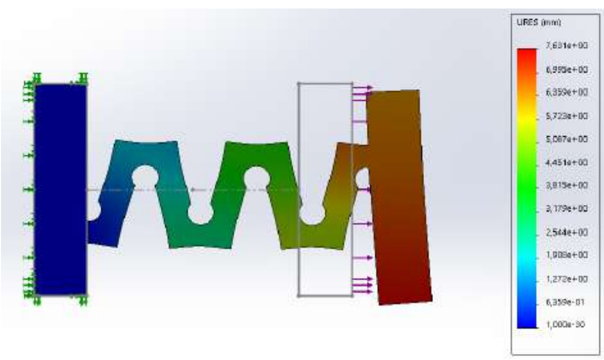

(g) The displacement in the structure as a result of Load Case 1: 5N of pulling force in the X-direction.

FIGURE 35. Visualisation of the simulation results of Load Case 1 and 2, performed with Structure Type 1, H = 10, R = 2, T = 2.

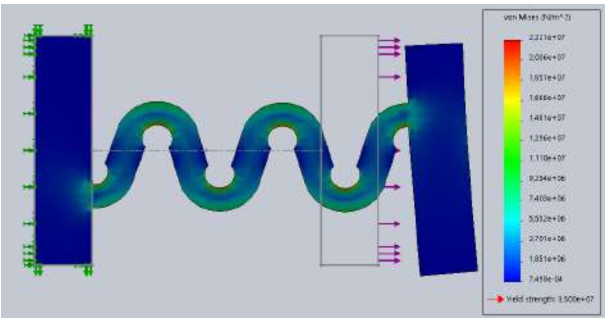

(a) The Von Mises Stress in the structure as a result of Load Case 1: 5N of pulling force in the X-direction.

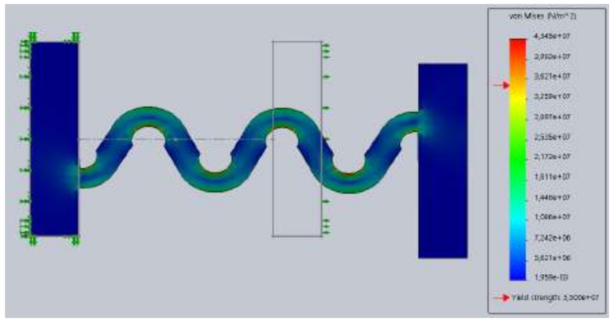

(b) The Von Mises Stress in the structure as a result of Load Case 2: 15 mm displacement in the X-direction.

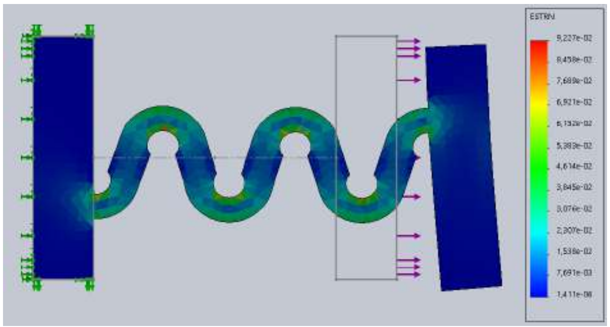

(c) The equivalent strain in the structure as a result of Load Case 1: 5N of pulling force in the X-direction.

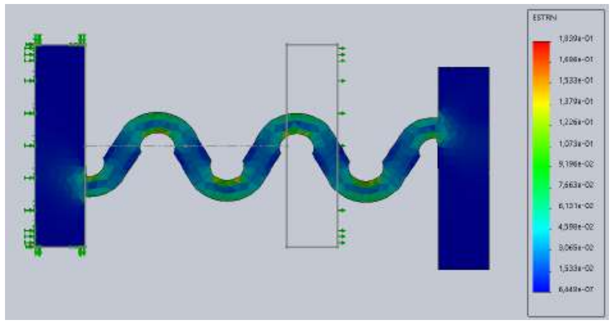

(d) The equivalent strain in the structure as a result of Load Case 2: 15 mm displacement in the X-direction

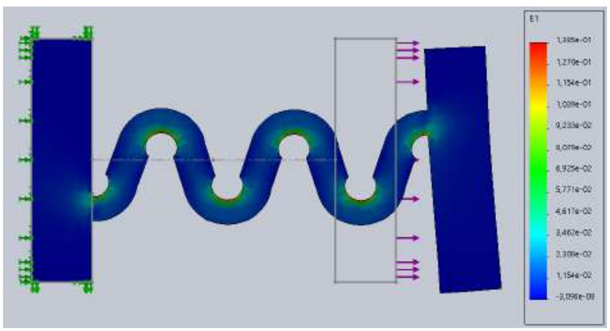

(e) The First principal strain in the structure as a result of Load Case 1: 5N of pulling force in the X-direction.

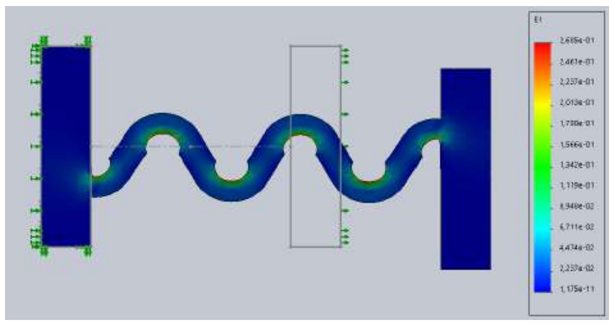

(f) The First principal strain in the structure as a result of Load Case 2: 15 mm displacement in the X-direction

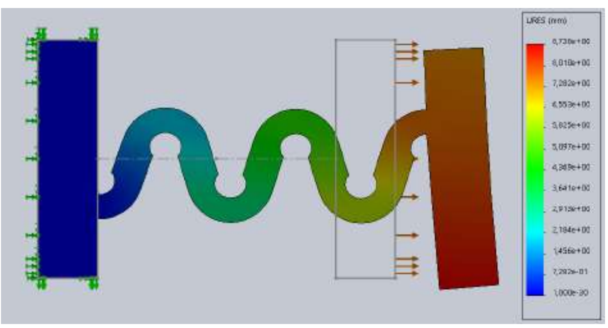

(g) The displacement in the structure as a result of Load Case 1: 5N of pulling force in the X-direction.

FIGURE 36. Visualisation of the simulation results of Load Case 1 and 2, performed with Structure Type 2, H = 10, R = 2, T = 2.

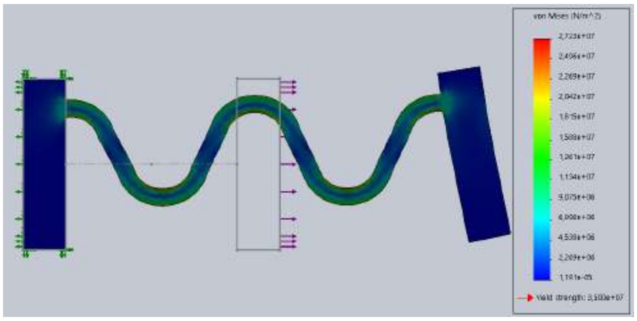

(a) The Von Mises Stress in the structure as a result of Load Case 1: 5N of pulling force in the X-direction.

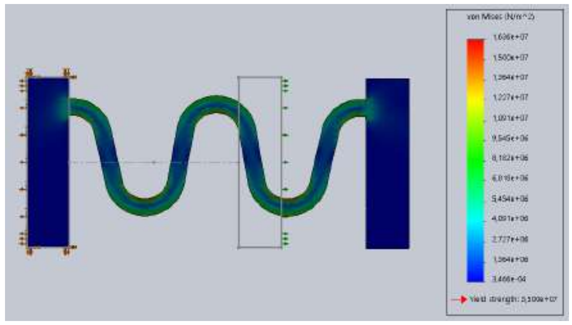

(b) The Von Mises Stress in the structure as a result of Load Case 2: 15 mm displacement in the X-direction.

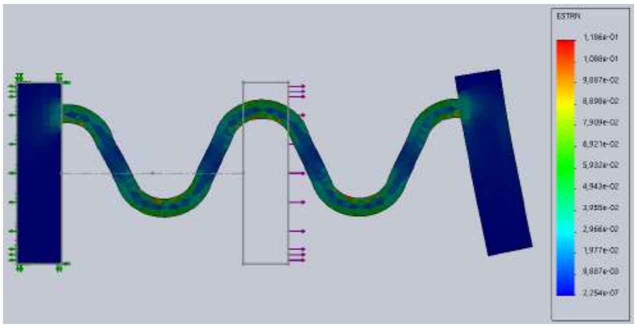

(c) The equivalent strain in the structure as a result of Load Case 1: 5N of pulling force in the X-direction.

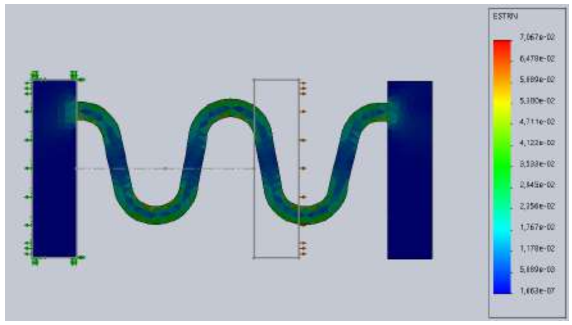

(d) The equivalent strain in the structure as a result of Load Case 2: 15 mm displacement in the X-direction

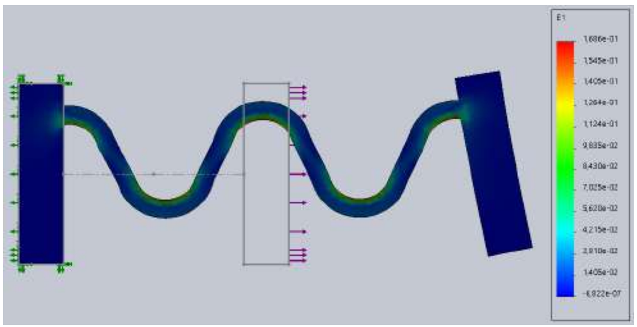

(e) The First principal strain in the structure as a result of Load Case 1: 5N of pulling force in the X-direction.

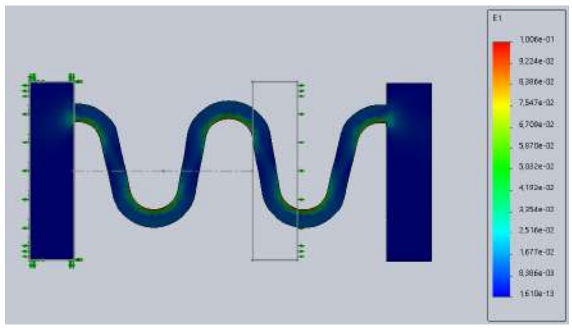

(f) The First principal strain in the structure as a result of Load Case 2: 15 mm displacement in the X-direction

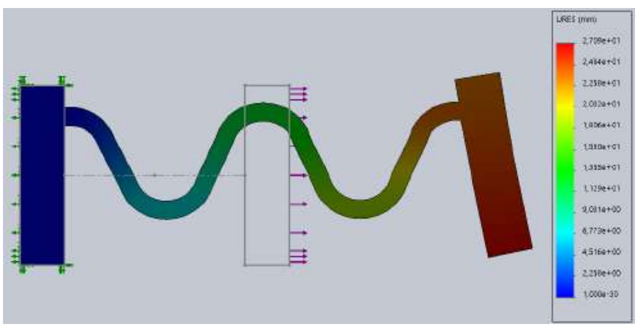

(g) The displacement in the structure as a result of Load Case 1: 5N of pulling force in the X-direction.

FIGURE 37. Visualisation of the simulation results of Load Case 1 and 2, performed with Structure Type 3, H = 15, R = 2, T = 2.

APPENDIX H THE TESTBED

Due to fragility of the patient group, the difficulty of getting in touch with a Duchenne patient in the correct phase of the disease and the Covid-19 epidemic, performing experiments within the target population could, unfortunately, not be executed. As testing with a healthy hand would be expected to lead to inaccurate results, instead a mock-up hand was developed for testing in a lab environment. By developing a dummy hand a full range of experiments can be performed and safety can be ensured before submitting it to the human hand as well.

The model of the thumb, must have accurate DOF of the thumb in the CMC joint, as otherwise, the orthosis can not be evaluated on grasping configurations. Furthermore, the testbed must be manufacturable in house, for allowance of quick iterations. Lastly, the testbed should be adapted to fit the developed thumb orthosis, as the orthosis was made based on an 3D scan of my own hand.

1. LITERATURE ON ANTHROPOMETRIC ROBOTIC HANDS

Literature has been scoured for mock-up hands and bio-mimetic prosthetic limbs, of which several results are indicated in Figure 38. Robotic hands built for manipulation are often anthropomorphic but not anatomically accurate [299], [300]. They are built with fewer degrees of freedom in order to approximate the grasping ability of the hand for a narrow set of task requirements, while simplifying the joint mechanisms [299]. This is applicable to the designs in figure 38(a), 38(d), 38(f), 38(g), 38(h) and 38(j).

(a) Bhadugale (2018) [301] (b) Deshpande (2013) [300] (c) Hughes 2018 [302], [303] (d) Miloradovic (2015) [304] (e) Xu (2016) [305] (f) Mohammadi (2020) [306]

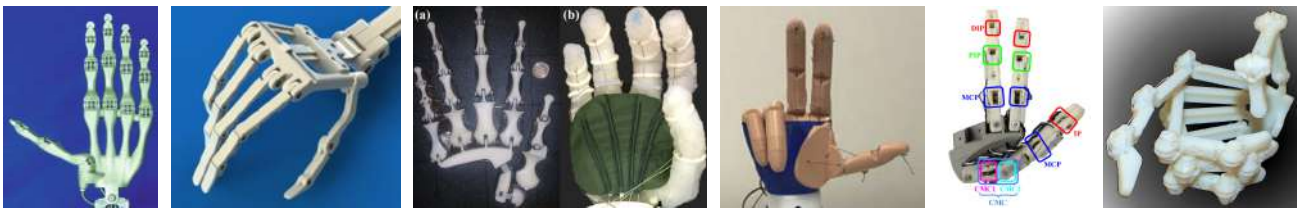

(g) Varol (2014) [307] (h) Otsuka (2010) [245] (i) Saharan (2017) [273] (j) Zhou (2019) [308] (k) Yousaf (2019) [309] (l) Sarkany (2013) [310]

FIGURE 38. Inspiration for testbed design retrieved from literature.

As the DIP and MCP joint of thumb are splinted within the orthosis, simplification of these joints is allowed. However, the CMC joint may not be simplified. In the case where the CMC joint is not properly represented, testing the effect of the applied forces by the orthosis on the hand can not be evaluated. The mock-up hand needed is a passive structure with the limitations in ROM and the behaviour of the human hand. Actuation of the hand itself is unnecessary as it is representative of a disabled hand. The anthropomorphic soft skeleton hand for piano playing, developed by Hughes et al. (2018), is a great example of such a passive mock-up hand [302]. As can be seen in Figure 38(c), the design is created by a multi-material 3D-printing of the skeletal and tendon system to obtain anisotropic flexure joints. Multi-material 3D printing at the TU Delft is not possible at the time, however, the applicability of this design as testbed should be re-evaluated when this possibility opens up.

The ACT hand in figure 38(b) has been designed as a tool to investigate human dexterity. It incorporates the biomechanical features of the human hand, and so allows for the identification of the critical factors that lead to dexterity in the human hand [300]. The hands in Figure 38(e) and 38(i) are based on the ACT hand design. The dummy hand by Saharan et al. (2017) is a simplification, approaching the CMC joint as a ball and socket and casting it in silicone to obtain an accurate hand shape. The bio-mimetic anthropomorphic robotic hand by Xu et al. (2016), in opposite, is a revised version of the ACT hand and eliminates all mechanical joints by adding plastic tendon and ligaments. Within this section it will be referred to as the BAR hand.

The performance of the thumb extensor mechanism is very sensitive to the shape of the underlying bones it is in contact with

[299]. Therefor, it would be beneficial to use the bone articulations to restrict ROM. The ACT hand as well as the BAR hand, both retain the complex geometry of the one surfaces by 3D printing artificial bones from the laser-scanned model of a cadaver skeleton hand to obtain the proper bone features [300], [305].

Matching the robotic thumb joints to the anatomic joints creates the proper relative motion between the bones [83]. The complexity of the thumb movements result mainly from the contact between the trapezium and first metacarpal bones at the CMC joint. Due to the irregular shape of the trapezium bone, the exact locations of its joint axes are still under debate, but the CMC joint has been commonly explained as a saddle joint that allows the thumb to have a wide ROM - up (adduction) and down (abduction), bent (flexion) and straightened (extension), and the ability to move across the palm (opposition), as indicated in Figure 39 [305].

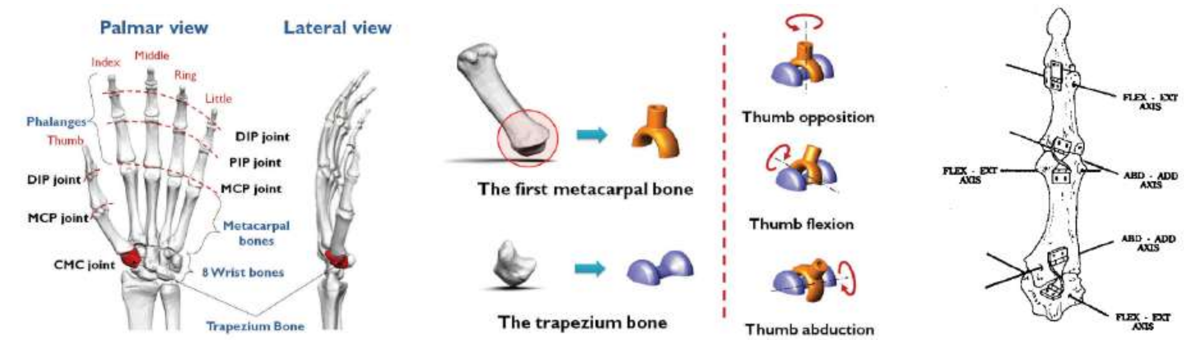

(a) Bone structure of the hand, with the CMC joint indicated in red [305]

(b) Motion descriptions of the thumb CMC joint [305]

(c) The rotational axes of the thumb by Hollister et al. (1995) [86]

FIGURE 39. Anatomy and descriptions of the thumb bone structures and rotational axes.

The ACT hand uses mechanical joints to facilitate these motions. The approach of development is described well, and so, this design was decided upon for the development of the testbed. In the design low-friction was achieved by implementing machined pin joints at each rotational axis [83]. The CMC and the MCP joints used to be considered universal joints, which have two perpendicular and intersecting axes, as was implemented by Saharan et al. [311]. However instead, the ACT hand approaches the thumb axes of rotation as described by Hollister et al. (1993 & 1995) with five non-orthogonal, non-intersecting DOFs as indicated in Figure 39(c) [84]–[86]. These five axes have been mechanically located in cadaver specimens and using them showed more accurate preservation of the workspace of the thumb [83].

Conform these axial descriptions of Hollister et al. each joint in the ACT hand contains a different mechanism to achieve proper joint motion. The DIP joint consist of a simple pin joint with the axis of rotation at the distal part of the Interphalangeal bone. The MCP joint is implemented by a gimbal mechanism, as both the FE and the AA axes lay within the distal part of the Metacarpal bone. This gimbal design is not suitable for the CMC joint, as it's two rotational axes are located in separate bones. Thus instead, the CMC joint is realized by two non-perpendicular, non-intersecting pin joints at the ends of a single-link arm. The pin joint at the proximal end of the MC bone coincides with the AA axis, whilst the pin joint at the trapezium allows for FE. A third axis in the CMC joint to account for the axial rotation of the thumb as in Figure 39, was dismissed as it was demonstrated that axial rotation for pronation-supination was not independent of the FE and AA angles [191]. The geometry of the articulating bone ends were maintained except for a narrow slot that allows the link arms to rotate around the axis pin. The span of the cavity enforces the joint ROM, whereas the length of the link arms determine the clearance between the two opposing surfaces [83], [300].

2. THE MOCK-UP THUMB

3D scanned CAD models of the hand bones, were retrieved from Pinshape.com. Here a project was published based on the BAR hand by Grayson, G. [82]. The bodies of the bones were scaled and mirrored in order to fit the orthosis made for the right hand. Rotational axes were implemented as shown in Figure 40, and bones were assigned mates in relation to each others articular surfaces. Then, volume was added to the bones, so the thumb fits the orthosis better. The entire structure was 3D printed by use of an Ultimaker 3, with PLA for the thumb and soluble PVA as support material. This model was then implemented in the 3D scan of my hand to create the full testbed hand.

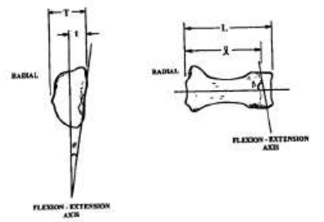

(a) Location of the FE axis in the distal end of the interphalangeal bone of the thumb. $\theta = 5 \pm 2°, t/T = 44 \pm 17\%, \beta = 83 \pm 4°, l/L = 90 \pm 5\%$ [85]

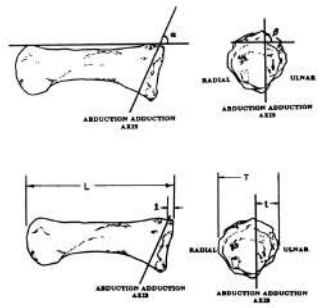

(b) Location of the FE axis in the distal end of the metacarpophalangeal bone of the thumb. $\beta = 5 \pm 2°, t/T = 57 \pm 17\%, \alpha = 101 \pm 6°, l/L = 87 \pm 5\%$ [85]

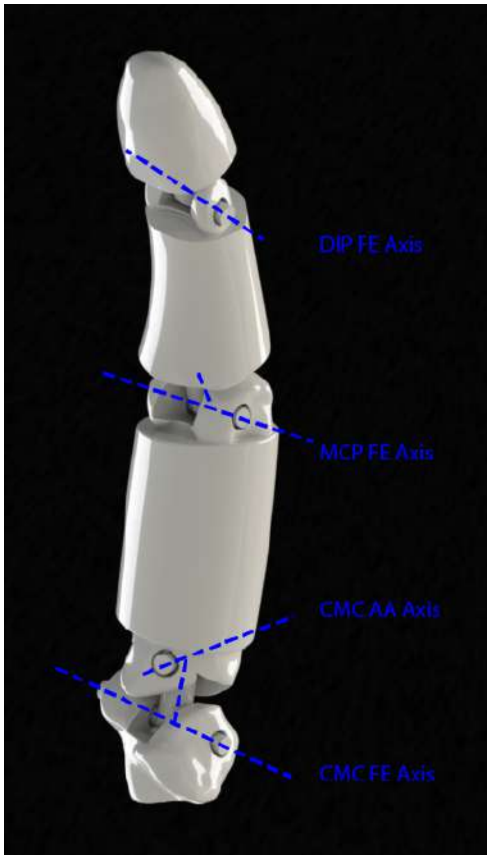

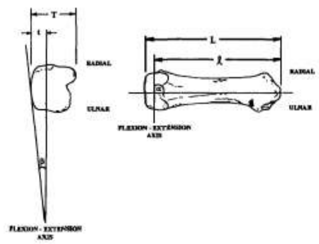

(c) Location of the AA axis in the proximal end of the metacarpophalangeal bone of the thumb. $\alpha = 83.6 \pm 14.2°, l/L = 12.5 \pm 6.2\%, \beta = 78.3 \pm 12.9°, t/T = 59.5 \pm 14.3\%$ [84]

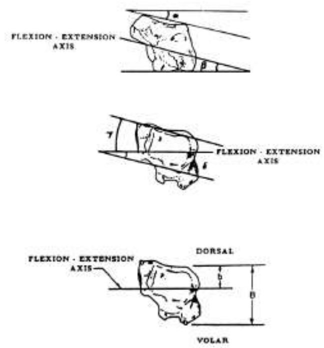

(d) Location of the FE axis the trapezium bone of the thumb. α = 13.6 $\pm 16.5°, \beta = 14.1 \pm 9.0°, \gamma = 14.7 \pm 9.0°, \delta = 8.4 \pm 4.7°, b/B = 36 \pm 13.6\%$ [84]

(e) SolidWorks model of the 3D printed mock-up thumb with the applied axes indicated in blue

FIGURE 40. Locations of the rotational axes as described by Hollister et al. [84]–[86] and the implementation within the CAD model.

3. THE TESTBED IN GENERAL

In addition to the thumb two set-ups were created for testing the orthosis on grip forces of the power grip, and whether or not, a pinch grip could be achieved. Both are illustrated in Figure 41. For the assessment of the pinch grip, an index finger was developed which indicates the ROM of the index finger 41(a). The area within the trench indicates the area that can be reached by the index finger tip. In pursuance of a successful pinch grip, the thumb must be able to reach the fingertip somewhere in this area. As the Symbihand actuates only the MCP and PIP joint of the digits, no angle was indicated at the DIP joint. Limits to the ROM are based on the ROM achieved with the Symbihand during the case study [7]. Secondly, the index finger for evaluation of the grip force was designed. Angles are based on values measured by Shimawaki et al. (2019) of a grip diameter of 6 cm [312]. This grip diameter was chosen as it large enough to be distinct form a pinch grip and smaller than the opening width needed for the majority of ADL tasks is 10 cm, which is set as a requirement in Section 2.

As the PVA support material is prone to errors, the base of the hand and the thumb should be printed in separate parts to ensure the proper functioning of the joint. Placing the mock-up thumb on the hand has been a process of iteration, as it is unclear at which location and orientation within the 3D scanned hand the trapezium should be placed. Also, the index fingers are printed separately from the hand base, so that, they are exchangeable. An exploded view and the assembly including the orthosis itself can be seen in Figure 42.

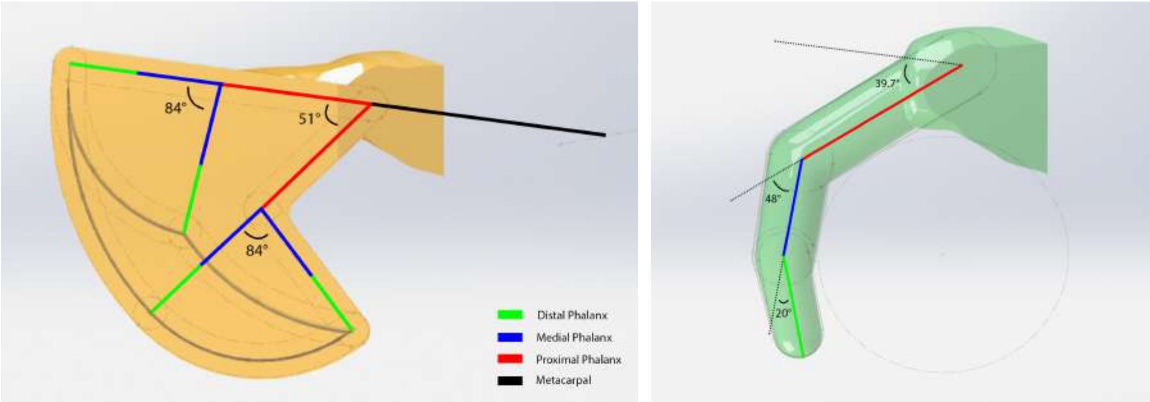

(a) ROM of the index finger with the Symbihand [7]. With the area the tip of the index finger can reach indicated within the rounded lines. For achieving a successful pinch grip the thumb must be able to reach some point within this indicated area.

(b) Index finger created for testing of the power grip force achievable by the thumb. Angles are based on the values reported by Shimawaki et al. (2019) for a grip diameter of 6 cm [312].

FIGURE 41. The two index finger set ups. Bones are indicated by the colors; black = metacarpal, red = proximal phalanx, blue = medial phalanx and green = distal phalanx. Length of the bones are based on values found by Buryanov (2010) [313].

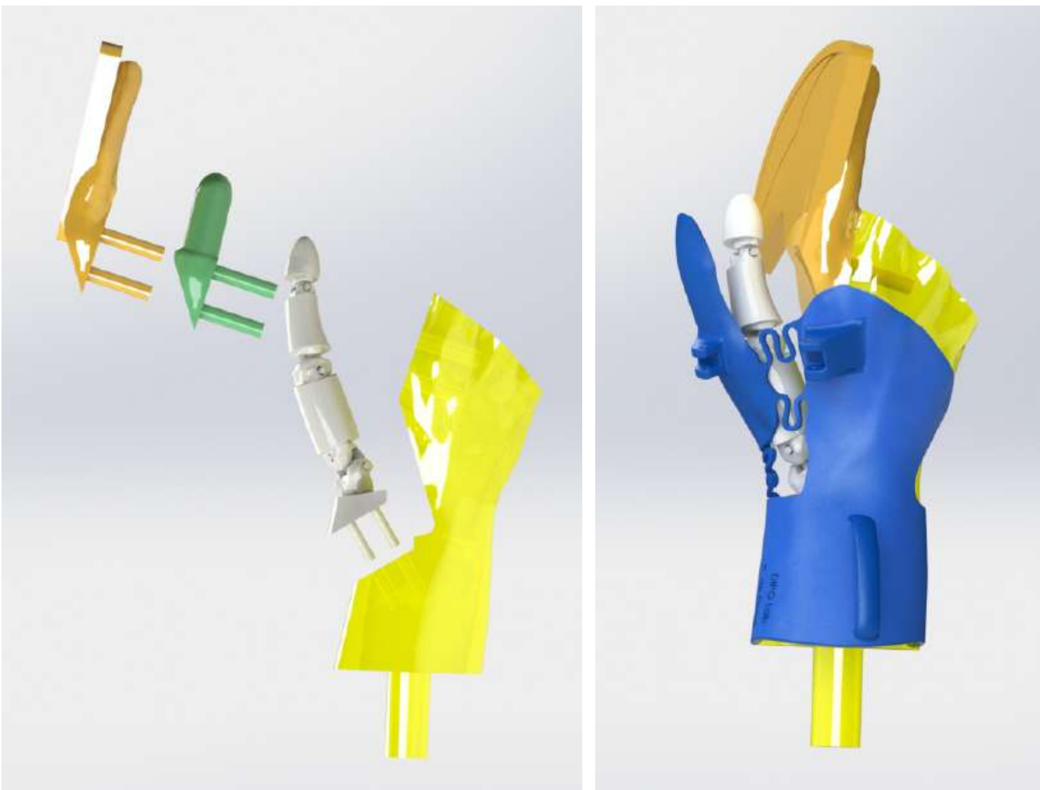

(a) Exploded view of the testbed

(b) Assembly of the testbed, including the hand orthosis

FIGURE 42. CAD models of the testbed and hand orthosis.

4. FURTHER RECOMMENDATIONS

3D printing of the testbed was succesfull when implementing fine precision. The movement of the thumb seems reasonably accurate, allowing the thumb to move to the index finger in a rather conical trajectory. One thing to note, is that at large ROM the thumb resists returning to it's initial position. This indicates that either the trapezium is misplaced on the mock-up hand, or that there are too many inaccuracies on the bone parts or the connecting joint. Which could be solved by perhaps printing the hand by use of SLS printing. Additionally, for more complicated test cases, or when a more accurate testbed is desirable, some improvements can be made. First of all the accuracy of the testbed regarding true thumb motions must be evaluated. The workspace of the thumb has been evaluated in literature and can be used for validation of the current design [38], [61], [71], [183], [314], [315]. Hereby, the position and orientation of the trapezium bone within the hand 3D scan can be optimized.

Secondly, the model can be improved by incorporating joint stiffness. One method for implementing joint stiffness, is by integrating leaf springs in the joints as was done by Bos (2020) [7]. This would mean that the thumb must be printed by selective laser sintering instead of using a fused deposition modelling technique. The use of SLS printing would also lead to more precise printing and so would achieve lower friction within the 3D printed joints. Another method for adding joint stiffness, is by adding the tendon and ligament structures as was done in the ACT and in the BAR hand [300], [305]. If to go as far as the BAR hand, even the mechanical joints can be eliminated in order to obtain maximum anatomical resemblance. The thumb including conventional mechanical joints, reproduces only those features required for equivalent kinematic function. Complete duplication of the complex articular cartilage topology and synovial tissue constraints around the bones could also create the appropriate degrees of freedom [83]. This was done by Xu et al., so that by disposing the conventional mechanical joints, also a curved rotation axis that supports rotation, sliding, translation and pivoting motions can be achieved [305]. To further approach anatomical correctness, the simplified MCP joint could be turned into a gimbal as was done by the ACT hand, or it could immediately be transformed towards the design of Xu et al. [305].

Lastly, the testbed hand could be lifted to a higher level by also implementing movable digits for the other digits of the hand. Hereby allowing for more extensive testing of the complete hand orthosis including the finger modules.

APPENDIX I MATLAB SCRIPT

1. CLOSE TEST CODE

```
%% Pinch Test results --> Force vs Pressure
% Patty de Groot - 4367960
% Master Thesis - Biomedical Engineering
% 30-01-2021
%% Set up
    clear all
    close all
    clc

    a = 0; % Figure number

%% Import Data - Test with Testbed Hand
    %Strings with file names
        filenamesH6  = {'H6 - 40-1.txt', 'H6 - 40-2.txt', 'H6 - 40-3.txt'};
            % Structure 1
        filenamesH10 = {'H10 - 40-1.txt', 'H10 - 40-2.txt', 'H10 - 40-3.txt'};
            % Structure 2
        filenamesC40 = {'Curly - 40-1.txt', 'Curly - 40-2.txt', 'Curly - 40-3.txt'};
            % Structure 3
        filenames3_1el  = {'Test_struc3_1.txt', 'Test_struc3_2.txt', 'Test_struc3_3.
           txt',}; % Structure 3 - 1 element

    %Read data from index number: --> index is stroke is larger than 0
        initialvaluesH6  = [10, 13, 15];                  % Index numbers
        initialvaluesH10 = [21, 14, 18];
        initialvaluesC40 = [17, 14, 12];
        initialvalues3_1el  = [19, 19, 14];

    %Read out useful data
    %[Hysteresis, work_close, work_open, close stroke, open stroke, close pressure,
       open pressure, all stroke, alle pressure]
        %Structure 1
            Test = 'Structure 1';
            HysteresisH6  = HysteresisFunction(filenamesH6, initialvaluesH6, a, Test
               );
            meanEL_H6 = mean(HysteresisH6(1:3,1));       % Calculate mean hysteresis
            stdEL_H6  = std(HysteresisH6(1:3,1));        % Calculate std hysteresis
            a = HysteresisH6(1,10);                      % Update figure number
        %Structure 2
            Test = 'Structure 2';
            HysteresisH10 = HysteresisFunction(filenamesH10, initialvaluesH10, a,
               Test);
            meanEL_H10 = mean(HysteresisH10(1:3,1));     % Calculate mean hysteresis
            stdEL_H10  = std(HysteresisH10(1:3,1));      % Calculate std hysteresis
            a = HysteresisH10(1,10);                     % Update figure number
        %Structure 3
            Test = 'Structure 3';
            HysteresisC40 = HysteresisFunction(filenamesC40, initialvaluesC40, a,
               Test);
            meanEL_C40 = mean(HysteresisC40(1:3,1));     % Calculate mean hysteresis
            stdEL_C40  = std(HysteresisC40(1:3,1));      % Calculate std hysteresis
            a = HysteresisC40(1,10);                     % Update figure number
```

```
        %Structure 3 - 1 element
            Test = 'Structure 3 - 1 flex element';
            Hysteresis3_1el = HysteresisFunction(filenames3_1el, initialvalues3_1el,
                a, Test);
            meanEL_3_1el = mean(Hysteresis3_1el(1:3,1)); % Calculate mean hysteresis
            stdEL_3_1el  = std(Hysteresis3_1el(1:3,1));  % Calculate std hysteresis
            a = Hysteresis3_1el(1,10);                   % Update figure number


%% Plot results - Testbed Hand
%Plot raw data
    a = a+1;                                                  % Update figure number
    figure(a)
    set(gcf,'position',[300,30,400,1000]);                    % [x0,y0,width,height]
    subplot(3,1,1)                                            % Pressure
        plot(HysteresisH6(:,9)); hold on
        plot(HysteresisH10(:,9)); hold on
        plot(HysteresisC40(:,9)); hold on
        xlabel('steps');                                      % Name axis
        ylabel('Pressure [MPa]');                             % Name axis
        title('Mean pressure');                               % Create plot title

    subplot(3,1,2)                                            % Master cylinder
       Stroke
        plot(HysteresisH6(:,8)); hold on
        plot(HysteresisH10(:,8)); hold on
        plot(HysteresisC40(:,8)); hold on
        xlabel('steps');                                      % Name axis
        ylabel('Stroke [mm]');                                % Name axis
        title('Mean stroke');                                 % Create plot title

    subplot(3,1,3)                                            % Hysteresis
         plot(HysteresisH6(:,8),HysteresisH6(:,9)); hold on
         plot(HysteresisH10(:,8),HysteresisH10(:,9)); hold on
         plot(HysteresisC40(:,8),HysteresisC40(:,9)); hold on
         xlabel('Stroke [mm]');                               % Name axis
         ylabel('Pressure [MPa]');                            % Name axis
         title('Stroke vs Pressure');                         % Create plot title
         legend('Structure 1','Structure 2', 'Structure 3'); % Create legend
         legend('Location','northwest');                      % Position legend
         sgtitle('Close Test - Raw data');                    % Create figure title

%% MPa plot Energy
% Calculate % of energy loss due to hysteresis
    lossH6  = round(meanEL_H6/HysteresisH6(1,2)*100,2);    % Energy loss structure 1
    lossH10 = round(meanEL_H10/HysteresisH10(1,2)*100,2); % Energy loss structure 2
    lossC40 = round(meanEL_C40/HysteresisC40(1,2)*100,2); % Energy loss structure 3

% MPa Plot Hysteresis
    a = a+1;                                                  % Update figure number
    figure(a)
    set(gcf,'position',[300,30,400,1000]);                    % [x0,y0,width,height]
    X = categorical({'Structure 1', 'Structure 2', 'Structure 3'})       % Name MPas
    Y = [HysteresisH6(1,3), HysteresisH10(1,3), HysteresisC40(1,3);meanEL_H6,
       meanEL_H10, meanEL_C40];                               % Y values of MPa
    MPa(X,Y ,'stacked')                          % Stack work returned & hysteresis
```

```
    % Create strings for each MPa count
        MPastrings = {[num2str(lossH6) ' %'], [num2str(lossH10) ' %'], [num2str(
            lossC40) ' %']};
    % Create text objects at each location
        text(X,Y(2,:),MPastrings,'horizontalalignment','center','verticalalignment',
            'bottom')
    xlabel('Structure #')
    ylabel('Energy [Nmm]')
    sgtitle('Energy loss')                                % Create figure title
    legend('Recovered energy', 'Hysteresis')              % Create legend
    legend('Location', 'northwest')                       % Set legend position

%% Test on healthy hand
   %Import Data
    %Strings with file names
        filenames1 = {'Person_test_struc1_1.txt'};            % Structure 1
        filenames2 = {'Person_test_struc2_2.txt', 'Person_test_struc2_3.txt'};
            % Structure 2
        filenames3 = {'Person_test_struc3_2.txt', 'Person_test_struc3_3.txt'};
            % Structure 3

    %Read data from index number: -->
        initialvalues1 = [22];
        initialvalues2 = [10, 17, 21];                        % Index number
        initialvalues3 = [19, 22, 15];

    %Read out useful data
    %[Hysteresis, work_close, work_open, close stroke, open stroke, close pressure,
       open pressure, all stroke, alle pressure]
        %Structure 1
            Test = 'Structure 1 - Healthy hand';
            Data1 = importdata('Person_test_struc1_1.txt');
            pData1 = Data1.data(initialvalues1(1):end,7)/10; % Pressure [MPa]
            sData1 = Data1.data(initialvalues1(1):end,9);     % Stroke [mm]

            [max_pData, k] = (max(pData1));
            closing_S1 = sData1(1:k);
            opening_S1 = sData1(k+1:end);
            closing_P1 = pData1(1:k);
            opening_P1 = pData1(k+1:end);

            work_close1 = (trapz(closing_S1, closing_P1));
                % Amount of work needed for closing
            work_open1  = (trapz(flip(opening_S1), flip(opening_P1)));
                % Amount of work returned during reopening
            EL1 = work_close1 - work_open1;                   % Hysteresis
            loss1  = round(EL1/work_close1*100,2);            % Energy loss

        %Structure 2
            Test = 'Structure 2 - Healthy hand';
            Hysteresis2  = HysteresisFunction(filenames2, initialvalues2, a, Test);
            meanEL_2 = mean(Hysteresis2(1:3,1));              % Mean hysteresis
            stdEL_2  = std(Hysteresis2(1:3,1));               % Std hysteresis
            a = Hysteresis2(1,10);                            % Update figure number
            loss2  = round(meanEL_2/Hysteresis2(1,2)*100,2); % Energy loss
```

```
        %Structure 3
            Test = 'Structure 3 - Healthy hand';
            Hysteresis3  = HysteresisFunction(filenames3, initialvalues3, a, Test);
            meanEL_3 = mean(Hysteresis3(1:3,1));                % Mean hysteresis
            stdEL_3  = std(Hysteresis3(1:3,1));                 % Std hysteresis
            a = Hysteresis3(1,10);                              % Update figure number
            loss3   = round(meanEL_3/Hysteresis3(1,2)*100,2);  % Energy loss

%% Plot - Healthy Hand
%Plot raw data
    a = a+1;                                                    % Update figure number
    figure(a)
    set(gcf,'position',[300,30,400,1000]);                     % [x0,y0,width,height]
    subplot(3,1,1)                                              % Pressure
        plot(pData1); hold on
        plot(Hysteresis2(:,9)); hold on
        plot(Hysteresis3(:,9)); hold on
        xlabel('steps');                                        % Name axis
        ylabel('Pressure [MPa]');                               % Name axis
        title('Mean pressure');                                 % Create plot title

    subplot(3,1,2)                                              % Master cylinder
       Stroke
        plot(sData1+29.6528); hold on
        plot(Hysteresis2(:,8)+29.6529); hold on
        plot(Hysteresis3(:,8)+24.3851); hold on
        xlabel('steps');                                        % Name axis
        ylabel('Stroke [mm]');                                  % Name axis
        title('Mean stroke');                                   % Create plot title

    subplot(3,1,3)                                              % Hysteresis
         plot(sData1+29.6528,pData1); hold on
         plot(Hysteresis2(:,8)+29.6529,Hysteresis2(:,9)); hold on
         plot(Hysteresis3(:,8)+24.3851,Hysteresis3(:,9)); hold on
         xlabel('Stroke [mm]');                                 % Name axis
         ylabel('Pressure [MPa]');                              % Name axis
         title('Stroke vs Pressure');                           % Create legend
         legend('Structure 1 - 2 elements', 'Structure 2 - 3 elements', 'Structure 3
             - 1 element')
         legend('Location','northwest');                        % Position legend
         sgtitle('Close Test with Healthy hand - Raw data'); % Create figure title

%% On Test Bed Hand
   %Structure 2 - no 10 sec wait
    filenamesH10_2  = {'Test_struc2_2.txt', 'Test_struc2_3.txt', 'Test_struc2_4.txt'
       };   % Structure 1
    initialvaluesH10_2 = [25, 15 ,14 17];                       % Index number

    Test = 'Structure 2 - without 10 sec wait on TBH';
    HysteresisH10_2 = HysteresisFunction(filenamesH10_2, initialvaluesH10_2, a, Test
       );
    meanEL_H10_2 = mean(HysteresisH10_2(1:3,1));                % Mean hysteresis
    stdEL_H10_2  = std(HysteresisH10_2(1:3,1));                 % Std hysteresis
    a = HysteresisH10_2(1,10);                                  % Update figure number
    lossH10_2  = round(meanEL_H10_2/HysteresisH10_2(1,2)*100,2); % Energy loss
```

```
%% Plot all in 1 plot
    %Plot
    a = a+1;
    figure(a)
    set(gcf,'position',[300,30,1500,600]); %set(gcf,'position',[x0,y0,width,height])
          % Graph size
    subplot(1,3,1)                                                   % Pressure
     plot(HysteresisH6(:,9)); hold on    % TBH Structure 1
     plot(HysteresisH10(:,9)); hold on   % TBH Structure 2
     plot(HysteresisC40(:,9)); hold on   % TBH Structure 3
     plot(pData1); hold on               % HH Structure 1
     plot(Hysteresis2(:,9)); hold on     % HH Structure 2
     plot(Hysteresis3(:,9)); hold on     % HH Structure 3
     plot(HysteresisH10_2(:,9)); hold on % TBH Structure 2 no 10 s
     plot(Hysteresis3_1el(:,9)); hold on % TBH Structure 3 1 element
    subplot(1,3,2)                                                    % Master cylinder
       stroke
     plot(HysteresisH6(:,8)); hold on
     plot(HysteresisH10(:,8)); hold on
     plot(HysteresisC40(:,8)); hold on
     plot(HysteresisH6(:,8)); hold on
     plot(HysteresisH10(:,8)); hold on
     plot(HysteresisC40(:,8)); hold on
     plot(HysteresisH10_2(:,8)); hold on
     plot(Hysteresis3_1el(:,8)); hold on
    subplot(1,3,3)                                                    % Stroke vs Pressure
     plot(HysteresisH6(:,8),HysteresisH6(:,9)); hold on
     plot(HysteresisH10(:,8),HysteresisH10(:,9)); hold on
     plot(HysteresisC40(:,8),HysteresisC40(:,9)); hold on
     plot(HysteresisH6(:,8),HysteresisH6(:,9)); hold on
     plot(HysteresisH10(:,8),HysteresisH10(:,9)); hold on
     plot(HysteresisC40(:,8),HysteresisC40(:,9)); hold on
     plot(HysteresisH10_2(:,8),HysteresisH10_2(:,9)); hold on
     plot(Hysteresis3_1el(:,8),Hysteresis3_1el(:,9)); hold on
     legend('TBH Str.1', 'TBH Str.2', 'TBH Str.3', 'HH Str.1 - 2 el.', 'HH Str.2', '
        HH Str.3 - 1 el', 'TBH Str.2 - no 10 s', 'TBH Str.3 - 1 el')
     legend('Location', 'northwest')                                  % Position legend
     sgtitle('Close test - All results');                             % Figure title

%% Functions
    function Hysteresis = HysteresisFunction(filenames, initialvalue, a, Test)
    a = a + 1;
        %Import data
            for i = 1: length(filenames)
                %Import data of all trials
                  Data(i)   = importdata(filenames{i});
                  pData{i} = Data(i).data(:,7)/10;                      % Pressure [MPa]
                  sData{i} = Data(i).data(:,9);                     % Stroke [mm]

                %Identify max values per trial
                  pmax(i) = max(pData{i});                          % Pressure [MPa]
                  smax(i) = max(sData{i});                          % Stroke [mm]
            end

            %Trim data to equal length
                %Determine trim length
```

```
    for i = 1:length(filenames)
        trim(1,i) = length(pData{i}(initialvalue(i):end));
    end
     %trim = [length(pData{1}(initialvalue(1):end)), length(pData{2}(
        initialvalue(2):end)), length(pData{3}(initialvalue(3):end))];
     trim = min(trim)-1;

    %Trim
     for i = 1:length(filenames)
      pData{i} = pData{i}(initialvalue(i):initialvalue(i)+trim);
        % Pressure [MPa]
      sData{i} = sData{i}(initialvalue(i):initialvalue(i)+trim);
        % Stroke [mm]
     end

%Calculate Hysteresis per trial
    for i = 1:length(filenames)
        [max_pData, k] = (max(pData{i}));
        closing_S = sData{i}(1:k);
        opening_S = sData{i}(k+1:end);
        closing_P = pData{i}(1:k);
        opening_P = pData{i}(k+1:end);

        work_close = (trapz(closing_S, closing_P));
            % Amount of work needed for closing
        work_open  = (trapz(flip(opening_S), flip(opening_P)));
            % Amount of work returned during reopening
        EL(i) = work_close - work_open; % Hysteresis

        P(:,i) = [pData{i}];
        S(:,i) = [sData{i}];
    end

%Calculate Mean values
    pMean = mean([P],2);
    sMean = mean([S],2);

%Calculate Mean Hysteresis
    [max_pMean, k] = (max(pMean));      % Terminal device fully closed
    close_S    = sMean(1:k);            % Displacement during closing
    open_S     = sMean((k+1):end);      % Displacement during reopening
       pull
    close_P    = pMean(1:k);            % Pressure during closing
    open_P     = pMean((k+1):end);      % Pressure during opening

    work_close = (trapz(close_S, close_P));
        % Amount of work needed for closing
    work_open  = (trapz(flip(open_S), flip(open_P)));
        % Amount of work returned during reopening

%Store Results
    Hysteresis = zeros(length(pMean),10);   % Allocate space for results
    Hysteresis(1:length(EL),1) = EL(1:end); % Hysteresis of each trail
    Hysteresis(length(EL)+1,1) = work_close - work_open; % Mean
    Hysteresis(1,2) = work_close;
        % Amount of work needed for closing
```

```
                Hysteresis(1,3) = work_open;
                    % Amount of work returned during reopening
                Hysteresis(1:length(close_S),4) = close_S; % Mean Closing stroke
                Hysteresis(1:length(open_S),5)  = open_S;  % Mean Opening stroke
                Hysteresis(1:length(close_P),6) = close_P; % Mean Closing pressure
                Hysteresis(1:length(open_P),7)  = open_P;  % Mean Opening pressure
                Hysteresis(:,8) = sMean;                   % Mean of stroke [mm]
                Hysteresis(:,9) = pMean;                   % Mean of pressure [mm]
                Hysteresis(1,10) = a;                      % Figure number

            %Plot each trial
                for i = 1:length(filenames)                      % For all trials
                    figure(a)
                    set(gcf,'position',[300,30,1000,400])        %[x0,y0,width,
                       height]
                     subplot(1,3,1)                              % Pressure [MPa]
                      h(i) = plot(pData{i}); hold on
                      xlabel('steps');                           % Name axis
                      ylabel('pressure [MPa]');                  % Name axis
                      title('Pressure');                         % Create plot title

                     subplot(1,3,2)                              % Master cylinder
                        stroke [mm]
                      plot(sData{i}); hold on
                      xlabel('steps');                           % Name axis
                      ylabel('stroke [mm]');                     % Name axis
                      title('Stroke');                           % Create plot title

                     subplot(1,3,3)                              % Stroke vs
                        Pressure
                      plot(sData{i},pData{i}); hold on
                      xlabel('stroke [mm]');                     % Name axis
                      ylabel('pressure [MPa]');                  % Name axis
                      title('Stroke vs Pressure');               % Create plot title
                end

                legend('Trial 1', 'Trial 2', 'Trial 3'); hold on % Create legend
                legend('Location','northwest');                  % Position legend
                sgtitle(['Close test:' ' '  Test ' - 4 MPa']);  % Create figure
                   title
    end
```

2. PINCH TEST CODE

```
% Pinch Test results --> Force vs Pressure
% Patty de Groot - 4367960
% Master Thesis  - TU Delft, Biomedical Engineering
% 30-01-2021
%% Set up
clear all
close all
clc

a = 0;  % Figure number

%% Import Data
    %Strings with file names
```

```
        filenamesH6  = {'H6 - Pinch 40-1.txt', 'H6 - Pinch 40-2.txt', 'H6 - Pinch
            40-3.txt'};      % Structure 1
        filenamesH10 = {'H10 - Pinch 40-1.txt', 'H10 - Pinch 40-2.txt', 'H10 - Pinch
            40-3.txt'};      % Structure 2
        filenamesC30 = {'Curly Pinch 30-1.txt', 'Curly Pinch 30-2.txt', 'Curly Pinch
            30-3.txt'};      % Structure 3 - 3 MPa
        filenamesC40 = {'Curly Pinch 40-1.txt', 'Curly Pinch 40-2.txt', 'Curly Pinch
            40-3.txt'};      % Structure 3 - 4 MPa

    %Read data from index number: --> index is pinch force is larger thant 0
        initialvaluesH6  = [126, 90, 95];     % Index number
        initialvaluesH10 = [158, 134, 117];
        initialvaluesC30 = [119, 121, 106];
        initialvaluesC40 = [129, 225, 173];

    %Read out useful data
    %[max pressure per trial, max force per trial, max mean pressure, max mean force
       , mean of pressure data, mean of force data]
        %Structure 1
            Test = 'Structure 1 - 4 [MPa]'
            PinchH6  = PinchFunction(filenamesH6, initialvaluesH6, Test, a);
            a = PinchH6(1,7);                % Update figure number
            meanH6 = mean(PinchH6(1:3,2));   % Calculate mean max force
            stdH6  = std(PinchH6(1:3,2));    % Calculate std max force
        %Structure 2
            Test = 'Structure 2 - 4 [MPa]'
            PinchH10 = PinchFunction(filenamesH10, initialvaluesH10, Test, a);
            a = PinchH10(1,7);               % Update figure number
            meanH10 = mean(PinchH10(1:3,2)); % Calculate mean max force
            stdH10  = std(PinchH10(1:3,2));  % Calculate std max force
        %Structure 3 - 3
            Test = 'Structure 3 - 3 [MPa]'
            PinchC30 = PinchFunction(filenamesC30, initialvaluesC30, Test, a);
            a = PinchC30(1,7);               % Update figure number
            meanC30 = mean(PinchC30(1:3,2)); % Calculate mean max force
            stdC30  = std(PinchC30(1:3,2));  % Calculate std max force
        %Structure 3 - 4
            Test = 'Structure 3 - 4 [MPa]'
            PinchC40 = PinchFunction(filenamesC40, initialvaluesC40, Test, a);
            a = PinchC40(1,7);               % Update figure number
            meanC40 = mean(PinchC40(1:3,2)); % Calculate mean max force
            stdC40  = std(PinchC40(1:3,2));  % Calculate std max force

%% Plot results
    %Determine index d at which the pressure is >4
        dH6  = find(PinchH6(:,5)>4,1);
        dH10 = find(PinchH10(:,5)>4,1);
        dC30 = find(PinchC30(:,5)>3,1);
        dC40 = find(PinchC40(:,5)>3.9,1);

    %Plot Raw data
        figure
        set(gcf,'position',[300,30,400,1000]); %[x0,y0,width,height]
        subplot(3,1,1)                         % Force [N]
            plot(PinchH6(:,6)); hold on
            plot(PinchH10(:,6)); hold on
```

```
        plot(PinchC30(:,6)); hold on
        plot(PinchC40(:,6)); hold on
        xlabel('steps');               % Name axis
        ylabel('Force [N]');           % Name axis
        title('Mean force');           % Create plot title

    subplot(3,1,2)                     % Pressure [MPa]
        plot(PinchH6(:,5)); hold on
        plot(PinchH10(:,5)); hold on
        plot(PinchC30(:,5)); hold on
        plot(PinchC40(:,5)); hold on
        xlabel('steps');               % Name axis
        ylabel('Pressure [MPa]');      % Name axis
        title('Mean pressure');        % Create plot title

    subplot(3,1,3)                     % Force vs pressure
        plot(PinchH6(1:dH6,5),PinchH6(1:dH6,6)); hold on
        plot(PinchH10(1:dH10,5),PinchH10(1:dH10,6)); hold on
        plot(PinchC30(1:dC30,5),PinchC30(1:dC30,6)); hold on
        plot(PinchC40(1:dC40,5),PinchC40(1:dC40,6)); hold on
        xlabel('Pressure [MPa]');      % Name axis
        ylabel('Force [N]');           % Name axis
        title('Pressure vs Force');    % Create plot title
        legend('Structure 1','Structure 2','Structure 3 - 3 MPa', 'Structure 3 -
            4 MPa'); % Create legend
        legend('Location','best');     % Position legend
        sgtitle('Pinch Test - Raw data') % Create figure title

%% Functions
  function Pinch = PinchFunction(filenames, initialvalue, Test, a)
  a = a + 1;                           % Increase figure number

    %Import data
        for i = 1: length(filenames)
            %Import data of all trials
              Data(i)  = importdata(filenames{i});
              pData{i} = Data(i).data(:,7)/10;  % Pressure [MPa]
              fData{i} = Data(i).data(:,11); % Force [N]

            %Identify max values per trial
              pmax(i) = max(pData{i});      % Pressure [MPa]
              fmax(i) = max(fData{i});      % Force [N]
        end

   %Trim data to equal length
        %Determine trim length
         trim = [length(pData{1}(initialvalue(1):end)), length(pData{2}(
             initialvalue(2):end)), length(pData{3}(initialvalue(3):end))];
         trim = min(trim)-1;

        %Trim
         for i = 1:3
          pData{i} = pData{i}(initialvalue(i):initialvalue(i)+trim); % Pressure
              [MPa]
          fData{i} = fData{i}(initialvalue(i):initialvalue(i)+trim); % Force [N]
         end
```

```
    %Calculate Mean values
         pMean = mean([pData{1}, pData{2}, pData{3}],2); % Mean pressure [MPa]
         fMean = mean([fData{1}, fData{2}, fData{3}],2); % Mean force [N]

    %Identify Max values of the mean
         max_pMean = max(pMean);                    % Max mean pressure [MPa]
         max_fMean = max(fMean);                    % Max mean force [N]

    %Store data
       Pinch = zeros(trim+1,6);                     % Allocate space for results
       Pinch(1:3,1)= pmax;                          % Max pressure [MPa]
       Pinch(1:3,2)= fmax;                          % Max force [N]
       Pinch(1,3)  = max_pMean;                     % Max mean pressure [MPa]
       Pinch(1,4)  = max_fMean;                     % Max mean force [N]
       Pinch(:,5)  = pMean; %smoothdata(pMean);     % Mean of pressure data [MPa]
       Pinch(:,6)  = fMean; %smoothdata(fMean);     % Mean of force data [N]
       Pinch(1,7)  = a;                             % Figure number

    %Plot each trial
         for i = 1:length(filenames)
             figure(a)
             set(gcf,'position',[300,30,1000,400]) %[x0,y0,width,height]
             subplot(1,3,1)                         % Pressure [MPa]
             plot(pData{i}); hold on
             xlabel('steps');                       % Name axis
             ylabel('pressure [MPa]');              % Name axis
             title('Pressure');                     % Create plot title

             subplot(1,3,2)                         % Force [N]
             plot(fData{i}); hold on
             xlabel('steps');                       % Name axis
             ylabel('force [N]');                   % Name axis
             title('Force');                        % Create plot title

             subplot(1,3,3)                         % Pressure vs Force
             plot(pData{i},fData{i}); hold on
             xlabel('pressure [MPa]');              % Name axis
             ylabel('force [N]');                   % Name axis
             title('Pressure vs Force');            % Create plot title
         end
             legend('Trial 1', 'Trial 2', 'Trial 3'); hold on % Create legend
             legend('Location','southeast');            % Position legend
             sgtitle(['Pinch test:' ' '  Test]);        % Create figure title
end
```

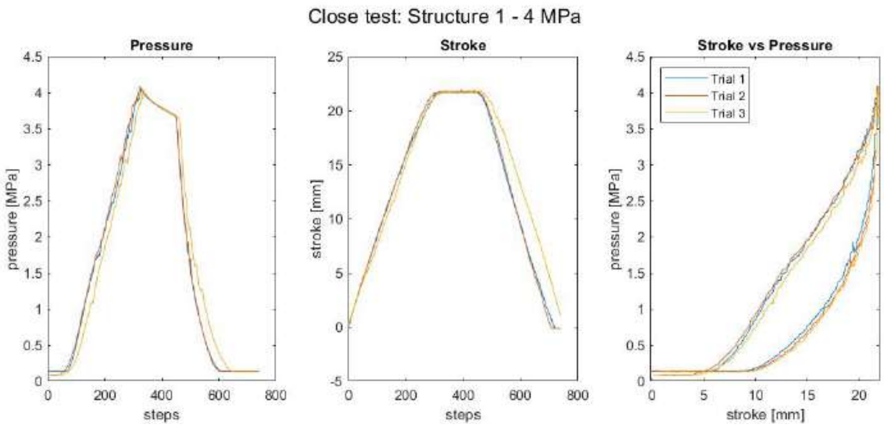
Close test: Structure 1 - 4 MPa
Pressure
pressure [MPa]
steps
Stroke
stroke [mm]
steps
Stroke vs Pressure
Trial 1
Trial 2
Trial 3
pressure [MPa]
stroke [mm]

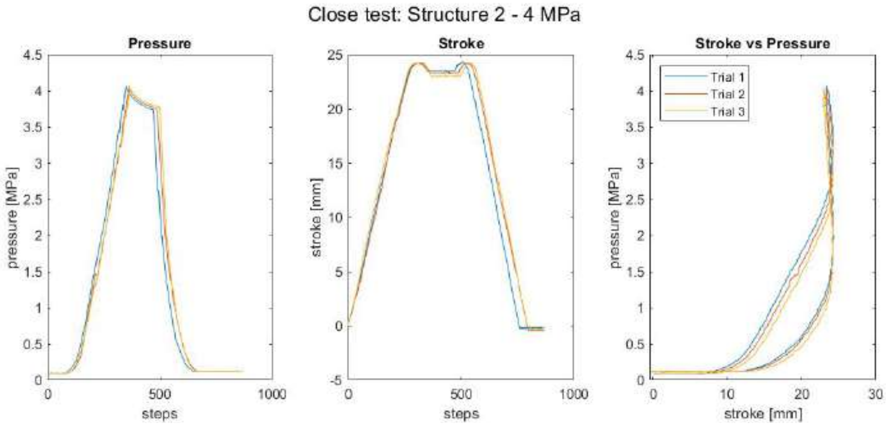
Close test: Structure 2 - 4 MPa
Pressure
pressure [MPa]
steps
Stroke
stroke [mm]
steps
Stroke vs Pressure
Trial 1
Trial 2
Trial 3
pressure [MPa]
stroke [mm]

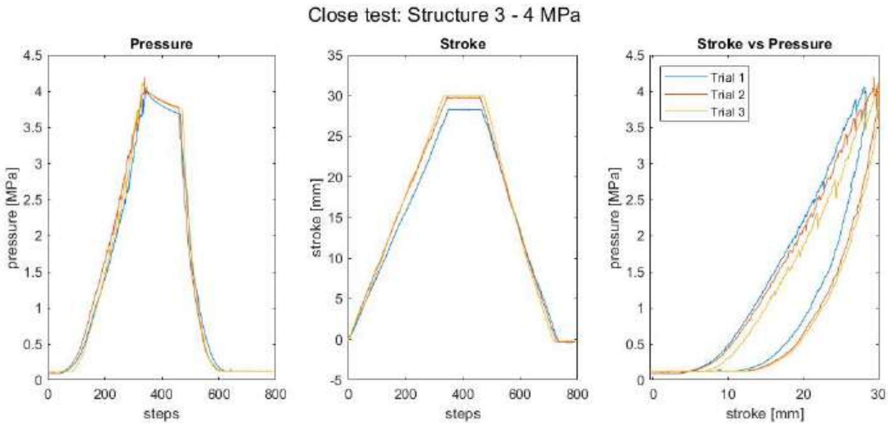
Close test: Structure 3 - 4 MPa
Pressure
pressure [MPa]
steps
Stroke
stroke [mm]
steps
Stroke vs Pressure
Trial 1
Trial 2
Trial 3
pressure [MPa]
stroke [mm]

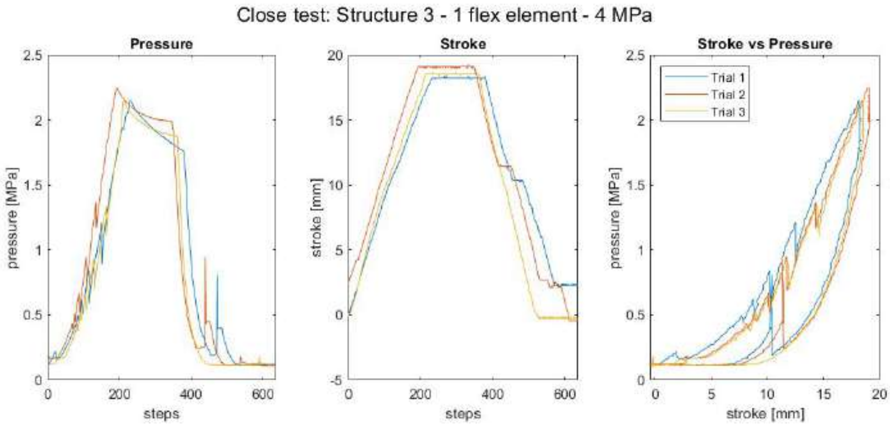
Close test: Structure 3 - 1 flex element - 4 MPa
Pressure
pressure [MPa]
steps
Stroke
stroke [mm]
steps
Stroke vs Pressure
Trial 1
Trial 2
Trial 3
pressure [MPa]
stroke [mm]

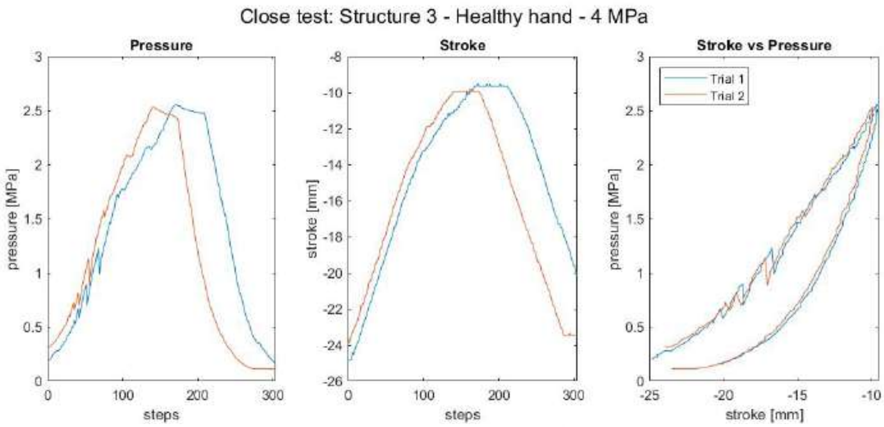
Close test: Structure 3 - Healthy hand - 4 MPa
Pressure
Stroke
Stroke vs Pressure
pressure [MPa]
stroke [mm]
steps
Trial 1
Trial 2

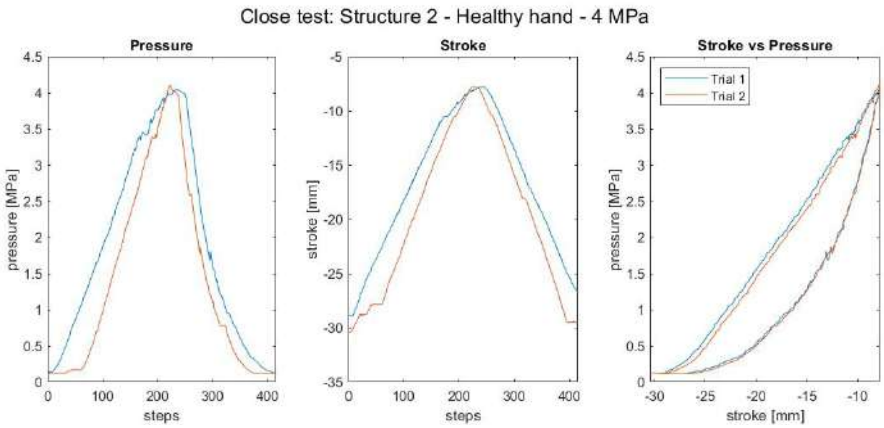
Close test: Structure 2 - Healthy hand - 4 MPa
Pressure
Stroke
Stroke vs Pressure
pressure [MPa]
stroke [mm]
steps
Trial 1
Trial 2

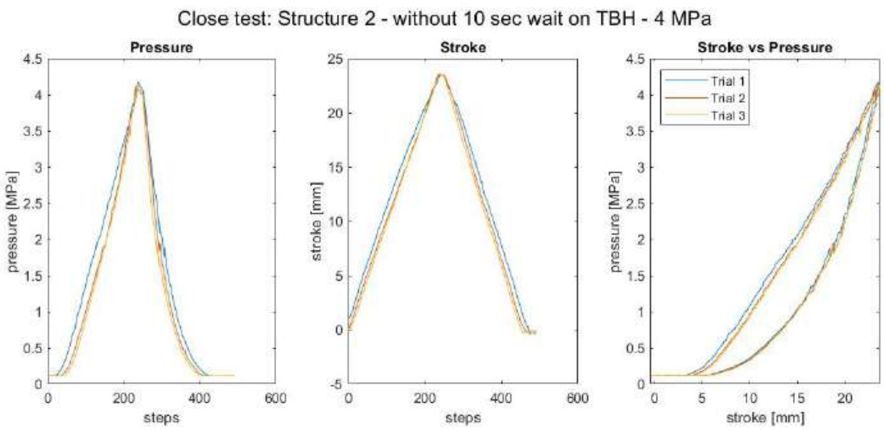
Close test: Structure 2 - without 10 sec wait on TBH - 4 MPa
Pressure
Stroke
Stroke vs Pressure
pressure [MPa]
stroke [mm]
steps
Trial 1
Trial 2
Trial 3

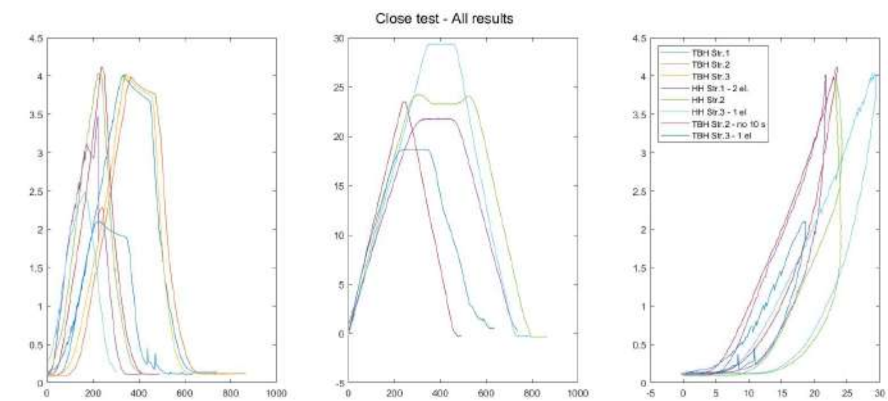
Close test - All results
TBH Str.1
TBH Str.2
TBH Str.3
HH Str.1 - 2 el.
HH Str.2
HH Str.3 - 1 el
TBH Str.2 - no 10 s
TBH Str.3 - 1 el

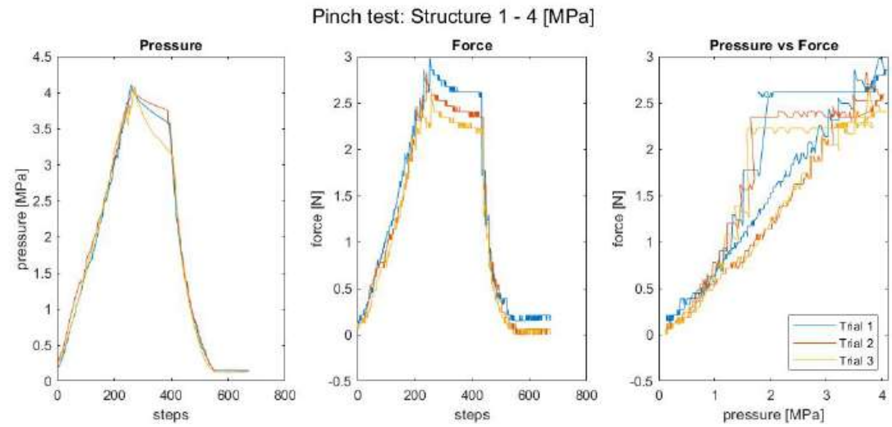
Pinch test: Structure 1 - 4 [MPa]
Pressure
pressure [MPa]
steps
Force
force [N]
steps
Pressure vs Force
force [N]
pressure [MPa]
Trial 1
Trial 2
Trial 3

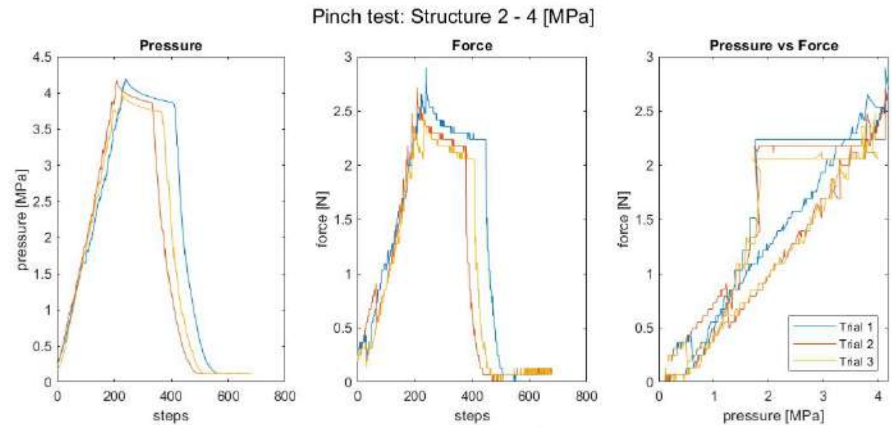
Pinch test: Structure 2 - 4 [MPa]
Pressure
pressure [MPa]
steps
Force
force [N]
steps
Pressure vs Force
force [N]
pressure [MPa]
Trial 1
Trial 2
Trial 3

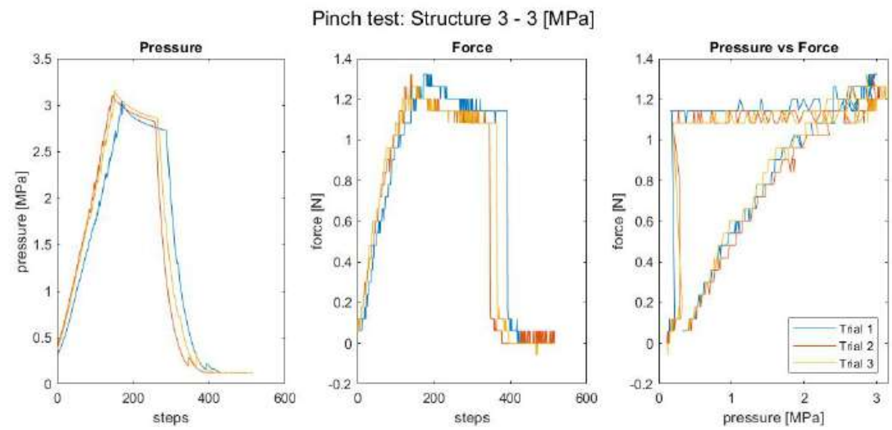
Pinch test: Structure 3 - 3 [MPa]
Pressure
pressure [MPa]
steps
Force
force [N]
steps
Pressure vs Force
force [N]
pressure [MPa]
Trial 1
Trial 2
Trial 3

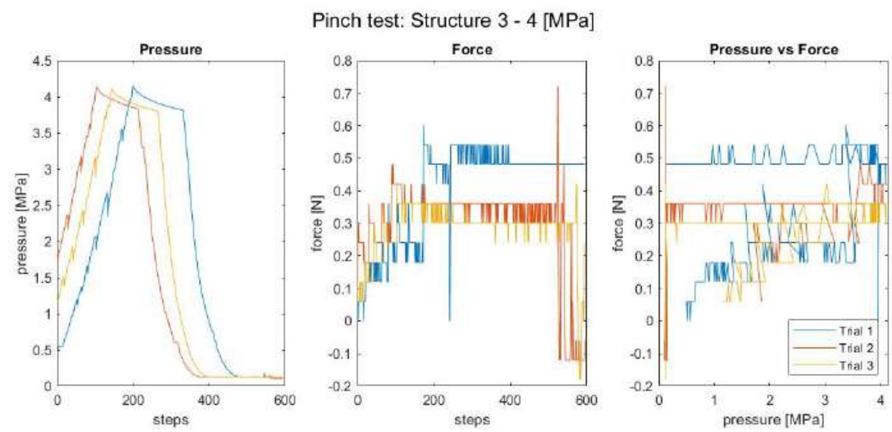
Pinch test: Structure 3 - 4 [MPa]
Pressure
pressure [MPa]
steps
Force
force [N]
steps
Pressure vs Force
force [N]
pressure [MPa]
Trial 1
Trial 2
Trial 3

APPENDIX J FASTENING

Although, this is not the main focus of this thesis, it was mentioned previously that one of the limitations of the Symbihand was discomfort experienced by the user. One main source of discomfort was the donning and doffing of the hand orthosis, as the sliding of the finger modules over the fingers was considered as painful in the case study. For this reason, a closer look is taken on potential fastening mechanisms for hand orthoses. Requirements have been described in Appendix D as: minimal palmar surface area; enough force to hold the orthosis; clamping force <32 mmHg (133 Pa), to prevent blood vessel obstruction; soft & smooth interface; donning doffing with hand deformities; painless donning & doffing and modularity, to allow for different hand sizes. In order to obtain an open palm for sensation, all other aspects must be applied dorsally as between the fingers few space is available. The fastening mechanism should so also be applicable within the space that is left by the actuation mechanism.

The literature study on fixture designs in dynamic hand orthoses in Section III was performed in September 2019. Within this study several different categories for fixture mechanisms have been identified: Gloves; Straps; End point inserts; Finger inserts; Hybrids and Miscellaneous. Miscellaneous contained magnets and one design of Hasegawa et al. (2015), which will be discussed later on [316]. The Symbihand design is included in the category of Finger inserts, but is considered uncomfortable. The category called 'Straps' contains all designs that use straps to envelop the finger and are either elastic, or fasten by the use of Velcro or buckles. The overall conclusion of the literature study was that designs of the fastening mechanisms has been highly overlooked and should be improved. For deciding upon a more promising fastening mechanism a closer look was taken on mechanisms, as well as, on emerging materials.

1. MECHANISMS

When applying a mechanism for fastening of the orthosis to the hand, during donning and doffing more space should be available then during the wearing time of the device. As the orthosis is worn, the fit should be snug to avoid chafing over the fingers due to actuation. A tightening mechanism is thus up for consideration, however these come in many different shapes and forms. An image search was performed on Google Images and on Pinterest to obtain some inspiration, results are indicated in Figure 1.

1) *Velcro:* is already used often for the fastening of hand orthoses. It is easy in use, readily obtainable and also used in many other applications. However, regarding cleanliness it is not ideal as it is a fabric and dirt can influence the strenght of the fixture.
2) *Compliant Grippers:* one source of inspiration are compliant grippers and mechanisms. These grippers are emerging mainly in the field of agriculture or minimal invasive surgery, where must be dealt with delicate objects. The grippers form to the object to be grasped and so would be beneficial in dealing with hand deformities where no finger is following standard anatomy. A drawback is that the grippers are quite spacious as they rely upon their geometry for grasping force.
3) *Simple clips:* mechanisms like clothespins or hair clips are easy clamping mechanisms. They use small springs to create a clamping force and can be opened by generating a counter-force with the fingers. These clips also come in compliant forms, which can easily be 3D printed, however here opening width depends on deformation of the structure and that might demand more space.
4) *Spring hose clamps:* used to tighten hoses around pipes. They come in many different sorts, such as ratchets, tie-wraps, geometric clamps, turning rods, or by locking mechanisms. Either they remain in circular shape and must be slid over the pipes or they create an opening so they can be put around the pipe. There is potential in applying one of these mechanisms as fastening method. However the sliding over the fingers must be avoided, especially as the act of having to open the structure and sliding them over the fingers might be difficult if there is more than one fixture per finger. Similar are Springform baking pans [317], that use a spring mechanism for tightly closing a baking tray.
5) *Boa Fasteners:* make use of cables and a turning mechanism to tighten the cable. They are often applied in snowboard shoes, but also in some wrist braces that are available on the market. The tightness of the fixture could be adjusted and by a locking mechanism the snug fit is maintained. However when miniaturized for the finger fixture, it might become a bit fiddling. Also, if one cable is used to tighten several fixtures at the same time with one larger fastener on the dorsal side of the hand, the tension on the cable might interfere with the actuation of the fingers.
6) *Memory Spring Steel:* is mostly known for its application in SlapWrap bracelets. They are made of concave spring steel strips and when slapped against the wrist they encircle around the object in a circular manner. Currently a company has also applied slap wraps for adding grip in weight lifting [318]. The mechanism is incredibly easy as the user would only have to lightly push his/her finger against the material and it would wrap around the finger. The only question is whether or not the material could apply enough force to allow for an open palm design. Otherwise, the material would have to envelop the finger and an additional fixture would need to be applied to hold the orthosis and to create a snug enough

fastening. Besides that, steel is not a soft interface so the mechanism should be covered with another material.

7) *Diaphragm Shutter/Iris mechanism:* work with two rings that are rotated in opposite direction to create an opening or closure. They are easy mechanisms, however they require too much space as a certain distance is needed between the inner and outer diameter. Added to that no more than one fixture per finger can be used with respect to easy donning, similar to the spring hose clamps.
8) *Magnets:* are easy fastening mechanisms, that can be applied to the end of straps. They can provide good normal forces, however some geometric linking must be added to counteract sliding forces. They are added to straps and therefor do envelop the fingers taking a way some of the palmar surface. The strenght of the magnets should also be taken into consideration, as the user might want to pick up products that react to magnetic fields.
9) *Interlinking/Form lock:* simple geometric locking of shapes to obtain a closure of a strap. Can be combined with a magnet for even stronger fastening. These are however nog adjustable to varying finger diameters.
10) *Inflatables:* soft actuators can also be used to create a clamping force on the hand. Auto-inflatable compression bandages have been developed by Webb et al. (2019) by pressing the fabric the material is actuated and inflates itself [319]. The inflation is however irreversible and could not be applied for fixture design. Soft actuators could also be of use, different types have been described in the Appendix E. It would be questionable if soft inflatable actuators would supply enough clamping force with low encumbrance to hold the orthosis, and it would need separate control and holding pressures to maintain the fixture. Hiramitsu et al. (2019) created a fabric of woven McKibben muscles, by inflating the actuators the fabric is able to move [320]. Lastly, new 3D printing technology enables the embedding of micro-fluidic channels in [321] [322], of which inflation is controlled by a micro fluidic chip and no external compressor is needed within the system. This is a nice concept, but would probably not generate enough force for holding the orthosis.

FIGURE 43. Exploration of fastening mechanisms using Google Images and Pinterest.

2. EMERGING MATERIALS

The fastening methods discussed previously are all mechanisms that have been under development for a while. However it might also be useful to evaluate more novel options on the field of emerging materials and production methods. One article was obtained within the literature review that can be related to this field. Hasegawa et al. (2015) combined memory metal with inflatable air-chambers to create a fixture that can be clamped upon the hand [316]. By inflating the air-chambers the metal strip is straightened and an opening is created, when the air is let out the metal returns to its resting position and creates a clamping force upon the fingers. The fastening developed by Hasegawa et al. uses six fixtures to connect an orthosis of 500 grams to the hand in a static situation. A continuous pressure of 0.05 MPa was needed to create a clamping force that was sufficient, but not so tight it resulted in blood flow obstruction [316]. As a continuous pressure is needed, this also demands a continuous pressure supply that needs to be generated.

Smart Memory Effect (SME): Materials can be deformed and fixed into a temporary shape and recover their original permanent shape only on exposure to an external stimulus [323]. These materials can be metals, polymers as well as composites and can respond to different kinds of stimuli.

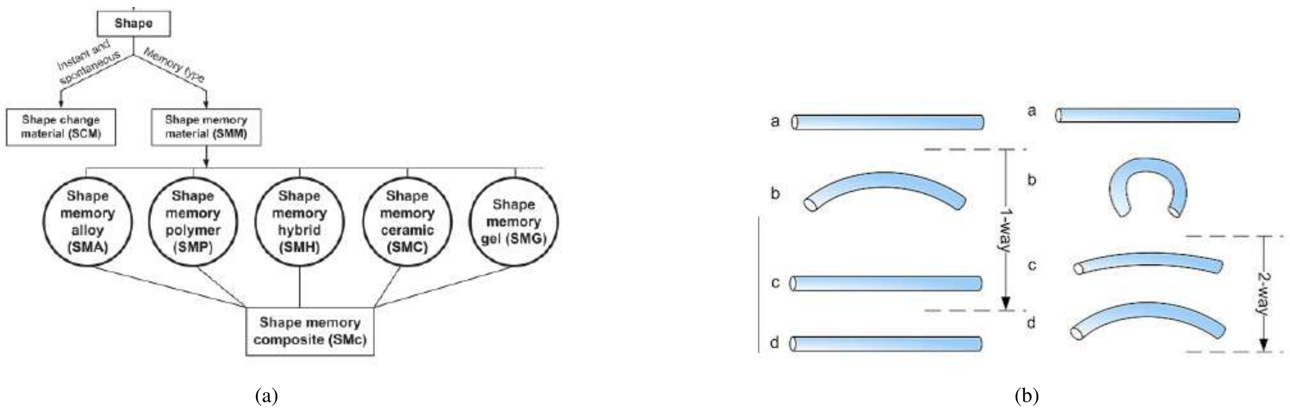

FIGURE 44. Smart memory material types and effects. A) categorisation of shape changing materials by Sun et al. (2019) [256]. B) illustration of the one and two way smart memory effect [324].

MATERIAL TYPES

1) *Smart memory alloys (SMAs):* can deform at a low-temperature and then recover to their prior shape upon heating above a particular temperature-related to the properties of alloy. SMAs mainly include three types: nickel-titanium (NiTi) alloys, copper–zinc–aluminum–nickel and copper–aluminum–nickel. The most used smart memory alloy is NiTi, as it is highly bio-compatible [324]. Responses are either triggered by thermal (environmental or electrically applied) or magnetic input (static or alternating fields) [256]. If SMAs were to be applied as fixture an activation mechanism containing electrical threads and a battery for heating needs to be implemented as well. Simpler thermo-responsive materials are unusable as they either need to be externally heated, also subjecting the and to the same heat source, or they respond to body warmth, but then are also highly sensitive to temperature fluctuations, not being able to guarantee continuous forces. At the same time the clamping forces that can be generated by the SMAs only of low amounts [256]. For obtaining a proper interface, the SMA should be covered with a soft material which also creates an insulating layer for warmth of the material. Smart memory alloy wires are also used to create temperature active auxetics, which are fabrics that can be shaped to the body by applying heat [325]–[327].
2) *Smart memory polymers (SMPs):* the shape-memory effect of SMPs depends on the existence of separated phases related to the coiled polymer structure and cross-links The advantage of SMPs over SMAs relies mostly on their intrinsic properties such as lower cost, lower density, easier processing, increased form freedom and larger attainable strains [324]. They can also be triggered by additional stimuli such as moisture, stretch, or light, etc., and they can be activated by more than one type of stimulus [256], [324], [328]. Photo-responsive SMPs by Lendlein et al. (2005), respond to UV light for obtaining mode 1 and UV light of a different wavelength for returning to original shape [323]. However, despite the properties of SMPs can be more easily tailored than SMAs, the successful synthesis of a particular SMP for a special application normally requires strong chemical/polymer background, years of experience and great efforts in trial and error. SMP can achieve high deflection, however can only generate low forces [256].
3) *Composites:* are different materials combined with one another in order to achieve the best properties of the merged materials. Also, smart memory materials can be integrated to create composites. For example molding SMA wires into polymer material to obtain the wrist band created by Tyas Franssen (2017) [329], or the SMP combination by Re:Flex [330]. Similar flexible materials can be combined with rigid structures to create joints, as was used to create the KinetX structures of MIT [331]. With advancing possibilities for multi-material 3D printing these structures are more and more easy to obtain [332]. Results can be compared to compliant mechanisms, where a simple applied force can cause controlled deformation of the structure. It is also possible to print ferromagnetic particles into a polymeric product, with the printing technology by MIT [333]. By controlling the magnetic poles of the particles, switching between different modes can be achieved by changing the magnetic field. By use of this technology a moving robotic structure was created as can be seen in Figure 2. Combinations are endless, and many of the discussed possibilities are still in their infancy or require state of the art production facilities.

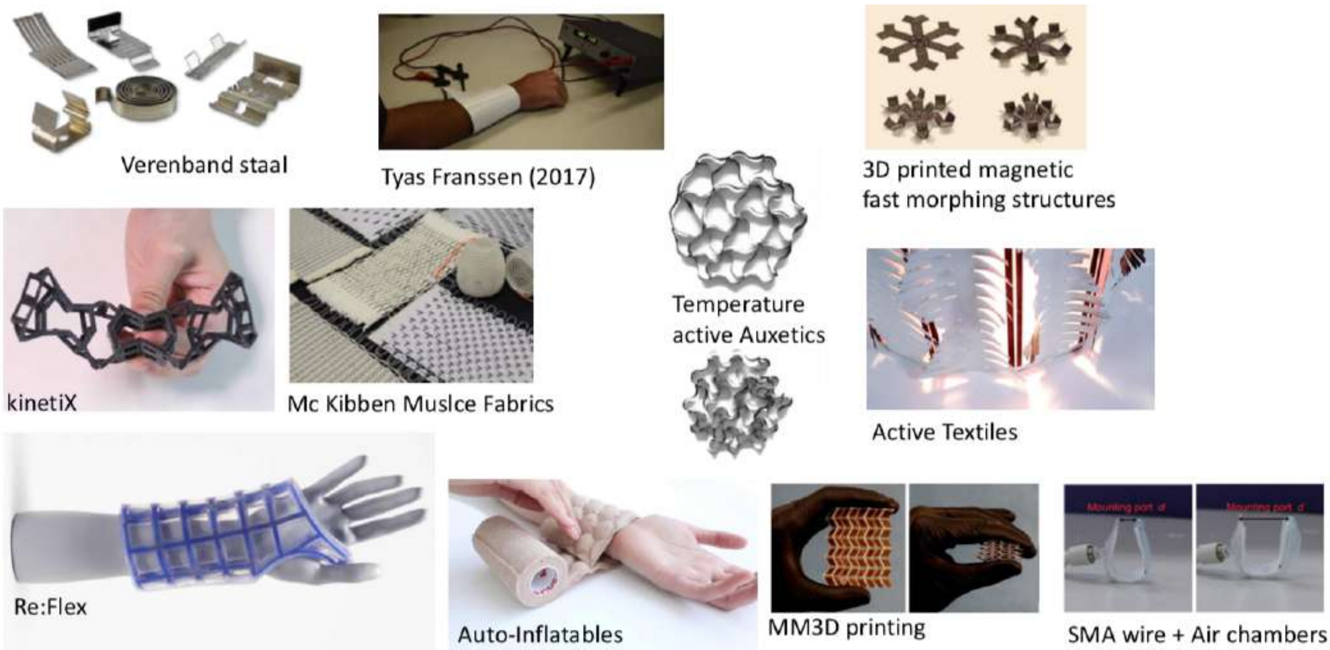

FIGURE 45. Exploration of smart materials using Google Images, Pinterest and YouTube. Verenbandstaal [] [X], Tyas Franssen (2017) [329], Temperature active auxetics [325], [326], 3D printed magnetic fast morphing structures [334], KinetiX [331], McKibben Muscle Fabrics [320], [335], Active Textiles [336], Re:Flex [330] Auto-inflatables [319], MM3D printing [332], SMA wire + Air chambers [316]

3. CONCEPTS OF CLAMPING FASTENING MECHANISMS

Many opportunities for fixture designs have been discussed, still, when returning to the core of the problem, none of them are ideal. A consideration must be made between simplicity and functionality. Electric-responsive Smart Memory Alloys (SMA) might be a possible solution, where an electrical current heats the metal and so opens the fixture, however, this would also oppose a need for the placement of batteries and wires. As a result, demands on weight and safety will become more important as the user should be able to operate the orthosis in all sorts of environments. The SMA should also be submerged in an insulating material, so that the user is not subjected to the applied current.

Other potential fixtures use inflatable or also hydraulic soft robotics to create a clamping force on the fingers. Question here, is whether enough force can be applied to hold the orthosis and if appropriate pressure can be maintained for longer amounts of time. Furthermore, Slap Wraps could be beneficial as it is a simple mechanism. Sliding motions should however be counteracted to make sure the wraps do not slide from the fingers or, if available, a stronger memory spring steel should be used so a clamping force can be generated. This could allow for an open palmar structure, enabling the users sensory function.

Smart Memory Polymers (SMPs), are probably unusable, as they can generate large actuation movements but can only withstand very small forces. A last interesting prospective might be the 3D printing of ferromagnetic particles. If the technology was better available, printing the material so that it would create a circle to enclose the finger when a magnet is applied would be promising. However this technology is not available at the TU Delft yet, and perhaps the magnetic field created to close the fixture is obstructing when holding materials that are attracted by magnetic fields.

Simple mechanical clamping might therefore be a better solution. With clamping mechanisms it must be taken into consideration that the clamping force must be high enough to hold the orthosis, but also low enough to avoid blood vessel obstruction. Slim enclosing mechanisms could also be a possibility, only if placed by avoiding the most sensitive regions of the hand. Adding actuation systems for the fastening mechanism is unacceptable, therefor, systems like McKibben Muscle fabrics and soft actuators are discarded.

IDEA GENERATION

By ideation several mechanical clamping mechanisms concepts have been evaluated. They are indicated in Figure 46 and evaluated in Table 17 with unweighted criteria and in with weighted criteria 18.

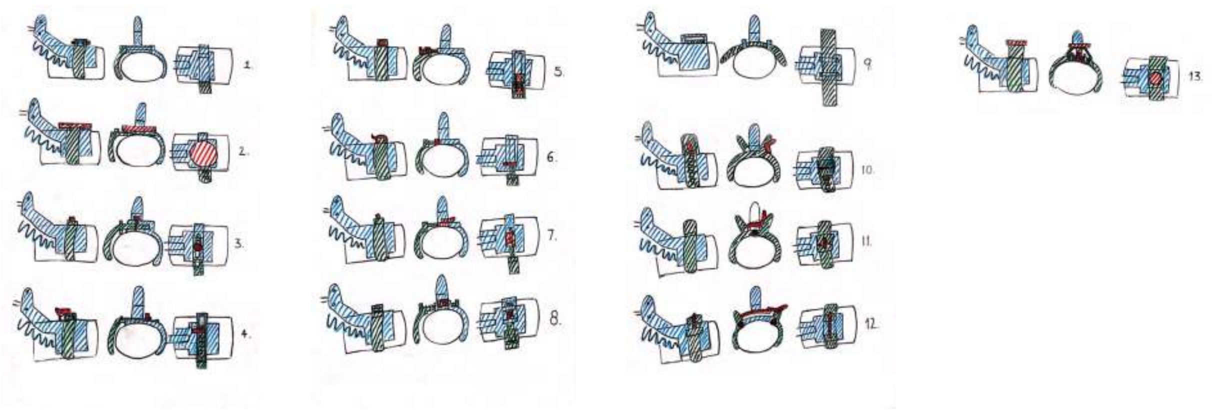

FIGURE 46. Concepts of potential clamping mechanisms for improved fastening design. 1) rails, 2) Kreg in-line mechanism, 3) slots, 5) twist lock / pen mechanism, 6 & 7) Ski-pole mechanism, 8 & 13) Worm wheel, 9) Slap-wrap, 4,10, 11, 12) Ratchet mechanisms.

	1	2	3	4	5	6	7	8	9	10	11	12	13
Adjustability	8	8	8	7	7	8	8	8	0	7	7	7	8
Fragility	6	7	7	4	6	7	7	7	9	4	4	4	4
Ease of donning	9	8	8	9	4	8	8	6	9	8	8	8	6
Space	7	7	7	7	8	7	6	6	9	4	4	4	3
Cleanliness	7	6	6	6	7	7	7	5	9	5	5	5	8
Durability	7	8	8	5	7	7	7	8	8	4	4	4	6
Weight	5	5	5	5	5	5	5	5	9	5	5	5	5
Scalability	8	8	8	8	7	7	7	8	8	6	6	6	5
TOTAL	57	57	57	51	51	56	55	53	61	43	42	42	45

TABLE 17. Evaluation of fastening concepts with unweighted criteria.

	Weight	1	2	3	4	5	6	7	8	9	10	11	12	13
Adjustability	2	8	8	8	7	7	8	8	8	0	7	7	7	8
Fragility	1	6	7	7	4	6	7	7	7	9	4	4	4	4
Ease of donning	2	9	8	8	9	4	8	8	6	9	8	8	8	6
Space	2	7	7	7	7	8	7	6	6	9	4	4	4	3
Cleanliness	1	7	6	6	6	7	7	7	5	9	5	5	5	8
Durability	0.5	7	8	8	5	7	7	7	8	8	4	4	4	6
Weight	1	5	5	5	5	5	5	5	5	9	5	5	5	5
Scalability	0.5	8	8	8	8	7	7	7	8	8	6	6	6	5
TOTAL	10	73.5	72	72	67.5	63	72	70	65	71	57	57	57	56.7

TABLE 18. Evaluation of fastening concepts with weighted criteria.

APPENDIX K TABLE OF ORTHOSIS FIXTURE DESIGNS REVIEWED

TABLE 19. End point fixture designs

Image	Name	Designer & Year	source
	Vanderbilt	Gasser 2017	[143]
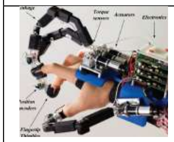	HEXOTRAC	Sarakoglou 2016	[142]
	MR Glove	Yap 2017	[264]

TABLE 20. Finger insert fixture designs

Image	Name	Designer & Year	source
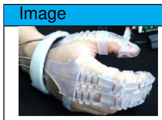	Exoglove Poly = SNU Exoglove (Flexible material)	Kang 2016	[138]
	-	Rahman 2013	[150]
	-	Sarwar2019	[151]
	M.ReS	Weiss 2013	[149]
	-	Yamaura 2009	[148]

TABLE 21. Miscellaneous fixture designs.

Image	Fixture	Name	Designer & Year	source
	No direct connection, assistance + resistance purely by forces	-	Cui 2015	[157]
	Shape memory alloy wire and air chamber	-	Hasegawa 2015	[316]
	Tape and Magnets	AMADEO	-	[159]

TABLE 22. Glove fixture designs.

Image	Name	Designer & Year	source
Closed Gloved			
	Shieldex117/17	Bahrami 2018	[284]
	-	Biggar 2016	[179]
	Gloreha	Borboni 2016	[201]
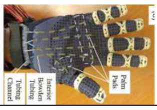	HEXOES	Burns 2017	[146]
	Lobster	Chen 2017	[208]
	PneuGlove	Connelly 2009	[213]
	Delph II	Delph 2013	[247]
	ASR Glove	Hadi 2018	[255]
	-	Kadowaki 2011	[232]
	GRIPIT	Kim 2017	[97]
	BiomHED	Lee 2014	[147]
	-	Moromugi 2009	[262]
	J-Glove	Ochoa 2011	[337]
	-	Park 2018	[137]
	-	Sasaki 2004	[248]
	AirExoGlove	Stilli 2018	[338]
	-	Sun 2019	[256]
	-	Takagi 2009	[216]
	-	Toochinda 2018	[257]
	-	Toya 2009	[258]
	-	In 2011	[103]
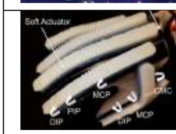	ExoGlove	Yap 2015	[269]
Open Gloves			
	SEM Glove	Nilsson 2012	[268]

TABLE 23. Straps fixture designs.

Image	Name	Designer & Year	source
Velcro			
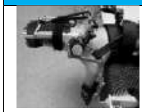	HandSOME	Brokaw 2011	[160]
	EXO = HEXOSYS	Iqbal 2010/2015	[234], [238]
	ReHand	Lince 2017	[237]
	-	Maeder-York 2014	[141]
	-	Nishad 2014	[210]
	-	Polotto 2012	[339]
	GraspyGlove	Popov 2017	[340]
	-	Refour 2019	[206]
	-	Richards 2015	[215]
	ExoK'ab	Sandoval-Gonzalez 2016	[341]
	-	Shiota 2019	[253]
	-	Tang 2011	[254]
Elastic			
	-	Arata 2013	[197]
	-	Lin 2018	[236]
	PM Hand	McConnell 2014	[240]
	-	Ong 2018	[274]
	iGrab	Saharan 2017	[273]
Elastic + Velcro			
	Exo-Finger	Otsuka 2010	[245]
Sliding Buckle			
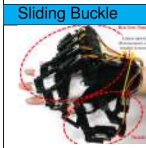	-	Jo 2017	[342]
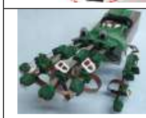	PEXO	Bützer 2019	[162]
Unknown strap type			
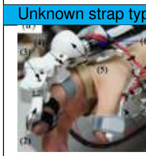	KULEX	Hong 2019	[272]
	BRAVO Hand Exoskeleton	Leonardis 2015	[196]
	SMART WHO	Makaran 1993	[235]
	-	Nycz 2016	[199]
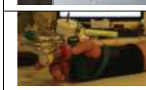	AssistOnFinger	Ertas 2014	[209]

TABLE 24. Hybrid fixture designs.

Image	Name	Designer & Year	source
End point + Straps			
	-	Chowdhury 2019	[133]
	MANDARIN	Hansen 2018	[283]
	SaeboFlex	Hoffman 2011	[343]
	-	Patino 2018	[144]
	-	Polygerinos 2015	[145]
	FEX	Sale 2017	[?]

Image	Name	Designer & Year	source
End point + Gloves			
	-	Cappello 2018	[153]
	-	Ferguson 2018	[154]
	SAFE Glove	Ma 2016	[155]
End point + Gloves + Straps			
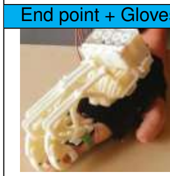	HES	Conti 2017	[156]
	Synergy Glove	Xiloyannis 2017	[136]
Gloves + Straps			
	IOTA	Aubin 2013	[89]
	iHandRehab	Li 2011	[152]
	SPAR Glove	Rose 2019	[139]
End point + Finger Inserts + Straps			
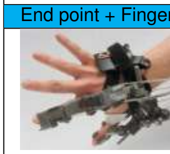	HX	Cempini 2015	[90]
	-	Lambercy 2013	[91]

End point + Finger Inserts			
	HANDEXOS	Chiri 2012	[202]
	FlexoGlove	Mohammadi 2018	[158]
	-	Tadano 2010	[219]
	-	Tjahyono	[220]
	-	Wege 2006	[261]
	-	Kuswanto 2018	[165]
Finger Inserts + Straps			
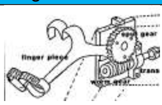	-	Benjuya 1990	[?]
	OFX	Heo 2014	[193]
	OHAE	Martinez 2010	[266]
	-	Tan 2017	[249]
	-	Tong 2010	[227]
	-	Wang 2018	[134]
	Symbihand	Nizamis 2019	[8]

TU Delft

Delft University of Technology, Faculty of Mechanical, Maritime and Materials Engineering
Department of Biomechanical Engineering, Delft Institute of Prosthetics and Orthotics